The mineral potential of New Zealand – Part 2: New Zealand mineral deposits and resources classified by their commodity and mineral deposit type

AB Christie RG Barker RL Brathwaite
MP Hill SM Rooyakkers CEJ de Ronde

GNS Science Consultancy Report 2024/62B
July 2024 – Revised September 2024

DISCLAIMER

This report has been prepared by the Institute of Geological and Nuclear Sciences Limited (GNS Science) exclusively for and under contract to the Ministry of Business, Innovation & Employment (MBIE). Unless otherwise agreed in writing by GNS Science, GNS Science accepts no responsibility for any use of or reliance on any contents of this report by any person other than MBIE and shall not be liable to any person other than MBIE, on any ground, for any loss, damage or expense arising from such use or reliance.

Use of Data:

Client consent required to use data.

BIBLIOGRAPHIC REFERENCE

Christie AB, Barker RG, Brathwaite RL, Hill MP, Rooyakkers SM, de Ronde CEJ. 2024. The mineral potential of New Zealand – Part 2: New Zealand mineral deposits and resources classified by their commodity and mineral deposit type. Lower Hutt (NZ): GNS Science. 233 p. Consultancy Report 2024/62B.

Note: In mid-September 2024, revised versions of both Parts 1 and 2 of this report were issued to update mineral resource statistics for Trans-Tasman Resources' ironsand prospect offshore from Pātea in southern Taranaki, as well as to clarify the current status of the mining proposal (Sections 6.2.2 and 6.2.5 in this document).

CONTENTS

1.0 INTRODUCTION 1

2.0 MINERAL DEPOSIT MODELS..2

3.0 ONSHORE METALLIC MINERALS 7

3.1 Aluminium (Al) 7

3.1.1 International Description..7

3.1.2 Lateritic Bauxite 7

3.2 Antimony (Sb)...9

3.2.1 International Description..9

3.2.2 Antimony in New Zealand 9

3.2.3 Orogenic Quartz Vein Sb 10

3.2.4 Hot Spring Sb–As... 12

3.3 Beryllium (Be)..13

3.3.1 International Description.. 13

3.3.2 Beryllium in New Zealand... 13

3.4 Chromium (Cr)..14

3.4.1 International Description.. 14

3.4.2 Chromium in New Zealand... 15

3.4.3 Podiform Chromite 16

3.5 Cobalt (Co)...18

3.5.1 International Description.. 18

3.5.2 New Zealand Cobalt Occurrences 18

3.6 Copper (Cu)..19

3.6.1 International Description.. 19

3.6.2 Copper in New Zealand.. 19

3.6.3 Production 19

3.6.4 Resources 21

3.6.5 Potential and Prospectivity 21

3.6.6 Volcanogenic Massive Sulfide Deposits 21

3.6.7 Serpentine-Hosted Fe-Cu 25

3.6.8 Porphyry Cu... 27

3.6.9 Copper Skarn 29

3.6.10 Hydrothermal Quartz and Sulfide Vein Copper of Uncertain Origin................ 29

3.7 Gallium (Ga)...33

3.7.1 International Description.. 33

3.7.2 New Zealand Occurrences of Gallium 33

3.8 Gold (Au)..33

3.8.1 International Description.. 33

3.8.2 Gold in New Zealand.. 34

3.8.3 Orogenic Shear Zone Au – Paleozoic....................................... 36

3.8.4 Orogenic Shear Zone Au – Mesozoic 42

3.8.5 *Low-Sulfidation Epithermal Au–Ag* Deposits.............................. 48

3.8.6 Intermediate-Sulfidation Epithermal Vein Zn-Pb-Cu-Ag-Au 60

3.8.7 High-Sulfidation Epithermal Au–Ag 62
3.8.8 Reduced-Granitic Intrusion-Related Au 63
3.8.9 Alkali Intrusion-Related Au 64
3.8.10 Gabbroid-Associated Au-Ni-Cu 65
3.8.11 Sediment (Carbonate)-Hosted Au–Ag (Carlin Type) 66
3.8.12 Gold Skarn 67
3.8.13 Detachment-Fault-Related Polymetallic Deposits 68
3.8.14 Placer Au, Onshore, Beach and Offshore 69
3.9 Iron (Fe) 71
3.9.1 International Description 71
3.9.2 New Zealand Occurrences of Iron 72
3.9.3 Shoreline Placer Fe 72
3.9.4 Bog Fe 77
3.9.5 Transported Residual Fe 77
3.10 Lithium (Li) 78
3.10.1 International Description 78
3.10.2 New Zealand Occurrences of Lithium 79
3.10.3 Li Pegmatites 79
3.11 Magnesium (Mg) 81
3.11.1 International Description 81
3.11.2 International Occurrences of Magnesium 81
3.11.3 New Zealand Occurrences of Magnesite 81
3.12 Manganese (Mn) 83
3.12.1 International Description 83
3.12.2 New Zealand Occurrences of Manganese 83
3.12.3 Volcanogenic Mn 84
3.13 Molybdenum (Mo) 87
3.13.1 International Description 87
3.13.2 New Zealand Occurrences of Molybdenum 87
3.13.3 Porphyry Mo 88
3.14 Nickel (Ni) 90
3.14.1 International Description 90
3.14.2 New Zealand Occurrences of Nickel 91
3.14.3 Dunitic Ni-Cu 93
3.14.4 Gabbroid-Associated Ni-Cu 94
3.14.5 Lateritic Ni 95
3.15 Platinum Group Metals (PGM) 96
3.15.1 International Description 96
3.15.2 Platinum Group Metals in New Zealand 96
3.15.3 Magmatic PGM 97
3.15.4 *Dunitic PGM* – Dun Mountain Ophiolite Belt 100
3.15.5 Placer PGM 101
3.16 Rare Earth Elements 104
3.16.1 International Description 104

3.16.2 New Zealand Occurrences of Rare Earth Elements 104
3.16.3 Carbonatite-Hosted REE (Rare Earth Elements).. 107
3.16.4 Alkali Complex-Hosted REE.. 107
3.16.5 REE-Bearing Monazite in Granitic and Metamorphic Rocks 108
3.16.6 REE Associated with the Paparoa Metamorphic Core Complex 109
3.16.7 Clay-Bearing REE 109
3.16.8 Placer REE 109
3.17 Silver (Ag)..110
3.17.1 International Description... 110
3.17.2 New Zealand Occurrences of Silver... 110
3.18 Tin (Sn)...113
3.18.1 International Description... 113
3.18.2 New Zealand Occurrences of Tin.. 113
3.18.3 Greisen Sn.. 114
3.18.4 Placer Sn 115
3.19 Titanium (Ti) 116
3.19.1 International Description... 116
3.19.2 New Zealand Occurrences of Ilmenite 116
3.19.3 Magmatic Fe-Ti-V... 117
3.19.4 By-Product Ti.. 119
3.19.5 Shoreline Placer Ti 119
3.20 Tungsten (W)..122
3.20.1 International Description... 122
3.20.2 New Zealand Occurrences of Tungsten... 122
3.20.3 Orogenic Scheelite-Bearing Quartz Veins 123
3.20.4 Greisen W-Sn 126
3.20.5 Tungsten Skarn 127
3.20.6 Stratabound W.. 128
3.21 Vanadium (V)..129
3.21.1 International Description... 129
3.21.2 Occurrence of Vanadium in New Zealand 129
3.22 Zinc (Zn) – Lead (Pb)..130
3.22.1 International Description... 130
3.22.2 New Zealand Occurrences of Zinc and Lead... 130
3.22.3 Zinc-Lead Skarn 131
3.22.4 Polymetallic Veins 132
3.22.5 Sediment-Hosted Zn-Pb... 134
3.22.6 Volcanogenic Massive Sulfide (VMS) Zn-Pb 135
3.23 Zirconium (Zr)...136
3.23.1 International Description... 136
3.23.2 New Zealand Occurrences of Zircon.. 136
3.23.3 Placer Zircon 137

4.0 ONSHORE NON-METALLIC MINERALS ... 138

4.1 Aggregate and Sand ... 138

4.1.1 Resources ... 143

4.1.2 Challenges ... 143

4.1.3 Opportunities ... 143

4.2 Barium (Ba) ... 145

4.2.1 International Description ... 145

4.2.2 New Zealand Occurrences of Barite ... 146

4.3 Building Stone ... 146

4.4 Bentonite Clay ... 147

4.4.1 International Description ... 147

4.4.2 New Zealand Occurrences of Bentonite Clay ... 147

4.5 Halloysite Clay [$Al_2SiO_5(OH)_4 \cdot nH_2O$] ... 148

4.6 Kaolinite Clay for Bricks, Pottery and Industry ... 149

4.6.1 International Description ... 149

4.6.2 New Zealand Occurrences of Kaolinite Clays ... 149

4.7 Diatomite ... 150

4.7.1 International Description ... 150

4.7.2 New Zealand Occurrences of Diatomite ... 150

4.8 Dolomite ... 151

4.8.1 International Description ... 151

4.8.2 New Zealand Occurrences of Dolomite ... 151

4.9 Feldspar ... 152

4.9.1 International Description ... 152

4.9.2 New Zealand Occurrences of Feldspar ... 152

4.10 Fluorite / Fluorspar (CaF_2) ... 153

4.10.1 International Description ... 153

4.10.2 New Zealand Occurrences of Fluorite ... 153

4.11 Garnet ... 154

4.11.1 International Description ... 154

4.11.2 New Zealand Occurrences of Garnet ... 154

4.12 Glauconite $(K,Na)(Fe,Al,Mg)_2(Si,Al)_4O_{10}(OH)_2$ ... 155

4.12.1 International Description ... 155

4.12.2 New Zealand Occurrences of Glauconite ... 155

4.13 Limestone ... 156

4.13.1 International Description ... 156

4.13.2 New Zealand Occurrences of Limestone ... 156

4.14 Magnesite ... 158

4.15 Marble ... 158

4.15.1 International Description ... 158

4.15.2 New Zealand Occurrences of Marble ... 158

4.16 Perlite ... 159

4.16.1 International Description ... 159

4.16.2 New Zealand Occurrences of Perlite ... 159

4.17 Phosphate 160
4.17.1 International Description 160
4.17.2 New Zealand Occurrences of Phosphate 160
4.18 Pounamu (Greenstone) 161
4.19 Potassium (K) – Potash (KCl, K_2O) 162
4.19.1 International Description 162
4.19.2 New Zealand Occurrences of Potash 162
4.20 Pumice 163
4.20.1 International Description 163
4.20.2 New Zealand Occurrences of Pumice 163
4.21 Salt 164
4.21.1 International Description 164
4.21.2 New Zealand Occurrences of Salt 164
4.22 Serpentinite 165
4.22.1 International Description 165
4.22.2 New Zealand Occurrences of Serpentinite 165
4.23 Silica 166
4.23.1 International Description 166
4.23.2 New Zealand Occurrences of Silica 166
4.24 Sulfur (S) 168
4.24.1 International Description 168
4.24.2 New Zealand Occurrences of Sulfur 168
4.25 Talc-Magnesite 170
4.26 Wollastonite ($CaSiO_3$) 170
4.26.1 International Description 170
4.26.2 New Zealand Occurrences of Wollastonite 170
4.27 Zeolite 171
4.27.1 International Description 171
4.27.2 New Zealand Occurrences of Zeolites 171
5.0 COAL 173
5.1 Coal Introduction 173
5.2 Coal Occurrence 173
5.2.1 North Island Coal 173
5.2.2 West Coast 173
5.2.3 Otago and Southland 174
5.3 History 175
5.4 Production 175
5.5 Usage and Consumption 177
5.6 Resources 178
5.7 Opportunities 179
5.8 Challenges 179

6.0 OFFSHORE METALLIC MINERALS.....180
6.1 Offshore Placer Gold.....180
6.1.1 Exploration.....180
6.2 Offshore Placer Titanomagnetite Ironsand.....181
6.2.1 Exploration.....182
6.2.2 Resources.....184
6.2.3 Mining Proposal.....184
6.2.4 Challenges to Mining.....184
6.2.5 Status.....184
6.3 Offshore Placer Ilmenite.....184
6.4 Offshore Volcanogenic Massive Sulfide Mineralisation.....185
6.4.1 Introduction.....185
6.4.2 Research Exploration.....186
6.4.3 Mineral Exploration.....188
6.4.4 Prospectivity Categories.....188
6.4.5 Category ‘A’ Volcanoes – High Prospectivity.....188
6.4.6 Category ‘B’ Volcanoes – Medium Prospectivity.....190
6.4.7 Category ‘C’ Volcanoes – Low Prospectivity.....190
6.4.8 Category ‘D’ Volcanoes/Regions – Prospectivity Unknown.....190
6.4.9 Research Required to Increase Prospectivity.....191
6.5 Offshore Ferromanganese Nodules.....195
6.5.1 Introduction and Overview.....195
6.5.2 Distribution.....196
6.5.3 Nodule Compositions and Economic Potential.....196
7.0 OFFSHORE NON-METALLIC MINERALS.....198
7.1 Chatham Rise Phosphorite.....198
7.1.1 Exploration.....199
7.1.2 Resources.....200
8.0 ACKNOWLEDGEMENTS.....201
9.0 REFERENCES.....201

TABLES

Table 2.1 Onshore elements, minerals and materials described in this part of the report, including relevant mineral deposit models, deposit types and New Zealand deposit examples where available......2
Table 2.2 Offshore elements, minerals and materials described in this part of the report.....6
Table 3.1 Major minerals, world production, reserves and resources and major uses of aluminium......7
Table 3.2 Features of the *Lateritic bauxite* international mineral deposit model......7
Table 3.3 Major minerals, world production, reserves and resources and major uses of antimony......9
Table 3.4 Features of the equivalent international mineral deposit models to the *Orogenic quartz vein Sb* model used in this report......10
Table 3.5 *Orogenic quartz vein Sb* model occurrences.....11

Table 3.6 *Hot spring Sb–As* model occurrences in New Zealand 12

Table 3.7 Major minerals, world production, reserves and resources and major uses of beryllium....13

Table 3.8 Major minerals, world production, reserves and resources and major uses of chromium. 14

Table 3.9 Features of the *Podiform chromite* international mineral deposit model. 16

Table 3.10 *Podiform chromite* and other chromite occurrences in New Zealand 17

Table 3.11 Major minerals, world production, reserves and resources and major uses of cobalt. 18

Table 3.12 Major minerals, world production, reserves and resources and major uses of copper. 19

Table 3.13 Deposits with recorded copper production 20

Table 3.14 Resource estimates from the literature. 21

Table 3.15 Features of the Ophiolite-hosted *VMS Cu (Cyprus type)* international mineral deposit model. 22

Table 3.16 *VMS Cu (Cyprus type)* deposits 23

Table 3.17 Features of the *VMS Cu (Besshi type)* international mineral deposit model. 24

Table 3.18 *VMS Cu (Besshi type)* deposits 24

Table 3.19 Volcanogenic massive sulfide stratiform lenses and disseminations in the Southern Alps 25

Table 3.20 Occurrences of *Serpentine-hosted Fe-Cu* model 26

Table 3.21 Features of the *Porphyry Cu* international mineral deposit model. 27

Table 3.22 *Porphyry Cu* occurrences 28

Table 3.23 Features of the *Copper skarn* international mineral deposit model. 29

Table 3.24 Copper-bearing vein, disseminated and stratiform deposits of uncertain genesis and classification 30

Table 3.25 Copper-bearing vein, disseminated and stratiform deposits of uncertain genesis and classification 32

Table 3.26 Major minerals, world production, reserves and resources and major uses of gallium. 33

Table 3.27 Major minerals, world production, reserves and resources and major uses of gold. 33

Table 3.28 New Zealand gold production 35

Table 3.29 New Zealand gold and silver production 2021 and 2022. 36

Table 3.30 Features of international mineral deposit models equivalent to the *Orogenic shear zone Au – Paleozoic* mineral deposit model. 36

Table 3.31 Estimated resources in the Reefton orogenic gold deposits. 39

Table 3.32 *Orogenic shear zone Au – Paleozoic* model occurrences in the Buller Terrane of the West Coast and Fiordland 40

Table 3.33 Features of international mineral deposit models equivalent to the *Orogenic shear zone Au – Mesozoic* mineral deposit model. 42

Table 3.34 Joint Ore Reserves Committee (JORC)-compliant Reserve (0.6 Moz Au) and Resource (Moz) estimates for Macraes 31 December 2023 44

Table 3.35 *Orogenic shear zone Au – Mesozoic* model occurrences in the Haast Schist and Mesozoic greywacke 45

Table 3.36 Features of international mineral deposit models equivalent to the *Low-sulfidation epithermal Au–Ag* mineral deposit model. 48

Table 3.37 Resource estimates for *Low-sulfidation epithermal Au–Ag* deposits of the Hauraki Goldfield. 54

Table 3.38 *Low-sulfidation epithermal Au–Ag* model occurrences 55

Table 3.39 Features of the *Intermediate-sulfidation epithermal vein Zn-Pb-Cu-Ag-Au* international mineral deposit model. 60

Table 3.40 *Intermediate-sulfidation epithermal Zn Pb-Cu-Ag-Au* occurrences 61

Table 3.41 Features of international mineral deposit models equivalent to the *High-sulfidation epithermal Au–Ag* model used in this report. 62

Table 3.42 Features of international mineral deposit models equivalent to the *Reduced-granitic intrusion-related Au* model used in this report. 63

Table 3.43 Features of the *Alkali intrusion-related Au* international mineral deposit model. 64

Table 3.44 Features of international mineral deposit models equivalent to the *Sediment (carbonate)-hosted Au–Ag (Carlin type)* model used in this report. 66

Table 3.45 Features of the *Gold skarn* international mineral deposit model. 67

Table 3.46 Features of the *Detachment fault-related polymetallic deposits* international mineral deposit model. 68

Table 3.47 Features of international mineral deposit models equivalent to the *Placer Au, onshore, beach and offshore* model used in this report. 69

Table 3.48 Major minerals, world production, reserves and resources and major uses of iron. 71

Table 3.49 Features of international mineral deposit models equivalent to the *Shoreline placer Fe* model used in this report. 72

Table 3.50 Resource estimates for titanomagnetite ironsand resources. 75

Table 3.51 Ironsand resources, west coast, North Island. 75

Table 3.52 *Bog Fe* deposit model occurrences 77

Table 3.53 Iron occurrences additional to the titanomagnetite and *Bog Fe* and *Transported Residual Fe* deposits 78

Table 3.54 Major minerals, world production, reserves and resources and major uses of lithium. 78

Table 3.55 Features of the *Li pegmatites* mineral deposit model. 79

Table 3.56 Major minerals, world production, reserves and resources and major uses of magnesium 81

Table 3.57 Major minerals, world production, reserves and resources and major uses of manganese. 83

Table 3.58 Features of the *Volcanogenic Mn* international mineral deposit model. 84

Table 3.59 *Volcanogenic Mn* model occurrences 85

Table 3.60 Major minerals, world production, reserves and resources and major uses of molybdenum 87

Table 3.61 Features of the *Porphyry Mo* international mineral deposit model 88

Table 3.62 *Porphyry Mo* occurrences 89

Table 3.63 Major minerals, world production, reserves and resources and major uses of nickel. 90

Table 3.64 Features of international mineral deposit models equivalent to the *Dunitic Ni-Cu* model used in this report. 93

Table 3.65 Features of the *Gabbroid-associated Ni-Cu* international mineral deposit model. 94

Table 3.66 *Gabbroid-associated Ni-Cu* model occurrences 95

Table 3.67 Features of the *Lateritic Ni* international mineral deposit model. 95

Table 3.68 Major minerals, world production, reserves and resources and major uses for platinum group metals. 96

Table 3.69 Features of international mineral deposit models relevant to the *Magmatic PGM* model and *Alaskan-type* sub-model used in this report. 97

Table 3.70 Prospects explored for *Magmatic PGM* 98

Table 3.71 Prospect explored for *Dunitic PGM* 100

Table 3.72 Features of international mineral deposit models equivalent to the *Placer PGM* model used in this report. 101

Table 3.73 *Placer PGM* model occurrences 103

Table 3.74 Major elements, ore minerals, world production, reserves and resources and major uses of rare earth elements, as well as associates scandium, yttrium and thorium. 104

Table 3.75 Features of international mineral deposit models equivalent to the *Carbonatite-hosted REE* model used in this report. 107

Table 3.76 Features of international mineral deposit models equivalent to the *REE-bearing monazite in granitic and metamorphic rocks* model used in this report. 108
Table 3.77 Major minerals, world production, reserves and resources and major uses for silver. 110
Table 3.78 Silver occurrences 112
Table 3.79 Major minerals, world production, reserves and resources and major uses for tin. 113
Table 3.80 Features of international mineral deposit models equivalent to the *Greisen Sn* model used in this report. 114
Table 3.81 *Greisen Sn* model occurrence 114
Table 3.82 Features of international mineral deposit models equivalent to the *Placer Sn* model used in this report. 115
Table 3.83 Major minerals, world production, reserves and resources and major uses for titanium. 116
Table 3.84 Features of international mineral deposit models equivalent to the *Magmatic Fe-Ti-V* deposit model used in this report. 117
Table 3.85 *Magmatic Fe-Ti-V* model occurrences 118
Table 3.86 Features of the *Shoreline placer Ti* international mineral deposit model. 119
Table 3.87 *Shoreline placer Ti* model occurrences in the eastern Coromandel Peninsula, North Island 119
Table 3.88 South Island shoreline placer titanium ilmenite resources 120
Table 3.89 Major minerals, world production, reserves and resources and major uses for tungsten. 122
Table 3.90 *Vein Ti* model occurrences 124
Table 3.91 Prospective resources at Glenorchy calculated from a GIS compilation of historic data 125
Table 3.92 Features of international mineral deposit models equivalent to the *Greisen W-Sn* model used in this report. 126
Table 3.93 *Greisen W-Sn* model occurrences 126
Table 3.94 Features of international mineral deposit models equivalent to the *Tungsten skarn* model used in this report. 127
Table 3.95 Features of international mineral deposit models equivalent to the *Stratabound W* model used in this report. 128
Table 3.96 Major minerals, world production, reserves and resources and major uses for vanadium. 129
Table 3.97 Major minerals, world production, reserves and resources and major uses for lead and zinc. 130
Table 3.98 Features of the *Zinc-lead skarn* international mineral deposit model. 131
Table 3.99 Features of the *Polymetallic veins* international mineral deposit model. 132
Table 3.100 *Polymetallic vein* model occurrences 133
Table 3.101 Features of international mineral deposit models equivalent to the *Sediment-hosted Zn-Pb* model used in this report. 134
Table 3.102 Occurrence of *Sediment-hosted Zn-Pb* deposits 134
Table 3.103 Features of international mineral deposit models equivalent to the *VMS Zn-Pb* deposits model used in this report. 135
Table 3.104 Major minerals, world production, reserves and resources and major uses for zirconium. 136
Table 3.105 Features of international mineral deposit models equivalent to the *Placer zircon* model used in this report. 137
Table 4.1 Size of aggregate operations 141
Table 4.2 World production, reserves and resources and major uses of barite 145
Table 4.3 World production, reserves and resources and major uses of bentonite clay. 147
Table 4.4 World production, reserves and resources and major uses of kaolinite clay. 149
Table 4.5 World mine production, reserves and resources and major uses of diatomite. 150
Table 4.6 World mine production, reserves and resources and major uses of dolomite. 151

Table 4.7 Major minerals, world production, reserves and resources and major uses of feldspar. 152
Table 4.8 World mine production, reserves and resources and major uses of fluorspar. 153
Table 4.9 World mine production, reserves and resources and major uses of garnet. 154
Table 4.10 World production, reserves and resources and major uses of limestone. 156
Table 4.11 World production, reserves and resources and major uses of marble. 158
Table 4.12 World mine production, reserves and resources and major uses of perlite. 159
Table 4.13 World mine production, reserves and resources and major uses of phosphate. 160
Table 4.14 World production, reserves and resources and major uses of potash. 162
Table 4.15 World production, reserves and resources and major uses of pumice. 163
Table 4.16 World mine production, reserves and resources and major uses of salt. 164
Table 4.17 World production, reserves and resources and major uses of serpentinite. 165
Table 4.18 Element properties, major minerals, world production, reserves and resources and major uses of silicon/silica. 166
Table 4.19 Element properties, major minerals, world production, reserves and resources and major uses of sulfur. 168
Table 4.20 Sulfur occurrences 169
Table 4.21 World production, reserves and resources and major uses of wollastonite. 170
Table 4.22 Major minerals, world production, reserves and resources and major uses of zeolite. 171
Table 5.1 Operating coal mines at the end of 2022 176
Table 5.2 Coal production by rank and region for 2023 176
Table 6.1 Kermadec arc volcano inventory and prospectivity rank 193
Table 6.2 Mean concentrations of selected elements in nodules from the northeast part of the Campbell field and four other fields in the Pacific and Indian Oceans 197
Table 7.1 Trace element abundances in Chatham Rise sediments, phosphorite nodules and glauconite-rich sands 198
Table 7.2 Exploration and sampling surveys of the Chatham Rise phosphorite 200
Table 7.3 Statement of Mineral Resources (phosphorite) for Mining Permit 55549, Chatham Rise 200

FIGURES

Figure 3.1 Location of lateritic bauxite deposits in Northland and the Tiwai Point smelter in Southland 8
Figure 3.2 Location of antimony (stibnite) deposits in New Zealand 9
Figure 3.3 Location of beryllium deposits in New Zealand 14
Figure 3.4 Location of chromite deposits in New Zealand 15
Figure 3.5 Location of copper deposits 20
Figure 3.6 Locations of main volcanogenic massive sulfide copper deposits 22
Figure 3.7 Main areas of past gold mining and potential for future discoveries 34
Figure 3.8 Location of Paleozoic orogenic gold deposits, groups and their historic gold production up to 1952; geology of the Reefton Goldfield 38
Figure 3.9 *Orogenic shear zone Au – Paleozoic* mineralisation prospectivity map 39
Figure 3.10 Drilling on the Bendigo-Ophir prospect on the Rise & Shine Shear Zone 43
Figure 3.11 *Orogenic shear zone Au – Mesozoic* mineralisation results 44
Figure 3.12 Location of epithermal gold deposits, North Island. 49
Figure 3.13 Geology and location of epithermal Au–Ag mines and prospects in the Coromandel Volcanic Zone – Hauraki Goldfield 50

Figure 3.14 Relative size of past Au–Ag production, Au:Ag ratios and dominant vein orientation of epithermal Au–Ag deposits of the Hauraki Goldfield 51
Figure 3.15 Geology and location of epithermal Au–Ag prospects and geothermal fields in the Taupō Volcanic Zone....52
Figure 3.16 Geology and location of epithermal Au–Ag deposits and prospects in Northland 53
Figure 3.17 Prospectivity map for epithermal gold-silver deposits in the Coromandel Peninsula, Hauraki Goldfield 59
Figure 3.18 Diagrammatic cross-section through the metamorphic core complex in the Paparoa Range....68
Figure 3.19 Nearly all of the alluvial gold produced in New Zealand has been from the South Island 70
Figure 3.20 Location of iron deposits in New Zealand....72
Figure 3.21 Distribution of ironsand deposits and volcanic-source rocks along the west coast of the North Island 74
Figure 3.22 Prospectivity maps for hydrothermally altered rhyolitic lacustrine sediment-hosted lithium potential in the Taupō Volcanic Zone using a mineral systems approach 80
Figure 3.23 Location of magnesite (and talc) deposits in New Zealand 82
Figure 3.24 Location of manganese deposits (*Volcanogenic Mn*) in New Zealand 83
Figure 3.25 Location of molybdenum deposits in New Zealand 87
Figure 3.26 Location of nickel deposits in New Zealand....91
Figure 3.27 Location of mapped, ultramafic and mafic geology that could potentially host magmatic nickel and cobalt deposits in New Zealand....92
Figure 3.28 Location of platinum group metal occurrences 96
Figure 3.29 Geology of the Longwood Complex and environs, Southland 99
Figure 3.30 Location of the Median Batholith. 100
Figure 3.31 Location of the Dun Mountain Ophiolite Belt and prospects explored during the 1980s....101
Figure 3.32 Locations of detrital platinum group metals and *Placer PGM* where known 102
Figure 3.33 Location of rare earth element occurrences in New Zealand 105
Figure 3.34 The location of plutonic rocks and lithologies with rare earth element potential in New Zealand 106
Figure 3.35 Location of silver deposits in New Zealand 111
Figure 3.36 Location of tin occurrences in New Zealand....113
Figure 3.37 Location of titanium deposits in New Zealand 116
Figure 3.38 Mount George Gabbro of Cretaceous age at Mount George....118
Figure 3.39 Location of tungsten occurrences in New Zealand....122
Figure 3.40 Location of lead and zinc deposits in New Zealand....131
Figure 3.41 Location of zirconium deposits in New Zealand 136
Figure 4.1 New Zealand aggregate production statistics....138
Figure 4.2 Examples of extractive quarrying activity in New Zealand....139
Figure 4.3 Aggregate processing plant at Belmont quarry in Lower Hutt....140
Figure 4.4 Aggregate rock is crushed and screend to make various-sized products.....140
Figure 4.5 The occurrence of main aggregate source rocks in New Zealand....141
Figure 4.6 Profile of the construction materials in a road....142
Figure 4.7 Stabilisation of road aggregate to bond particles....142
Figure 4.8 Maps of the aggregate opportunity hard-rock model for the North Island and South Island....144
Figure 4.9 Maps of the aggregate opportunity gravel model for the North Island and South Island 145
Figure 4.10 Location of selected clay deposits in New Zealand 148

Figure 4.11 Locations of limestone, marble and dolomite deposits 157

Figure 4.12 Pounamu resources of New Zealand 161

Figure 4.13 Location of zeolite deposits in New Zealand 172

Figure 5.1 Coal regions and coalfields of the North Island and South Island, including small coal deposits for the latter 174

Figure 5.2 Coal consumption by sector for 2023 177

Figure 5.3 Coal consumption (PJ) by sector for 1992–2023....178

Figure 5.4 Share of total electricity generation by source, from 1990 to 2022 178

Figure 6.1 Schematic depiction of West Coast Late Pleistocene glaciers, terminal moraines and outwash systems 181

Figure 6.2 Past New Zealand sea levels 182

Figure 6.3 Mineral permits for offshore ironsand exploration in 2005, 2009 and August 2016 183

Figure 6.4 Area of Pacific Offshore Mining’s prospecting permit 52474 to explore for ilmenite sands offshore of Waihi Beach in the Coromandel Peninsula 185

Figure 6.5 Schematic model of Kermadec arc petrogenesis 186

Figure 6.6 Brothers volcano chimneys *in situ* 187

Figure 6.7 Recommended stages of exploration for seafloor massive sulfide deposits on the Kermadec Arc 191

Figure 6.8 Discoidal shaped ferromanganese nodule from site U1413-1 195

Figure 6.9 Schematic showing formation of hydrogenetic nodules via precipitation from seawater on the ocean floor, as well as diagenetic nodules via precipitation from pore fluids below the sediment-seawater interface 196

1.0 INTRODUCTION

This Part 2 of the report describes occurrences of mineral deposits and resources in more detail than Part 1. The descriptions are ordered under the element, mineral or material name, and many include sections of mineral deposit types for that element, mineral or material. Mineral sites are assigned identification codes from the Geological Resource Map (GERM) database and 1:1 million metallogenic map (MM) of Brathwaite and Pirajno (1993), where these are available. All mineral commodities described in Part 1 (Christie et al. 2024) are expanded on in Part 2, apart from offshore sand and glauconite, which are only included in Part 1.

2.0 MINERAL DEPOSIT MODELS

Mineral deposit models (e.g. Cox and Singer 1986; Kirkham et al. 1993; Eckstrand et al. 1995; Lefebure and Ray 1995; Lefebure and Höy 1996) describe the essential geological and geochemical attributes that are common to a number of similar mineral deposits that are presumed to have been formed by the same genetic process. The main attributes used in classifying a mineral deposit type are: tectonic setting, structural controls, host-rock lithology, form of the deposit, main economic elements or minerals, mineralogy of ore and host rocks and geochemical and geophysical characteristics. Mineral deposit models used in this report are listed in Table 2.1 (onshore elements, minerals and materials) and drawn mainly from international models assembled by the United States Geological Survey (USGS) and British Columbia Geological Survey (BCGS). Additionally, offshore mineral deposit types are listed in Table 2.2.

Deposit models are linked to grade-tonnage models, which show the range of grade and tonnage of different deposits of a specific type and derive statistical parameters such as the average grade and tonnage (Cox and Singer 1986). Grade-tonnage models are compiled from pre-mining resource estimates or from production figures for mined-out deposits. These figures vary according to mining conditions (e.g. mining method used) and economic factors (e.g. metal prices). For many of the models, the data are drawn from historic mining of higher grades and smaller volumes than are sought or mined at present.

Table 2.1 Onshore elements, minerals and materials described in this part of the report, including relevant mineral deposit models (in italics), deposit types and New Zealand deposit examples where available.

Element or Mineral	**Mineral Deposit Model or Type**	**Examples**
Metallic Minerals		
Aluminium (Al)	*Lateritic bauxite*	Kerikeri-Kaikohe-Kaeo, Northland
Antimony (Sb)	*Orogenic quartz vein Sb*	Endeavour Inlet, Marlborough
	Hot spring Sb–As	Rangitarore Hill (Lanigan’s Mine), Northland
Beryllium (Be)	*Be pegmatite*	Charleston, West Coast
Chromium (Cr)	*Podiform Cr*	Dun Mountain, East Nelson
Cobalt (Co)	By-product Co	
Copper (Cu)	*Volcanogenic massive sulfide (VMS) Cu*, sub-models:	
	• *VMS Cu (Cyprus type)*	Pakotai, Northland
	• *VMS Cu (Besshi type)*	Kawau Island, North Auckland
	• VMS lenses in the Pounamu Ultramafics	Wilberg Range
	Serpentine-hosted Fe–Cu	United Mine, Dun Mountain, East Nelson
	Porphyry Cu	Ohio Creek, north Thames, Coromandel Peninsula
	Copper skarn	Copperstain Creek, near Takaka, West Nelson
	Hydrothermal quartz and sulfide vein Cu of uncertain origin	Baton River, West Nelson
	Dissemination and stratiform concentrations in metamorphic rocks of Fiordland and Rakiura / Stewart Island	Mt Solitary, Fiordland

Element or Mineral	**Mineral Deposit Model or Type**	**Examples**
Gallium (Ga)	Geothermal gallium	Geothermal fields of the Taupō Volcanic Zone
Gold (Au)	Orogenic shear zone Au, sub-models:	
	• *Orogenic shear zone Au – Paleozoic*	Blackwater (Snowy River project), Reefton, West Coast
	• *Orogenic shear zone Au – Mesozoic*	Steep vein type: Bendigo field, Otago Thrust shear zone type: Macraes, Otago
	Epithermal Au, sub-models:	
	• *Low-sulfidation epithermal Au–Ag*	Waihi, Coromandel Peninsula
	• *Intermediate-sulfidation epithermal Zn-Pb-Cu-Ag-Au*	Tui, Coromandel Peninsula
	• *High-sulfidation epithermal Au–Ag*	Lookout Rocks, Coromandel Peninsula
	Reduced-granitic intrusion-related Au	None (potential on the West Coast)
	Alkali intrusion-related Au	Sams Creek, West Nelson
	Gabbroid-associated Au-Ni-Cu	Arethusa, Longwood Range, Southland
	Sediment (carbonate)-hosted (Carlin) type	None (potential in Northland)
	Gold skarn	None (potential in West Nelson)
	Detachment-fault-related polymetallic deposits	None (potential on the West Coast)
	Placer Au, sub-models:	
	• *Alluvial placer Au*	Ross, West Coast and Clutha River, Otago
	• *Beach placer Au*	Addisons Flat, Hou Hou Lead and Lamplough Lead, West Coast
	• *Marine place Au*	Harvester project, West Coast
Iron (Fe)	*Shoreline placer Fe*	Waikato North Head, South Auckland
	Bog Fe	Okaihau, Northland
	Transported residual Fe	Onekaka, West Nelson
Lithium (Li)	*Li pegmatites* (LCT [Lithium-Caesium-Tantalum] pegmatites)	None (potential in West Coast pegmatites)
	Li-bearing hydrothermal clays and lacustrine sediments	None (potential in the Taupō Volcanic Zone)
Magnesium (Mg)	Ultramafic-hosted *Talc-magnesite*	Cobb, West Nelson
Manganese (Mn)	*Volcanogenic Mn*	Parua Bay, Northland
Molybdenum (Mo)	*Porphyry Mo*	Taipo, West Nelson
Nickel (Ni)	*Dunitic Ni-Cu*	Red Hill Range, South Westland
	Gabbroid-associated Ni-Cu	Riwaka, West Nelson
	Lateritic Ni	Surville Cliffs, Northland
Platinum Group Metals (PGM)	*Magmatic PGM*	Longwood Range, Southland
	Dunitic PGM – Dun Mountain Ophiolite Belt	Mount Baldy, Matakitaki, south Nelson
	Placer PGM	Round Hill, Southland

Element or Mineral	**Mineral Deposit Model or Type**	**Examples**
Rare Earth Elements (REE)	*Carbonatite-hosted REE*	None (potential in the Alpine Dike Swarm, Westland)
	Alkali complex-hosted REE	French Creek Granite, Westland
	REE-bearing monazite in granitic and metamorphic rocks	None (potential in Foulwind and French Creek granites, West Coast)
	REE associated with the Paparoa metamorphic core complex	Paparoa Range, West Coast
	Clay-bearing REE	None (potential in Northland clays)
	Placer REE	By-product in West Coast ilmenite sand deposits
Silver (Ag)	*Epithermal Au–Ag*	Maratoto, Coromandel Peninsula
Tin (Sn)	*Greisen Sn*	Tin Range, Rakiura / Stewart Island
	Placer Sn	Tin Range, Rakiura / Stewart Island
Titanium (Ti)	*Magmatic Fe-Ti-V*	Mt George, Fiordland
	By-product Ti (in titanomagnetite ironsand)	Waikato North Head, South Auckland
	Shoreline placer Ti	Barrytown, West Coast
Tungsten (W)	*Vein W* (orogenic scheelite-bearing quartz veins)	Glenorchy, Otago
	Greisen W-Sn	Bateman Creek, West Coast
	Tungsten skarn	None
	Stratabound W	Lake Stanley, West Nelson
Vanadium (V)	By-product V (in titanomagnetite ironsand)	Waikato North Head, South Auckland
Zinc-lead (Zn-Pb)	*Zinc-Lead skarn*	Motukokaka (Piercy) Island, Northland
	Polymetallic veins	Richmond Hill, West Nelson
	Sediment-hosted Zn-Pb	Mt Irene, Fiordland
	Volcanic massive sulfide Zn-Pb	Johnston’s United, West Nelson
Zirconium (Zr)	*Placer Zr* (by-product in ilmenite sand)	Orepuke, Southland
Non-Metallic Minerals and Rocks		
Aggregate and sand	Hard-rock sources	Hunua and Drury quarries
	River-gravel sources	Manawatu, Waimakariri and Oreti rivers
Barite (Ba)	Vein barite	Thomson Hill, West Nelson
Bentonite clay	Freshwater bentonite	Coalgate, Canterbury
	Marine bentonite	Mangatu, East Coast, North Island
Halloysite clay	Halloysite clay from weathered rhyolite	Matauri Bay, Northland
Kaolinite clay	Kaolinite from surface weathering of clay-rich rocks	Port Waikato, South Auckland
	Kaolinite from acid leaching of mudstone – coal-measure clay	Malvern Hills
	Kaolinite from hydrothermal alteration of rhyolite	Hahei, Coromandel Peninsula, Waikato

Element or Mineral	**Mineral Deposit Model or Type**	**Examples**
Diatomite	Freshwater diatomite	Mercer
	Marine diatomite	Oamaru
Dolomite	Dolomitisation of limestone and marble	Mt Burnett, West Nelson
Feldspar	Feldspar in pegmatites	Charleston,
	Feldspar – weathered granite	Motueka area, West Nelson
	Feldspar-rich sand	Ruakaka, Northland
Fluorine (F) / fluorspar	*Vein F*	Thomson Hill, West Nelson
Garnet	*Placer garnet*	Westport
Glauconite	Marine greensand glauconite	Otaka, East Cape
Magnesite	*Talc-magnesite*	Cobb Valley, West Nelson
Marble	-	Ngarua, Takaka Hill, West Nelson
Limestone	-	Te Kūiti, Waikato
Perlite	Perlitic rhyolite	Maungati Dome, Atiamuri
Phosphate	Marine phosphate	Clarendon, Otago
Pounamu	-	Arahura River, Westland
Potassium (K) / potash	Weathered feldspar	Separation Point Granite, West Nelson
	Glauconite	Otaka, East Cape
Pumice	Alluvial pumice	Atiamuri
Salt (NaCl)	Evaporite salt	Lake Grassmere, Marlborough
Serpentinite	Ultramafic serpentinite	Mossburn, Southland
Silica (SiO_2)	Silica sand	Parengarenga, Northland
	Silica gravel	Pebbly Hills, Southland
	Amorphous silica	Tikitere, Rotorua
Sulfur (S)	Volcanogenic S	Lake Rotokawa, Waikato
	Hydrothermal pyrite S	Copperstain Creek, West Nelson
Talc-magnesite	Ultramafic-hosted *Talc-magnesite*	Cobb Valley, Northwest Nelson
Wollastonite	-	Holyoake Valley, West Nelson
Zeolite	Hydrothermal zeolite	Ngakuru, Waikao
	Metamorphic zeolite	Taringatura Hills, Southland
Coal		
Coal	Bituminous	Stockton, Buller, West Coast
	Sub-bituminous	Rotowaro, Waikato
	Lignite	New Vale, Waimumu, Southland

Table 2.2 Offshore elements, minerals and materials described in this part of the report, including relevant deposit models and New Zealand deposit examples where available.

Element or Mineral	Mineral Deposit Type	Examples
Metallic Minerals		
Copper (± zinc, ± lead, ± silver, ± gold)	Volcanogenic massive sulphide	Brothers volcano, Kemadec Arc
Iron (titanomagnetite)	Placer titanomagnetite	Offshore Pātea, Taranaki
Gold	Marine placer Au	Harvester project, West Coast
Manganese	Ferromanganese nodules	Campbell Plateau
Titanium (ilmenite)	Placer ilmenite	Offshore Waihi Beach
Non-Metallic Minerals and Materials		
Potassium (glauconite) (see Part 1)	Marine glauconite	Chatham Rise
Phosphate	Phosphorite nodules	Chatham Rise
Sand (see Part 1)	Marine sand	Kaipara Harbour, Northland and North Auckland

3.0 ONSHORE METALLIC MINERALS

3.1 Aluminium (Al)

3.1.1 International Description

International data for aluminium are listed in Table 3.1.

Table 3.1 Major minerals, world production, reserves and resources and major uses of aluminium.

Aluminium (Al)		
International	**Ore Minerals**: Bauxite – a mixture of oxide minerals, principally gibbsite $Al(OH)_3$ and boehmite AlO(OH) but also may have andalusite Al_2SiO_5, and alunite $Kal_3(SO_4)_2(OH)_6$	
	World production (2023) (USGS 2024)	400 Mt of bauxite ore; 142 Mt of alumina (Al_2O_3)
	Major world bauxite producers (% of average total 2022)	Australia (26%), China (24%), Guinea (23%), Brazil (9%), Indonesia (6%), India (4%), Russia (1%), Saudi Arabia (1%), Kazakhstan (1%), Vietnam (1%)
	World reserves (USGS 2024)	30 Bt of bauxite
	World resources (USGS 2024)	55–75 Bt
	Uses: Aluminium metal and alloys are used in transportation (e.g. manufacture of automobiles, aircraft, railway carriages, marine vessels and bicycles), building and construction (e.g. windows frames, doors, sheathing, roofing), packaging (e.g. cans, foil and frame), electricity-related items (e.g. conductor alloys, motors and transformers) and house-hold items (e.g. cooking utensils, furniture).	

3.1.2 Lateritic Bauxite

3.1.2.1 International Mineral Deposit Model

Features of the *Lateritic bauxite* international mineral deposit model are listed in Table 3.2.

Table 3.2 Features of the *Lateritic bauxite* international mineral deposit model.

International Mineral Deposit Model – *Lateritic Bauxite*	
Reference	USGS model 38b Laterite-type bauxite (Cox and Singer 1986)
Description	Bauxite is residual material in subsoil formed by weathering of aluminous silicate rocks under tropical or semi-tropical conditions. It consists mainly of gibbsite or a mixture of gibbsite and boehmite in a gangue mineral assemblage of hematite, goethite, anatase and, locally, quartz. Ore textures are pisolitic, massive, earthy and nodular. A typical bauxite contains 35–65% Al_2O_3, 2–10% SiO_2, 2–10% Fe_2O_3, 1–3% TiO_2 and 10–30% combined water. For aluminium ore, bauxite should contain preferably at least 35% Al_2O_3 and less than 5% SiO_2, 6% Fe_2O_3 and 3% TiO_2.
International Examples	Jamaica; Surinam; Weipa, Jarrahdale, Coore and Mitchell Plateau (Australia); Georgia–Alabama (USA)
Grade-Tonnage Model	USGS model 38b 50th percentile = 25 Mt at 45% Al_2O_3 (Cox and Singer 1986).

3.1.2.2 New Zealand Occurrences of Lateritic Bauxite *Deposits*

Bauxite deposits are found in Northland, within a triangular area between Kerikeri, Kaikohe, and Kaeo (MM I5; GERM P04/e18, 19, 26, 41, 42, 43) (Figure 3.1). Late Miocene to Early Pleistocene Kerikeri Basalt has been extensively altered to halloysite, and, where rainfall and leaching has been sufficient, gibbsite (bauxite) has been produced from the halloysite-altered material (Carr et al. 1980). At Otoroa (Matauri Bay area), where the largest resources are known, the average thickness of the gibbsite-rich profiles is between 3 and 4.6 m and the maximum thickness is 12 m.

Prospecting and research by DSIR (Department of Scientific and Industrial Research) resulted in a resource estimate for the Otoroa area of 20 Mt of bauxite, typically grading 37.4% Al_2O_3 (equivalent to 30.6% extractable alumina), 5.5% SiO_2, 23.3% Fe_2O_3, 2.3% FeO and 6.4% TiO_2 (Kear et al. 1961). Additional auger drilling by Comalco / Consolidated Zinc (Evans 1963) and, later, Magellan (Pearson 1973), confirmed the DSIR resource estimate of the Otoroa deposit and identified another 15 small deposits nearby, collectively containing about 9.25 Mt of bauxite with 30% alumina or better. The largest of these deposits contained about 2.4 Mt.

Figure 3.1 Location of lateritic bauxite deposits in Northland and the Tiwai Point smelter in Southland, where aluminium is produced by electrolytic smelting alumina imported from Queensland, Australia (after Christie et al. [1993]).

Previously estimated resources for the Kerikeri-Kaikohe-Kaeo area are 30 Mt of bauxite at 30% Al_2O_3 (alumina). Beneficiation tests showed that the Otoroa bauxite could be upgraded from 30% extractable alumina to approximately 44% by wet screening, but this increase in grade was coupled with a more than 40% reduction in the tonnage of the alumina resource to about 8 Mt Al_2O_3. The area of this resource is only a very small part of the total area of young basalt, therefore there is likely to be some additional potential.

Aluminium is currently produced at the Tiwai Point aluminium smelter, with bauxite ore imported from Queensland, Australia.

Key References: Kear et al. (1961); Brathwaite and Pirajno (1993); Christie et al. (1993); Christie and Barker (2007).

3.2 Antimony (Sb)

3.2.1 International Description

International data for antimony are listed in Table 3.3.

Table 3.3 Major minerals, world production, reserves and resources and major uses of antimony.

Antimony (Sb)		
International	**Ore Minerals:** Stibnite Sb_2S_3	
	World production	83,000 t in 2023, but a high of 178,000 t in 2011
	Major world producers (% of average total 2022)	China (55%), Russia (18%), Tajikistan (15%), Australia (2%), Burma (2%), Bolivia (2%), Turkey (1%), Mexico (1%)
	Uses: Antimony is used as a fire retardant in construction and defence applications and as an alloying agent in lead-acid batteries and small arms munitions.	

3.2.2 Antimony in New Zealand

The antimony mineral stibnite (Sb_2S_3) occurs principally in association with orogenic gold-bearing quartz veins in greywacke in Westland and in schist in Marlborough and Otago (*Orogenic quartz vein Sb*, see Section 3.2.3) (Figure 3.2). Other occurrences include those in quartz veins in Mesozoic greywacke in Northland (Rangitarore Hill or Lanigan's Mine, Waikare Inlet) and in epithermal quartz veins and sinters associated with late Cenozoic volcanism in Northland (Puhipuhi, Ngawha), Coromandel Peninsula (e.g. Te Ahumata, Mahakirau and Thames), and the Taupō Volcanic Zone (Hot Spring Sb, see Section 3.2.4).

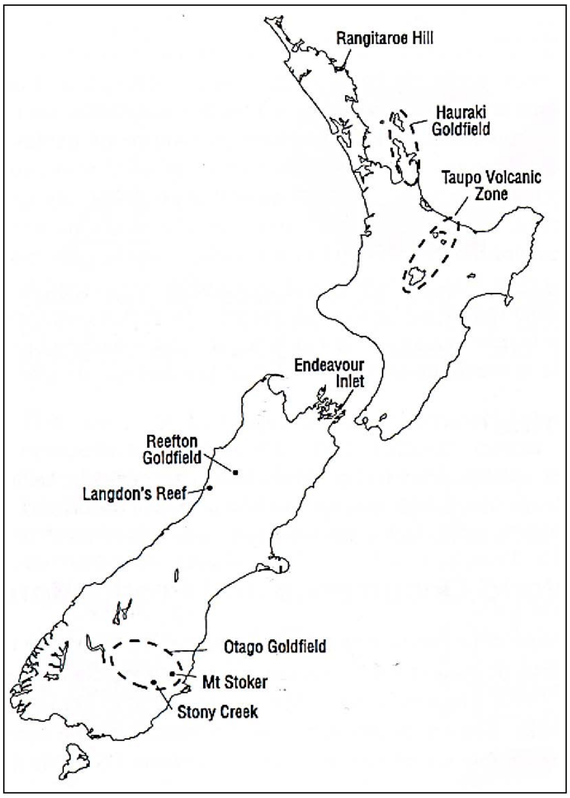

Figure 3.2 Location of antimony (stibnite) deposits in New Zealand (after Christie and Brathwaite [1993]).

Key References: Williams (1974); Pirajno (1979); Brathwaite and Pirajno (1993); Christie and Brathwaite (1993); Price (2016).

3.2.3 Orogenic Quartz Vein Sb

3.2.3.1 International Mineral Deposit Model

Features of the *Orogenic quartz vein Sb* mineral deposit model are listed in Table 3.4.

Table 3.4 Features of the equivalent international mineral deposit models to the *Orogenic quartz vein Sb* model used in this report.

International Mineral Deposit Model – Simple Sb Deposits; Stibnite Veins and Disseminations	
Reference	USGS model 27d Simple Sb deposits (Cox and Singer 1986); BCGS model I09 Stibnite veins and disseminations (Lefebure and Höy 1996)
Description	Stibnite veins, pods and disseminations in or adjacent to brecciated or sheared fault zones
International Examples	Amphoe Phra Saeng (Thailand); Caracota (Bolivia); Coimadai, Victoria (Australia); Last Chance, Nevada (USA); Lake George, New Brunswick (Canada)
Grade-Tonnage Model	USGS model 27d 50th percentile = 180 t at 35% Sb

3.2.3.2 New Zealand Occurrences of Orogenic Quartz Vein Sb *Deposits*

Stibnite occurs in orogenic gold-bearing quartz lodes in lower Paleozoic-age greywacke in Westland (Reefton Goldfield and at Langdons and Croesus Knob reefs in the Paparoa Range), and in schist in Marlborough (Endeavour Inlet) and Otago (Hindon, Waipori, Carrick and Nenthorn) (Table 3.5). Some quartz lodes in Reefton are particularly rich in stibnite where it was reported from mines at Blackwater, Globe Hill, Crushington, Capleston-Specimen Hill, Big River, Ajax, Murray Creek, Blacks Point-Painkiller, Merrijigs and Alexander River. Mineralisation in the Murray Creek area was especially antimony-rich, with up to 7% reported in ore concentrates by Henderson (1917) and abundant stibnite reported from the Golden Treasure lode by Downey (1928) and Suggate (1957). A discrete antimony-bearing lode, the Bonanza lode, was described from Aulds Creek by McKay (1883). Williams (1974) noted that, at the Blackwater mine, a discrete stibnite lode was found in the country rock not far from the main lode. Reconnaissance geochemical exploration for antimony in the Reefton Goldfield (Riley and Ball 1971, 1972a, 1972b; Viljoen 1972) highlighted several potential targets where new resources might be found.

A total of 3900 t of antimony ore has been produced, of which 3000 t was from Endeavour Inlet (late 1800s). Antimony could be produced as a by-product of mining some orogenic gold deposits. Siren Gold is currently exploring for antimony at Auld Creek and other Reefton gold deposits.

Resources at Endeavour Inlet (MM C30; GERM P26/e34–37) have been estimated at 25,000 t at 15% Sb (3750 t Sb). Other known antimony deposits are small.

Table 3.5 *Orogenic quartz vein Sb* model occurrences (data modified after Brathwaite and Pirajno [1993]). Minerals: Au = gold; Sb = antimony, W = tungsten, As = native arsenic; aspy = arsenopyrite, Ci sulf = bismuth sulfides; gn = galena; py = pyrite, sch = scheelite; sp = sphalerite.

Region	**Occurrence**	**MM** [1]	**GERM** [2]	**Production (t)**	**Deposit Form**	**Minerals Major (minor)**	**Host Rocks**
Marlborough	Endeavour Inlet	C30	P26/e34–37	~1000 Sb ore	Sb-Au-quartz veins	sb,(aspy, py, gold)	Quartzofeldspathic chlorite schist
	Jacksons Head	-	Q26/e2	-	Sb-quartz veins	-	Chlorite schist
	Resolution Bay	-	Q27/e1	-	Sb-quartz veins	-	Chlorite schist
West Coast	Murray Creek group	A62	L30/e215	1.234 Au	Au quartz veins	py, sb, aspy, gold	Greywacke, argillite
	Ajax group	A63	-	3.007 Au	Au quartz veins	py, aspy, sb, gold	Greywacke, argillite
	Blacks Point-Painkiller group	A64	-	0.221 Au	Au quartz veins	py, aspy, sb, gold	Greywacke, argillite
	Crushington group	A65	-	12.635 Au	Au quartz veins	py, aspy, sb, gold	Greywacke, argillite
	Globe Hill Group	A68	L30/e235 (Globe Progress mine)	13.198 Au (historic)	Au quartz veins	py, aspy, sb, gold	Greywacke, argillite
	Big River group	A70	L31/e34 (Big River mine)	3.841 Au	Au quartz veins	py, sb, aspy, gold	Greywacke, argillite
	Alexander group	A73	L31/e39 (Alexander mine)	1.280 Au	Au quartz veins	py, aspy, sb, gold	Greywacke, argillite
	Langdons	A83	K31/e64	0.049 Au	Au-Sb quartz veins	py, sb, gold	Greywacke, argillite
	Croesus Knob reefs	A80	K31/e66	0.082 Au	Quartz veins	py, sp, gn, aspy, sb, gold	Greywacke, argillite
Otago	Rogers Gully, Macetown	C67	F41/e48	-	Sb quartz veins	Sb	Pelitic schist and greenschist
	Carrick	C71	F42/e26, 27	0.453 Au	Au quartz veins	py, gold, aspy, ±sb, (sp, cp)	Quartzofeldspathic chlorite schist
	Nenthorn	C85	I43/e23, e28, e31	0.222 Au	Au quartz veins	py, sb, gold, (sp, Bi sulf, gn)	Quartzofeldspathic chlorite schist
	Barewood	C86	I43/e34, e36	0.420 Au, 12 W	Au-W quartz veins	py, sch, sb, gold, (gn)	Quartzofeldspathic chlorite schist
	Hindon (Mt Stoker)	C87	I43/e24	0.049 W, Au	Au quartz veins	py, sb, gold	Quartzofeldspathic chlorite schist

[1] MM = Metallogenic map code (Brathwaite and Pirajno 1993).

[2] GERM = Geological Resource Map code.

3.2.4 Hot Spring Sb–As

3.2.4.1 International Mineral Deposit Model

In the *Hot spring Sb–As* mineral deposit model, quartz veins and sinters are formed at the surface and in the near surface environments of epithermal systems. These are hosted in volcanic and sedimentary rocks and contain stibnite, pyrite and cinnabar. There is no well-documented international model.

3.2.4.2 New Zealand Occurrences of Hot Spring Sb–As *Deposits*

Occurrences of *Hot Spring Sb–As* deposits are listed in Table 3.6. At Rangitarore Hill (Lanigan's Mine), 10 km southeast of Russell, stibnite is found within a 3-m-wide silicified crush zone, dipping 80° SW, in Waipapa Group greywacke (Ferrar 1925). The deposit was first mined in 1907, and 115 t of ore, at an average grade of 50–60% Sb, was extracted and exported. Fricker (1970) reported analyses of up to 40% Sb and 0.51% Hg in samples taken from the lode.

At Puhipuhi, stibnite occurs in sinter and silicified greywacke associated with mercury deposits. At Ngawha, minor stibnite is associated with mercury in Pleistocene lake sediments and is related to the active Ngawha geothermal system.

In the Hauraki Goldfield, stibnite is found in some epithermal quartz veins, particularly at Te Ahumata (Great Barrier Island; Ramsay and Kobe 1974), Mahakirau (Fraser and Adams 1907; Robson 1979) and Thames (Fraser 1910; Merchant 1978, 1986).

Table 3.6 *Hot spring Sb–As* model occurrences in New Zealand. Minerals: ag sulfosalts = silver sulfosalts; aspy = arsenopyrite; cin = cinnabar; Hg = mercury; el = electrum; marc = marcasite; pyrg = pyrargyrite; py = pyrite; real = realgar; sb= stibnite; td = tetrahedrite; tel = tellurides.

Occurrence	MM[1]	GERM[2]	Production (t)	Deposit Form	Minerals Major (minor)	Host Rocks
Te Pene	I4	P04/e52	-	Quartz veins	sb, aspy	Greywacke
Rangitarore Hill (Lanigan's Mine)	I13	Q05/e13	58 Sb	Quartz veins	Sb	Silicified greywacke
Ngawha	I12	P05/e56	33 Hg	Stratabound dissemination	cin, Hg, sb, real	Lake beds, basalt
Puhipuhi	I15	Q06/e70	55 Hg	Stratabound	cin, marc, py, sb	Sinter, silicified greywacke
Te Ahumata	I22	S09/e1	1.295 Ag–Au	Quartz veins	py, pyrarg, el, sb, ag sulfosalts	Rhyolite, andesite and porphyry
Mahakirau	I42	T11/e29.30, 33	0.017 Au–Ag	Quartz veins	py, sb, el	Andesite flows and tuffs
Thames	I54	-	67.095 Au–Ag	Quartz veins	py, pyrg, el, sb, (sp, cp, td, tel)	Andesite flows and breccias

[1] MM = Metallogenic map code (Brathwaite and Pirajno 1993).

[2] GERM = Geological Resource Map code.

3.3 Beryllium (Be)

3.3.1 International Description

International data for beryllium are listed in Table 3.7.

Table 3.7 Major minerals, world production, reserves and resources and major uses of beryllium.

Beryllium (Be)		
International	**Ore Minerals:** Barylite $BaBe_2Si_2O_7$, bertrandite $Be_4Si_2O_7(OH)_2$, beryl $Be_3Al_2Si_6O_{18}$, chrysoberyl $BeAl_2O_4$, eudidymite $NaBeSi_3O_7(OH$, helvite $Mn,Fe,Zn)_4Be_3Si_3O_{12}S$, phenakite/phenacite Be_2SiO_4	
	World production (USGS 2024)	330 t in 2023 from a high of 337 t in 2014
	Major world producers (% of average total 2023) (USGS 2024)	USA (58%), China (22%), Brazil (12%), Mozambique (7%)
	World resources (USGS 2024)	100,000 t (60% in the USA)
	World reserves (USGS 2024)	N/A
	Uses: Beryllium is widely used in automotive, aerospace and electronics applications. It also has many applications in the defence sector.	

In the *Be Pegmatite* mineral deposit model (Bradley et al. 2017), beryl occurs in coarsely crystalline pegmatite dikes located peripheral to granitic intrusions. The pegmatites are composed of quartz, sodic plagioclase and microcline with or without spodumene, muscovite or lepidolite.

3.3.2 Beryllium in New Zealand

Beryl occurs in pegmatite dikes and quartz veins and in trace quantities in West Coast beach sand (Figure 3.3).

Be Pegmatite occurrences are found near Charleston on the West Coast and on the north shore of Paterson Inlet, Rakiura / Stewart Island. The pegmatites near Charleston are hosted in banded granitic Constant Gneiss and contain coarse-grained quartz, feldspar, muscovite and biotite. Beryl occurs as columnar, pale green to colourless crystals up to 125 mm across and containing 12.82% BeO (Hutton and Seelye 1945; NZGS 1970a). At Paterson Inlet, beryl occurs as fine-grained crystals in association with abundant tourmaline (McKay 1890). Hutton and Seelye (1945) referred to the existence of beryl at Dusky Sound but gave no specific location or reference.

A quartz vein occurrence at Canaan Valley, Pikikiruna range (Figure 3.3; GERM N26/e510), is associated with Separation Point Granite and contains rare, blue and colourless beryl crystals and scheelite (Williams et al. 1959). The beryl is mostly very fine grained, but a few crystals up to 8 mm in size are present. Beryl is also present in nearby stream alluvium (NZGS 1970a).

Analyses from the ilmenite-bearing beach sand on the West Coast during prospecting in the 1970s showed traces of beryl. In the Birchfield area, it comprised 0.01% of the heavy-mineral fraction and 0.02% at Hokitika (Zuckerman 1972a; Painter 1973). Hutton (1950) noted that some West Coast dredge concentrates contained rare grains of gadolinite that were probably eroded from pegmatites in the Karamea granite.

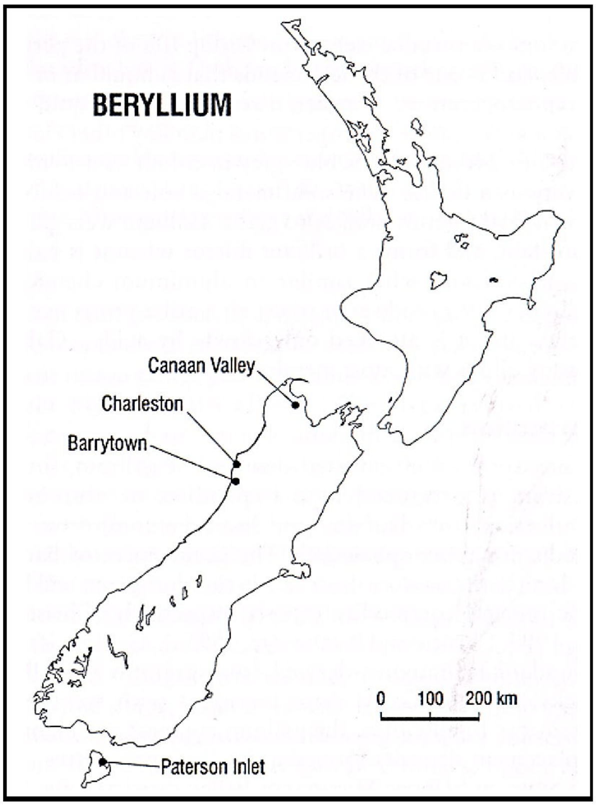

Figure 3.3 Location of beryllium deposits in New Zealand (after Christie and Brathwaite [1999a]).

Key References: Brathwaite and Pirajno (1983); Christie and Brathwaite (1999a).

3.4 Chromium (Cr)

3.4.1 International Description

International data for chromium are listed in Table 3.8.

Table 3.8 Major minerals, world production, reserves and resources and major uses of chromium.

Chromium (Cr)		
International	**Ore Minerals:** Chromite $FeCr_2O_4$. Because of substitution, natural chromite has the general formula of $(Fe,Mg)O(Cr,Al,Fe)_2O_3$.	
	World production of chromite ore (USGS 2024)	41 Mt (2023)
	Major world producers in 2023 (USGS 2024)	South Africa (44%), Kazakhstan (15%), Turkey (15%), India (10%), Finland (5%)
	World reserves of chromite ore in 2023 (USGS 2024)	560 Mt
	World resources of chromite ore in 2023 (USGS 2024)	>12 Bt
	Uses: The creation of metal alloys accounts for 85% of the available chromium's usage, for example, stainless steel (>11% Cr) and Inconel nickel superalloys (18.6% Cr). The remainder of chromium is used in electroplating, pigments, timber preservatives and the refractory and foundry industries.	

3.4.2 Chromium in New Zealand

Chromite is found in *Podiform chromite* deposits described in the *Podiform chromite* model section below, as well as in small peridotite and serpentinite bodies near North Cape, Wellsford and Piopio in the North Island (Figure 3.4).

At North Cape, minor disseminated chromite is found in serpentinite at Surville Cliffs in Northland. Bennett (1976) noted that the cumulate harzburgite-lherzolite zone of the Murimotu Intrusives contains disseminated chromite and that a possible underlying tectonite harzburgite zone with podiform chromite could lie offshore.

In the South Island, chromite is also present in the ultramafic rocks of the Cobb Igneous Complex, in the vicinity of the magnesite and asbestos mines, mainly:

> *"as highly irregular masses from 5 cm to 4 m in size, in the serpentinised orthopyroxenite masses which cut peridotite."* (Hunter 1977)

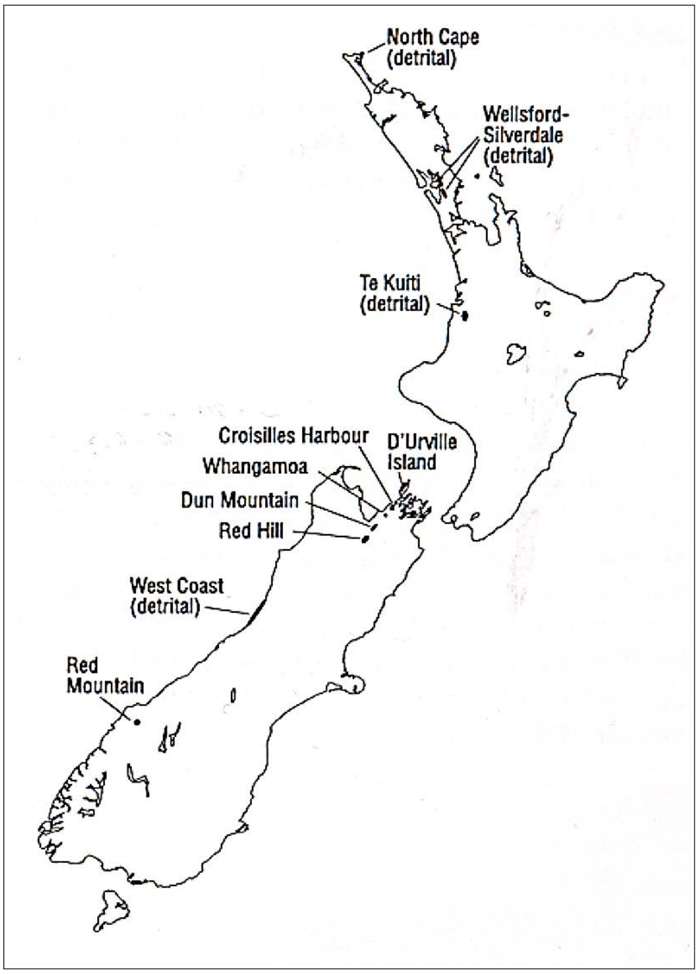

Figure 3.4 Location of chromite deposits in New Zealand (after Christie et al. [1994]).

Key References: Williams (1974); Brathwaite and Pirajno (1993); Christie et al. (1994); Brathwaite et al. (2012c, 2016).

3.4.3 Podiform Chromite

3.4.3.1 International Mineral Deposit Model

Features of the *Podiform chromite* mineral deposit model are listed in Table 3.9.

Table 3.9 Features of the *Podiform chromite* international mineral deposit model.

International Mineral Deposit Model – *Podiform Chromite*	
Reference	USGS models 8a (minor) and 8b (major) Podiform chromite (Cox and Singer 1986); BCGS model M03 Podiform chromite (Lefebure and Höy 1996); and USGS Podiform chromite model (Mosier et al. 2012).
Description	Deposits of massive chromitite occur as pods, tabular lenses or layers within ophiolitic ultramafic rocks. The deposits are formed as a primary magmatic differentiate during early olivine and chrome-spinel crystal fractionation of basaltic liquid at an oceanic spreading centre. The host rocks represent obducted fragments of oceanic, lower crustal and upper mantle ultramafic rocks within accreted oceanic terranes.
International Examples	Guleman ore field (Turkey); Kalimash-Kukes-Tropoje district, Bulquize and Todo Manco-Bater-Martanesh district (Mirdita ophiolite) (Albania); Tiébaghi ophiolite and Massif du Sud, (New Caledonia); Acoje and Masinloc-Coto (Zambales range / ophiolite), Luzon (Philippines); Batamshinsk, Stepninsk, Tagashaisai and Main SE ore fields (Kempirsai massif), Southern Urals (Russia); Xeraivado and Skoumtsa mines (Vourinos ophiolite) (Greece); Semail ophiolite (Oman); Luobusa, Donqiao, Sartohay, Yushi, Solun, Wudu and Hegenshan deposits (China).
Grade-Tonnage Model	Grades range from 20 to 60% Cr_2O_3 and tonnages range from several thousand to several million tonnes. USGS model 8b major podiform chromite deposits 50th percentile = 20,000 t at 46% Cr_2O_3 (9200 t Cr_2O_3) and trace Rh, Ir, Ru, Pd and Pt (Cox and Singer 1986).

3.4.3.2 New Zealand Occurrences of Podiform Chromite *Deposits*

In the South Island, chromite is found as pods or disseminations in ultramafic rocks of the Dun Mountain Ophiolite Belt (Permian) and is most abundant in the Nelson Mineral Belt from Croisilles Harbour to the Wairau River (Johnston 1987; Brathwaite et al. 2016, 2017a), as well as at Red Mountain in west Otago (Figure 3.4 and Table 3.10). The deposits were formed during partial melting of ultramafic mantle rocks.

Recorded production from the Dun Mountain area was 5870 t of ore (20–54% Cr_2O_3) between 1858 and 1866. About 200 t of ore was produced from Croiselles Harbour between 1900 and 1902.

Table 3.10 *Podiform chromite* and other chromite occurrences in New Zealand (data modified after Brathwaite and Pirajno [1993]).

Region	Occurrence	MM [1]	GERM [2]	Production (t)	Deposit Form	Minerals Major (minor)	Host Rocks
Northland	Surville Cliffs	-	N02/e18	-	Lenses	Chromite	Serpentinite
West Nelson	Cobb magnesite mine	-	M26/e599	-	Lenses	Magnesite, talc	Serpentinite
	Cobb asbestos mine	-	M27/e596	-	Lenses	asbestos	Serpentinised harzburgite
East Nelson	Croisilles	B4	O26/e549	~50	Podiform lenses	Chromite	Serpentinite
	Maungatapu	B6	O27/e574	Very small	Podiform lenses	Chromite	Serpentinised peridotite
	Dun Mountain	B15	O27/e573	~1400	Podiform lenses	Chromite	Serpentinised dunite and harzburgite
	Jackson Creek	B16	O27/e572	Very small	Podiform lenses	Chromite	Serpentinised dunite and harzburgite
	Miner Creek	B17	O27/e576	Very small	Podiform lenses	Chromite	Serpentinised dunite and harzburgite
	Serpentine Valley	B18	N28/e557	Very small	Podiform lenses	Chromite	Serpentinised dunite and harzburgite
	Chromite Creek	B19	N28/e578	Very small	Podiform lenses	Chromite	Serpentinised dunite and harzburgite
	Mt Starveall	B20	N28/e580	Very small	Podiform lenses	Chromite	Serpentinised peridotite
	Little Ben Nevis	B21	N28/e579	Very small	Podiform lenses	Chromite	Serpentinised dunite and harzburgite
	Chrome Trig, Red Hills	B22	E39/e5	Very small	Podiform lenses	Chromite	Serpentinised dunite and harzburgite
Otago Southland	Red Spur	B24	E38/e3	-	Podiform lenses	Chromite	Peridotite
	Martyr Hill	B26	E28/e5	-	Chromatite	Chromite	Peridotite
	Red Hills Trig	B28	E39/e5	-	Chromatite layers	Chromite	Dunite, peridotite
	Steep Creek, Little Red Hill	B31	E39/e8	-	Podiform	Chromite	Dunite
	Stag Pass	-	E39/e7	-	Podiform chromite	Chromite boulders	-
	Simonin Stream	-	E39/e6	-	Podiform chromite	Chromite	-
	Greenhills	B43	-	-	Disseminated in layers	Chromite	Dunite

[1] MM = Metallogenic map code (Brathwaite and Pirajno 1993).

[2] GERM = Geological Resource Map code.

3.5 Cobalt (Co)

3.5.1 International Description

International data for cobalt are listed in Table 3.11. Cobalt production is mostly as a by-product of nickel mining.

Table 3.11 Major minerals, world production, reserves and resources and major uses of cobalt.

Cobalt (Co)		
International	**Ore Minerals:** Cobaltite (CoAsS), safflorite $CoAs_2$, glaucodot (Co,Fe)As, skutterudite $CoAs_3$ and smaltite $CoAs_2$	
	World mine production in 2023 (USGS 2024)	230,000 t
	Major world producers (% of total 2023 world production) (USGS 2024)	Democratic Republic of Congo (74%), Indonesia (10%), Russia (3%), Australia (3%), Madagascar (3%), Philippines (2%), Cuba (2%), New Caledonia (1%), Papua New Guinea (1%), Turkey (1%)
	World reserves (USGS 2024)	11 Mt
	World resources (USGS 2024)	25 Mt (plus more than 120 Mt in seafloor polymetallic nodules)
	Uses: Cobalt is a key constituent of most lithium-ion batteries used in electric vehicles, consumer goods and stationary energy storage. It is also used in nickel-based alloys and tool materials.	

3.5.2 New Zealand Cobalt Occurrences

A limited range of cobalt-bearing minerals have been observed in New Zealand and include the following: wairauite, cobaltite, glaucodot and linnaeite (Railton and Watters 1990; Durance et al. 2018). Wairauite was first identified in the Red Hills in Marlborough as minute grains in serpentinite (Challis and Long 1964). Bell et al. (1911) noted nickel and cobalt in analyses of ore from copper mines in the east Nelson Dun Mountain Ophiolite Belt.

Any likely future production of cobalt in New Zealand would be as a by-product of mining one of New Zealand's nickel prospects, e.g. Riwaka.

Key References: Williams (1974); Brathwaite and Pirajno (1993); Durance et al. (2018).

3.6 Copper (Cu)

3.6.1 International Description

International data for copper are listed in Table 3.12.

Table 3.12 Major minerals, world production, reserves and resources and major uses of copper.

Copper (Cu)		
International	**Ore Minerals:** Azurite $Cu_3(CO_3)_2(OH)_2$, bornite Cu_5FeS_4, chalcopyrite $CuFeS_2$, native copper Cu, cuprite Cu_2O, chalcocite Cu_2S, covellite CuS, enargite Cu_3AsS_4, malachite $Cu_2CO_3(OH)_2$, tetrahedrite $(CuFeZnAg)_{12}Sb_4S_{13}$	
	World production (USGS 2024)	22 Mt in 2023
	Major world producers (% of average total 2022) (USGS 2024)	Chile (24%), Democratic Republic of Congo (10%), Peru (10%), China (9%) USA (6%), Russia (5%)
	World reserves (USGS 2024)	1 Bt
	World resources in 2015 (USGS 2024)	2.1 Bt identified (plus an estimated 3.5 Bt undiscovered)
	Uses: Copper is used as a conductor of heat and electricity, as a building material and as a constituent of various metal alloys, such as sterling silver used in jewellery, cupronickel used to make marine hardware and coins and constantan used in strain gauges and thermocouples for temperature measurement. Copper compounds are used as bacteriostatic agents, fungicides and wood preservatives.	

3.6.2 Copper in New Zealand

New Zealand has a wide variety of copper deposits; these have been classified and grouped here by international mineral deposit models: *Porphyry Cu*, *Porphyry Mo-Cu*, *Volcanogenic massive sulfide*, *Serpentine-hosted Fe-Cu*, *Gabbroid-associated Ni-Cu*, *Intermediate sulfidation epithermal Au*, orogenic and *Copper skarn* deposits. The primary origin and potential genetic classification of some quartz vein and disseminated stratabound/stratiform deposits, particularly in Fiordland, is difficult to determine because of insufficient information; therefore these are listed in separate tables.

3.6.3 Production

A little more than 7500 t of copper ore has been mined in New Zealand (Table 3.13) since the country’s first underground mine was opened on Kawau Island in 1842. This production was mainly from *Volcanogenic massive sulfide* (Kawau Island, Pakotai, Pupke, Parakao, Te Kumi, Maharahara, Moke Creek, Waitahuna), *Serpentinite-hosted* (Dun Mountain, D’Urville Island), *Hydrothermal (epithermal) vein* (Tui Mine) and *Porphyry Cu* (Miners Head, Great Barrier Island) deposits (Figure 3.5).

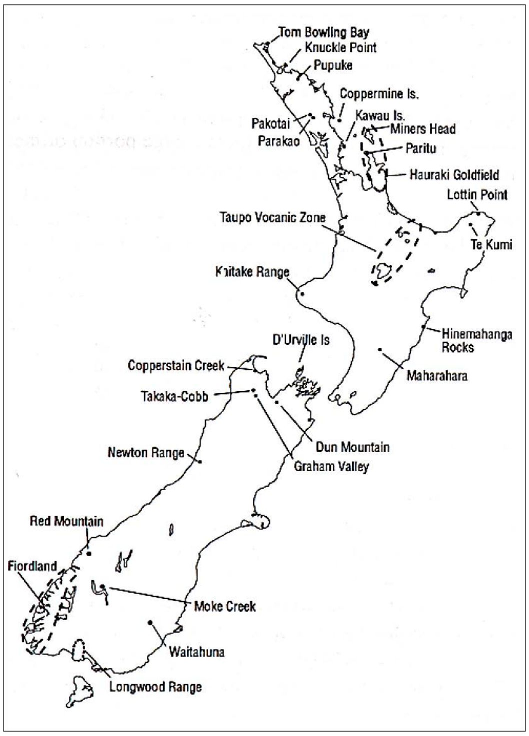

Figure 3.5 Location of copper deposits (after Christie and Brathwaite [1994]).

Table 3.13 Deposits with recorded copper production. VMS = Volcanogenic massive sulfide; conc = concentrate. Note: Ore production and years from Williams (1974), Brathwaite and Pirajno (1993) and Christie and Brathwaite (1994).

Deposit	MM [1]	GERM [2]	Deposit Type	Ore Production (t)	Grade	Years
Parakao	E5	P07/e20	VMS	1040	-	1961–1966
Pupuke	E2	P04/e30	VMS	30	conc	1892–1912, 1964–1968
Pakotai	E4	P06/e23–25	VMS	1400	conc	1947–1951
Kawau Island	C14	R09/e56	VMS	2500	-	1846–1860
Miners Head, Great Barrier Island	I20	S08/e2	Porphyry Cu	2325	conc	1857–1867
Tui Mine	I81	T13/e53	Epithermal	404	From conc	1967–1974
Te Kumi	C21	Y15/e12	VMS	Very small	-	1917–1920
D’Urville Island	B1–3	P25/e1–3, 5, P26/e41–47	Serpentine-hosted Fe-Cu	5	-	1879–1880
Dun Mountain	B7, 9–13	O27/e524–526, 528–530, 532–535	Serpentine-hosted Fe-Cu	930	conc	1886, 1908–1909
Maharahara	C23	T23/e37	VMS	50	2% Cu	1881–1891, 1930
Moke Creek	C61	F42/e85	VMS	c. 3	conc	?1880s–1968
Waitahuna	C97	H44/e14	VMS	17	conc	1880s

[1] MM = Metallogenic map code (Brathwaite and Pirajno 1993).

[2] GERM = Geological Resource Map code.

3.6.4 Resources

Previously published information on copper resources is available for some deposits in the mineral research and exploration literature (Table 3.14; Part 1, Table 7.2).

Table 3.14 Resource estimates from the literature.

Deposit	MM [1]	GERM [2]	Deposit Type	Ore (t)	Grade (% Cu)	Copper (t)	Reference
Monowai [3]	I49	T11/e26	Epithermal vein	143,000 38,000	0.6 0.5	858 190	Roberts (1989)
Tui Mine	I81	T13/e53	Epithermal vein	140,000	0.5	700	Bates (1989b)
Copperstain Creek	A9	M25/e542	Copper skarn, porphyry Mo	10,000,000	0.15	-	Smale (1970), Wodzicki (1972)

[1] MM = Metallogenic map code (Brathwaite and Pirajno 1993).

[2] GERM = Geological Resource Map code.

[3] The two separate resource estimates (ore, grade and tonnage) for the Monowai deposit represent two categories reported by Roberts (1989), corresponding to high-grade and low-grade resources. The low-grade estimate is for low gold and higher copper grades, while high-grade represents high gold and lower copper grades.

3.6.5 Potential and Prospectivity

Although the known copper deposits in New Zealand are all small, the varied geology and number of deposits show significant potential for future copper production, possibly as a by-product of mining other metals. Different types of deposits, such as the porphyry copper, volcanogenic massive sulfide and sediment-hosted deposits, will inevitably be sought for copper in future mineral exploration. Based on international examples and this assessment, the porphyry Cu deposits are likely to yield the largest resources of copper.

Key References: Williams (1974); Brathwaite and Pirajno (1993); Christie and Brathwaite (1994, 2006); Turnbull et al. (2023).

3.6.6 Volcanogenic Massive Sulfide Deposits

Volcanogenic massive sulfide (VMS) deposits are formed by seafloor hydrothermal systems generated by submarine volcanic activity. The known VMS deposits in New Zealand consist of small sulfide lenses composed mainly of pyrite and chalcopyrite that are associated with (a) marine basalts of Cretaceous age in Northland and East Cape (*VMS Cu [Cyprus type]*), (b) chert and pillow lava in greywacke sequences of Permian–Jurassic age and their metamorphic equivalents (*VMS Cu [Besshi type]*) and (c) greenschists (metabasalts) and metaserpentinite of Permian–Triassic age in Westland. Exploration from the 1970s has focused mainly on prospects at Lottin Point and Te Kumi near East Cape, as well as the Maharahara deposit in the Ruahine Ranges (Figure 3.6).

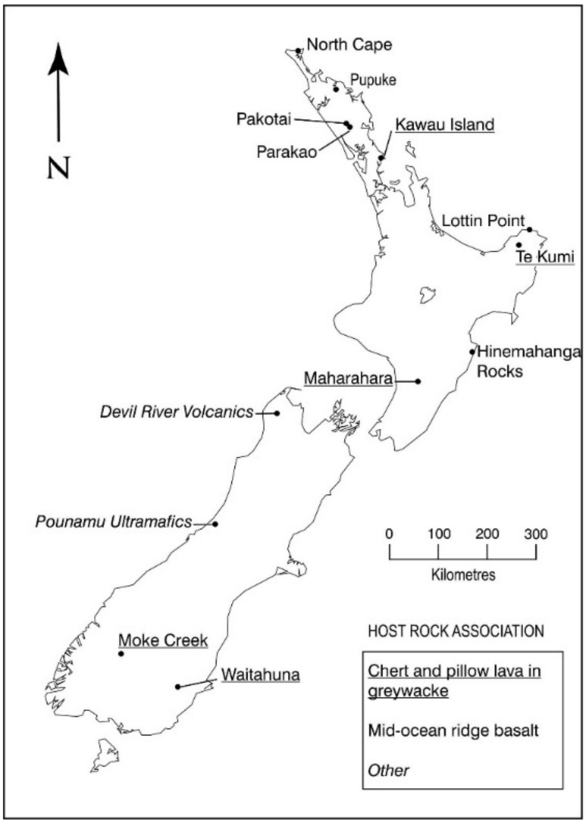

Figure 3.6 Locations of main volcanogenic massive sulfide copper deposits (after Christie and Brathwaite [2006]).

3.6.6.1 VMS Cu (Cyprus Type) *Deposits in Northland and East Cape*

International Mineral Deposit Model

Features of the *VMS Cu (Cyprus type)* model are listed in Table 3.15.

Table 3.15 Features of the Ophiolite-hosted *VMS Cu (Cyprus type)* international mineral deposit model.

International Mineral Deposit Model – *VMS Cu (Cyprus Type)*	
Reference	USGS model 24a Cyprus massive sulfide (Cox and Singer 1986); BCGS model G05 Cyprus massive sulfide Cu (Zn) (Lefebure and Ray 1995); and USGS Volcanogenic massive sulfide occurrence model (Shanks and Thurston 2012).
Description	Seafloor deposition of sulfide mounds contemporaneous with mafic volcanism, such as spreading ridges and back-arc basins. Deposits typically comprise one or more lenses of massive pyrite and chalcopyrite hosted by mafic volcanic rocks and underlain by a well-developed pipe-shaped stockwork zone. Lenses are commonly in tholeiitic or calcalkaline marine basalts, commonly pillowed, near a transition with overlying argillaceous sediments. Many lenses appear to be structurally controlled, aligned near steep, normal faults. The main minerals are pyrite, chalcopyrite, magnetite and sphalerite, with lesser marcasite, galena, pyrrhotite, cubanite, stannite-besterite and hematite, in a gangue mineral assemblage of talc, chert, magnetite and chlorite.
International Examples	Cyprus; York Harbour and Betts Cove, Newfoundland (Canada); Turner-Albright (USA); Lokken (Norway).
Grade-Tonnage Model	USGS model 24a 50th percentile = 1.6 Mt at 1.7% Cu (27,200 t Cu), possible by-product Ag, Au, Pb and/or Zn (0–33 g/t Ag; 0–1.9 g/t Au, 0–2.1% Zn) (Cox and Singer 1986). See also Lefebure and Höy (1996; Table 7) for BCGS model G05.

New Zealand Occurrences of *VMS Cu (Cyprus Type)* Deposits

Previously mined copper deposits at Pupuke, Pakotai and Parakao in Northland, as well as copper shows at Lottin Point in East Cape, are associated with Cretaceous ophiolite sequences (Tangihua Complex and Matakoa Volcanics, respectively) (Table 3.16). Several other copper occurrences are associated with the ophiolite sequences near North Cape. Recent geochemical trace and rare earth element studies have indicated that they contain island arc tholeiites, in addition to mid-ocean ridge basalts, and were formed in a suprasubduction zone setting close to their Late Oligocene obduction site (e.g. Nicholson and Black 2004; Whattam et al. 2004, 2005).

Key References: Mason (1973); Roser (1983); Mason and Kobe (1989); Brathwaite and Christie (2006); Brathwaite et al. (2008, 2012b).

Table 3.16 *VMS Cu (Cyprus type)* deposits (data modified after Table 16 of Brathwaite and Pirajno [1993]). Minerals: bn = bornite, cp = chalcopyrite, Cu = native copper, cup = cuprite, gn = galena, hm = hematite, mt = magnetite, marc = marcasite, py = pyrite, sp = sphalerite.

Region	Occurrence	MM [1]	GERM [2]	Production (t)	Deposit Form	Minerals Major (minor)	Host Rocks
Northland	Pupuke	E2	P04/e30	30 Cu conc	Stratiform lenses	py, marc, cp	Shale, dolerite, basalt
	Pakotai	E4	P06/e23, e24, e25	1381 Cu conc	Stratiform lenses	py, cp, (sp)	Shale, basalt, andesite
	Parakao	E5	P07/e20	1026 Cu conc	Stratiform lenses	py, cp	Shale, chert, dolerite
	Purua	E6	Q06/e117	-	Stratabound	cp, bn, (mt, hm)	Basalt
East Cape	Upongongaruru	E8	-	-	Stratiform lenses	py, cp, mt	Argillite, basalt
	Lottin Point	E9	Y14/e11–13	-	Stratiform lens	py, cp, (gn, sp)	Argillite, chert, basalt
Hawke's Bay	Hinemahanga (Kairakau) Rocks	E11	-	-	Disseminated	Cu, cup	Limestone, basalt

[1] MM = Metallogenic map code (Brathwaite and Pirajno 1993).

[2] GERM = Geological Resource Map code.

3.6.6.2 *VMS Cu (Besshi Type)*

International Mineral Deposit Model

Features of the *VMS Cu (Besshi type)* mineral deposit model are listed in Table 3.17.

Table 3.17 Features of the *VMS Cu (Besshi type)* international mineral deposit model.

International Mineral Deposit Model – *VMS Cu (Besshi Type)*	
Reference	USGS model 24b Besshi massive sulfide (Cox and Singer 1986); BCGS model G04 Besshi massive sulfide Zn-Cu-Pb (Lefebure and Ray 1995); and USGS Volcanogenic massive sulfide occurrence model (Shanks and Thurston 2012).
Description	Thin, sheet-like bodies of massive to well-laminated pyrite, pyrrhotite and chalcopyrite within thinly laminated clastic sediments and marine volcanic rocks; basaltic tuffs and flows, shale and siltstone, commonly calcareous; less commonly chert and iron formations. The deposits represent seafloor deposition of sulfide mounds in back-arc basins, or several other tectonic settings, contemporaneous with volcanism.
International Examples	Besshi and Motoyasu (Japan); Greens Creek, Alaska (USA); Kieslager (Austria); Raul (Peru)
Grade-Tonnage Model	USGS model 24b 50th percentile = 0.22 Mt at 1.5% Cu (3300 t Cu), possible by-product Ag, Au and/or Zn (2–9 g/t Ag, 0.4–2% Zn) (Cox and Singer 1986). See also Lefebure and Höy (1995, Table 6) for BCGS model G04.

New Zealand Occurrences of *VMS Cu (Besshi Type)* Deposits

In both the North and South Islands, several small copper deposits occur in Torlesse Supergroup and Waipapa Group greywacke, as well as Haast Schist associated with cherts and/or spilitic pillow lavas (Table 3.18).

Key References: Williams (1974); Lowery (1979); Roser (1983); Brathwaite and Pirajno (1993); Christie and Brathwaite (2006).

Table 3.18 *VMS Cu (Besshi type)* deposits (data modified after Tables 14a and 14c of Brathwaite and Pirajno [1993]). conc = concentrate. Minerals: cp = chalcopyrite, mt = magnetite, marc = marcasite, po = pyrrhotite, py = pyrite, sp = sphalerite.

Occurrence	MM [1]	GERM [2]	Production (t)	Deposit Form	Minerals Major (minor)	Host Rocks
Kawau Island	C14	R09/e56	~2500 Cu ore	Stratiform lenses	cp, py, marc, (sp)	Chert, green argillite
Te Kumi	C21	Y15/e12	Very small	Stratiform	py, cp, (mt, sp)	Argillite, spilite
Makaretu	C22	U22/e3	-	Stratiform	py, cp	Red chert, spilite
Maharahara	C23	T23/e37	50 Cu conc	-	py, cp, (sp, po)	Red chert
Makatote Stream	-	U25/e31	-	-	-	-
Moke Creek	C61	E41/e85	~3 Cu conc	Stratiform	sp, py, po, (cp)	Greenschist metavolcanics
Waitahuna	C97	H44/e14	17 Cu conc	Stratiform sulfide	cp, py, marc, po, (sp)	Greenschist metavolcanics

[1] MM = Metallogenic map code (Brathwaite and Pirajno 1993).

[2] GERM = Geological Resource Map code.

3.6.6.3 VMS Lenses in the Pounamu Ultramafics

Small massive sulfide lenses are present in greenschist metavolcanics and metaserpentinite of the Pounamu Ultramafics on the western side of the Southern Alps in Westland (Table 3.19). The Pounamau Ultramafics are interpreted as ophiolite (ocean crust) basement to the Torlesse terrane (Cooper and Reay 1983). Copper-bearing sulfide lenses have been found in the Newton Range (J33/e85, e86; Beck 1965), Diedrich, Meta and Bowen ranges (MacKenzie 1984), Whitcombe River area (Cooper and Reay 1983) and in the Wilberg Range (Gardiner RT 1971; Coleman 1980). Those in the Wilberg Range appear to be the largest, with a mineralised zone 3–9 m wide and 1500 m long containing numerous pyrite-chalcopyrite lenses (30–90 cm wide) (MacPherson 1970). Later exploration in the same area (Coleman 1980) identified a much more extensive zone of mineralisation comprising many small pods of massive sulfide within greenschist, with grades between 0.5 and 2.0% Cu. An analysis from the Diedrich Range returned 5.1% Cu and 3.9 ppm Ag.

Table 3.19 Volcanogenic massive sulfide stratiform lenses and disseminations in the Southern Alps (data modified after Table 14c of Brathwaite and Pirajno [1993]). Minerals: cp = chalcopyrite, mt = magnetite, mal = malachite, po = pyrrhotite, py = pyrite.

Occurrence	MM [1]	GERM [2]	Production (t)	Deposit Form	Minerals Major (minor)	Host Rocks
Newton Range	C45	J33/e86	Stratiform lens	po, py, cp, mt	Serpentinite, biotite and quartz schist	Newton Range
Whakarira George	C46	J33/e85	Stratiform lens	py, cp, mt	Talc schist	Whakarira George
Noisy Creek	C47	J34/e1	Stratiform disseminated	py, cp, mal	Metaserpentinite, greenschist metavolcanics	Noisy Creek
Wilberg Range	C48	I34/e14	Stratiform lens	py, cp	Greenschist metavolcanics and metasediments	Wilberg Range

[1] MM = Metallogenic map code (Brathwaite and Pirajno 1993).

[2] GERM = Geological Resource Map code.

3.6.7 Serpentine-Hosted Fe-Cu

Small shear-controlled lenses of copper mineralisation are present in serpentinised ultramafic rocks of the Dun Mountain Ophiolite Belt in the Nelson region (D’Urville Island and Dun Mountain) and in Southland (Red Mountain) (Table 3.20). There has been historic mining at D’Urville Island and Dun Mountain (e.g. United Mine 700 t copper ore) in Nelson. Although there is no corresponding international mineral deposit model, these have many features of the *Dunitic Ni-Cu* deposits of Cox and Singer (1986) (see Section 3.14) but without recorded nickel minerals.

Key References: Williams (1974); Johnston (1987); Brathwaite and Pirajno (1993).

Table 3.20 Occurrences of *Serpentine-hosted Fe-Cu* model (data modified after Table 13a of Brathwaite and Pirajno [1993]). Minerals: cc = chalcocite, cp = chalcopyrite, Cu = native copper, cup = cuprite, mt = magnetite, mal = malacite, po = pyrrhotite, py = pyrite.

Occurrence		**MM** [1]	**GERM** [2]	**Production (t)**	**Deposit Form**	**Minerals Major (minor)**	**Host Rocks**
D'Uberville Island	Otu Point	B1	P25/e1	-	Stratabound lenses	py, cp, mal	Basaltic tuffs and lavas
	Out Bay	-	P25/e2,3,5	-	-	-	-
	Punaatawheke Bay	B2	P25/e20	-	Disseminated/ stratabound	py, mt, cp, (Cu)	Basaltic tuffs and lavas
	Copper Mine Bay	B3	P26/e41–47	5	Lenses in shear	cup, Cu, cc	Serpentinite
Dun Mountain	Windy Point Group	B7	(O27/e524, 525, 526, 528, 529)	~3	Lenses in shear zones	po, cp, mt, Cu, cup	Serpentinite
	Duckpond	B8	Q27/e595	Very small	Lenses in shear zones	po, cup, mal, mt	Serpentinite
	Mt Claude	B9	O27/e532	5–6	Lenses in shear zones	cup, mal, mt	Serpentinite
	Imperial	B10	O27/e533	Very small	Lenses in shear zones	po, mal	Serpentinite
	Monster	B11	O27/e530	200	Lenses in shear zones	po, cp, mal	Serpentinite
	United	B12	O27/e535	700	Lenses in shear zones	po, cp, cup, Cu	Serpentinite
	Champion	B13	O27/e534	30	Lenses in shear zones	po, Cu, cp	Serpentinite
	Johnstons United	B14	N28/e536	Very small	Lenses in shear zones	po, cu oxides	Serpentinite

[1] MM = Metallogenic map code (Brathwaite and Pirajno 1993).

[2] GERM = Geological Resource Map code.

3.6.8 Porphyry Cu

3.6.8.1 International Mineral Deposit Model

Features of the *Porphyry Cu* mineral deposit model are listed in Table 3.21.

Table 3.21 Features of the *Porphyry Cu* international mineral deposit model.

International Mineral Deposit Model – *Porphyry Cu*	
Reference	USGS model 17 Porphyry copper (Cox and Singer 1986); BCGS model L04 Porphyry Cu ± Mo ± Au (Lefebure and Ray 1995); USGS Porphyry copper deposit model (John et al. 2010)
Description	Quartz vein stockwork, breccia and disseminated Cu ± Au ± Mo mineralisation is centred around small cylindrical porphyry stocks or swarms of dikes typically of intermediate to felsic calc-alkaline composition. In some cases, the mineralised intrusions represent cupolas of larger underlying plutons or batholiths. Undeformed deposits commonly have circular or elliptical shapes in plane view, with diameters typically between 0.1 and 1.0 km and vertical dimensions similar to their horizontal dimensions. The vertical extent of hypogene ore is generally 1–1.5 km or less. Copper-mineralised rock can continue several kilometres deeper at uneconomic grades. Zonal patterns of hydrothermal alteration are generally present, typically from central potassic (quartz, K-feldspar, biotite) through sericitic (quartz, sericite, pyrite) and advanced argillic (quartz, kaolinite, alunite) to distal propylitic (chlorite, epidote, carbonate). The main metallic minerals are chalcopyrite and pyrite, with local bornite and magnetite. Copper grades vary from several tenths of 1% to greater than 1% with an average of 0.44% Cu in producing deposits (John et al. 2010).
International Examples	Ray, Kalamazoo, Santa Rita and Yerrington/Ann-Mason, Arizona; Butte, Montana; Bingham, Utah (USA); Chuquicamata, La Escondida, El Salvador, Refugio and El Teniente (Chile); Alumbera (Argentina); Far South East (Philippines); Batu Hijau and Grassberg (Indonesia); Panguna (Papua New Guinea); Cadia (Australia)
Grade-Tonnage Model	USGS model 17 50th percentile = 140 Mt at 0.54% Cu (756,000 t Cu), possible by-product Ag, Au and/or Mo (Cox and Singer 1986). See also Lefebure and Höy (1996, Table 19) for BCGS model L04.

3.6.8.2 New Zealand Occurrences of Porphyry Cu *Deposits*

Porphyry-style mineralisation occurs associated with Miocene-age intrusive rocks (e.g. quartz diorites and quartz monzonites) at Knuckle Point, Coppermine Island and Whangārei Heads in Northland, as well as Miners Head (Great Barrier Island), Paritu, Manaia and Ohio Creek (Thames) in the Coromandel Volcanic Zone (Figure 3.5 and Table 3.22). Copper occurrences in the South Island of possibly porphyry Cu style include: Piano Clearing (GERM L27/e562), Copper Creek Reef (Mt Radiant; L27/e504), Little Wanganui (L27/e567) and Campbell Creek (M26/e537), all on the West Coast, and Ruggedy Range (D48/e7) on Rakiura / Stewart Island.

Miners Head, Great Barrier Island, is the only example previously mined, which produced 2500 t copper ore (hand-picked concentrate). At Ohio Creek, exploration, including six diamond drillholes totalling some 2530 m, was carried out by Amoco Minerals (Merchant 1978,1986; Dimo et al. 1982, Brathwaite et al. 2001). The drillholes intersected a quartz vein stockwork containing pyrite-chalcopyrite mineralisation, with an average grade of 0.18% Cu.

Key References: Wodzicki and Thompson (1970); Brathwaite and Pirajno (1993); Brathwaite et al. (2001); Turnbull et al. (2023).

Table 3.22 *Porphyry Cu* occurrences (data modified after Tables 21a and 21b of Brathwaite and Pirajno [1993]). Minerals: cc = chalcocite, cp = chalcopyrite, gn = galena, mt = magnetite, mal = malacite, marc = marcasite, mo = molybdenite, po = pyrrhotite, py = pyrite, sp = sphalerite.

Region	Occurrence	MM [1]	GERM [2]	Production (t)	Deposit Form	Minerals Major (minor)	Host Rocks
Northland	Kerr Point	-	N02/e17	-	-	-	-
	Pihakoa Point	I1	O03/e8	-	Stockwork, disseminated	py, cp	Diorite
	Knuckle Point	I2	O03/e7	-	Stockwork, disseminated	cp, py, mal	Diorite
	Kauri Mountain		R07/e9	-	-	-	-
	Coppermine Island	I18	R07/e10	-	Stockwork, disseminated	py, cp, po, (marc, mo)	Diorite and dacite breccia
	Whangārei Heads, Reef Bay	I17	-	-	Sulfide vein	py, sp, gn, cp	Andesite porphyry, siltstone
Coromandel Volcanic Zone	Dolphin Creek, Great Barrier Island	I19	S08/e3, e4	-	Vein/breccia zone	gn, sp, cp	Felsic dike, greywacke
	Miners Head, Great Barrier Island	I20	S08/e2	2300 Cu concentrate	Stockwork, disseminated	cp, py, (gn, sp, po)	Diorite porphyry, greywacke
	Paritu	I24	S10/e4	-	Stockwork, disseminated	py, cp, mt	Granodiorite and quartz diorite
	Manaia (Kakatarahae Stream)	I43	T11/e17	-	Stockwork, disseminated	py, cp, mt, (sp, gn, mo)	Diorite porphyry, greywacke
	Puru-Upper Waiomu	I50	T11/e80, T12/e19	-	Stockwork, disseminated	py, cp, (mo, cc)	Quartz dorite porphyry
	Ohio Creek	I52	T12/e47	-	Stockwork, disseminated	py, cp, (mo)	Diorite porphyry

[1] MM = Metallogenic map code (Brathwaite and Pirajno 1993).

[2] GERM = Geological Resource Map code.

3.6.9 Copper Skarn

3.6.9.1 International Mineral Deposit Model

Features of the *Copper skarn* mineral deposit model are listed in Table 3.23.

Table 3.23 Features of the *Copper skarn* international mineral deposit model.

International Mineral Deposit Model – *Copper Skarn*	
Reference	USGS model 18b copper skarn (Cox and Singer 1986); and BCGS model K01 copper skarns (Lefebure and Ray 1995).
Description	Deposits consist of Cu–Ag sulfide minerals as replacement bodies in contact metasomatic rocks where limestone is intruded by felsic stocks.
International Examples	Ruth, Mason Valley, Victoria and Copper Canyon, Nevada; Carr Fork, Utah (USA); Ok Tedi (Papua New Guinea)
Grade-Tonnage Model	USGS model 18b 50th percentile = 0.56 Mt and 1.7% Cu (9520 t Cu), possible by-product Ag and Au (Cox and Singer 1986). See also Lefebure and Höy (1996, Table 14) for BCGS model K01.

3.6.9.2 New Zealand Occurrences of Copper Skarn *Deposits*

At Copperstain Creek, about 11 km west of Takaka, copper mineralisation is associated with skarns developed by the intrusion of small granodiorite porphyry stocks and sills into Lower Paleozoic sedimentary rocks of Mount Arthur Marble and Onekaka Schist (Wodzicki 1972; GERM M0825; Brathwaite et al. 2004). Wodzicki (1972) suggested that there is a lateral metal zonation, from molybdenum in the granodiorite, out through copper, to lead-zinc in peripheral locations. Mount Arthur (M27/e17), Arthur Range (M27/e556) and Leslie River (M27/e561) copper occurrences also have a skarn association. Resources at Copperstain Creek were estimated at 10 Mt at 0.15% Cu (Smale 1970; Wodzicki 1972).

Key References: Smale (1970); Wodzicki (1972); Brathwaite and Pirajno (1993); Brathwaite et al. (2004).

3.6.10 Hydrothermal Quartz and Sulfide Vein Copper of Uncertain Origin

In addition to the epithermal quartz veins, chalcopyrite is found in quartz and sulfide veins of several other types of geological settings and formation processes, for example, hydrothermal-magmatic and hydrothermal-metamorphic, and, in many cases, their specific genesis is uncertain. Host rocks include granitic, metasedimentary and other metamorphic rocks. Veins found in and adjacent to granitic intrusions are possibly formed by magmatic-related hydrothermal fluids. This classification is used to group quartz veins listed in Table 3.24 that have insufficient information to readily assign them to other genetic models, such as the orogenic and epithermal quartz veins.

Table 3.24 Copper-bearing vein, disseminated and stratiform deposits of uncertain genesis and classification (after Christie and Brathwaite [1999b]). Minerals: bn = bornite, cc = chalcocite, cp = chalcopyrite, cv = covellite, gn = galena, hm = hematite, mal = malachite, marc = marcasite, mo = molybdenite, mt = magnetite, pent = pentlandite, po = pyrrhotite, py = pyrite, sp = sphalerite.

Brathwaite and Pirajno (1993)	Occurrence	MM [1]	GERM [2]	Deposit Form or Type	Minerals Major (Minor)	Host Rocks	Genesis
Vein deposits, Western Province, West Nelson	Loveridge Creek	-	M27/e546	Quartz veins	cp, gn, py	Argillite and quartzite	Hydrothermal
	Mount Arthur	-	M27/e16, 17	Quartz veins	-	Lamprophyre sill	Hydrothermal
	Mossey Creek	-	M27/e13	Quartz veins	-	Pyroxene-feldspar porphyry	Hydrothermal
	Middle Wangapeka River	-	M28/e551	Quartz veins	cp, bn, hm, cc, mal	Sandstone, chert	Hydrothermal
	Patriarch Range area	-	M28/e548	Quartz veins	py, marc,	Hornblende porphyry in siltstone, sandstone and shale	Hydrothermal
	Baton River	-	M27/e545	Quartz veins	cp, py	Basaltic lava and tuff	Hydrothermal
	Bastite Creek	-	M27/e543	Quartz veins	cp, cv, cc, py, mt	Serpentinised ultramafics	Hydrothermal
	Mount Benson	-	M26/e42	Quartz veins	-	Quartzose sedimentary rock	Hydrothermal
	Anatoki Range	-	M26/e23	Quartz veins	-	Metasediments and volcanics	Hydrothermal
	Hardy Ridge	-	M26/e10	Quartz veins	-	Volcanics	Hydrothermal
	Copper Mine	A4	M25/e522	Quartz veins	cp, py, (bn)	Chloritoid schist	Hydrothermal
	Mt Evans	A12	N26/e507	Quartz veins	py, cp (mo, aikinite)	Granite	Hydrothermal
	Copper Creek	A28	L27/e504	Quartz veins	py, cp	Biotite granite	Hydrothermal
	Mackays Reef	A31	L28/e538	Quartz veins	py, cp, (gn, sp)	Foliated granite	Hydrothermal
	Wangapeka River	A35	-	Sulfide veins	cp, (bn, hm)	Sandstone	Hydrothermal

Brathwaite and Pirajno (1993)	Occurrence	MM[1]	GERM[2]	Deposit Form or Type	Minerals Major (Minor)	Host Rocks	Genesis
Vein deposits, Western Province, Westland	Waiwhio Creek	A78	-	Quartz veins	py, cp	Greywacke, argillite	Hydrothermal
	Waiahio Creek		K31/e60	Quartz veins	py, cp, mal	Greywacke, argillite	Hydrothermal-magmatic
	Aynsley Creek	-	K31/e71	Quartz veins	-	Quartz float	Hydrothermal-magmatic
Western Province, Fiordland and Rakiura / Stewart Island	Milford Sound	A89	D40/e7	Sulfide vein	cp	Mafic orthogneiss	Magmatic segregation?
	Bligh Sound	A90	C41/e6	Sulfide vein	cp	Mafic orthogneiss	Magmatic segregation?
	George Sound	A91	C41/e5 or e9 (entrance)	Sulfide vein	py, cp	Dioritic gneiss	Magmatic segregation?
	Doubtful Sound	A99	C41/e5 or e9 (entrance)	Sulfide vein	po, cp, py	Amphibolite gneiss	Hydrothermal-metamorphic

[1] MM = Metallogenic map code (Brathwaite and Pirajno 1993).

[2] GERM = Geological Resource Map code.

3.6.10.1 Disseminations and Stratiform Concentrations of Copper in Metamorphic Rocks of Fiordland and Rakiura / Stewart Island

Disseminations and stratiform concentrations of copper have been recorded in metamorphic rocks of Fiordland and Rakiura / Stewart Island as listed in Table 3.25. There is minimal information available for the individual deposits; therefore, their origin is uncertain and no resource assessment has been made.

Table 3.25 Copper-bearing vein, disseminated and stratiform deposits of uncertain genesis and classification (after Christie and Brathwaite [1999b]). Minerals: cp = chalcopyrite, mt = magnetite, marc = marcasite, pent = pentlandite, po = pyrrhotite, py = pyrite.

Brathwaite and Pirajno (1993)	Occurrence	MM [1]	GERM [2]	Deposit Form or Type	Minerals Major (Minor)	Host Rocks	Genesis
Disseminated and stratiform deposits, Western Province, Fiordland and Rakiura / Stewart Island	Camera Lake	A92	D41/e2	Disseminated	po, cp, marc	Anorthosite	Magmatic segregation?
	Falls Creek	A93	D41/e3	Disseminated	py, cp, po, mt	Gabbro	Magmatic segregation?
	Aragorn Peak	A94	D41/e6	Disseminated	py, mt, po, cp	Gabbro, granite	Hydrothermal-metasomatic
	U Pass West	A95	D41/e4	Disseminated	py, cp, mt	Diorite	Hydrothermal-replacement
	Mt Luxmore	A97	C43/e7	Disseminated	cp, cup	epidiorite	Hydrothermal
	Mt Solitary Copper Lode	A102	B44/e2	Disseminated in amphibolite band	po, pent, cp	Diorite, gneiss, amphibolite	Magmatic segregation?
	Mt Solitary	A103	B44/e5	Disseminated	po, cp, pent	Metadiorite, peridotite	Magmatic segregation
	Lake Hauroko (Cu, Ni)	A105	C44/e3	Disseminated	py, po, cp	Gabbro, pyroxenite	Magmatic segregation
Stratiform deposits	Wet Jacket Arm	A100	(B44/e3)	Stratiform	po, cp, sp	Mafic gabbro	Hydrothermal
	Mt Ponder	A101	B44/e11	Stratiform	py, po, cp, mt	Hornblende schist, quartz schist	Hydrothermal

[1] MM = Metallogenic map code (Brathwaite and Pirajno 1993).

[2] GERM = Geological Resource Map code.

3.7 Gallium (Ga)

3.7.1 International Description

International data for gallium are listed in Table 3.26.

Table 3.26 Major minerals, world production, reserves and resources and major uses of gallium.

Gallium (Ga)		
International	**Ore Minerals:** Bauxite $Al_2O_3.2H_2O$ (Ga substitutes for Al), sphalerite ZnS (trace Ga), germanite $Cu_{26}Fe_4Ge_4S_{32}$, renierite $(Cu,Zn)_{11}(Ge,As)_2Fe_4S_{16}$	
	World mine production in 2023 (USGS 2024)	610,000 kg
	Major world producers (% of total world mine production in 2023)	China (98%), Russia (0.8%), Japan (0.5%), Republic of Korea (0.3%)
	World reserves (USGS 2024)	1.1 M kg (production capacity)
	World resources (USGS 2024)	> 1 Mt in bauxite, but less than 10% is potentially recoverable
	Uses: Widely used in electronic and optical systems, particularly in integrated circuits, lighting and CIGS (copper indium gallium selenide) solar cells. Its use in photovoltaics may grow in the future.	
	Notes: Gallium is almost exclusively produced as a by-product of bauxite (aluminium) mining. However, it can also be a by-product of zinc mining from the mineral sphalerite.	

3.7.2 New Zealand Occurrences of Gallium

Gallium is present in muds and sinters of geothermal fields of the Taupō Volcanic Zone (Crump 1994). Reported gallium concentrations range between 8 and 144 ppm in 48 surface samples from 11 major geothermal fields. Crump (1994) considered that, in the mud samples, the gallium was probably present in kaolinite, substituting for aluminium. Samples with high gallium concentrations (>70 ppm) also contain high concentrations of antimony (400 to >5000 ppm) and arsenic (800 to >10,000 ppm). These two elements form colloids that are efficient scavengers of metals. Co-precipitation of gallium with these colloids is a possible deposition mechanism.

3.8 Gold (Au)

3.8.1 International Description

International data for gold are listed in Table 3.27.

Table 3.27 Major minerals, world production, reserves and resources and major uses of gold.

Gold (Au)		
International	**Ore Minerals:** Calaverite $AuTe_2$, electrum AuAg, gold (native) Au, nagyagite (black tellurium) $Pb_5Au(Te,Sb)_4S_{5–8}$, petzite $(Au,Ag)_2Te$, polybasite $(Au,Cu)_{16}Sb_2S_{11}$ and sylvanite $(Au,Ag)Te_2$	
	World mine production (2023)	3644 t
	Major world producers (% of total world mine production in 2023)	China (11%), Russia (9%), Australia 9%), Canada (5%), USA (5%), Ghana (4%), Peru (4%), Indonesia (4%), Mexico (3%)
	World reserves (USGS 2024)	59,000 t
	World resources (USGS 2024)	N/A
	Uses: Jewellery, electronics, coinage, medicine, medals, trophies and decoration (foil).	

3.8.2 Gold in New Zealand

Gold occurs primarily in quartz veins deposited from hydrothermal fluids in fault zones at medium (orogenic or mesothermal) or shallow (epithermal) depths in the crust. Because of its high density and chemical stability, gold eroded from vein deposits, particularly from orogenic (mesothermal) veins, is concentrated by water flow in river-bed gravels (alluvial) and beach sands to form placer gold deposits. There are a large number of alluvial gold plants in operation in the West Coast region, and some are also present in the Otago and Southland regions.

Past production consists of about 20 Moz from hard-rock gold deposits and 18 Moz from placer gold deposits to date (Figure 3.7 and Table 3.28). Annual production in 2021 and 2022 is listed in Table 3.29. Resources are listed in Part 1 (Table 7.2) and in some sections below.

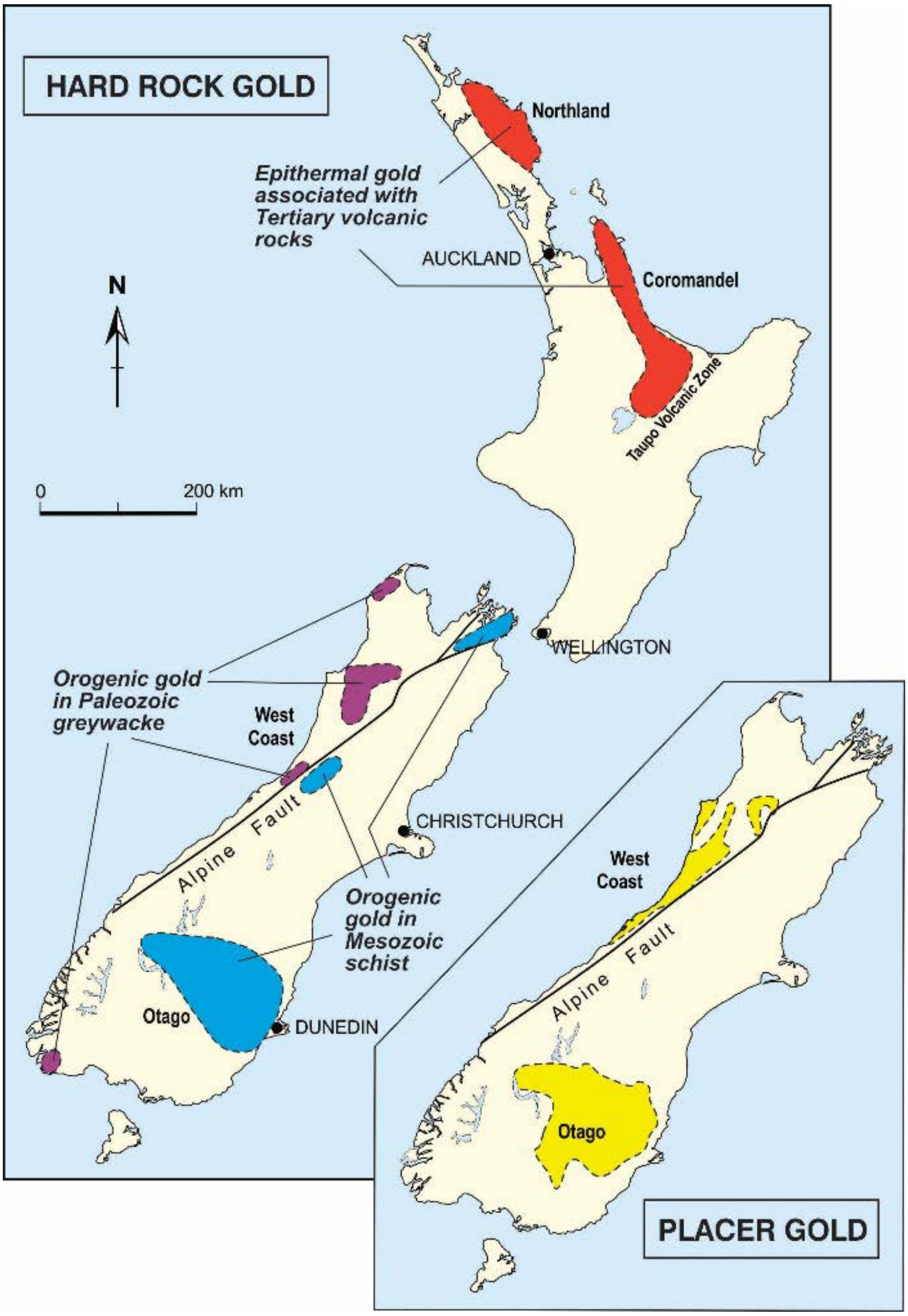

Figure 3.7 Main areas of past gold mining and potential for future discoveries (after Christie and Barker [2013]).

Table 3.28 New Zealand gold production (modified after Christie [2019]).

Gold Deposit Type	Host Rocks	Estimated Total Production	Estimated Total Production	Annual Production in 2022	Major Production	Minor Production	Significant Mines and Deposits
		1860–1952	1980–2022				
Orogenic	Paleozoic greywacke	2 Moz Au	0.7 Moz Au (Globe)	-	Reefton and Lyell goldfields	Golden Blocks, Mt Greenland and Preservation Inlet	Globe Progress, Blackwater, Keep-It-Dark, (Crushington mine group), Big River
	Mesozoic schist (and greywacke)	<1 Moz Au	>5 Moz Au (Macraes)	143,688 oz Au	Otago	Marlborough, Southern Alps	Macraes and Rise & Shine
Epithermal	Cenozoic volcanic rocks (and underlying Mesozoic basement greywacke)	8 Moz Au	>3 Moz Au (Waihi, Golden Cross, Karangahake and Broken Hills)	39,114 oz Au	Hauraki Goldfield	-	Waihi (Martha, Favona, Correnso), Golden Cross, Karangahake (Talisman), Komata, Thames mine group, Coromandel mine group
Placer	Cretaceous to Recent sedimentary rocks and sediments	16 Moz Au	>3 Moz Au >200 mining operations	31,776 oz Au	West Coast, Otago and Southland	West Nelson and Marlborough	Grey River, Arahura, Rimu, Ross, Mikonui, Shotover, Clutha, Nokomai, Wakaia

Key References: Williams (1974); Brathwaite and Pirajno (1993); Christie and Brathwaite (1996c, 1997a).

Table 3.29 New Zealand gold and silver production 2021 and 2022 (Source: New Zealand Petroleum & Minerals).

Metal	Mines	2021		2022	
		Quantity (oz)	**Value (NZ$)**	**Quantity (oz)**	**Value (NZ$)**
Gold	Waihi mines	27,685	69,376,628	39,114	110,910,386
	Macraes mines	130,330	332,840,799	143,688	412,346,542
	Other hard rock	1	2,438	5.5	14,675
	Placer West Coast	26,431	64,631,428	29,079	80,127,516
	Placer Otago/Southland	809	1,817,613	1214	3,032,261
	Placer Marlborough	11	27,147	14.8	39,803
	Placer Nelson/Tasman	1697	4,147,993	1468	3,857,539
		2021		**2022**	
	Total gold production (oz) and values ($NZ)	186,977	472,844,046	214,583	610,328,723
Silver	Waihi	93,045	3,254,829	120,058	4,118,710
	Macraes mine	5172	182,840	6041	155,571
		2021		**2022**	
	Total silver production (oz) and values ($NZ)	98,217	3,437,670	126,098	4,274,281
	Total gold and silver produced (oz) and values ($NZ)	285,181	476,281,716	340,681	614,603,004

3.8.3 Orogenic Shear Zone Au – Paleozoic

3.8.3.1 International Mineral Deposit Model

Features of the *Orogenic shear zone Au – Paleozoic* mineral deposit model are listed in Table 3.30.

Table 3.30 Features of international mineral deposit models equivalent to the *Orogenic shear zone Au – Paleozoic* mineral deposit model.

International Mineral Deposit Model – *Orogenic Shear Zone Au – Paleozoic*	
Reference	BCGS model I03 Turbidite-hosted Au veins (Lefebure and Höy 1996); Orogenic gold deposits (Groves et al. 1998; Goldfarb et al. 2001, 2005); and GNS Science turbidite-hosted mesothermal gold deposit Model 1A Paleozoic mesothermal Au (Christie 2002).
Description	Gold-bearing quartz veins, segregations, lodes and sheeted zones hosted by fractures, faults, folds and openings in anticlines, synclines and along bedding planes in turbidites and associated poorly sorted clastic sedimentary rocks (Lefebure and Höy 1996). The predominant host-rock types are greywacke, siliceous wacke, shale and carbonaceous shale. Bedded cherts, iron formations, fine-grained impure carbonate rocks; minor polymictic conglomerate, tuffaceous members and minor marine volcanic flows may also be part of the stratigraphic sequence. There are younger granitic intrusions in many belts. Metamorphic grade is generally greenschist but may reach amphibolite rank.

International Mineral Deposit Model – *Orogenic Shear Zone Au – Paleozoic*	
International Examples	Bendigo, Ballarat, Castlemaine and Stawell (Victoria, Australia) and Goldenville and other deposits in the Meguma Group (Nova Scotia, Canada).
Grade-Tonnage Model	USGS model 38a 50th percentile = 30,000 t at 16 g/t Au for 15,400 oz Au. Christie and Brathwaite (1999b) suggested that, based on some large occurrences in New Zealand (e.g. Blackwater >1.4 Moz Au production and resources; Globe Progress 1.2 Moz Au production), a more representative model was 250,000 oz of contained Au. A higher figure could be justified by production of correlative deposits in Victoria, which had a total historic production of more than 30 Moz, with 17 Moz produced from one goldfield, Bendigo.

3.8.3.2 New Zealand Occurrences of Orogenic Shear Zone Au – Paleozoic *Deposits*

Orogenic, turbidite-hosted, quartz-vein gold deposits in Western Province Ordovician metagreywacke include deposits at Golden Blocks and Aorere in Northwest Nelson; Mokihinui, Lyell, Reefton, Langdons and Mt Greenland on the West Coast; and Preservation Inlet in Fiordland (Figure 3.8a).

Characteristic features of the Western Province Paleozoic orogenic shear zone Au deposits and some exploration parameters were summarised by Christie (2019). The deposits exhibit many similarities to orogenic gold deposits in Victoria, Australia (e.g. Bendigo and Ballarat). Most are hosted in Ordovician greywacke and argillite (Greenland Group); notable exceptions are deposits at Golden Blocks and Preservation Inlet, which are hosted in graptolitic black slate-greywacke sequences of Golden Bay Group and Greenland group, respectively. The host rocks are weakly metamorphosed up to lower greenschist facies, with metamorphic mineral assemblages of quartz, albite, muscovite and chlorite. The deposits consist of quartz veins that were formed in steeply dipping shear and fault structures. In Blackwater, in the Reefton Goldfield, the largest vein averages 0.61 m wide, has a strike length of 1070 m, and was mined to a depth of 830 m, with an average grade of 21.9 g/t Au (15 g/t Au recovered grade). Additionally, some deposits such as Globe Progress have clay-rich breccia zones bordering the main quartz veins. The veins contain native gold, pyrite and arsenopyrite, with stibnite, chalcopyrite and galena locally present. The vein quartz typically exhibits ribbon-banded, crack-seal textures. Wallrock hydrothermal alteration consists of secondary illite/sericite, pyrite, chlorite and carbonate in narrow zones, generally less than 1 m in width, enveloping the quartz lodes. A much wider alteration halo is present at Globe Progress where alteration extends outward for c. 30 m from the main vein.

Reefton: The most important deposits are those in the Reefton area, where over 67 t of gold were produced from 84 mines between 1870 and 1951 (Barry 1993; Christie et al. 2006b). The gold quartz lodes are contained within a NNE-trending belt of Greenland Group metasedimentary rocks, some 34 km in length by 10 km in width, which is in intrusive and/or fault contact along its eastern side with granites of Devonian and Cretaceous ages (Figure 3.8b). To the south, the belt passes under Quaternary cover and to the north is cut off by granite.

The largest historic gold producers were the Blackwater (732,907 oz Au between 1909 and 1951) and Globe Progress (418,343 oz Au between 1879 and 1920) underground mines in the Reefton Goldfield. Between 2007 and 2015, Globe Progress was mined as an open pit to produce 536,494 oz Au (McIntosh and Cooksey 2016). At Blackwater, Federation Mining's recent Snowy River project has included a 3.3-km-long twin tunnel decline from the Snowy River to reach the Birthday Reef below the historic workings at the Blackwater gold mine.[1]

---

[1] https://federationmining.com.au/blackwater-gold/

They are currently undertaking an extensive diamond drilling programme to prepare a new Joint Ore Reserves Committee (JORC)-compliant Mineral Resource statement.

Lyell: A number of gold-bearing quartz lodes, varying from 0.3 to 6 m in width, were worked or prospected over a 5-km-long zone extending NNW from Lyell Creek to New Creek. Most of the production was from the United Alpine mine (2.504 t Au, 1874–1912) from a short but thick ore shoot mined down to 500 m (Downey 1928; Barry 1996). Around Lyell Creek, a phyllitic argillite unit carrying minor pyrite and arsenopyrite hosts the quartz lodes (M1321). In the New Creek area, the country rocks are intruded and baked (producing hornfels) by granite dikes (Morgan and Bartrum 1915). Modern exploration was summarised by Christie (2016a) and consisted predominantly of stream sediment and soil geochemical surveys.

Exploration: In addition to Tasman Mining's Snowy River project, in 2024, Rua Gold (Reefton Gold Ltd; Aldrich 2024) is exploring a northern group of vein systems, including the former Capleston, Murray Creek, Ajax and Crushington mining areas. They recently discovered a new vein system (Pactolus) southeast of the Capleston system. Siren Gold (Reefton Resources Pty Ltd) is exploring a southern group of vein systems, including the Auld Creek, Cumberland, Alexander River and Big River former mining areas. They have released several gold resource estimates for these areas (see Part 1, Table 7.2).

Opportunities: Crown Minerals (2002) mapped and ranked prospectivity based on a GIS-based study of research and exploration data (Figure 3.9).

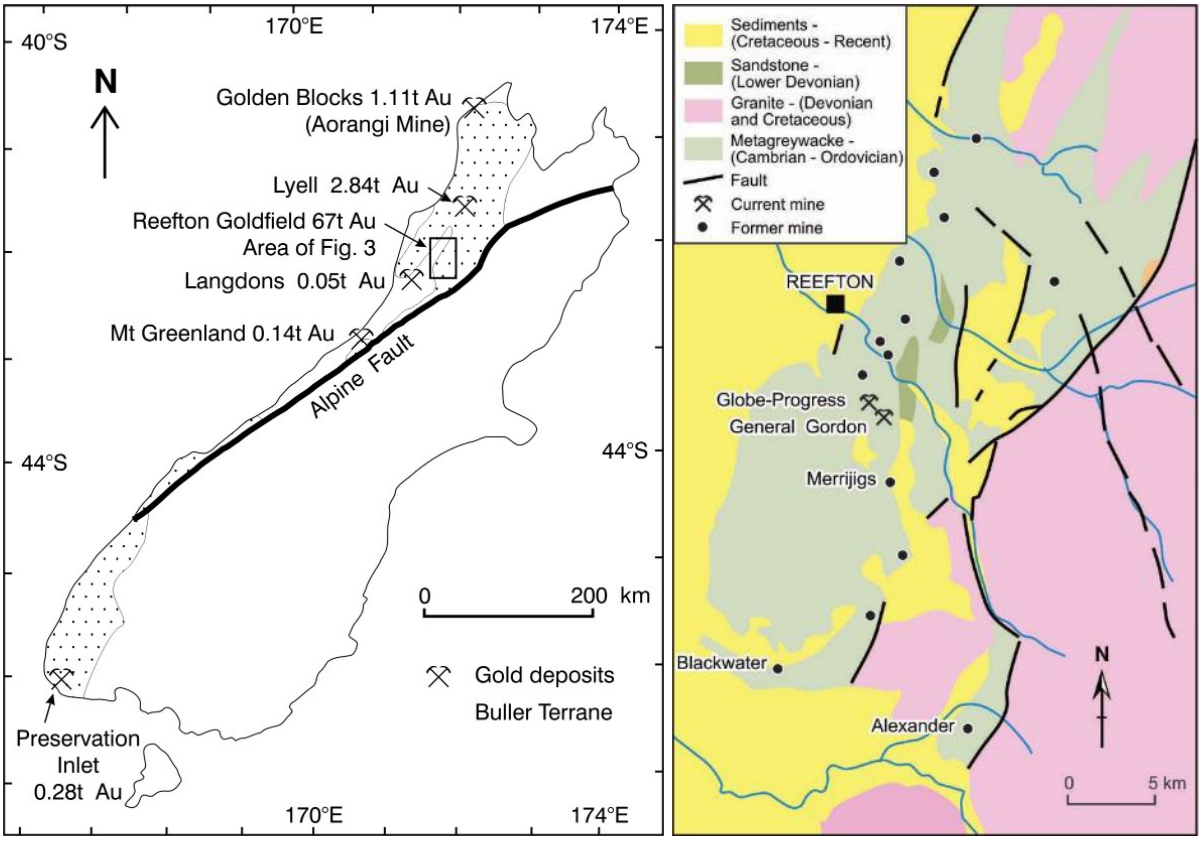

Figure 3.8 (a) Location of Paleozoic orogenic gold deposits, groups and their historic gold production up to 1952 (after Christie and Brathwaite [2003]). (b) Geology of the Reefton Goldfield (after Christie and Barker [2013]).

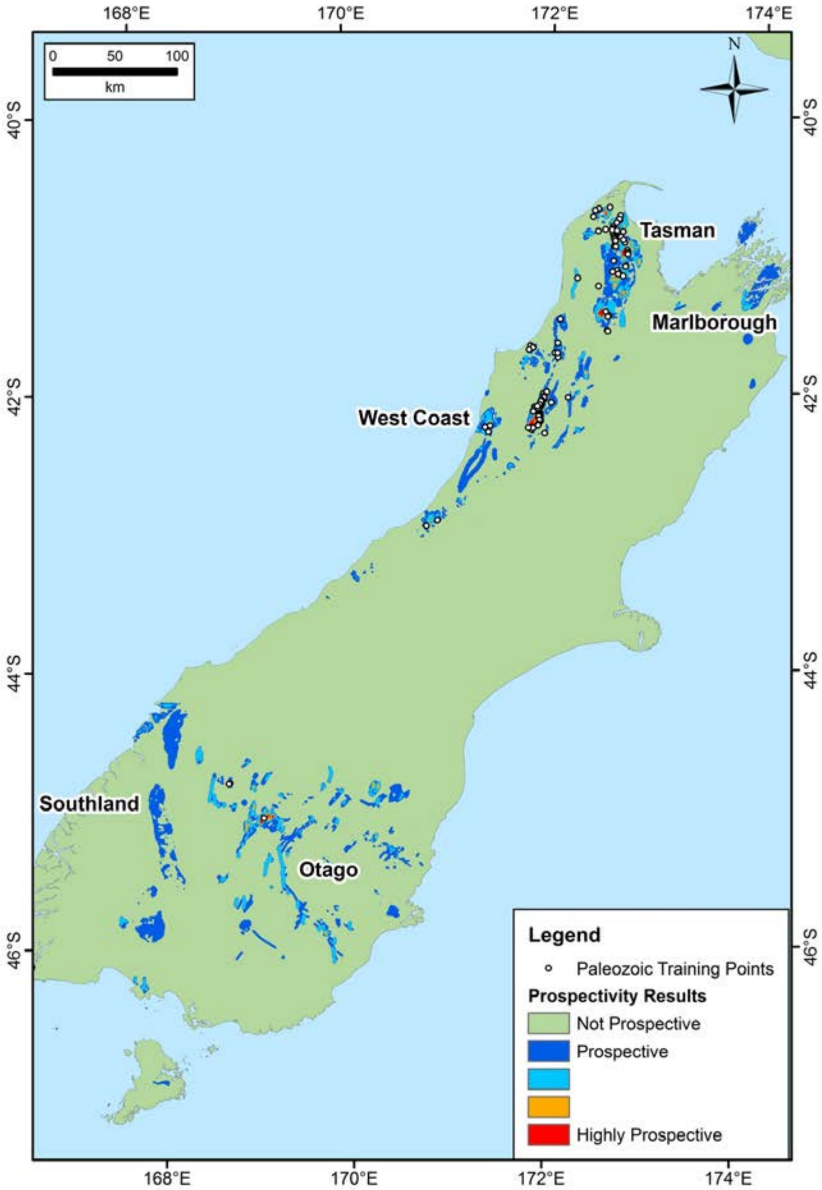

Figure 3.9 *Orogenic shear zone Au – Paleozoic* mineralisation prospectivity map showing the most prospective areas in red, moderately prospective areas in orange and light blue and areas above the prior probability in dark blue (after Kenex 2011).

Resource estimates for *Orogenic shear zone Au – Paleozoic* deposits in the Reefton Goldfield are listed in Table 3.31.

Table 3.31 Estimated resources in the Reefton orogenic gold deposits.

Deposit	Type	Resource	Categories	Date	Reference
Supreme	JORC	103,000 oz Au	Inferred Resources	April 2023	Siren Gold
Big River	JORC	105,000 oz Au	Inferred Resources	April 2023	Siren Gold
Blackwater / Snowy River project	JORC	785,000 oz Au	Indicated Resources + Inferred Resources	-	Federation Mining
Alexander River	JORC	170,000 oz Au	Inferred Resources	2023	Siren Gold

Occurrences of *Orogenic shear zone Au – Paleozoic* deposits are listed in Table 3.32.

Table 3.32 *Orogenic shear zone Au – Paleozoic* model occurrences in the Buller Terrane of the West Coast and Fiordland (data modified after Brathwaite and Pirajno 1993). Minerals: aspy = arsenopyrite; bourn = bournonite; cp = chalcopyrite; el = electrum; gn = galena; marc = marcasite; py = pyrite; sp = sphalerite.

Region	Area	Occurrence	MM [1]	GERM [2]	Production (t)	Deposit Form	Minerals Major (minor)	Host Rocks
West Nelson	-	Golden Blocks	A1	M25/e604–608	1.110 Au	Au quartz veins	marc, py, gold	Carbonaceous slate, quartzite (chert)
West Coast	Reefton Goldfield	Larry Creek-Caledonian group	A56	L30/e196, 197	0.164 Au	Au quartz veins	py, aspy, gold, (gn)	Greywacke, argillite
		Italian Gully group	A57	L30/e195	0.034 Au	Au quartz veins	py, aspy, sb, gold	Greywacke, argillite
		Capleston-Specimen Hill group	A58	L30/e203–211	4.325 Au	Au quartz veins	py, aspy, sb, gold	Greywacke, argillite
		Kirwan Hill	A60	L30/e198	0.342 Au	Au quartz veins	aspy, py, gold	Greywacke, argillite
		Wheel Creek	A61	L30/e250	-	Quartz veins	gold	Greywacke, argillite
		Murray Creek group	A62	L30/e136, 212–217	1.234 Au	Au quartz veins	py, sb, aspy, gold	Greywacke, argillite
		Ajax group	A63	L30/e219, 222	3.007 Au	Au quartz veins	py, aspy, sb, gold	Greywacke, argillite
		Blacks Point-Painkiller group	A64	L30/e231–234	0.221 Au	Au quartz veins	py, aspy, sb, gold	Greywacke, argillite
		Globe Progres	A68	L30/e235	13.198	Au quartz veins	py, aspy, sb, gold	Greywacke, argillite
		Crushington group	A65	L30/e223–225, 227, 228	12.635	Au quartz veins	py, aspy, sb, gold	Greywacke, argillite
		Maori Gully group	A67	L30/e229, 230, 296	0.013 Au	Au quartz veins	py, gold	Greywacke, argillite
		Merrijigs group	A69	L30/e236–239; L31/e18–24, 27	1.200 Au	Au quartz veins	py, aspy, sb, gold	Greywacke, argillite
		Big River group	A70	L31/e34–38	3.841 Au	Au quartz veins	py, sb, aspy, gold	Greywacke, argillite
		Millerton	A71	L31/e48	0.052	Au quartz veins	py, gold	Greywacke, argillite
		Alexander River group	A73	L31/e39	1.280 Au	Au quartz veins	py, aspy, sb, gold	Greywacke, argillite
		Blackwater	A72	L31/e29–31	22.810 Au	Au quartz veins	py, aspy, gold	Greywacke, argillite

Region	Area	Occurrence	MM [1]	GERM [2]	Production (t)	Deposit Form	Minerals Major (minor)	Host Rocks
West Coast	Lyell Goldfield	New Creek	A45	-	Very small	Au quartz veins	py, lollingite, gold	Greywacke and argillite (semi-schistose)
		Lyell	A46	L29/e134 (Alpine United mine)	2.841 Au	Au quartz veins	py, aspy, gold	Greywacke, argillite
	-	Mohikinui	-	L28/e559	-	-	-	-
		Red Queen	A41	-	0.103 Au	Quartz veins	py, gold	Greywacke, argillite
		Waimangaroa	A42	-	0.203 Au	Quartz veins, disseminated	py, gold	Hornfelsed greywacke
		Taffy [3]	A79	-	0.031 Au	Quartz vein stockwork	py, gold	Greywacke, argillite
		Croesus Knob [3]	A80	-	0.082 Au	Quartz vein	py, sp, gn, aspy, sb, gold	Greywacke, argillite
		Roaring Meg Creek [3]	A81	-	0.001 Au	Quartz veins	py, gold	Greywacke, argillite
		Minerva [3]	A82	-	0.024 Au	Quartz veins	py, gold	Greywacke, argillite
		Langdons	A83	K31/e64	0.049 Au	Au-Sb quartz veins	py, sb, gold	Greywacke, argillite
		Donellys Creek [3]	A85	-	0.024	Quartz veins	gold	Greywacke, argillite
		Mt. Greenland	A86	J33/e76, 78	0.137 Au	Au quartz veins	py, cp, (gold, bourn)	Greywacke, argillite
		Mt Rangitoto [3]	A87	-	-	Quartz-sulfide veins	py, sp, gn, aspy, cp, (el)	Greywacke, argillite, granite
Fiordland	Preservation Inlet	Cuttle Cove	A107	-	001 Au	Au quartz veins	Gold	Greywacke, argillite
		Morning Star	A108	B46/e5	0.234 Au	Au quartz veins	Gold	Graphitic slate
		Golden Site	A109	B46/e2	0.044 Au	Au quartz veins	Gold	Quartzose greywacke, slate

[1] MM = Metallogenic map code (Brathwaite and Pirajno 1993); [2] GERM = Geological Resource Map code; [3] The genesis of Taffy, Croesus Knob, Roaring Meg Creek, Minerva, Donellys Creek and Mt Rangitoto deposits is uncertain; these may be magmatic-related.

Key References: Downey (1928); Williams (1974); Brathwaite and Pirajno (1993); Christie et al. (2006b); Allibone et al. (2018a); Christie (2019).

3.8.4 Orogenic Shear Zone Au – Mesozoic

3.8.4.1 International Mineral Deposit Model

Features of the *Orogenic shear zone Au – Mesozoic* mineral deposit model are listed in Table 3.33.

Table 3.33 Features of international mineral deposit models equivalent to the *Orogenic shear zone Au – Mesozoic* mineral deposit model.

International Mineral Deposit Model – *Orogenic Shear Zone Au – Mesozoic*	
Reference	USGS model 36a low-sulfide Au-quartz veins (Cox and Singer 1986); BCGS model I03 turbidite-hosted Au veins (Lefebure and Höy 1996); Orogenic gold deposits (Groves et al. 1998; Goldfarb et al. 2001, 2005); and GNS Science turbidite-hosted mesothermal gold deposit Model 1B Mesozoic mesothermal Au (Christie 2002)
Description	Similar features to the Paleozoic orogenic shear zone gold model
International Examples	Alaska-Juneau, Treadwell and Kensington, Alaska; Mother Lode, Alleghany and Grass Valley, California (USA); Sheba, Mitchell and Hunter, Yukon (Canada).
Grade-Tonnage Model	Grade-tonnage data: Model 36a 50th percentile = 0.03 Mt and 16 g/t Au (15,400 oz Au), possible by-product Ag, Sb, W (Cox and Singer 1986). These low tonnage and grade figures are biased by data from historic small high-grade mines. Christie and Brathwaite (1999b) suggested that, based on the occurrence of Macraes (>5 Moz Au production) in Otago, a more representative model was 250,000 oz of contained Au.

3.8.4.2 New Zealand Occurrences of Orogenic Shear Zone Au – Mesozoic *Deposits*

Gold-bearing quartz lodes and disseminated mineralisation are hosted in the Mesozoic Haast Schist of Otago, Marlborough and the Southern Alps (Skinner and Brathwaite 1999; Craw and MacKenzie 2016; Christie 2019). Although they accounted for only 2.6% of New Zealand's total pre-1980 gold production, the deposit at Macraes is now New Zealand's largest known gold deposit worked by the largest operating gold mine. Most are Cretaceous age; however, Cenozoic-age gold-bearing quartz-carbonate veins in greenschist facies rocks of the Southern Alps are suggested as younger analogues of the Cretaceous-age vein deposits in Otago (Craw et al. 1987, 2006; Craw 2006; Pitcairn et al. 2006, 2014).

Characteristic features of the Eastern Province Mesozoic orogenic shear zone Au deposits and some exploration parameters were summarised by Christie (2019). The quartz veins are typically less than 1 m wide, localised along single or multiple parallel shear zones that generally dip steeply, have normal dip-slip displacements and are discordant to the schist foliation. A notable exception is at Macraes mine in Otago, where mineralisation occurs in shear veins and stockwork veins and is disseminated within the 26-km-long, NW-striking and gently south-dipping (c. 30°) Hyde–Macraes Shear Zone. Gold ore is mined from a series of open pits and an underground mine. The current mining operation began late in 1990 and has now produced more than 5 Moz Au, with a current annual production of c. 200,000 oz Au per year (Craw and MacKenzie 2016; Doyle et al. 2016).

Scheelite was mined from lodes at Wakamarina, Glenorchy, Macraes and Barewood and is present in many others. Stibnite was mined at Endeavour Inlet and Carrick and is also present at Macetown, Hindon, Nenthorn and Waipori. Many of the lodes were only worked in the oxidised zone and became uneconomic when the finer-grained, refractory gold of the primary zone was reached, typically only 20–30 m below the surface.

In 2024, exploration for Mesozoic-age orogenic gold deposits in Otago features Santana Minerals' resource definition and exploration on the Rise & Shine Shear Zone (Figure 3.10) and various projects by other companies, including: Midway Resources (Mareburn), Mineral Rangahau, Newpeak NZ (Garibaldi and Raggedy Range), KO Gold NZ (Rough Ridge South, Carrick Range, Tokomairiro, Glenpark and Smylers prospects), Gondwana Gold NZ (Teviot East), Nimitz Resources, New Age Exploration (Lammerlaw) and Lammerlaw Resources (Lammerlaw). New Age Exploration also has an exploration project in Marlborough.

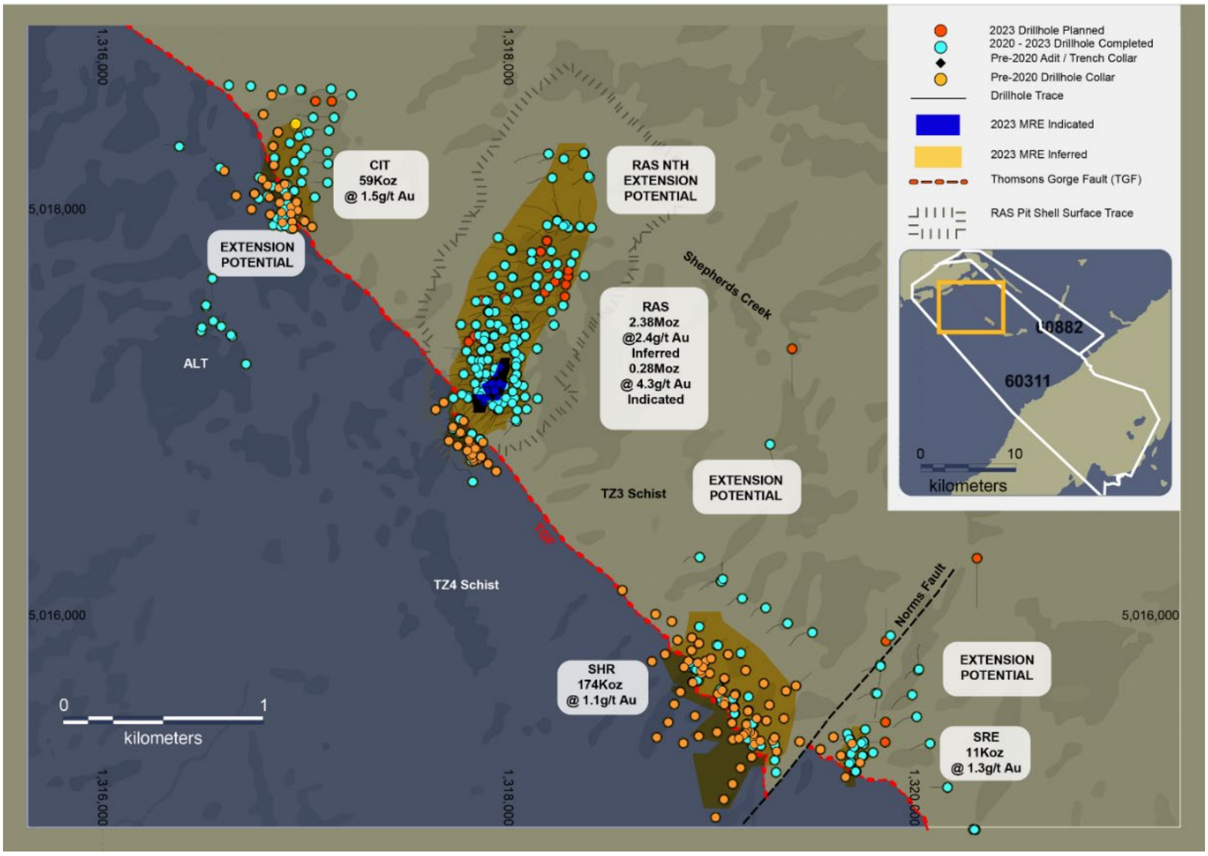

Figure 3.10 Drilling on the Bendigo-Ophir prospect on the Rise & Shine Shear Zone (RSSZ) (Source: Santana Minerals). The project contains a new Mineral Resource Estimate (MRE2024) of 2.45 Moz gold at 2.0g/t (0.5 g/t Au lower cut-off grade with top-cut), an estimate based on drill results to January 2024 and reported in February 2024. The Bendigo-Ophir resources occur in four deposits that extend in a northerly direction within the RSSZ, which hosts gold mineralisation over a recognised strike length of >20 km.

Studies by Crown Minerals (1992) and Kenex (2011) have mapped and ranked prospectivity based on a GIS-based study of research and exploration data (Figure 3.11).

Total gold production from the *Orogenic shear zone Au – Mesozoic* deposits is more than >5 Moz Au. Reported Reserve and Resource estimates are listed in Table 3.34, and a list of deposits is presented in Table 3.35.

Table 3.34 Joint Ore Reserves Committee (JORC)-compliant Reserve (0.6 Moz Au) and Resource (Moz) estimates for Macraes 31 December 2023 (Grant et al. 2024; OceanaGold 2024). See Figure 3.10 for Resources at Rise & Shine Shear Zone and Part 1 (Table 7.2) for Ophir.

Project Area	Reserves							Resources					
	Proven		Probable		Proven and Probable			Measured		Inferred		Inferred	
	(Mt)	(Au g/t)	(Mt)	(Au g/t)	(Mt)	(Au g/t)	(Au Moz)	(Mt)	(Au g/t)	(Mt)	(Au g/t)	(Mt)	(Au g/t)
Macraes underground	0.2	2.0	2.8	1.97	3.0	1.97	0.19	0.3	2.60	7.6	2.43	7.9	2.43
Macraes open pits	6.0	0.51	13.6	0.71	19.6	0.65	0.41	10.2	0.73	23.5	0.63	33.8	0.66
Macraes total	6.2	0.55	16.4	0.92	22.5	0.82	0.60	10.5	0.78	31.2	3.1	41.7	1.00

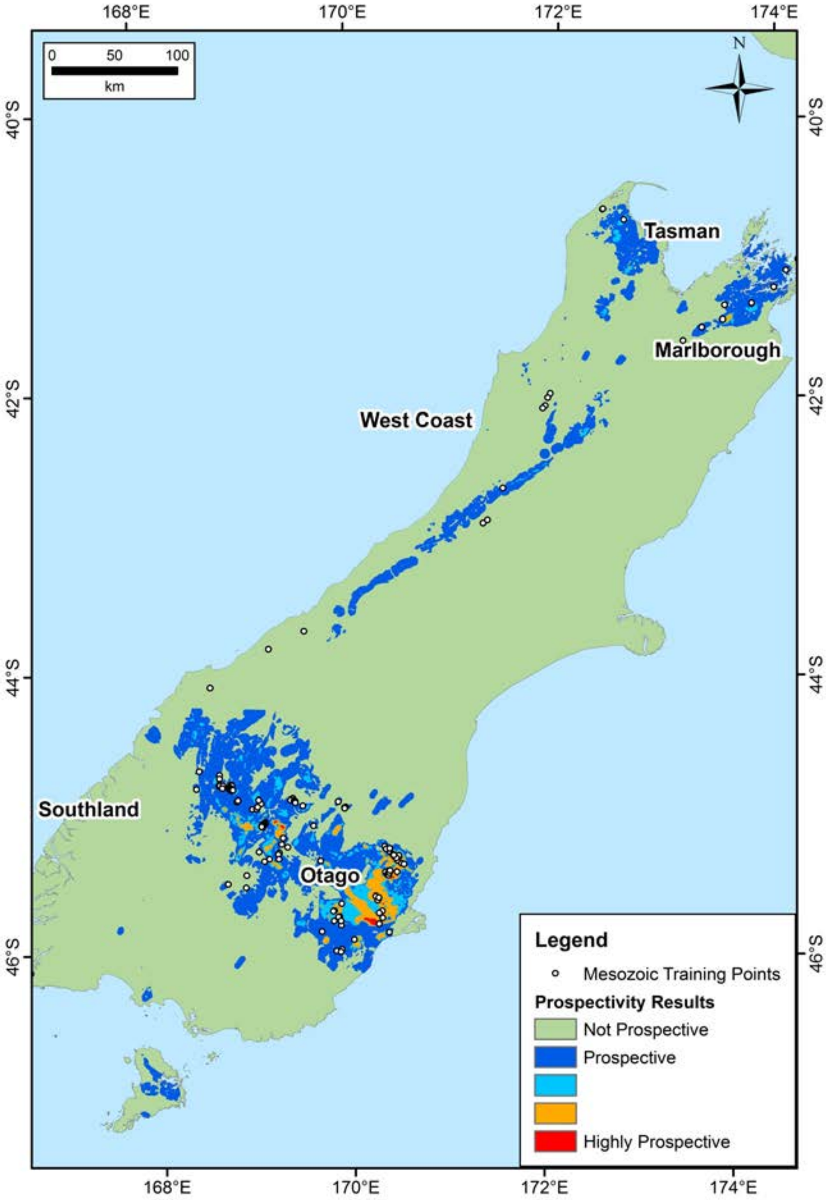

Figure 3.11 *Orogenic shear zone Au – Mesozoic* mineralisation results showing the most prospective areas in red, moderately prospective areas in orange and light blue and areas above the prior probability in dark blue over the extent of the study area (after Kenex [2011]).

Table 3.35 *Orogenic shear zone Au – Mesozoic* model occurrences in the Haast Schist and Mesozoic greywacke (data modified after Brathwaite and Pirajno [1993]). Minerals: aspy = arsenopyrite; Bi sulf = bismuth sulfides; bourn = bournonite; cp = chalcopyrite; gn = galena; py = pyrite; sb = stibnite; sch = scheelite; sp = sphalerite.

Region	Occurrence	MM [1]	GERM [2]	Production (t)	Deposit Form	Minerals Major (minor)	Host Rocks
Wellington	Galatea	C25	R27/e67	Very small	Au quartz veins	Gold	Argillite
	Terawhiti Ridge	C26	Q27/e12, 13	Very small	Au quartz veins	py, gold	Greywacke, argillite
	Breakneck Ridge, Terawhiti	C27	-	Very small	Au quartz veins	Gold	Greywacke, argillite
	Bakers Hill	C28	R27/e79	Very small	Au quartz veins	Gold	Greywacke, argillite
Marlborough	Ravenscliff	C29	-	Very small	Au quartz veins	Gold	Quartzofeldspathic chlorite schist
	Golden Point	C31	-	Very small	Au quartz veins	Gold	Quartzofeldspathic chlorite schist
	Waikakaho	C32	-	Very small	Au quartz veins	Gold	Quartzofeldspathic chlorite schist
	Wakamarina	C33	O27/e592, O28/e20	Very small	W–Au quartz veins	sch, py, gold	Quartzofeldspathic chlorite schist
	Sutherlands	C35	O28/e613	Very small	Au–W quartz veins	sch, gold	Quartzofeldspathic chlorite schist
	Jubilee	C36	O28/e16, 612	Very small	Au quartz veins	Gold	Quartzofeldspathic chlorite schist
	Top Valley	C37	O28/e615	Very small	W–Au quartz veins	sch, (aspy, py, sb)	Quartzofeldspathic chlorite schist
Southern Alps	Poerua	C38	K32/e83	0.001 Au	Au quartz veins	po, cp, (gold)	Quartzofeldspathic garnet schist
	Taipo Corner	C39	K33/e53	-	Au quartz veins	py, (gold)	Schistose greywacke
	McQuilkans Reef	C40	K33/e54	-	Au quartz veins	py, cp, hm, (gold)	Chlorite schist
	Gold Creek, Taipo River	C41	-	-	Au quartz veins	py, (gold)	Metagreywacke
	Wilsons Reward	C42	K33/e51	-	Au quartz veins	py, cp, (gold)	Greywacke, argillite
	Fiddes Reef	C43	K33/e50	-	Au quartz veins	py, cp, (gold)	Greywacke, argillite
	Pfahlerts Reef	C44	K33/e49	-	Au quartz veins	py, cp, hm, (gold)	Greywacke, argillite

Region	Occurrence	MM[1]	GERM[2]	Production (t)	Deposit Form	Minerals Major (minor)	Host Rocks
Otago	Bullendale, Skippers	C62	E41/e115–121, 123; F41/e58, 118	1.089	Au quartz veins	py, aspy, gold, (cp)	Pelitic schist and greenschist
	Copper Creek, Skippers	C63		Very small	Au quartz veins	py, sb, gold	Pelitic schist and greenschist
	Crystal Reef, Skippers	C64		0.05 Au	Au quartz veins	aspy, py, gold	Pelitic schist and greenschist
	Skippers Reef, Skippers	C65		0.07 Au	Au quartz veins	py, aspy, gold	Pelitic schist and greenschist
	Cotters Creek, Skippers	C66		Very small	Au quartz veins	py, aspy, gold	Pelitic schist and greenschist
	Macetown Field	C68	F41/e25–33, 35–57	1.283 Au	Au quartz veins	py, gold, (aspy)	Pelitic schist and greenschist
	Arrow Field	C69	F41/e59, 61–67	0.044 Au	Au quartz veins	py, gold	Quartzofelspathic and pelitic chlorite schist
	Carrick Field	C71	F41/e17; F42/e2–25	0.453 Au	Au quartz veins	py, gold, aspy, ±sb, (sp, cp)	Quartzofelspathic chlorite schist
	Bendigo Field	C72	G41/e16, 17	5.039 Au	Au quartz veins	aspy, gold, (gn, sp)	Quartzofelspathic chlorite schist
	Alta	C73	G41/e19	Very small	Au-W quartz veins	sch, gold	Quartzofelspathic chlorite schist
	Rise and Shine	C74	G41/e20	-	Au quartz veins	py, aspy, gold	Quartzofelspathic chlorite schist
	Conroys	C75	G42/e88	0.017 Au	Au quartz veins	py, gold	Quartzofelspathic and pelitic chlorite schist
	Whites Reef	C76	G42/e24	0.205 Au	Au quartz veins	py, gold	Quartzofelspathic and pelitic chlorite schist
	Nicholsons Reef	C77	G42/e26	Small	Au quartz veins	aspy, gold, (sch)	Quartzofelspathic chlorite schist
	Ophir	C78	G41/e90	0.038 Au	Au quartz veins	py, gold	Quartzofelspathic chlorite schist
	Rough Ridge (Oturehua)	C79	H41/e18, e72	0.147 Au	Au quartz veins	py, aspy, gold, (sp, bourn)	Quartzofelspathic chlorite schist
	Golden Gully	C81	H43/e8	0.007 Au	Au quartz veins	py, gold	Quartzofelspathic chlorite schist
	Nunns (Mareburn)	C82	I42/e76	0.020 Au	Au-W quartz veins	sch, gold	Quartzofelspathic chlorite schist

Region	Occurrence	MM [1]	GERM [2]	Production (t)	Deposit Form	Minerals Major (minor)	Host Rocks
Otago	Macraes field	C83	I42/e14, 28, 29, 46, 49, 53, 56	~640 W 3.331 Au	Au–W quartz veins and Au disseminated	py, aspy, sch, gold	Quartzofelspathic and pelitic (graphitic) chlorite schist
	Bonanza	C84	I43/e18	0.062 Au	Au quartz veins	py, gold	Quartzofelspathic chlorite schist
	Nenthorn	C85	I43/e23, 27–32	0.112 Au	Au quartz veins	py, sb, gold, (sp, Bi sulf, gn)	Quartzofelspathic chlorite schist
	Barewood	C86	I43/e25, 34, 36	0.420 Au 12 W	Au–W	py, sch, sb, gold, (gn)	Quartzofelspathic chlorite schist
	Hindon	C87	I43/e24	0.049 Au	Au quartz veins	py, sb, gold	Quartzofelspathic chlorite schist
	Saddle Hill	C88	I44/e38	0.016 Au	Au quartz veins	py, sch, gold	Quartzofelspathic chlorite schist
	Bootlemans, Waipori	C89	H44/e1	Very small	Au quartz veins	gold	Quartzofelspathic chlorite schist
	Cosmopolitan-Cox's, Waipori	C92	H44/e7	Very small	Au–W quartz veins	gold, sch	Quartzofelspathic chlorite schist
	Bella, Waipori	C94	H44/e8	Very small	Au–W quartz veins	gold, sch	Quartzofelspathic chlorite schist
	ABC-Nuggety Gully, Waipori	C95	H44/e42	Very small	Au quartz veins	gold	Quartzofelspathic chlorite schist
	QPC-Canton Waipori	C96	H44/e12	0.421 Au	Au quartz veins	py, aspy, gold	Quartzofelspathic chlorite schist
	Gabriels Gully	C99	H44/e13	0.035	Au quartz veins	gold	Pelitic chlorite schist
	Canada-Ocean View	C100	H45/e8	0.110	Au quartz veins	py, gold, (gn)	Quartzofelspathic chlorite schist

[1] MM = Metallogenic map code (Brathwaite and Pirajno 1993).

[2] GERM = Geological Resource Map code.

Key References: Brathwaite and Pirajno (1993); Craw and MacKenzie (2016); Allibone et al. (2017, 2018b); Christie (2019); Grant et al. (2024).

3.8.5 *Low-Sulfidation Epithermal Au–Ag* Deposits

3.8.5.1 International Mineral Deposit Model

Features of the *Low-sulfidation epithermal Au–Ag* mineral deposit model are listed in Table 3.36.

Table 3.36 Features of international mineral deposit models equivalent to the *Low-sulfidation epithermal Au–Ag* mineral deposit model.

International Mineral Deposit Model – *Low-Sulfidation Epithermal Au–Ag*	
Reference	USGS model 25c Comstock epithermal veins (Cox and Singer 1986) and BCGS model H05 Epithermal Au–Ag: low sulfidation (Lefebure and Höy 1996). Hot spring Au–Ag sub-class: • USGS model 25a Hot-spring Au–Ag (Cox and Singer 1986); and • BCGS model H03 Hot-spring Au–Ag (Lefebure and Höy 1996).
Description	Au + Ag ± Zn ± Pb ± Cu-bearing quartz veins, quartz vein stockworks and hydrothermal breccias hosted in andesitic, dacitic and rhyolitic lavas, breccias and tuffs, and adjacent basement sedimentary rocks, typically greywacke. The deposits form at depths between ~1500 m and the surface. The main ore minerals are electrum and acanthite with ubiquitous pyrite, and some deposits contain significant sphalerite, galena and chalcopyrite at depth. Quartz and calcite are the main gangue minerals, with Mn-carbonate, adularia and inesite present in some deposits. Bladed quartz and quartz pseudomorphous after calcite lattice textures are common in some veins. A Hot spring Au–Ag sub-class consists of deposits formed in the uppermost parts of epithermal systems that develop mineralised siliceous caps a few metres to hundreds of metres below surface, with subaerial siliceous sinter deposits at the water table and hydrothermal eruption breccias above. The mineralogy is typically pyrite, marcasite, electrum, stibnite, sulfosalt minerals, realgar and cinnabar in a gangue mineral assemblage of quartz and chalcedony, calcite, dolomite and barite.
International Examples	Comstock, Nevada (USA); Guanajuato (low Au:Ag ratio), Mexico; Hishikari (Japan). Hot spring examples include: McLaughlin, California; Round Mountain, Nevada; Delamar, Idaho (USA); Fruta del Norte (Ecuador).
Grade-Tonnage Model	See Lefebure and Höy et al. (1996, Table 9) for BCGS model H05. The median size of 41 low-sulfidation deposits listed for USGS model 25c was 0.77 Mt at 7.5 g/t Au and 110 g/t Ag (186,000 oz Au and 2,723,000 oz Ag) (Cox and Singer 1986). These figures are compiled from historic mining of small high-grade deposits and may be under-estimates.

3.8.5.2 New Zealand Occurrences of **Low-Sulfidation Epithermal Au–Ag** *Deposits*

Low-sulfidation epithermal Au–Ag deposits occur associated with Miocene to Recent volcanism in the Northland, Coromandel and Taupō volcanic zones (Figure 3.12), although all gold production has been from the Hauraki Goldfield in the Coromandel Volcanic Zone. In the Taupō Volcanic Zone, gold and silver deposition is occurring in active geothermal systems and provides key insights into epithermal processes that have aided gold exploration in New Zealand and elsewhere.

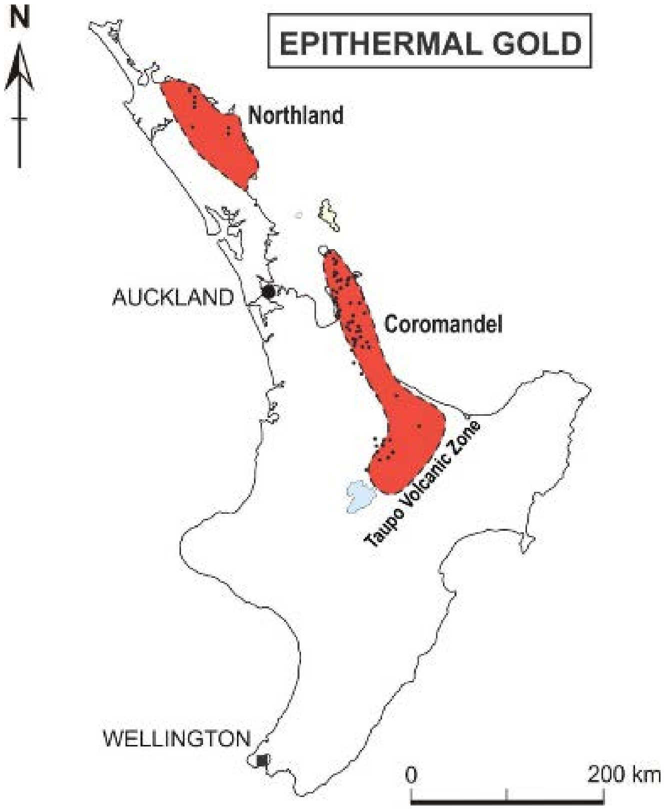

Figure 3.12 Location of epithermal gold deposits, North Island.

The Hauraki Goldfield, which extends southwards from Great Barrier Island to Muirs Reef near Te Puke (Figures 3.13 and 3.14), contains about 50 known epithermal Au–Ag quartz vein deposits that produced about 44 Moz of Au–Ag bullion between the 1860s and 1952, mostly from veins hosted by Miocene andesite and dacite. Miocene–Pliocene rhyolitic rocks host some deposits, but these were generally small producers. A new phase of mining commenced in 1988 at Waihi (Martha open pit), followed by Golden Cross in 1991, Favona in 2000, Trio (with Amaranth and Union) in 2003, Correnso in 2009 and continues today with underground mining under the Martha open pit. Characteristic features and a mineral systems exploration model for epithermal deposits in the Hauraki Goldfield was described by Christie (2019).

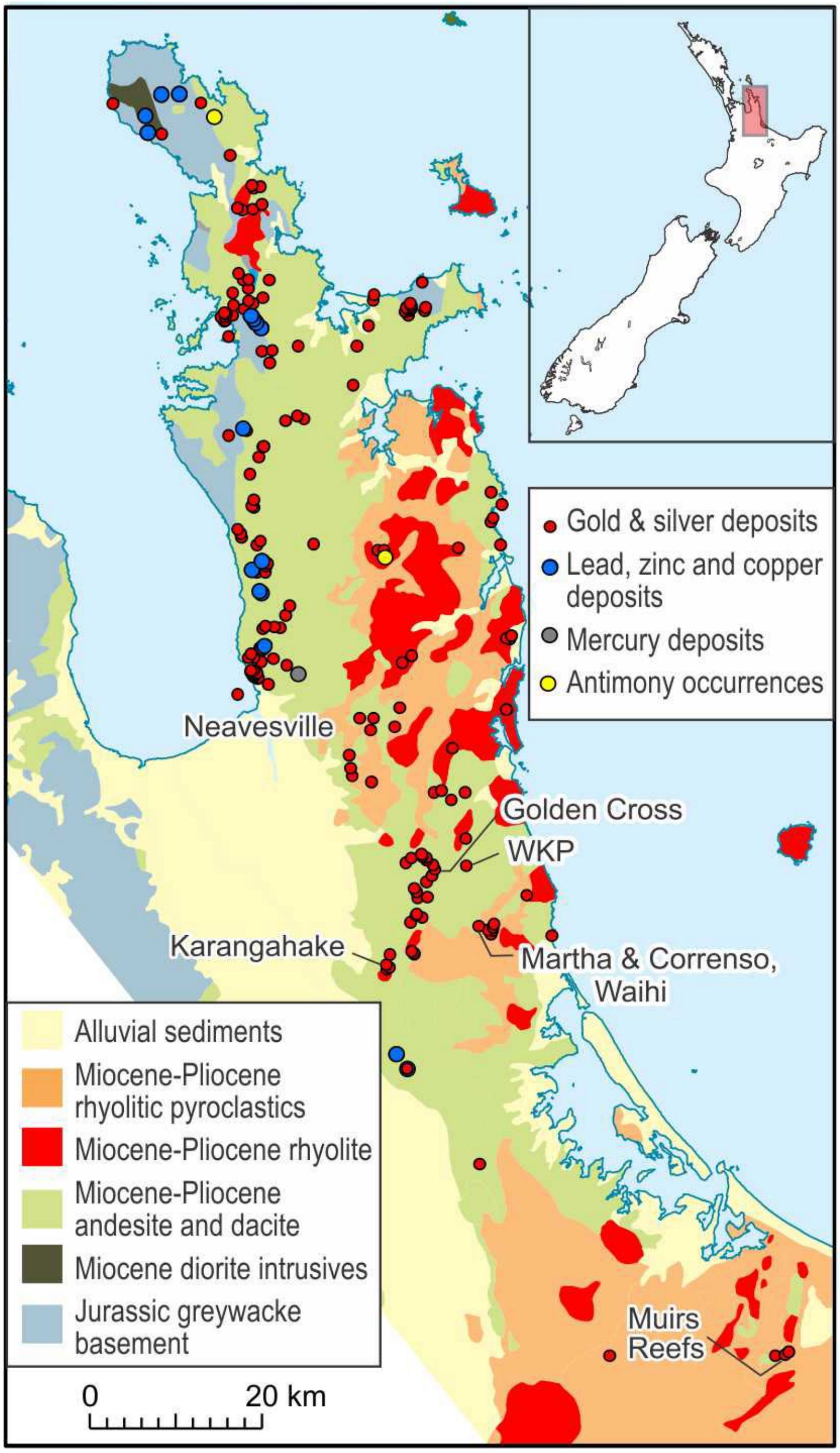

Figure 3.13 Geology and location of epithermal Au–Ag mines and prospects in the Coromandel Volcanic Zone – Hauraki Goldfield (after Christie et al. [2019]).

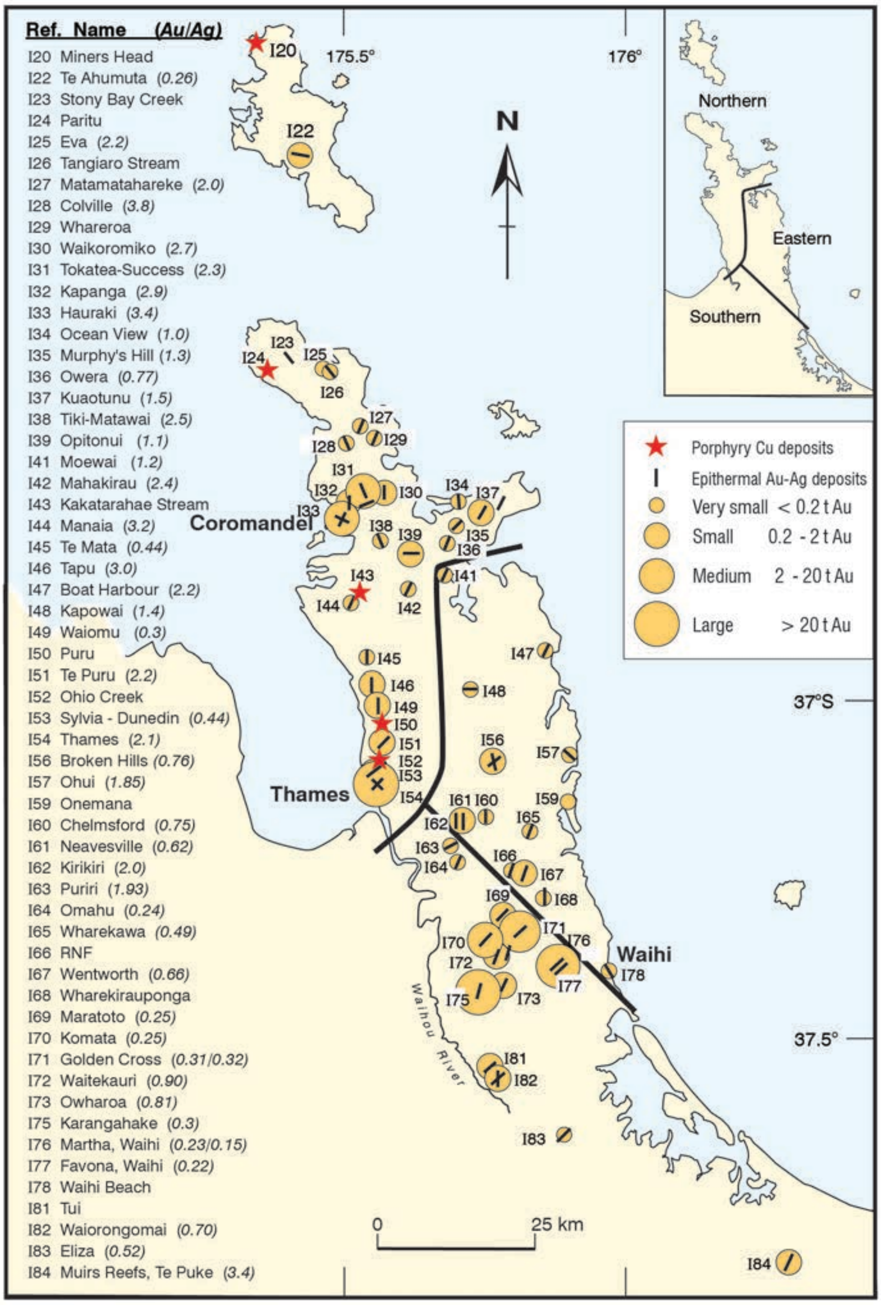

Figure 3.14 Relative size of past Au–Ag production, Au:Ag ratios and dominant vein orientation of epithermal Au–Ag deposits of the Hauraki Goldfield (after Christie et al. [2019]). The direction of bar symbols shows the dominant strike of veins. Deposit reference codes are from Brathwaite and Pirajno (1993). Inset map shows broad geographic groupings of deposits into northern, southern and eastern provinces based on mineralisation style described by Christie et al. (2006a, 2007).

In the Hauraki Goldfield, Au–Ag mineralised quartz veins generally dip steeply, strike N–ENE and are 1–5 m wide (rarely up to 30 m wide) and up to 800 m in length. Historically, these were mined over a vertical interval of 170–330 m but were mined up to 700 m at Karangahake and 600 m at Waihi. Individual deposits occur as vein systems occupying areas up to 3 km^2 (e.g. Waihi and Karangahake) that are surrounded by areas of up to 14 km^2 of hydrothermally altered rocks. The gold mostly occurs as electrum and is associated with pyrite, and, in some veins, various Ag-, Cu-, Pb- and Zn- sulfides and sulfosalts; selenides and tellurides. Silver to gold ratios are typically 1:1 to 10:1, but are much higher in the Ag-rich deposits at Te Ahumata and Maratoto. Base metal-rich mineralisation is present at the Tui Mine, which was mined for Pb-Zn-Cu during 1967–1972. Mineral exploration in the Hauraki Goldfield was reviewed by Barker and Christie (2016a).

The Martha mine is the largest producer, with 35 Moz of Au–Ag bullion produced from underground workings between 1878 and 1952 (Brathwaite and Faure 2002). The mine was re-opened in 1988 as an open pit. Four major veins (Martha, Welcome, Empire and Royal) and numerous smaller veins strike in a north-easterly direction and form a braided vein system over 2.5 km long by 600 m wide, extending to a depth of over 600 m. Several other vein systems have also been found in the Waihi area. Historical mining at Union Hill south of Martha focused on the Union and Amaranth veins. Underground mining has been on new discoveries of the Favona (-Moonlight), Trio and Correnso vein systems (Torckler et al. 2016) and more recently on veins adjacent and beneath the Marth open pit (Maton et al. 2021).

Small quantities of ore-grade gold and silver have been and are actively being deposited by geothermal fluids in several geothermal fields of the Taupō Volcanic Zone, including Ohaaki (Broadlands), Rotokawa, Waiotapu and Kawerau (Figure 3.15). Gold-silver mineralisation is also present in fossil geothermal systems in the Taupō Volcanic Zone, with 12 prospects identified and explored to date (Barker and Christie 2016b). Most drilling has been at the Ohakuri prospect.

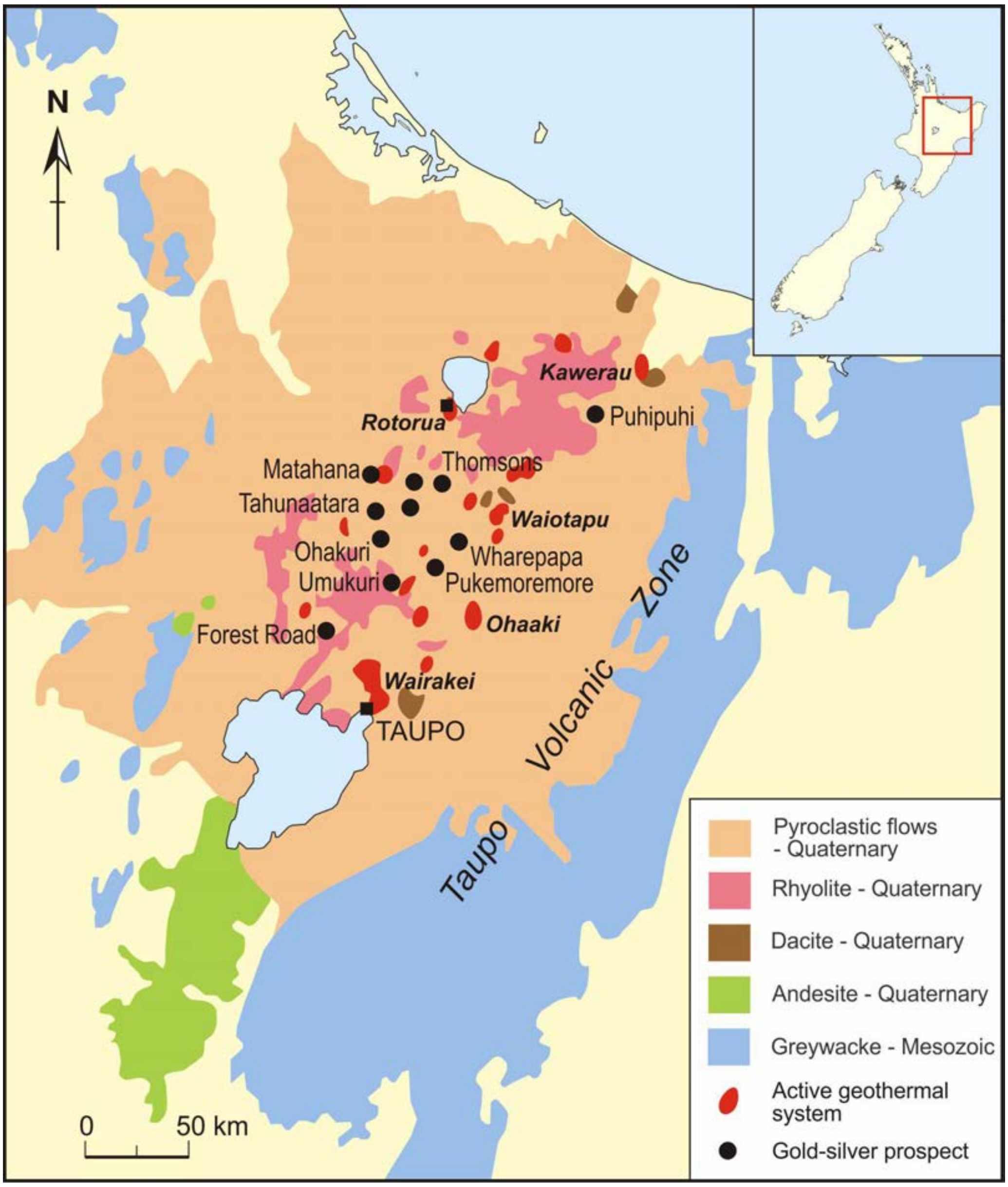

Figure 3.15 Geology and location of epithermal Au–Ag prospects and geothermal fields in the Taupō Volcanic Zone (after Christie et al. [2019]).

Ten hot-springs-type epithermal deposits have been explored in Northland (Barker and Christie 2016c). Small quantities of silver and mercury have been produced at Puhipuhi, north of Whangārei, and mercury at Ngawha, near Kaikohe (Figure 3.16). Reconnaissance drilling to intersect feeder quartz veins at Puhipuhi intersected potentially economic gold grades (Grieve et al. 2006; Beach and Hobbins 2016).

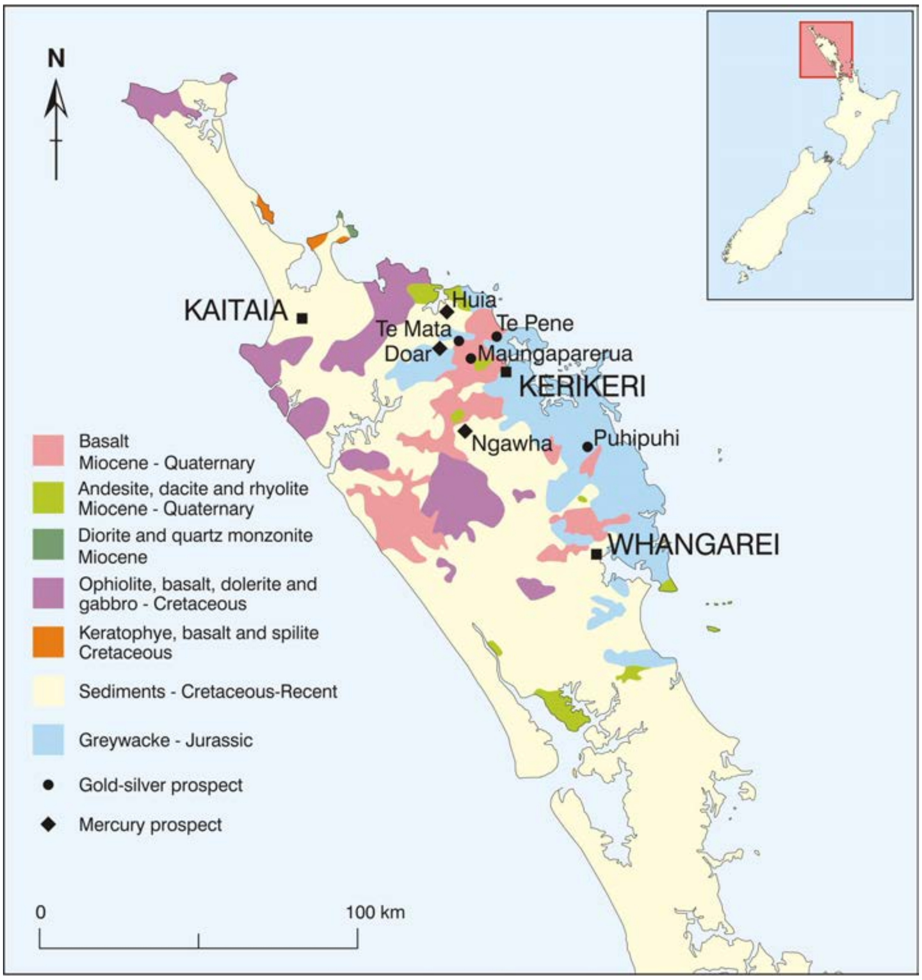

Figure 3.16 Geology and location of epithermal Au–Ag deposits and prospects in Northland (after Christie et al. [2019]).

Exploration highlights: From the 1980s, there has been a succession of new vein discoveries at Golden Cross and in the Waihi area that have since been mined. Significant resources have been discovered at the Wharekirauponga deposit north of Waihi, and the development of a new gold-silver mine is being investigated.

Current exploration: Exploration in the Hauraki Goldfield is currently being carried out by a number of companies, including OceanaGold (Dome Field, Twin Hills, Neavesville, Wharekirauponga, Waihi North and Golden Cross prospects), Reefton Gold (Rua Gold; Glamorgan prospect), Cladan Industries (Waihi East prospect), Nimitz Resources (Muirs Reefs prospect) and Midway Resources (Muirs area).

In Northland, exploration is being carried out by Mineralogy International on the Hazelbrook, Pungaere and Puhipuhi prospects.

In the Taupō Volcanic Zone, companies actively exploring include Bathurst Minerals, Green Energy Minerals (Maroa prospect), Mineralogy International (Paeroa Range, Whirinaki and Reporoa prospects) and Zedex Gold (Ohakuri and Forest Road prospects).

Production and resources: The mines in Waihi produce about 3700 kg Au (120,000 oz Au) and 7800 kg Ag (250,000 oz Ag) annually. Reported resource estimates are listed in Table 3.37.

Table 3.37 Resource estimates for *Low-sulfidation epithermal Au–Ag* deposits of the Hauraki Goldfield.

(A) Reserves – JORC									
Project Area	**Probable**			**Proven and Probable**					**Reference**
	(Mt)	**(Au g/t)**	**(Ag g/t)**	**(Mt)**	**(Au g/t)**	**(Ag g/t)**	**(Au Moz)**	**(Ag Moz)**	
Martha Underground	3.30	4.51	15	3.30	4.51	15	0.48	1.5	OceanaGold (2024)

(B) Resources – JORC									
Project Area	**Indicated**			**Inferred**			**Total**		**Reference**
	(Mt)	**(Au g/t)**	**(Ag g/t)**	**(Mt)**	**(Au g/t)**	**(Ag g/t)**	**(Au Moz)**	**(Ag Moz)**	
Wharekirauponga	2.0	15.9	25.3	1.2	9.0	17	1.41	1.3	OceanaGold (2024)
Martha Underground	6.4	5.43	23.0	3.1	4.7	24	1.62	7.2	OceanaGold (2024)
Martha and Gladstone open pits	7.2	1.73	12.7	5.7	1.7	16	0.7	5.9	OceanaGold (2024)
Talisman, Karangahake	-	-	-	-	-	-	0.350	-	New Talisman Gold Mines (2022)

(C) Resources – Estimates				
Project Area	**Au Moz**	**Ag Moz**	**Resource Type**	**References**
Monowai	0.169	0.921	Resources ‘defined and estimated’	Roberts (1989)
Thames area	0.894	0.500	Resources ‘defined and estimated’	Mineral Resources of New Zealand (1998)
Neavesville	0.260	0.868	-	ACM NZ Ltd (Barker and Christie 2016a)
Scotia, Waitekauri	0.146	0.100	Resources (inferred)	Couper (1981a, 1982, 1983)
Maoriland, Waitekauri	0.096	0.570	Resources (inferred)	Couper (1981b)
Waiorongomai	0.045	0.270	Resources (inferred) (plus Pb, Zn, Cu)	Bates (1989b)
Muirs	0.219	-	Resources (inferred resources)	Grieve (2013)

Occurrences of *Low-sulfidation epithermal Au–Ag* deposits are listed in Table 3.38.

Table 3.38 *Low-sulfidation epithermal Au–Ag* model occurrences (data modified after Brathwaite and Pirajno [1993]). Minerals: ac = acanthite; Ag sulf = silver sulfosalts; As = native arsenic; aspy = arsenopyrite; Au = native gold; Au-Ag-As-Se sulfosalts = gold-silver-arsenic-selenium sulfosalts ; Bi sulf = bismuth sulfides; bourn = bournonite; cin = cinnabar; cp = chalcopyrite; cup = cuprite; el = electrum; gn = galena; hes = hessite; Hg = native mercury; marc = marcasite; orp = orpiment; po = pyrrhotite; proust = proustite; py = pyrite; pyrarg = pyrargyrite; real = realgar; sb = stibnite; sch = scheelite; sp = sphalerite; tel = tellurides; td = tetrahedrite.

Region	Occurrence	MM[1]	GERM[2]	Production (t)	Deposit Form	Minerals Major (minor)	Host Rocks
Northland	Huia (Hazelbrook including Toolshed and Backyard)	-	P04/e56, 57)	-	Quartz veins	-	-
	Te Pene	I4	P04/e52	-	Quartz veins	sb, aspy	Greywacke
	Te Mata	I8	P04/e53, e59	-	Quartz veins	As, orp, real, py, marc	Siltstone, greywacke
	Ngawha	I12	P05/e92	33 Hg	Stratabound, disseminated	cin, hg, sb, real	Lake beds, basalt
	Waikaire	-	Q05/e27	-	Quartz veins	sb	Greywacke
	Puketotara	-	P05/e110	-	Quartz veins	cin, cp, sp, py, marc	Basalt and interbedded lacustrine sediments
	Parekura	-	Q05/e18	-	Quartz veins		Greywacke
	Puhipuhi	I14	-	0.042 Ag	Quartz veins	marc, py, proust, (td, cp)	Silicified greywacke
	Puhipuhi	I15	Q06/e73	55 Hg	Stratabound	cin, marc, py, sb	Sinter, silicified greywacke
Hauraki Goldfield	Te Ahumata	I22	S09/e1	1.295 Ag–Au	Quartz veins	py, pyrarg, el, sb, Ag sulfosalts	Rhyolite, andesite and porphyry
	Eva	I25	S10/e3	0.015 Au–Ag	Quartz vein	el	Andesite
	Tangiaro Stream	I26	T10/e12	-	Quartz vein	py, aspy, (td, cp, sp, el)	Andesite
	Matamataharakeke	I27	-	0.001 Au–Ag	Quartz veins	py, aspy, el	Andesite tuffs and breccias
	Colville	I28	T10/e23, 25, 26	0.021 Au–Ag	Quartz veins	py, aspy, el	Rhyolite flows and tuffs
	Whareoa	I29	T10/e33	0.010 Au–Ag	Quartz veins	aspy, (el, cp, sp, gn)	Andesite tuffs
	Waikoromiko	I30	T10/e71	0.409 Au–Ag	Quartz veins	py, el	Andesite

Region	Occurrence	MM[1]	GERM[2]	Production (t)	Deposit Form	Minerals Major (minor)	Host Rocks
Hauraki Goldfield	Tokatea – Success	I31	T10/e27, 29, 31, 69	3.940 Au–Ag	Quartz veins	py, el, (hes, sp, gn)	Andesite, greywacke
	Royal Oak, Coromandel	-	T10/e69	-	Quartz veins	py, el	Greywacke
	Kapanga, Coromandel	I32	T10/e20	2.299 Au–Ag	Quartz veins	py, aspy, el	Andesite breccias and flows
	Hauraki, Coromandel	I33	T10/e14–17	5.121 Au–Ag	Quartz veins	py, aspy, el, sb	Andesite breccias and flows
	Preceeces Point	-	T11/e13	-	Quartz veins	py, el	Andesitic tuff and lava flows
	Whangapoua (Lillis)	-	T10/e35	-	Quartz veins	py, el, Au	Andesite, tuff and breccia
	Ocean View, Matarangi	I34	T10/eI37, 38	0.487 Au–Ag	Quartz veins	el	Andesite
	Murphys Hill	I35	T11/e36	0.002 Au–Ag	Quartz veins	el	Andesite
	Owera	I36		0.069 Au–Ag	Quartz veins	el	Andesite
	Kuaotunu	I37	T10/e39–43, 48	2.969 Au–Ag	Quartz veins	py, el, (aspy, po, sp, gn)	Andesite, greywacke
	Tiki-Matawai	I38	T11/e75, 76	0.336 Au–Ag	Quartz veins	py, el, (sp, cp, gn, sb)	Greywacke
	Opitonui	I39	T11/e31	0.968 Au–Ag	Quartz veins	el	Andesite
	Moewai	I41	T11/e78	0.003 Au–Ag	Quartz veins	el	Andesite
	Mahakirau	I42	T11/e29, 30, 33	0.017 Au–Ag	Quartz veins	py, sb, el	Andesite flows and tuffs
	Manaia River	I44	T11/e23, 28	0.009 Au–Ag	Quartz veins	py, el	Greywacke
	Te Mata	I45	T11/e20–22, 24–27	0.007 Au–Ag	Quartz veins	el	Andesite
	Tapu	I46	T11/e15, 16, 18, 56, 68	0.472 Au–Ag	Quartz veins	py, el	Andesite, greywacke
	Boat Harbour	I47	T11/e37	0.003 Au–Ag	Quartz veins	py, el	Andesite, greywacke
	Kapowai	I48	T11/e34, 35, 47	0.192 Au–Ag	Quartz veins	py, el	Rhyolite tuffs and flows
	Te Puru	I51	T12/e20, 22–24, 88	0.487 Au–Ag	Quartz veins	py, el	Andesite flows and breccias
	Sylvia-Dunedin	I53	T12/e36, 46, 47	5.403 Au–Ag	Quartz veins	py, gn, sp, cp, el	Andesite

Region	Occurrence	MM[1]	GERM[2]	Production (t)	Deposit Form	Minerals Major (minor)	Host Rocks
Hauraki Goldfield	Thames	I54	T12/e17, 22, 54, 69–85, 87	67.095 Au–Ag	Quartz veins	py, pyrarg, el, sb, (sp, cp, td, tel)	Andesite flows and breccias
	Ohui	I57	T12/e42, 43, 44	0.007 Au–Ag	Quartz veins	py, el	Rhyolite
	Broken Hills	I56	T12/e37	1.716 Au–Ag	Quartz veins and breccia pipe	py, marc, ac, el, (Au-Ag-As-Se sulfosalts)	Rhyolite
	Golden Hills	I56	T12/e35				
	Onemana	I59	T12/e90, 93	-	hydrothermal breccia	py, el	Rhyolite, rhyolite breccia
	Chelmsford	I60	T12/e34	0.097 Au–Ag	Quartz veins	el	Andesite
	Neavesville	I61	T12/e30, 31	0.097 Au–Ag	Quartz veins	py, el, mrc, (cp)	Rhyolite tuffs, andesite
	Kirikiri	I62	T12/e29	0.017 Au–Ag	Quartz veins	el	Andesite
	Puriri	I63	T12/e26	0.050 Au–Ag	Quartz veins	py, el	Andesite
	Omahu	I64	T12/e27, 28, 32	0.062 Au–Ag	Quartz veins	py, el	Andesite
	Wharekawa	I65	-	0.410 Au–Ag	Quartz veins	el	Rhyolitic pyroclastics
	RNF	I66	T12/e91	-	Quartz veins	py, el	Rhyolitic pyroclastics, andesite
	Wentworth	I67	T12/e40, 41	0.516 Au–Ag	Quartz veins	py, el	Andesite
	Wharekirauponga	I68	T12/e45	0.001 Au–Ag	Quartz veins	py, el	Rhyolite flows and tuffs
	Waiharakeke	-	T13/e6	-	Quartz veins	-	Dacite flows and tuff
	Maratoto group	I69	T13/e29, 34, 43–46	5.972 Au–Ag	Quartz veins	py, marc, gn, sp, cp, ac, hes, el	Andesite breccias and flows
	Komata	I70	T13/e27	16,668 Au–Ag	Quartz veins	py, ac, el, (sp, gn, cp)	Rhyolite, andesite breccias and flows
	Golden Cross	I71	T13/e41, 42	12,204 Au–Ag	Quartz veins	py, marc, el, ac, (pyrarg)	Andesite and dacite lavas and pyroclastics
	Waitekauri group	I72	T13/e28, 30, 33, 37, 38, 40	4.437 Au–Ag	Quartz veins	py, cp, gn, sp, el	Andesite and dacite breccia

Region	Occurrence	MM [1]	GERM [2]	Production (t)	Deposit Form	Minerals Major (minor)	Host Rocks
Hauraki Goldfield	Owharoa	I73	T13/e31	3.865 Au–Ag	Quartz veins	py, marc, ac, el, (cin)	Dacite and rhyodacite
	Rahu	-	T13/e57	-	Quartz veins	py, marc, ac, el	Rhyolitic tuff and sediment
	Karangahake	I75	T13/e58, 59, 61	126,712 Au–Ag	Quartz veins	py, sp, gn, cp, el, ac	Andesite breccias and flows overlain by rhyolite lava
	Martha, Waihi	I76	T13/e47–52	1122.223 Au–Ag	Quartz veins	py, sp, gn, el, ac	Quartz andesite flows and breccias
	Union Hill, Waihi	I77	-	4.376 Au–Ag	Quartz veins	py, cp, gn, sp, ac	Andesite flows
	Favona	-	T13/e52	-	Quartz veins	py, cp, gn, sp, ac	Andesite flows
	Corenso	-	-	-	Quartz veins	py, cp, gn, sp, ac	Andesite flows
	Waihi Beach	I78	U13/e1	0.001 Au–Ag	Quartz veins	py, el	Rhyolite
	Tui	I81	T13/e53	7291 Zn 4424 Pb 404 Cu	Quartz veins	sp, gn, cp, py, (marc, td, cin)	Andesite flows and pyroclastics
	Waiorongomai	I82	T13/e54	2.123 Au–Ag	Quartz veins	py, cp, gn, sp, el	Dacite, andesite flows
	Eliza	I83	T14/e100	0.001 Au–Ag	Quartz veins	py, el, (sp, gl, cp)	Andesite
	Muirs Reefs (Te Puke)	I84	U14/e100, 101	1.685 Au–Ag	Quartz veins	py, el	Andesite overlain by rhyolite
Taupō Volcanic Zone	Puhipuhi or Goldmine Hill	-	V16/e12	-	Quartz veins	py (el, ac)	Dacite
	Horohoro	I90	-	-	Chalcedony lens, sinter	py	Sinter, pumice, sand and gravel
	Matahana	-	-	-	Silicified breccia, quartz veins	py	Ignimbrite, breccia
	Thomsons	-	-	-	Quartz veins, sinter	py	Ignimbrite rhyolite
	Ohakuri	I93	U17/e105	-	Quartz and pyrite veins	py	Ignimbrite
	Wharepapa	-	-	-	Quartz veins	py	Ignimbrite
	Umukuri	-	-	-	Sinter, veins	py	Ignimbrite
	Forest Road	-	-	-	Quartz veins	py	Ignimbrite

[1] MM = Metallogenic map code (Brathwaite and Pirajno 1993).

[2] GERM = Geological Resource Map code.

Opportunities: Crown Minerals (2003) mapped and ranked prospectivity based on a GIS-based study of research and exploration data (Figure 3.17).

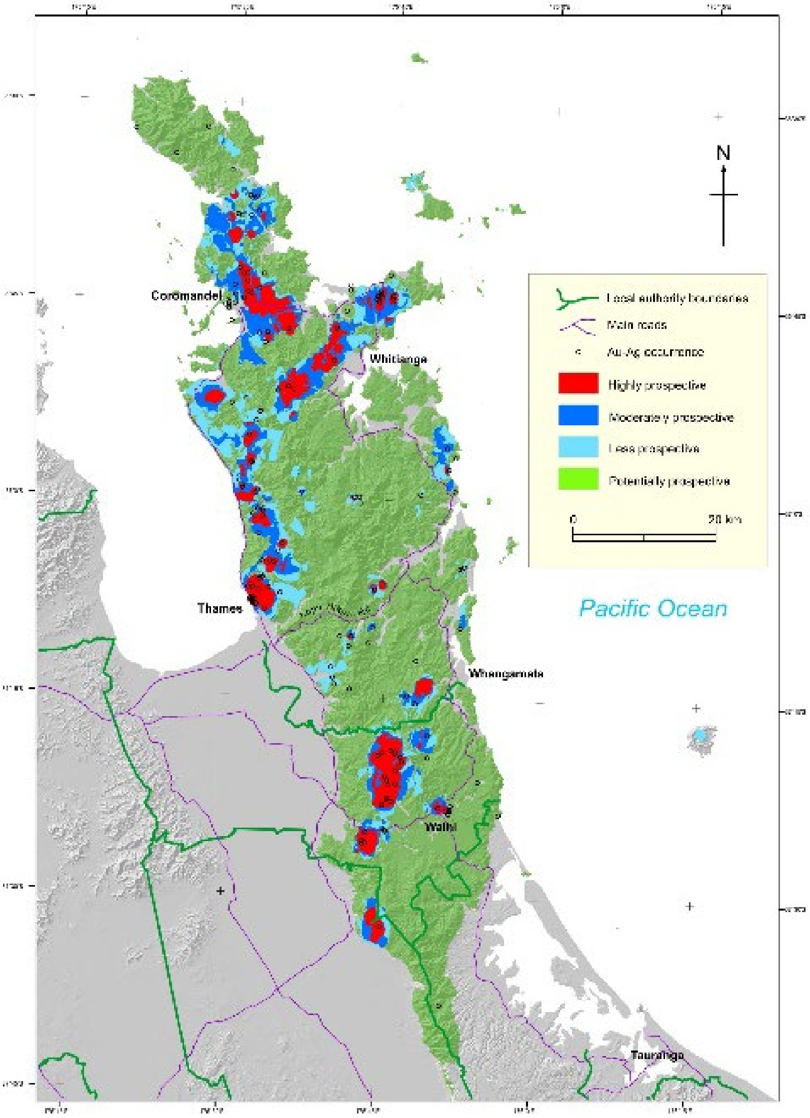

Figure 3.17 Prospectivity map for epithermal gold-silver deposits in the Coromandel Peninsula, Hauraki Goldfield (modified after Rattenbury and Partington [2003]).

Key References: Downey (1935); Brathwaite et al. (1989); Brathwaite and Pirajno (1993); Christie et al. (2007); Christie (2019).

3.8.6 Intermediate-Sulfidation Epithermal Vein Zn-Pb-Cu-Ag-Au

3.8.6.1 International Mineral Deposit Model

Features of the *Intermediate-sulfidation epithermal vein Zn-Pb-Cu-Ag-Au* model are listed in Table 3.39.

Table 3.39 Features of the *Intermediate-sulfidation epithermal vein Zn-Pb-Cu-Ag-Au* international mineral deposit model.

International Mineral Deposit Model – *Intermediate Sulfidation Epithermal Vein Zn-Pb-Cu-Ag-Au*	
Reference	USGS model 25b Creede epithermal veins (Cox and Singer 1986)
Description	Sulfide-rich veins containing sphalerite, galena, silver sulfide and sulfosalt minerals in a quartz and carbonate gangue. These veins are typically hosted in volcanic rocks but can also be hosted by metasediments and subvolcanic intrusive rocks. The veins are typically steeply dipping, narrow, tabular or splayed. They commonly occur as sets of parallel and offset veins. Individual veins vary from centimetres up to more than 3 m wide and can be followed from a few hundred to more than 1000 m in length and depth. Veins may grade into broad zones of stockwork or breccia.
International Examples	Comstock and Tonopah, Nevada; Creede, Colorado (USA); Fresnillo, Guanajuato, Pachuca and Tayoltita (Mexico); Casapalca and Finlansdia (Peru); Toyoha (Japan); Baguio (Philippines)
Grade-Tonnage Model	There is no published grade-tonnage model. Among the largest deposits: Comstock Lode, USA, produced ~8.3 Moz Au and ~192 Moz Ag; Tayoltita, Mexico, produced 4.89 Moz Au and 305 Moz Ag; Tonopah, USA, produced ~1.86 Moz Au and ~174 Moz Ag; Creede, USA, produced ~0.15 Moz Au and ~84 Moz Ag; Guanajuato, Mexico, produced 5.14 Moz Au and 1.1 Goz Ag; Pachuca-Real del Monte district, Mexico, produced 6.4 Moz Au and 1.3 Goz Ag (John et al. 2018). Peñasquito prospect, Mexico, has pre-mining reserves of ~9.7 Moz Au, ~530 Moz Ag, ~1.7 Mt Pb and ~4.1 Mt Zn.

3.8.6.2 New Zealand Occurrences of Intermediate-Sulfidation Epithermal Vein Zn-Pb-Cu-Ag-Au *Deposits*

Some of the epithermal quartz vein deposits in the Hauraki Goldfield are rich in base metals (Table 3.40); note that some are also listed as low-sulfidation epithermal Au–Ag deposits in Table 3.38). Tui was mined during 1967–1972, producing zinc, lead, copper, silver and gold concentrates exported to Japan.

Table 3.40 *Intermediate-sulfidation epithermal Zn Pb-Cu-Ag-Au* occurrences (data modified after Brathwaite and Pirajno [1993]). Minerals: cin = cinnabar; cp = chalcopyrite; el = electrum; gn = galena; marc = marcasite; py = pyrite; sp = sphalerite; td = tetrahedrite.

Region	Occurrence	MM [1]	GERM [2]	Production (t)	Deposit Form	Minerals Major (minor)	Host Rocks
Hauraki Goldfield (Coromandel Volcanic Zone)	Stony Bay-Ongohi Stream, Paritu	I23	S10/e5, 6, 8	None	Quartz veins	gn, sp, cp, py	Quartz diorite, greywacke
	Petote and Aitken streams, Coromandel	-	T10/e50, 51, 52, T11/e46	None	Quartz veins	gn, sp, cp, py	Greywacke
	Te Mata	-	T11/e20–22, 24–27	-	Quartz veins	py, gn, sp, cp, el	Andesite flows and breccias
	Tapu	-	T11/e15, 16, 18, 56, 68	-	Quartz veins	py, gn, sp, cp, el	Andesite flows and breccias
	Te Puru	I51	T12/e20, 22–24, 88	0.487 Au–Ag	Quartz veins	py, el	Andesite flows and breccias
	Sylvia	I53	T12/e46	5.403 Au–Ag	Quartz veins	py, gn, sp, cp, el	Andesite
	Tui	I81	T13/e53	7291 Zn	Quartz veins	sp, gn, cp, py, (marc, td, cin)	Andesite flows and pyroclastics
	Wairorongomai	I82	T13/e54	2.123 Au–Ag	Quartz veins	py, cp, gn, sp, el	Dacite, andesite flows

[1] MM = Metallogenic map code (Brathwaite and Pirajno 1993).

[2] GERM = Geological Resource Map code.

3.8.7 High-Sulfidation Epithermal Au–Ag

3.8.7.1 International Mineral Deposit Model

Features of the *High-sulfidation epithermal Au–Ag* mineral deposit model are listed in Table 3.41.

Table 3.41 Features of international mineral deposit models equivalent to the *High-sulfidation epithermal Au–Ag* model used in this report.

International Mineral Deposit Model – *High-Sulfidation Epithermal Au–Ag*	
Reference	USGS model 25e Epithermal quartz-alunite Au (Cox and Singer 1986); and BCGS model H04 Epithermal Au-Ag-Cu: high sulfidation (Lefebure and Höy 1996).
Description	High-sulfidation, acid-sulfate or quartz-alunite deposits are characterised by the presence of sulfide minerals with a high sulfur/metal ratio, such as enargite/luzonite and tetrahedrite. They are associated with calcalkalic andesite, dacite and rhyodacite and were probably formed within or below stratovolcanoes and above porphyry copper systems. Advanced argillic alteration with alunite and pyrophyllite, as well as acid-leached rock represented by 'vugg', 'slaggy', residual silica are characteristic.
International Examples	Goldfield, Nevada; Summitville, Colorado (USA); Nansatsu (Japan); El Indio (Chile); Temora, New South Wales (Australia); Yanacocha (Peru); Pueblo Viejo (Dominica); Lepanto and Nalesbitan (Philippines)
Grade-Tonnage Model	Model 25e 50th percentile = 1.6 Mt and 8.4 g/t Au and 18 g/t Ag (432,154 oz Au, 926,045 oz Ag), possible by-product Cu (Cox and Singer 1986). See also BCGS model H04 in which Panteleyev (Lefebure and Höy 1996) noted that underground mines range in size from 2 to 25 Mt, with grades from 178 g/t Au, 109 g/t Ag and 3.87% Cu (El Indio) to 2.8 g/t Au, 11.3 g/t Ag and 1.8% Cu (Lepanto), whereas open-pit mines typically grade about 4 g/t Au. Recently, some large high-sulfidation gold deposits have been developed in Peru, ranging in size up to the Yanacocha deposit, which contains more than 30 Moz of Au.

3.8.7.2 New Zealand Occurrences of High-Sulfidation Epithermal Au–Ag *Deposits*

There are no known unequivocal examples of *High-sulfidation epithermal Au–Ag* deposits in the Hauraki Goldfield, but the characteristic style of alteration associated with these deposits is present in Coromandel Group rocks at Lookout Rocks, Pumpkin Hill and Black Jack (Kuaotunu). Also, enargite, a characteristic mineral of high-sulfidation deposits, is present in some of the Thames veins.

Given the likely proximity to porphyry-copper-style mineralisation, high-sulfidation epithermal deposits are more likely to be found in the eastern parts of Northland and western parts of the Hauraki Goldfield because of their deeper levels of erosion, exposing the deeper style of mineralisation. There is also potential for undiscovered deposits buried beneath cover rocks.

3.8.8 Reduced-Granitic Intrusion-Related Au

3.8.8.1 International Mineral Deposit Model

Features of the *Reduced-granitic intrusion-related Au* mineral deposit model are listed in Table 3.42.

Table 3.42 Features of international mineral deposit models equivalent to the *Reduced-granitic intrusion-related Au* model used in this report.

International Mineral Deposit Model – *Reduced-Granitic Intrusion-Related Au*	
Reference	Reduced granitic intrusion-related Au (Thompson and Newberry 2000; Hart 2007); intrusion-related Au (Lang et al. 2000; Lang and Baker 2001; Hart 2005); granite-related Au deposits associated with W granites (Baker et al. 2005); BCGS model L02 Plutonic related Au quartz veins and veinlets (Lefebure and Hart 2005)
Description	Quartz vein stockworks with Au-Bi-Mo-W-Sb ± Sn associated with moderately reduced (ilmenite-series) granites and granodiorites. The main metallic minerals are pyrrhotite, pyrite, arsenopyrite, molybdenite, scheelite and bismuth and telluride minerals.
International Examples	Fort Knox, Alaska; Bald Mountain, Nevada (USA); Dublin Gulch and Scheelite Dome (intrusion-related gold deposit and skarn), Yukon (Canada); Timbarra, New South Wales (Australia); Morila in Mali and Bonikro in Côte d'Ivoire (both intrusion-related gold deposit over-printed with orogenic gold) (West Africa)
Grade-Tonnage Model	The main example is Fort Knox, Alaska, which has resources of approximately 6.5 Moz Au. Other deposits include Donlin Creek (10.4 Moz Au), Vasilkovskoe (9.5 Moz Au), Pogo (4.9 Moz Au) and Kidston (4.5 Moz Au).

3.8.8.2 New Zealand Occurrences of Reduced-Granitic Intrusion-Related Au *Deposits*

There are no known examples of these types of deposits in New Zealand, with the one known intrusion-related gold deposit, Sams Creek, better classified as an alkali intrusion-related gold deposit (discussed in the next section).

In exploration for reduced granitic intrusion-related gold, GIS prospectivity modelling by Kenex using regional geochemical data revealed an association of Au and Bi in several granite intrusions of the West Coast region (Mustard and Partington 2005; Partington 2009). The Buller George, Mt Rangitoto and Mt Greenland areas were considered the most prospective. Past stream-sediment surveys (e.g. REGCHEM database; Christie and Stewart 2016) returned concentrations of up to 70 ppm Bi in the Buckland Granite and 150 ppm Bi in the Mt Rangitoto area. Follow-up sampling and analyses of granites from Mt Greenland and the Buckland granite by Auzex Resources identified bismuth and tellurium in analyses of disseminated pyrite and arsenopyrite (Mustard and Partington 2005).

3.8.9 Alkali Intrusion-Related Au

3.8.9.1 International Mineral Deposit Model

Features of the *Alkali intrusion-related Au* mineral deposit model are listed in Table 3.43.

Table 3.43 Features of the *Alkali intrusion-related Au* international mineral deposit model.

International Mineral Deposit Model – *Alkali Intrusion-Related Au*	
Reference	BCGS model H08 Alkalic Intrusion-related Au–Ag (Lefebure and Höy 1996).
Description	Alkali intrusion-related gold deposits are typically magmatic-hydrothermal or phreatomagmatic pipe-like breccias associated with the intrusion of stocks, plugs, sills or dikes into a wide variety of host rocks ranging in age from Precambrian to Tertiary (Sillitoe 1991). As-Au-Ag ± Zn ± Pb mineralisation occurs in quartz-vein stockworks hosted by silicified and carbonate-altered alkalic intrusive rocks. The main metallic minerals are pyrite and arsenopyrite, with minor sphalerite, galena, gold, chalcopyrite, pyrrhotite and graphite.
International Examples	Kidston and Mount Leyshon, Queensland (Australia); Montana Tunnels (26.6 Mt at 0.61 g/t Au), Golden Sunlight (42.8 Mt at 1.9 g/t) and Zortman Landusky (55.7 Mt at 0.68 g/t Au) Montana; Colosseum, California (USA).
Grade-Tonnage Model	Montana Tunnels (26.6 Mt at 0.61 g/t Au), Golden Sunlight (42.8 Mt at 1.9 g/t) and Zortman Landusky (55.7 Mt at 0.68 g/t Au).

3.8.9.2 New Zealand Occurrences of Alkali Intrusion-Related Au *Deposits*

To date, only one deposit is known in New Zealand: Sams Creek (MM A15; GERM M26/e38) in west Nelson. The main features of the Sams Creek deposit and a mineral systems exploration model were described by Christie (2019). The mineralisation is hosted in a peralkaline granite dike emplaced in lower Paleozoic age sedimentary rocks (Tulloch 1992; Brathwaite et al. 2006; Faure and Brathwaite 2006). The porphyritic Sams Creek granite consists of phenocrysts of perthite, arfvedsonite-riebeckite amphibole and quartz, with accessory ilmenite and rutile (Faure and Brathwaite 2006; Tulloch and Dunlap 2006). The main phase of mineralisation consists of veins of gold-bearing arsenopyrite-pyrite-quartz-siderite, with minor galena, sphalerite, pyrrhotite and graphite.

There is uncertainty over the age of the dike and timing of gold mineralisation in relation to emplacement of the dike. Tulloch and Dunlap (2006) reported a Carboniferous age of 319 ± 8 Ma for the dike based on Ar-Ar dating of amphibole, whereas Phillips (2015) reported a Cretaceous age of 109 ± 9 Ma from U-Pb dating of zircon. The linking of mineralisation with D3 by Angus et al. (2016) suggests that mineralisation occurred well after dike emplacement, possibly related to a younger granite phase located deeper than the current depth drilled.

The dike is up to 60 m wide and has a strike length of c. 20 km. Most exploration to date has been on a 600-m-long zone known as the Main Zone.

Indicated and Inferred Resources at Sams Creek (consistent with the 2012 JORC Code), are estimated to be 8.9 Mt at 2.82 g/t Au for 807,772 oz Au (Siren Gold).

Key References: Brathwaite et al. (2006); Faure and Brathwaite (2006); Tulloch and Dunlap (2006); Phillips et al. (2013); Phillips (2014, 2015); Angus et al. (2016).

3.8.10 Gabbroid-Associated Au-Ni-Cu

This is a gold-rich version of the *Gabbroid-associated Au-Ni-Cu* model listed under Section 3.14. The gold is associated with disseminated sulfide mineralisation in mafic rocks.

The Asbestos Creek (M27/e21) and Meter Creek (M26/e43–45, 47 and M27/e22, 23) areas of the Takaka Valley contain Au-Cu-Ni mineralisation, with local Pt and/or Bi, which has been prospected by Kennecott (Smale 1971) and CRA (Stegman 1987, 1988a, 1988c). The mineralisation occurs within the Cambrian Devil River Volcanics as vein stockworks with pyrrhotite, chalcopyrite, pyrite and pentlandite. The host rocks comprise metasediments cut by diorite and porphyritic andesite dikes.

Otama Complex: A gold-bearing lode (at 6 g/t) was reported near the Otama Complex in the vicinity of Waikaia Hill (Stewart 1906). Traces of gold were also detected in a geochemical survey of the Otama Igneous Complex (Lay 1976). Locally derived gold from the Otama Igneous Complex has been suggested as a possible source for unusually coarse detrital flakes recovered at Charlton and Waimumu (MacArthur 1984; Mutch and Baker 1989).

Longwood Range: Gold-bearing quartz lodes were unsuccessfully worked in the 1870s to 1880s at several locations on the flanks of the Longwood Range, with the largest production from the Arethusa Claim (D46/e44, e45; Wood 1966; Nicolson et al. 1988). Sigma re-investigated the deposits in the 1980s and considered that the Upper Merrivale Goldfield, between Foals Creek and Buckton Creek on the northeastern Longwoods, was the most promising prospect for further work, although this was not carried out (Nicolson et al. 1988). At the ‘Foals Creek’ prospect, the quartz lodes are hosted in quartz-sericite-pyrite altered diorite within an anomalous zone of 1300 m x 200 m defined by drainage, soil, outcrop and float geochemical samples. The best channel samples of exposed mineralisation were 1.2 m at 12 ppm Au, and 0.3 m at 130 ppm Au and 12 ppm Ag.

Disseminated gold, with associated platinum, has been reported in plutonic rocks on the southern tops of the Longwood Complex (D46/e43; Challis and Lauder 1977; Nicolson et al. 1988). The best gold assay obtained by Sigma was 0.2 ppm (with 0.5 ppm Pt and 0.3 ppm Pd), although the best total precious metals assay was 0.1 ppm Au, 0.6 ppm Pt and 0.5 ppm Pd, both on float rocks (Nicolson et al. 1988).

3.8.11 Sediment (Carbonate)-Hosted Au–Ag (Carlin Type)

3.8.11.1 International Mineral Deposit Model

Features of the *Sediment (carbonate)-hosted Au–Ag (Carlin type)* mineral deposit model are listed in Table 3.44.

Table 3.44 Features of international mineral deposit models equivalent to the *Sediment (carbonate)-hosted Au–Ag (Carlin type)* model used in this report.

International Mineral Deposit Model – *Sediment (Carbonate)-Hosted Au–Ag (Carlin Type)*	
Reference	USGS model 26a Carbonate-hosted gold-silver (Cox and Singer 1986); and BCGS model E03 Carbonate-hosted disseminated Au–Ag (Lefebure and Höy 1996).
Description	Very fine-grained gold and sulfides disseminated in zones of decarbonated calcareous rocks and associated jasperoids. Gold occurs evenly distributed throughout the host rocks in stratabound concordant zones and in discordant breccias. The host rocks are thin-bedded carbonaceous shales and silty or argillaceous carbonaceous limestone or dolomite, mostly of Cambrian to Devonian age. Cretaceous- and Cenozoic-age felsic intrusive rocks are found in, or nearby, many deposits. The deposits are generally tabular, stratabound bodies localised at contacts between contrasting lithologies. Bodies are irregular in shape but commonly straddle lithological contacts which, in some cases, are thrust faults. Felsic plutons and dikes are also mineralised at some deposits. Silica replacement of carbonate is accompanied by volume loss so that brecciation of host rocks is common. Tectonic brecciation adjacent to steep normal faults is also common. Generally less than 1% fine-grained sulfides are disseminated throughout the host rock. Native gold (micron-sized), pyrite, realgar, orpiment, as well as local arsenopyrite, cinnabar, fluorite, barite and stibnite, occur in a gangue mineral assemblage of quartz, calcite, barite and carbonaceous matter.
International Examples	Carlin, Post, Gold Quarry, Getchell, Cortez, Gold Acres, Jerrit Canyon, Nevada; Mercur, Utah (USA)
Grade-Tonnage Model	USGS model 26a 50th percentile = 5.1 Mt and 2.5 g/t Au (410,000 oz Au), possible by-product Ag (Cox and Singer 1986). Mosier et al. (1992) reported the median size of 39 United States deposits as 6.6 Mt grading 2.3 g/t Au (488,000 oz Au), with most deposits in the range between 1 and 50 Mt, with grades from 1.0 to 6 g/t. However, two zones of the Carlin trend are significantly larger, Gold Quarry-Deep West-Maggie Creek, with 464 Mt at 1.32 g/t Au, and Goldstrike-Post-Blue Star-Genesis-Bobcat-North Star, with 307 Mt at 2.89 g/t Au.

3.8.11.2 New Zealand Occurrences of Sediment (Carbonate)-Hosted Au–Ag (Carlin Type) *Deposits*

Exploration for Carlin-type deposits has been carried out in Northland, and some formations of Northwest Nelson may also be prospective. The continental setting of North American deposits is a negative factor for New Zealand potential.

3.8.12 Gold Skarn

3.8.12.1 International Mineral Deposit Model

Features of the *Gold skarn* mineral deposit model are listed in Table 3.45.

Table 3.45 Features of the *Gold skarn* international mineral deposit model.

International Mineral Deposit Model – *Gold Skarn*	
Reference	BCGS model K04 gold skarns (Lefebure and Ray 1995).
Description	Gold-dominant mineralisation associated with skarns developed by metasomatic and hydrothermal processes where plutons intrude carbonate-bearing rocks. Gold skarns are hosted by sedimentary carbonates, calcareous clastics, volcaniclastics or (rarely) volcanic flows. They are commonly related to high- to intermediate-level stocks, sills and dikes of gabbro, diorite, quartz diorite or granodiorite composition. There is a worldwide spatial, temporal and genetic association between porphyry copper provinces and calcic Au skarns. Gold skarns vary in form from irregular lenses and veins to tabular or stratiform orebodies, with lengths ranging up to many hundreds of metres. Rare examples occur as vertical pipe-like bodies along permeable structures. Orebodies form veins or stratiform tabular lenses containing ore mineral assemblages of native gold, chalcopyrite, pyrrhotite, arsenopyrite and tellurides. The skarn gangue consists of Ca-Fe-Mg silicate minerals, such as clinopyroxene, garnet and epidote.
International Examples	Nickel Plate, British Columbia (Canada); Fortitude, McCoy and Tomboy-Minnie, Nevada; Buckhorn Mountain, Washington; Diamond Hill, New World district and Butte Highlands, Montana; Nixon Fork, Alaska (USA); Thanksgiving (Philippines); Browns Creek and Junction Reefs-Sheahan-Grants, New South Wales; Mount Biggenden, Queensland; Savage Lode, Coogee, Western Australia (Australia); Nambija (Ecuador); Wabu, Irian Jaya (Indonesia)
Grade-Tonnage Model	Skarn deposits range from 0.4 to 10 Mt and grade from 2 to 15 g/t Au. Nickel Plate in British Columbia, Canada, has produced over 8 Mt grading 7.4 g/t Au (Lefebure and Ray 1995).

3.8.12.2 New Zealand Occurrences of Gold Skarn *Deposits*

There are no known *Gold skarn* occurrences in New Zealand, and there has been no exploration for this type of deposit despite suitable geological environments, for example, intrusions into Mt Arthur Marble in northwest Nelson.

3.8.13 Detachment-Fault-Related Polymetallic Deposits

3.8.13.1 International Mineral Deposit Model

Features of the *Detachment-fault-related polymetallic deposits* mineral deposit model are listed in Table 3.46.

Table 3.46 Features of the *Detachment fault-related polymetallic deposits* international mineral deposit model.

International Mineral Deposit Model – *Detachment-Fault-Related Polymetallic Deposits*	
Reference	Detachment fault-related mineral deposits (Long 2004).
Description	Massive replacements, stockworks and veins of iron and copper oxides and locally sulfides along detachment-fault structures. These deposits sometimes contain economic concentrations of gold and silver. Distal veins of quartz-barite-fluorite-Mn oxides are emplaced along high-angle faults in the upper plate of detachment-faulted terranes.
International Examples	Bullard, Copperstone, Osborne, Planet, Harris, Tiger Wash and Newsboy, Arizona (USA).
Grade-Tonnage Model	The Copperstone deposit has resources of 386,000 oz Au at 2.6 g/t, and the Newsboy deposit has 67,500 at 1.54 g/t (Long 2004).

3.8.13.2 New Zealand Occurrences of Detachment-Fault-Related Polymetallic Deposits

Tulloch (1988b, 1995) suggested that gold anomalies, with associated Ag, As, Sb and Cu, in exploration stream-sediment geochemical surveys of the Paparoa Range may be related to a detachment-fault system associated with the Paparoa Metamorphic Core Complex (Figure 3.18). Silver, fluorite, barite, sulfide and uranium occurrences in the lower Buller Gorge were considered to have formed by hydrothermal activity associated with the Ohika detachment fault (Tulloch 1988b, 1995; Tulloch and Kimbrough 1989).

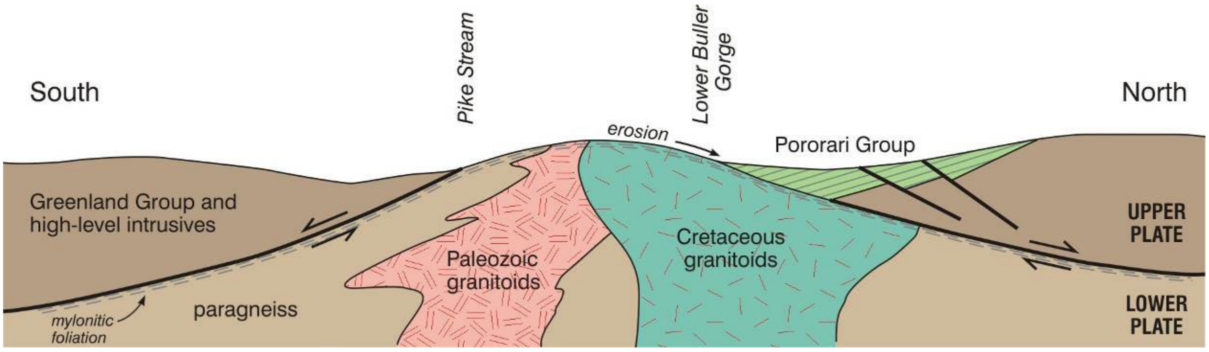

Figure 3.18 Diagrammatic cross-section through the metamorphic core complex in the Paparoa Range. The lower plate was uplifted along shallow-dipping mylonitic detachment faults, displacing the upper plate of early Paleozoic Greenland Group and some small granitoid intrusives. The extensional deformation also resulted in the formation of fault-bounded basins in the upper plate that were rapidly filled with Pororari Group terrestrial sediments derived from the eroding lower plate (after Nathan et al. [2002]).

3.8.14 Placer Au, Onshore, Beach and Offshore

3.8.14.1 *International Mineral Deposit Model*

Features of the *Placer Au, onshore, beach and offshore* mineral deposit model are listed in Table 3.47.

Table 3.47 Features of international mineral deposit models equivalent to the *Placer Au, onshore, beach and offshore* model used in this report.

International Mineral Deposit Model – *Placer Au, Onshore, Beach and Offshore*	
Reference	**Onshore:** • USGS model 39a Placer Au-PGE (Cox and Singer 1986); • BCGS model C01 Surficial placers (Lefebure and Ray 1995); and • BCGS model C02 Buried-channel placers (Lefebure and Ray 1995). **Offshore:** BCGS model C03 Marine placers (Lefebure and Ray 1995).
Description	**Onshore:** Detrital gold grains and (rarely) nuggets in gravel, sand, silt and clay, and their consolidated equivalents, in alluvial, beach (‘blacksand leads’) and fluvioglacial deposits. Alluvial deposits typically formed as channel-lag and gravel-bar deposits, as well as beneath boulders where gradients flatten and river velocities lessen. Winnowing action of surf caused gold concentrations in raised, present and submerged beaches. **Offshore:** Detrital gold and other heavy minerals occurring at the present or paleo-seafloor surface. These usually occur in Holocene raised or submarine beach or strandline deposits along wave-dominated shorelines but can also be found in coastal dunes, drowned fluvial channels or as offshore relict lag concentrations.
International Examples	**Onshore:** Sierra Nevada, California (USA); Victoria (Australia); Klondike, Yukon (Canada); Rio Tapajos (Brazil); Yana-Kolyma belt (Russia). **Offshore:** Nome, Alaska (USA); Bermagui (Australia); Country Harbour, Nova Scotia (Canada).
Grade-Tonnage Model	**Onshore:** Deposits are small to high tonnage (0.1–100 Mt) but low grade (0.05–5 g/t Au). Placer concentrations are highly variable both within and between individual deposits. Modern operations in the South Island work deposits typically between 1000 and 60,000 oz Au (e.g. Manhire et al. 2006). **Offshore:** Deposits are typically high tonnage (0.1–100 Mt) but low grade (0.05–0.25 g/t Au).

3.8.14.2 *New Zealand Occurrences of* Placer Au, Onshore, Beach and Offshore *Deposits*

Giant placer gold fields are present in Cenozoic gravel and sand in Westland and Otago–Southland, and smaller placers are found in west Nelson and Marlborough (Figure 3.19). About 18 Moz of gold were produced in the past, initially during the gold rushes of the 1860s and 1870s and later by sluicing and dredging operations, particularly in the early 1900s and 1930s. Small quantities of platinum group metals were a by-product of placer gold mining at Round Hill and Orepuki in Southland. Since 1980, there have been a large number of small- and medium-scale gold recovery operations using hydraulic excavators and mobile gold recovery plants, with a peak exceeding 150 operations in the late 1980s. The rapid throughput and relative mobility of these plants have enabled mining of ground that was not accessible or too small in volume for mining by large bucket-line dredges. The largest operations have been at Rimu, Arahura, Ross, Mikonui, Shotover Gorge, Kawarau Gorge, Island Block, Nokomai and Waikaia. Additionally, one bucket line dredge, the Grey River Dredge, has operated intermittently near Ngahere since 1988, but it is currently under maintenance. Current annual production from placer gold deposits in New Zealand is c. 32,000 oz Au.

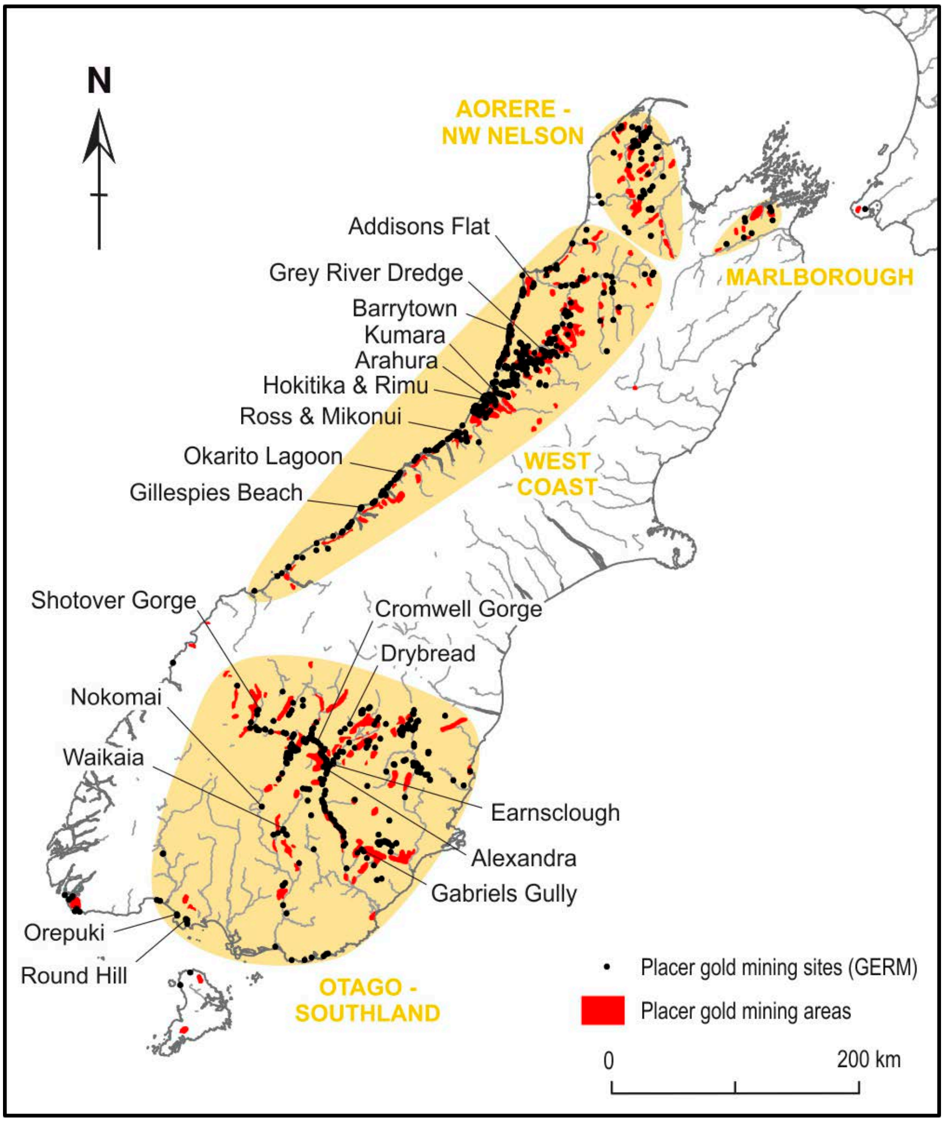

Figure 3.19 Nearly all of the alluvial gold produced in New Zealand has been from the South Island. These gold fields are still producing, mainly from small-scale operations using mining equipment rather than the picks and shovels of the gold-rush miners (after Christie [2016c]).

Gold placers in Otago and Southland were formed by erosion of the Haast Schist and deposition of auriferous conglomerates during several major fluvial depositional phases since the Cretaceous. On the West Coast, gold placers are found in late Pleistocene and recent alluvial and fluvioglacial gravels eroded from the uplifting Southern Alps. The alternating glacial and interglacial periods formed deposits associated with buried river channels, fluvial deposits, glacial meltwater channels and degraded terraces. An important factor in developing economic gold concentrations was the re-working, recycling and concentration of gold through the stratigraphic successions, resulting in some of the youngest placers being the richest. In Otago and Southland, another factor has been the authigenic growth of gold particles by chemical dissolution, transport and accretion processes, increasing the grain size of some gold particles.

Beach placers are found on the west and south coasts of the South Island in present-day beaches, older post-glacial beach deposits and the raised beach deposits of successive marine interglacials that underlie the remnants of coastal terraces. Gold is concentrated with other heavy minerals into lenticular ‘blacksand leads’. The largest deposits on the West Coast were leads in Addisons Flat and adjacent terraces near Westport, in terraces near Charleston and Barrytown, the Hou Hou Lead and associated leads west of Kumara, the Lamplough Lead north of Hokitika, and leads near Okarito Lagoon and on Gillespies Beach.

Current production: In Westland, Otago and Southland, there are about 123 alluvial mining operations and more than 200 hobby-scale river and beach operations, each consisting of excavators that supply gravel to mobile gold screens (e.g. Cotton and Rose 2006; Manhire et al. 2006; Christie and Herridge 2016; Cotton and Wood 2016; Henderson et al. 2016). A new bucket-ladder dredge operated on the Grey River briefly in 1989 and, after modification, started up again in 1992 but closed in 2015 (Cotton and Birchfield 2006). Large backhoe-fed floating plants have operated recently in the Arahura River in Westland, in eastern Otago and at Waikaia in Southland (Manhire et al. 2006; Becker and Batt 2016).

There is little exploration information available for assessment of undiscovered resources. Total resource estimates have been previously reported as 10 Moz of gold by Douch (1988) and 22 Moz of gold for the West Coast alone by Jury and Hancock (1989). Christie and Brathwaite (1999b) suggested a more conservative estimate of 2 Moz in the Marlborough, West Coast, Otago and Southland regions.

Key References: Brathwaite and Pirajno (1993); Becker and Batt (2016); Cotton and Wood (2016).

3.9 Iron (Fe)

3.9.1 International Description

International data for iron are listed in Table 3.48.

Table 3.48 Major minerals, world production, reserves and resources and major uses of iron.

Iron (Fe)		
International	**Ore Minerals:** Chamosite $(Fe,Mg,Al)_6(Si,Al)_4O_{10}.(OH)_8$, goethite $Fe_2O_3.H_2O$, hematite Fe_2O_3, native iron Fe, magnetite Fe_3O_4, marcasite FeS_2, melanterite $FeSO_4.7H_2O$, pyrite FeS_2, pyrrhotite FeS, siderite $FeCO_3$, titanomagnetite (Magnetite-ulvöspinel mixture) Fe_3O_4 + Fe_2TiO_4 and vivianite $Fe_3P_2O_8.8H_2O$	
	World production	2.5 Bt of ore with 1.5 Bt of iron content
	Major world producers (% of average total)	Australia (38%, Brazil (18%), China (11%), India (11%), Russia (4%), Iran (3%), Canada (3%), South Africa (2%), Kazakhstan (2%), USA (2%), Sweden (1%), Ukraine (1%)
	World reserves (USGS 2024)	190 Bt ore with 87 Bt iron content
	World resources (USGS 2024)	More than 800 Bt of ore containing more than 230 Bt of iron.
	Uses: Making steel and various alloys, machinery and tools, rails, automobiles, ship hulls, concrete reinforcing bars, as well as the load-carrying framework of buildings, catalysts and compounds.	

3.9.2 New Zealand Occurrences of Iron

New Zealand iron deposits (Figure 3.20) are classified under four main mineral deposit types: *Shoreline placer Fe*, *Bog Fe*, *Transported residual Fe* and *Magmatic Fe-Ti-V* (see Titanium; Section 3.19).

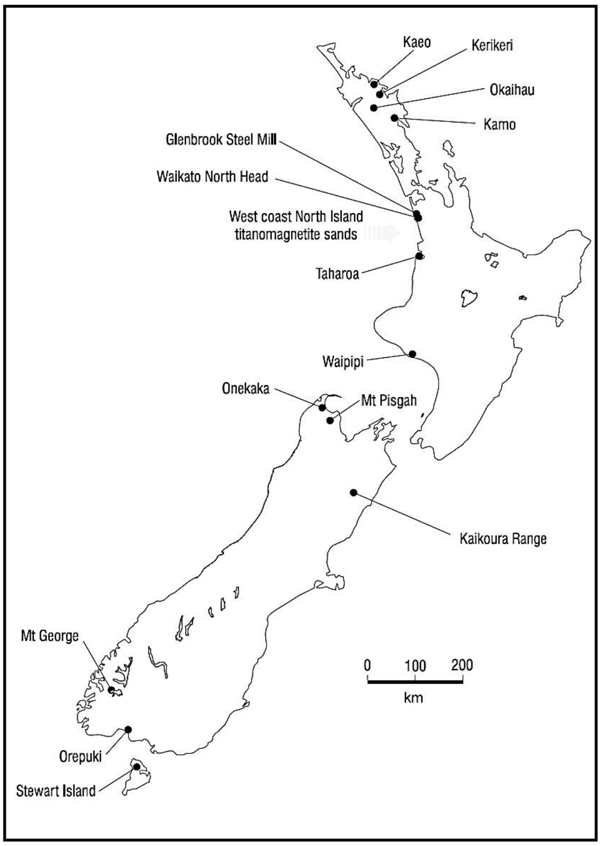

Figure 3.20 Location of iron deposits in New Zealand (after Christie and Brathwaite [1997b]).

3.9.3 Shoreline Placer Fe

3.9.3.1 International Mineral Deposit Model

Features of the *Shoreline placer Fe* mineral deposit model are listed in Table 3.49.

Table 3.49 Features of international mineral deposit models equivalent to the *Shoreline placer Fe* model used in this report.

International Mineral Deposit Model – *Shoreline Placer Fe*	
Reference	BCGS model C01 Surficial placers (Lefebure and Ray 1995); USGS model for heavy-mineral sands in coastal environments (Van Gosen et al. 2014)
Description	Detrital iron minerals and other heavy minerals concentrated by shallow marine, beach and dune processes. Elongate ‘shoestring’ ore bodies parallel to coastal beaches and dunes.
International Examples	Bardaskan, Khorasan-e-Razavi (Iran); Kerala (India)
Grade-Tonnage Model	Individual economic deposits typically have 10 Mt of sand at >2% heavy minerals and may occur in districts with >1 Bt of sand averaging 5% heavy minerals (Van Gosen et al. 2014). Titanomagnetite/magnetite contents of the heavy-mineral sand fraction are variable between deposits.

3.9.3.2 New Zealand Occurrences of Shoreline Placer Fe *Deposits*

Titanomagnetite ironsand (blacksand) forms Quaternary onshore beach and dune deposits and offshore marine deposits along 480 km of coastline from Kaipara Harbour south to Wanganui on the west coast of the North Island (Figure 3.21). The onshore deposits include the present beach and dune sand, as well as older coastal sand deposits that have been preserved by uplift due to faulting and/or lowering of sea level. In addition to titanomagnetite, the sands contain plagioclase, pyroxenes (mostly augite), hornblende, rock fragments and minor quartz, K-feldspar and olivine. North of the Waikato River, ilmenite becomes a significant component

The main source of titanomagnetite in the ironsands is from erosion of the late Pleistocene–Holocene andesite volcanoes of the Taranaki Mounga volcanic field, although, from the mouth of the Waikato River northwards, there is a minor contribution from Pleistocene ignimbrites and rhyolites of the Taupō Volcanic Zone, mainly transported by the Waikato River (Brathwaite et al. 2017b, 2021). Coastal sands eroded from the Taranaki volcanoes and their extensive ring plain deposits have been transported from Cape Egmont northwards and southwards by a long-period swell from the southern ocean, coupled with the prevailing southwesterly wind and wave action, and subsequently concentrated by wave and wind action into beach and dune lag deposits. Deposits present offshore on the continental shelf were probably concentrated as coastal deposits when sea level was lower than at present, and then re-worked under littoral conditions during the Holocene transgression.

Exploration during the 1940s to 1960s (e.g. Kear 1979) discovered several large ironsand deposits, and mining operations were established at the three largest: Waikato North Head in 1969, Waipipi in 1971 and Taharoa in 1972. The Waikato North Head and Taharoa mines continue today, but Waipipi closed in 1987.

Mining at Waikato North Head and Taharoa processes sand with c 18–25% titanomagnetite. This is concentrated by gravity and magnetic methods to produce a product with approximately 80% titanomagnetite. This material has a chemical composition of approximately 57% iron, 7.7% titanium dioxide and 0.4% vanadium oxide. New Zealand produces more than 2 Mt of ironsand concentrate annually. Production from Waikato North Head is used for making steel at the Glenbrook steel mill, whereas all of the ironsand concentrate from Taharoa is exported to steel mills in Asia.

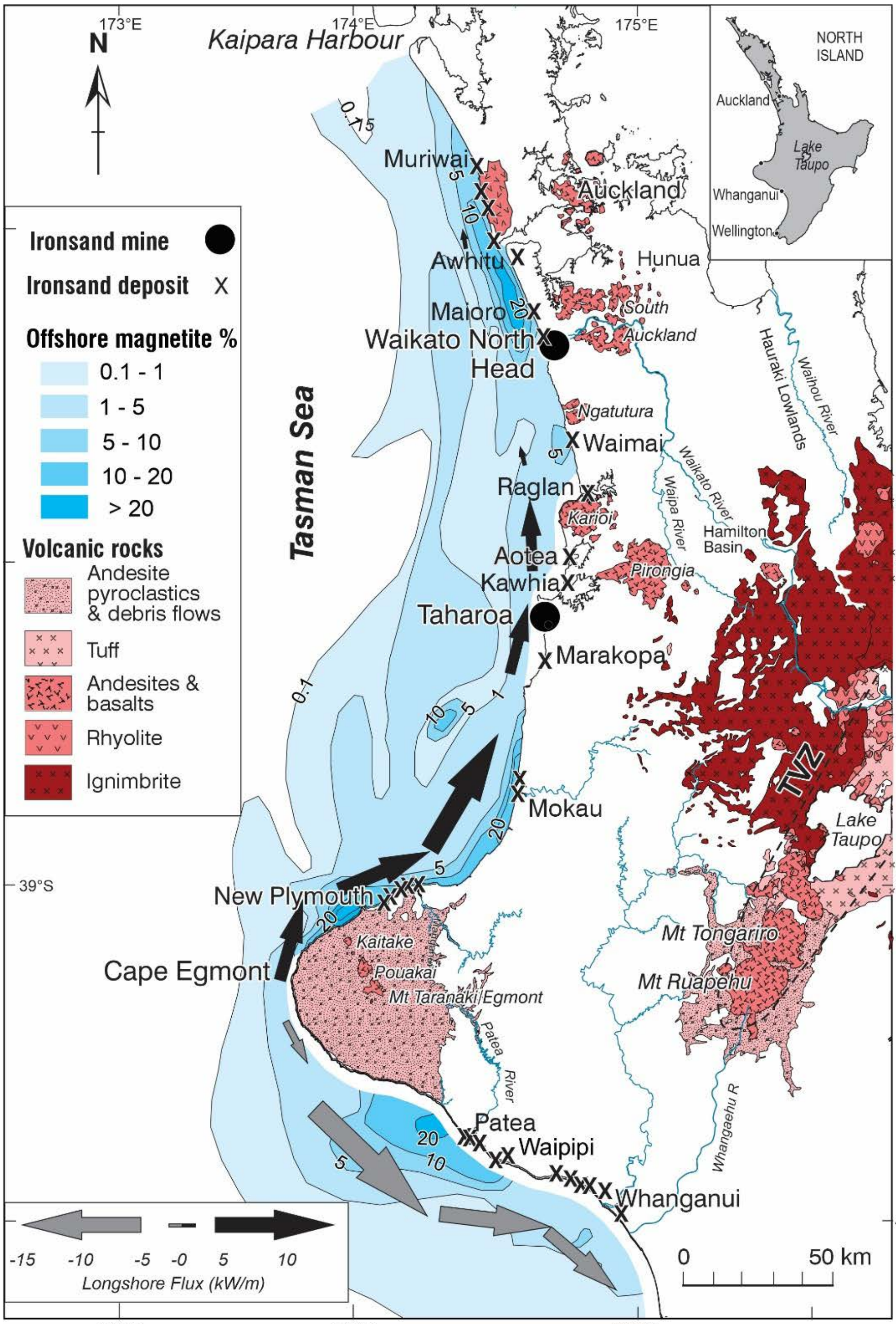

Figure 3.21 Distribution of ironsand deposits and volcanic-source rocks along the west coast of the North Island, showing the location of the operating mines at Waikato North Head and Taharoa and the former mine at Waipipi (from Brathwaite et al. [2017b]). The offshore magnetite wt.% contours are from Carter (1980). The black and grey arrows show the magnitude of northwards and southwards longshore current directions. TVZ = Taupō Volcanic Zone.

Production is currently from mines at Waikato North Head and Taharoa. The Waikato North Head mine produces about 1 Mt/yr of concentrate for making steel at Glenbrook and for export. A vanadium-rich slag is produced as a by-product at the Glenbrook steel mill and is exported. The Taharoa mine produces about 1.2 Mt/yr of titanomagnetite concentrate for export. A total of 15.7 Mt of concentrate for export were produced from Waipipi in southern Taranaki when it operated between 1971 and 1987.

Estimated in-ground resources at operating mines are: Waikato North Head – 140 Mt of concentrate; Taharoa – 208 Mt of concentrate (Table 3.50). A small resource remains at the Waipipi deposit. Rough estimates of other resources are known (Table 3.51) and amount to a total of 874 Mt, including Waikato North Head and Taharoa. The concentrate contains 55–56% Fe, 7–9% TiO_2 and 0.3–0.4% V_2O_5.

For many of the deposits, exploration drilling has been only on a reconnaissance scale and was carried out in the 1940s, 1950s and early 1960s; therefore, there is scope for improving the resource estimates with modern exploration. For example, the Aotea deposit was estimated to contain a large volume of ironsand (500 Mt of sand) but insufficient drilling was done in this early phase of exploration to estimate the grade in terms of Mt concentrate and percentage of Fe. Since then, drilling from 2009 resulted in a 2014 indicated plus inferred resource estimate of 29.547 Mt of concentrate at 53.1% Fe (Wood et al. 2016).

Waikato North Head production is limited by the capacity of the Glenbrook steel mill to 1.2 Mt of concentrate annually. Taharoa has previously produced up to 2 Mt in a year. Assuming increasing markets (e.g. China), ironsand production could be 3.2 Mt from the current operations and more if another mine is developed. In addition to by-product vanadium-rich slag, there is potential to produce a titanium mineral-rich concentrate from the ironsand mining.

Table 3.50 Resource estimates for titanomagnetite ironsand resources.

Deposit	Resource Category	Ironsand (Mt)	Magnetic Content (%)	Magnetics (Mt)	Fe (%)	Source
Aotea	Inferred	202.6	14.6	29.5	53.1	Wood et al. (2016)
Taharoa	Measured	27.4	31.6	8.7	-	Mauk et al. (2016)
	Indicated	341.8	23.6	82.2	-	
	inferred	5	11.1	0.6	-	
Waikato North Head	Measured	374.3	20.5	76.7	-	Mauk et al. (2016)
	Indicated	312.3	13.2	41.2		
	Inferred	43	6	2.6		
Total	**-**	**1176.8**	**-**	**222.1**	**-**	

Table 3.51 Ironsand resources, west coast, North Island (after Brathwaite [1990]).

Deposit	MM[1]	GERM[2]	Quantity of Sand (Mt)	Grade (% Magnetics)	Quantity of Concentrate (Mt)
Muriwai[3]	G1	Q11/e32	90	15	13
Bethells[3]	G2	Q11/e33	20	15	3
Piha[3]	G3	Q11/e34	3.45	24	0.8
Whatipu[3]	G4	Q11/e35	17	31	5.3
Irwins[3]	G5	R12/e35	20	18	5
Maioro North[3]	G6	R12/e36	200	10	20
Maioro South[4]	G7	R13/e18	150	21	30
Maioro South[3]	G7	R13/e18	50	12	6
Waikato North Head[4]	G8	R13/e1	780	18	140
Port Waikato	G9	R13/e19	-	-	-

Deposit	MM [1]	GERM [2]	Quantity of Sand (Mt)	Grade (% Magnetics)	Quantity of Concentrate (Mt)
Waimai [3]	G10	R14/e16	98	44	43
Raglan [4]	G11	R14/e11	78.7	19.7	15.5
Raglan [3]	G11	R14/e11	49.0	20.4	10.0
Aotea [3]	G12	R15/e5	500	-	-
Kawhia [3]	G13	R15/e6	1500	13	200
Taharoa [4]	G14	R16/e1	593	35	208
Harihari [3]	G15	R16/e7	1	58	1
Marakopa [3]	G16	R16/e8	55	45	25
Awakino [3]	G17	R17/e19	9	63	5.8
Mokau [3]	G18	R18/e47	10.5	37	3.9
Waitara	G19	Q19/e98	-	-	-
Waiongana	G20	Q19/e99	-	-	-
Waihowaka	G21	Q19/e100	-	-	-
Fitzroy	G23	P19/e74	-	-	-
New Plymouth [3]	-	-	33	24	8
Patea [3]	G24	Q21/e18, Q22/e5	73.5	33	23.5
Waipipi [4]	G25	Q22/e1	153	26	40
Nukumaru	G26	R22/e60	-	-	-
Okehu	G27	R22/e61	-	-	-
Kai Iwi	G28	R22/e62	-	-	-
Wanganui [3]	-	R22/e75	236	16	37
Rapanui	G29	R22/e63	300	10	30
Westmere	G30	R22/e64	-	-	-
Total	**-**	**-**	**-**	**-**	**873.8**

[1] MM = Metallogenic map code (Brathwaite and Pirajno 1993).

[2] GERM = Geological Resource Map code.

[3] Inferred estimate.

[4] Indicated and/or measured estimate.

Where both inferred and indicated figures are listed, these are added together to give a total resource.

Key References: Kear (1979); Brathwaite (1990); Christie and Brathwaite (1997b); Briggs et al. (2009); Brathwaite and Christie (2014, 2015); Brathwaite et al. (2017b, 2021).

3.9.4 Bog Fe

Limonitic *Bog Fe* is formed from leaching of iron-bearing rocks, such as basalt by carbonated surface and ground waters with subsequent deposition at the surface as ferric hydroxides. In New Zealand, limonitic bog-iron deposits occur in Northland near Kaeo, Okaihau, Kerikeri and Kamo (Table 3.52). These have been formed from leaching of iron from Kerikeri Basalt. The deposit near Okaihau was intermittently worked until 1961, producing a total of 39,111 t of iron ore.

Key References: Williams (1974); Brathwaite and Pirajno (1993); Christie and Brathwaite (1997b).

Table 3.52 *Bog Fe* deposit model occurrences (data modified after Brathwaite and Pirajno [1993]).

Occurrence	MM [1]	GERM [2]	Production (t)	Deposit Form	Minerals Major (Minor)	Host Rocks
Potaetupuhi Bush	-	-	-	Laterite	Limonite	-
Kaeo	-	P04/e54	-	Stratiform	Limonite	Andesite breccia
Okaihau	I11	P05/e67	40,000 Fe ore	Laterite pods	Limonite	Basalt
Kerikeri	-	P05/e69	-	laterite	limonite	basalt
Kamo	I16	-	9000 Fe ore	Laterite sheets	Limonite	Basalt

[1] MM = Metallogenic map code (Brathwaite and Pirajno 1993).

[2] GERM = Geological Resource Map code.

3.9.5 Transported Residual Fe

A deposit of residual limonite is present in a belt from Ironstone Creek, Onekaka, north to the Parapara Inlet (Figure 3.20). The material overlies Ordovician-age marble but is thought to be laterite, transported from the Tertiary-age peneplain and deposited in caves within the marble. The iron was possibly derived from iron sulfide disseminations in nearby schist. About 813,000 t were mined between 1922 and 1935 to produce 40,640 t of pig iron (Grindley and Watters 1965). Landreth (1946) estimated resources of 9.65 Mt at a grade of 40% Fe.

Key References: Williams (1994); Brathwaite and Pirajno (1993); Christie and Brathwaite (1997b).

Occurrences of miscellaneous iron deposits are listed in Table 3.53.

Table 3.53 Iron occurrences additional to the titanomagnetite and *Bog Fe* deposits listed above. Minerals: hm = hematite; il = ilmenite; mt = magnetite; rt = rutile.

Occurrence	MM [1]	GERM [2]	Production (t)	Deposit Form	Minerals Major (Minor)	Host Rocks	Genesis
Onekaka	A8	M25/e585, M25/e584	>40,000 Fe	Stratiform pods	Limonite	Weathered marble and schist	Surficial chemical concentration
Mr Pisgah	A10	N26/e586	-	Magnetite-ilmenite layer	mt, il, (hm, rt)	Diorite	Magmatic segregation
Mt George	A98	C43/e4	-	Layered zone	il, mt	Metagabbro	Magmatic segregation
Dromedary	B44	-	-	Stratiform	mt	Cemented blacksand in sandstone	Placer
Catlins River	B45	-	-	Stratiform	mt	Cemented blacksand in sandstone	Placer

[1] MM = Metallogenic map code (Brathwaite and Pirajno 1993).

[2] GERM = Geological Resource Map code.

3.10 Lithium (Li)

3.10.1 International Description

International data for lithium are listed in Table 3.54.

Table 3.54 Major minerals, world production, reserves and major uses of lithium.

Lithium (Li)		
International	**Ore Minerals:** Pentalite $LiAl(Si_2O_5)_2$, lepidolite $K(Li,Al)_3(Al,Si,Rb)_4O_{10}(F,OH)_2$, spondumene $LiAl(SiO_3)_2$	
	World production 2023 (USGS 2024)	180,000 t
	Major world producers (% of 2023 total world mine production) (USGA 2024)	Australia (48%), Chile (24%), China (18%), Argentina (5%), Brazil (3%), Canada (2%), Zimbabwe (2%)
	World reserves (USGS 2024)	28 Mt
	World resources (USGS 2024)	105 Mt
	Uses: Batteries, ceramics/glass and lubricating greases. Lithium is a key constituent of lithium-ion batteries used in electric vehicles, consumer devices and energy storage.	

3.10.2 New Zealand Occurrences of Lithium

Turnbull et al. (2018) reported that lithium is found in New Zealand associated with pegmatites (i.e. Lithium-Caesium-Tantalum [LCT] pegmatites) and hydrothermally altered rhyolitic, lacustrine sediment-hosted deposits – see their model descriptions below.

Key References: Christie and Brathwaite (1999b); Turnbull et al. (2018, 2019).

3.10.3 Li Pegmatites

3.10.3.1 International Mineral Deposit Model

Features of the *Li pegmatites* mineral deposit model are listed in Table 3.55.

Table 3.55 Features of the *Li pegmatites* mineral deposit model.

International Mineral Deposit Model – *Li Pegmatites* and *LCT Pegmatites*	
Reference	Bradley et al. (2017)
Description	Lithium-bearing granite pegmatites are found as dikes peripheral to granite intrusions and were formed by crystallisation of late-stage residual fluids (Turnbull et al. 2018). Lithium occurs in a paragenetic range from early-stage minerals, such iron-rich spodumene, through intermediate stages (spodumene, petalite, lepidolite and amblygonite) to lower-temperature hydrothermal alteration products such as eucryptite, bikitaite and cookeite.
International Examples	King Mountain, North Carolina; Black Hills, South Dakota (USA); Bernic Lake, Manitoba (Tanco pegmatite); CV5, Corvette, Quebec (Canada); Aracuai, Minas Gerais (Brazil); Altai Mountains (China); Chita region (Russia); Bikita mine (Bikita pegmatite) (Zimbabwe); Karibib (Rubicon and Helicon pegmatites) (Namibia); 'tin mineral province' in Zaire; Greenbushes pegmatite field, Western Australia (Australia).
Grade-Tonnage Model	No published data. Bradley et al. (2017) listed data for 10 deposits ranging from 1.6 Mt at 1.2% Li_2O to 70.4 Mt at 2.6% Li_2O. Grades of the 10 ranged from 0.7% to 2.76% Li_2O.

3.10.3.2 New Zealand Occurrences of Li Pegmatites

Pegmatites associated with strongly fractionated I-S-type felsic plutonic rocks are most likely to be associated with granitoids of the Karamea, Ridge, Rahu and Foulwind petrogenetic intrusive suites of the Tuhua Intrusives (Turnbull et al. 2018). These rocks of early Paleozoic to Cretaceous age are found in west Nelson, West Coast, Fiordland and Rakiura / Stewart Island. van de Ven et al. (2020) described a strategy for exploring for LCT pegmatites in the Hohonu Batholith.

3.10.3.3 Lithium-Bearing Hydrothermal Clays and Lacustrine Sediments

Lithium is leached from rhyolitic rocks by meteoric and hydrothermal fluids, then enriched and structurally bound in volcanic-derived clays (hectorite) by hydrothermal alteration of rhyolitic lacustrine sediments.

A GIS-based prospectivity study by Turnbull et al. (2018) indicated that the Taupō Volcanic Zone was the most prospective area for hydrothermally altered volcaniclastic/lacustrine sediments, particularly in the Huka Falls Formation (Huka Group), Ngakuru Formation and Waitemata Group sediments (Figure 3.22). In a follow-up study focusing on the Taupō Volcanic Zone, Turnbull et al. (2019) noted that localised areas within or proximal to the Wairakei, Tauhara, Mokai, Rotokawa, Ngatamariki, Ohaaki, Waiotapu and Rotorua geothermal fields have the highest potential for lithium mineralisation.

Felsic volcanic rocks in the Coromandel Peninsula and on Great Barrier Island may also be prospective for lithium.

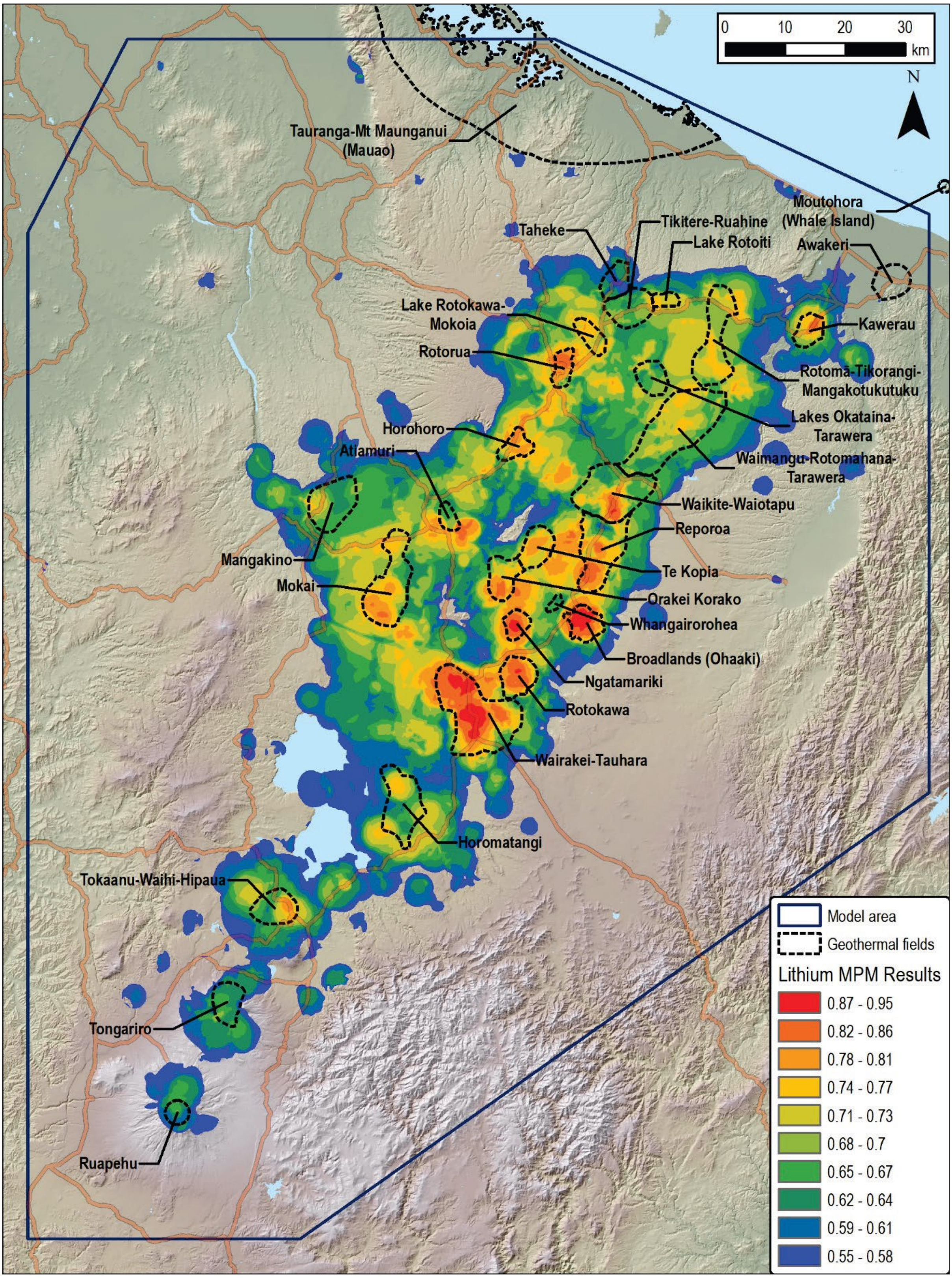

Figure 3.22 Prospectivity maps for hydrothermally altered rhyolitic lacustrine sediment-hosted lithium potential in the Taupō Volcanic Zone using a mineral systems approach. Warm colours represent higher potential (after Turnbull et al. [2019]).

3.11 Magnesium (Mg)

3.11.1 International Description

International data for magnesium are listed in Table 3.56.

Table 3.56 Major minerals, world production, reserves and resources and major uses of magnesium.

Magnesium (Mg)		
International	**Ore Minerals:** Bischofite $MgCl_2.6H_2O$, brucite $Mg(OH)_2$, dolomite $CaCO_3.MgCO_3$, epsomite $MgSO_4 \cdot 7H_2O$, magnesite $MgCO_3$, periclase MgO and talc (steatite; soapstone) $Mg_3Si_4O_{10}(OH)_2$	
	World mine production in 2023 (USGS 2024)	22 Mt of magnesite
	Major world producers of magnesite (% of total world mine production 2023) (USGS 2024)	China (59%), Turkey (8%), Brazil (8%), Russia (4%), Australia (4%), Austria (4%), Spain (3%), Slovakia (2%), Greece (2%), Saudi Arabia (2%)
	World reserves (USGS 2024)	7.7 Bt magnesite
	World resources (USGS 2024)	13 Bt magnesite
	Uses: Transport automotive, packaging and construction. Its use is growing in light-weighting for road vehicles and military applications.	

3.11.2 International Occurrences of Magnesium

Magnesium deposits include deposits of magnesite, seawater and brines, and contact metamorphic deposits of brucite along granite-dolomite contacts (e.g. Malyy Khingan, Russia; Marble Canyon, Texas, USA). Magnesia is produced from surface or subterranean brines in the USA, the Netherlands, Israel and Mexico.

Natural magnesite occurs in a few, but very large, high-grade (70–90% $MgCO_3$) crystalline magnesite deposits and a large number of small, lower-grade (>12% $MgCO_3$) deposits of amorphous or cryptocrystalline magnesite. The crystalline deposits form by replacement of sedimentary dolomite by magnesite, either by hydrothermal alteration or metamorphism. International examples include: Veitsch, Styria, Austria; Slovakia; Navarra, Spain; Satka, Russia; Serra des Eguas, Bahia, Brazil; Mount Brussilof, British Columbia, Canada; Gabbs, Nevada, USA; and Jabal Al Rokhan, Saudi Arabia.

Rogers (1996) developed a grade tonnage model for 14 crystalline and amorphous magnesite deposits (model B11; Rogers et al. 1995) from world-wide localities with a 50th percentile of 28.6 Mt at 91.6% MgO_3.

3.11.3 New Zealand Occurrences of Magnesite

Magnesite occurs with talc in *Talc-magnesite* deposits hosted in ultramafic rocks in Northwest Nelson, Westland, north Otago and Southland (NZGS 1970b; Williams 1974) (Figure 3.23).

The Cobb-Upper Takaka district was a small producer of talc-magnesite for agriculture and industry from 1944 to the 1980s. The talc-magnesite and quartz-magnesite lenses are derived from serpentinite of the Cobb Igneous Complex outcropping southwards between the Cobb and headwaters of the Takaka River (Wellman 1942, 1943; Williams 1974).

Ultramafic bodies containing lenses of serpentinite, talc-magnesite and steatite, up to 200 m in length, occur within the Waingaro Schist at Richmond Hill near Collingwood (Riley 1972; Thompson 1989). Talc-magnesite also occurs along shear zones in the serpentinitic matrix of the Patuki and Croisilles melanges of east Nelson. Although some is of very high grade, the quantities available are small.

Talc-magnesite is present as segregations and veins within serpentinite of the Pounamu Ultramafics (NZGS 1970b). All known deposits are small, and access is difficult. Minor talc-magnesite occurrences are also present in ultramafic rocks in northern Otago and Southland.

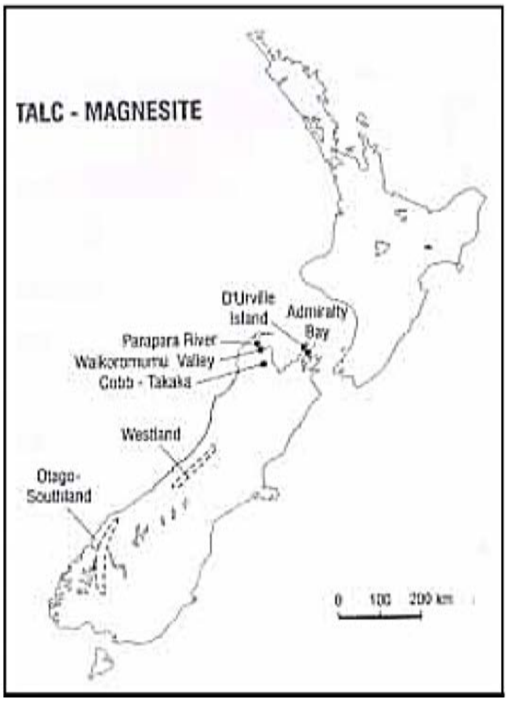

Figure 3.23 Location of magnesite (and talc) deposits in New Zealand (Christie and Brathwaite [1999a]).

Key References: NZGS (1970b); Williams (1974); Thompson (1989); Christie and Brathwaite (1999a).

3.12 Manganese (Mn)

3.12.1 International Description

International data for manganese are listed in Table 3.57.

Table 3.57 Major minerals, world production, reserves and resources and major uses of manganese.

Manganese (Mn)		
International	**Ore Minerals:** Braunite $3(Mn,Fe)_2O_3MnSiO_3$, manganite $Mn_2O_3.H_2O$, psilomelane $BaMn_9O_{16}(OH)_4$, pyrolusite MnO_2, piemontite $Ca_2(Mn,Fe^{3+},Al)_2AlO{\cdot}OH(Si_2O_7)(SiO_4)$, rhodochrosite $MnCO_3$ and wad (Mn oxides with variable composition)	
	World mine production in 2023 (USGS 2024)	20 Mt
	Major world producers (% of average total 2015–2019)	South Africa (36%), Gabon (23%), Australia (15%), Ghana (4%), China (4%), India (4%), Brazil (3%), Cộte de Ivoire (2%)
	World reserves (USGS 2024)	1.9 Bt
	World resources (USGS 2024)	Large. South Africa accounts for 70% of world's manganese resources.
	Uses: The dominant use of manganese is in steel, but it is also a key constituent of lithium-ion batteries for electric vehicles and a host of other purposes.	

3.12.2 New Zealand Occurrences of Manganese

Manganese occurs in *Volcanogenic Mn* type deposits in both the North and South Islands (Figure 3.24).

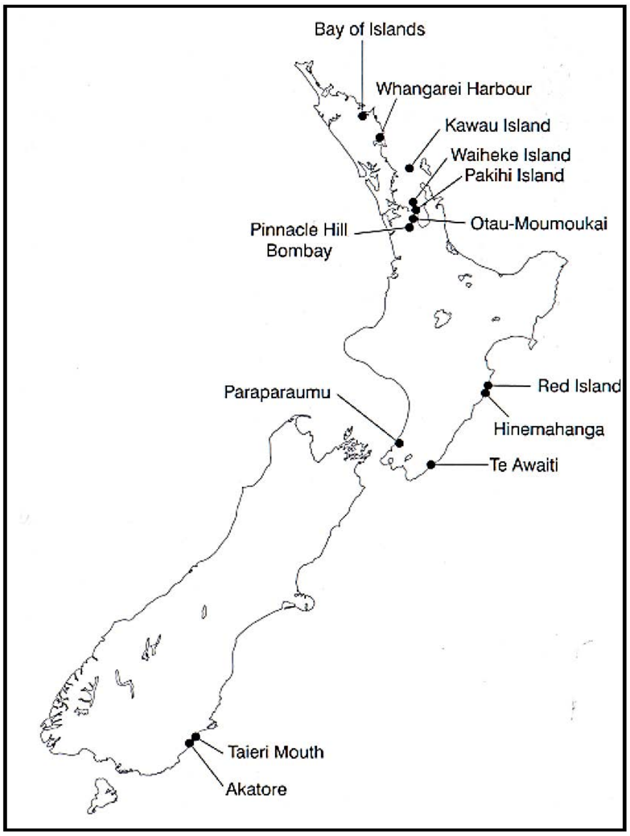

Figure 3.24 Location of manganese deposits (*Volcanogenic Mn*) in New Zealand (after Christie [1995]).

3.12.3 Volcanogenic Mn

3.12.3.1 International Mineral Deposit Model

Features of the *Volcanogenic Mn* mineral deposit model are listed in Table 3.58.

Table 3.58 Features of the *Volcanogenic Mn* international mineral deposit model.

International Mineral Deposit Model – *Volcanogenic Mn*	
Reference	USGS model 24c Volcanogenic Mn (Cox and Singer 1986)
Description	Lenses and stratiform bodies of manganese oxide, carbonate and silicate in chert associated with sedimentary and mafic volcanic rocks. Their genesis is related to volcanogenic processes. Host rocks include chert, shale, sandstone, greywacke, jasper, basaltic lava and tuff and serpentinite. The ore minerals occur in fine-grained massive crystalline aggregates, or botryoidal, colloform and lensoid masses, veinlets and disseminations. The main ore minerals are psilomelane, pyrolusite, rhodochrosite, hausmannite, braunite and neotocite.
International Examples	Olympic Peninsula, Washington; Franciscan Type, California (USA)
Grade-Tonnage Model	USGS model 24c 50th percentile = 47,000 t at 42% Mn (Cox and Singer 1986).

3.12.3.2 New Zealand Occurrences of Volcanogenic Mn *Deposits*

Small manganese deposits occur in association with spilitic red-rock suite rocks in the Permian–Jurassic greywacke and argillite of the North Island (Waipapa Group and Torlesse Supergroup), as well as their metamorphosed equivalents in the South Island (Haast Schist) (Table 3.59). The red rocks consist of mafic lava, chert, jasperite and volcaniclastic argillite. The manganese deposits are usually hosted by red argillite and chert.

New Zealand’s first metal-mining operation was the extraction of manganese from an adit on Kawau Island in 1842. Subsequent production was mainly from deposits in Northland, Bombay (South Auckland) and Taieri Mouth (Otago), continuing intermittently until 1960 to produce a total of 26,102 t of ore, mostly at grades of 40–50% metallic manganese.

Table 3.59 *Volcanogenic Mn* model occurrences (data modified after Brathwaite and Pirajno [1993]). Minerals: crypt = cryptomelane; hm = hematite; mang = manganite; Mn oxides = manganese oxides; psm = psilomelane.

Region	Occurrence	MM [1]	GERM [2]	Production (t)	Deposit Form	Minerals Major (Minor)	Host Rocks
Northland	Kairawaru Bay	C1	P04/e27	-	Stratiform beds	crypt, Mn oxides	Red argillite, spilite
	Wharengaere Road	C2	P04/e55	-	Stratiform beds	braunite, crypt, Mn oxides	Chert
	Mataka	C3	-	-	Stratiform	Mn oxides	Chert
	Pokaka Mt	C4	P05/e111	-	Stratiform	crypt, psm, Mn oxides	Chert, argillite
	Urupukapuka	C5	Q05/e26	-	Stratiform pods	pyrolusite	Red chert, greywacke
	Tikitikiora – Tikiora Hill	C6	Q05/e15	200 Mn ore	Stratiform lenses	braunite, crypt, Mn oxides	Chert, red argillite
	Frenchman's Hill	C7	Q05/e16	Very small	Stratiform lenses	Mn oxides	Chert
	Kiripaka Hill	C8	Q05/e11	Very small	Stratiform	crypt, Mn and Fe oxides	Chert, argillite
	Helena Bay	C9	-	50 Mn ore	Stratiform	pyrolusite	Chert
	Ruapekapeka	-	Q06/e64	-	-	-	-
	Otonga	C10	Q06/e94 and Q06/e103	Very small	Stratiform layer	psm, Mn and Fe oxides	Red clay on greywacke
	Patua Island	C11	-	-	Stratiform	psm, pyrolusite	Red chert, argillite, spilite
	Parua Bay	C12	Q07/e67	200 Mn ore	Stratiform lenses	jacobsite, psm, Mn oxides	Red argillite, chert, greywacke
	Manganese Point	C13	Q07/e66	-	Stratiform	crypt, psm	Red chert, argillite, spilite
	Kawau Island	C15	R09/e56	Very small	Stratiform lenses	Mn oxides	Chert, green argillite
Auckland	Waiheke Island	C16	S11/e24–26, e31–36	Very small	Stratiform lenses	craunite, mang	Chert, red argillite
	Pakihi Island	C17	S11/e38	Very small	Stratiform lenses	crypt, braunite	Red argillite

Region	Occurrence	MM [1]	GERM [2]	Production (t)	Deposit Form	Minerals Major (Minor)	Host Rocks
South Auckland	Otau	C18	-	5760 Mn ore	Stratiform lenses	braunite, crypt, (hm)	Chert, red argillite, spilite
	Moumoukai	C19	S12/e43	1900 Mn ore	Stratiform lenses	crypt, psm, (hm, pyrolusite)	Chert, red argillite
	Pinnacle Hill	C20	S12/e3, S12/e21	550 Mn ore	Stratiform lenses	braunite, psm, crypt, pyrolusite	Chert, red argillite
Wellington	Paraparaumu	C24	-	-	Stratiform	rhodochrosite, calcite, Mn oxides	Chert, argillite, pillow lava
Marlborough	Onamalutu	C34	Q28/e636	-	Stratiform lenses	hm, piemontite, spessartine	Metachert, quartzofeldspathic schist
Otago	Tooth Peak	C70	E41/e25	-	Stratiform bands	Mn oxides	Argillite and chert, pillow lavas
	Akatore	C101	-	~100 Mn concentrate	Stratiform bed	pyrolusite, mang	Chert, mafic tuff and lava

[1] MM = Metallogenic map code (Brathwaite and Pirajno 1993).

[2] GERM = Geological Resource Map code.

Key References: Reed (1960); Sekula (1972); Stanaway (1972); Stanaway et al. (1978), Roser (1983); Brathwaite and Pirajno (1993).

3.13 Molybdenum (Mo)

3.13.1 International Description

International data for molybdenum are listed in Table 3.60.

Table 3.60 Major minerals, world production, reserves and resources and major uses of molybdenum.

Molybdenum (Mo)		
International	**Ore Minerals:** Molybdenite MoS_2, wulfenite $PbMoO_4$ and powellite $Ca(MoW)O_4$	
	World mine production in 2023 (USGS 2024)	260,000 t
	Major world producers (% of 2023 total world production)	China (42%), Chile (18%), Peru (14%), USA (13%), Mexico (6%), Armenia (3%)
	World reserves (USGS 2024)	15 Mt
	World resources (USGS 2024)	20 Mt
	Uses: Steel, alloys and chemicals.	

3.13.2 New Zealand Occurrences of Molybdenum

Molybdenum is presently associated with igneous intrusions in the South Island, mostly as *Porphyry Mo* deposits and epithermal vein deposits in the Hauraki Goldfield – both low-sulfidation and intermediate-sulfidation epithermal deposits (Figure 3.25).

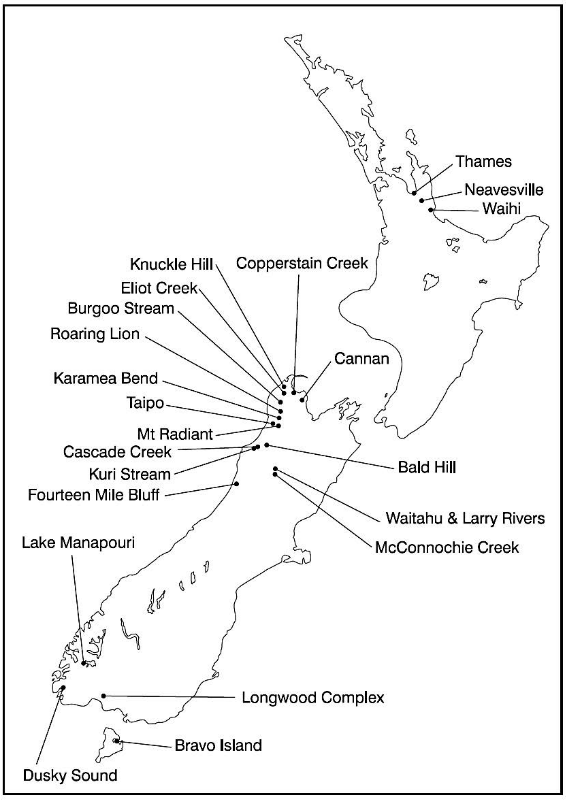

Figure 3.25 Location of molybdenum deposits in New Zealand (after Christie and Brathwaite [1995c]).

Key References: Williams (1974); Eggers and Adams (1979); Tulloch and Rabone (1993); Brathwaite and Pirajno (1993); Christie and Brathwaite (1995c).

3.13.3 Porphyry Mo

3.13.3.1 International Mineral Deposit Model

Features of the *Porphyry Mo* mineral deposit model are listed in Table 3.61.

Table 3.61 Features of the *Porphyry Mo* international mineral deposit model.

International Mineral Deposit Model – *Porphyry Mo*	
Reference	USGS model 21b Porphyry Mo, low-F (Cox and Singer 1986); BCGS model L05 Porphyry Mo (low-F-type) (Lefebure and Ray 1995); and USGS Arc-related porphyry molybdenum deposit model (Taylor et al. 2012).
Description	Stockwork of molybdenite-bearing quartz veinlets and fractures in granitic rocks and associated country rocks. Deposits are low-grade but large and amenable to bulk-mining methods.
International Examples	Endako and Boss Mountain, British Columbia; Red Mountain, Yukon (Canada); Quart Hill, Alaska; Cannivan, Montana; Thompson Creek, Idaho (USA); Compaccha (Peru), East Kounrad (Russia); Jinduicheng (China)
Grade-Tonnage Model	USGS Model 21b (low F) 50th percentile = 94 Mt and 0.085% Mo (Cox and Singer 1986). See also Lefebure and Höy (1996, Table 20) model L05. Copper is generally low-grade (e.g. Endako 0.002% Cu, Glacier Gulch 0.04% Cu, Kitsault 0.004% Cu, Quartz Hill 0.003% Cu, Red Bird 0.07% Cu and Adanac/Ruby Creek 0.001% Cu; John and Taylor 2016).

3.13.3.2 New Zealand Occurrences of Porphyry Mo *Deposits*

Exploration in the late 1960s to early 1980s discovered several *Porphyry Mo* deposits in the northwestern part of the South Island (Table 3.62). These are genetically related to the emplacement of Late Cretaceous (120–106 Ma) I-type Separation Point suite granitoids into the Paleozoic S-type granites of the Karamea suite (e.g. Karamea Batholith) or adjacent quartzose metasedimentary rocks of the Aorere and Greenland groups. Most of the deposits are hosted by the metasedimentary rocks or by the intrusive Cretaceous granitic stocks, with a few (e.g. Taipo Spur) hosted in Paleozoic Karamea suite granite.

The geochemistry of the molybdenum-bearing granitoids is characterised by low K_2O, Rb and F, as well as high Sr and Ti, confirming the classification of the deposits as Mo end members of the porphyry Cu-Mo family, also known as quartz-monzonite-type, granodiorite-type and calc-alkaline-type porphyry molybdenum rather than Climax type (Tulloch and Rabone 1993).

A slightly older (133.5 Ma) porphyry Mo deposit (Brathwaite et al. 2004) is associated with the copper skarn mineralisation at Copperstain Creek.

Key References: Eggers and Adams (1979); Rabone (1989a, 1989b); Tulloch and Rabone (1993).

Table 3.62 *Porphyry Mo* occurrences (data modified after Tables 12a, 12b and 12c of Brathwaite and Pirajno [1993]). Minerals: cp = chalcopyrite, cup = cuprite, gn = galena, hm = hematite, mt = magnetite, mo = molybdenite, po = pyrrhotite, py = pyrite, sb = stibnite, sch = scheelite, sp = sphalerite, td = tetrahedrite.

Occurrence	**MM** [1]	**GERM** [2]	**Deposit Form**	**Minerals Major (Minor)**	**Host Rocks**
Copperstain Creek	A9	M25/e542	Disseminated	py, cp, mo	Skarn, schist, marble, granodiorite porphyry
Gold Creek	A13	N26/e508	Quartz vein stockwork	py, mo	Quartzite
Eliot Creek	A20	M25/e512	Quartz vein stockwork	mo, py, (cp, po, sp, gn, Bi-minerals)	Phyllite, quartzite, granodiorite
Knuckle Hill	-	M25/e517	Quartz vein stockwork	mo, py	Granite
Burgoo	A21	M25/e511	Quartz vein stockwork	mo, py	Phyllite, quartzite, granodiorite
Roaring Lion – Discovery	A22	M26/e516	Quartz vein stockwork	mo, py, (cp, gn, sp)	Hornfelsed quartzite and siltstone; granodiorite
Roaring Lion – Cobra	A23	M26/e515	Quartz vein stockwork	mo, py, (po, mt, cp, gn, sp)	Quartzite and hornfelsed sanstone
Roaring Lion – Grace	A24	M27/e514	Multiple quartz pegmatite veins	mo, py, (cp, sb)	Hornfelsed sandstone and siltsone; granite
Ugly	-	M27/e518	Quartz vein stockwork	mo, cp, gn, sp	Potassic granite, granodiorite
Karamea Bend	A25	M27/e513	Quartz vein stockwork	mo, py, (sp, cp, tennantite, gn, po, Bi-minerals)	Quartz-sericite schist and argillite; quartz monzonite and diorite
Kakapo	A26	M27/e509	Quartz vein stockwork	py, mo, (mt)	Quartz monazite and granodiorite
Allen River	-	M28/e501	Quartz vein stockwork	-	Porphyritic granite
Mt Scarlett	A27	L27/e503	Quartz veins	po, cp, mo	Biotite granite
Anaconda	A29	L27/e506	Quartz-sulfide vein	cp, mo, py	Granite gneiss
Copper Creek Reef, Mt Radiant	-	L27/e504	Quartz vein stockwork	cp, py, bn, cup, sch	Porphyritic biotite granite
Stormy Ridge area	-	L27/e559	Quartz vein stockwork	mo, py	Porphyry granite, granodiorite
Mt Radiant	A30	L28/e505	Quartz and pegmatite veins	py, cp, mo, (td, bn, emplectite)	Foliated granite and granite gneiss; quartz monxonite and granodiorite
Taipo	A32	M28/e502	Multiple quartz veins	py, mo, (mt, hm)	Porphyritic granite; microgranite

Occurrence	MM [1]	GERM [2]	Deposit Form	Minerals Major (Minor)	Host Rocks
Bald Hill	A44	L29/e142	Quartz vein stockwork	mo, py, (cp, bismuthinite)	Hornfelsed greywacke and argillite; trondhjemite porphyry
Cascade Stream	A48	K29/e74	Quartz vein stockwork	py, cp, mo, mt	Hornfelsed greywacke; quartz porphyry
Kuri Stream	A49	K29/e73	Quartz vein	py, mo, cp	Greywacke
McConnochie Creek	A66	L30/e252	Quartz veins	cp, mo, py, bismuth	Greywacke, argillite; granite
Fourteen Mile Bluff	-	J31/e25	Quartz vein stockwork	mo, py	Greywacke intruded by granite
Seventeen Mile Bluff	A77	J31/e26	Quartz vein stockwork	mo, py, cp, (sp, Bi-minerals)	Hornfelsed greywacke; granite

[1] MM = Metallogenic map code (Brathwaite and Pirajno 1993).

[2] GERM = Geological Resource Map code.

3.14 Nickel (Ni)

3.14.1 International Description

International data for nickel are listed in Table 3.63.

Table 3.63 Major minerals, world production, reserves and resources and major uses of nickel.

<table>
<tr><th colspan="3">Nickel (Ni)</th></tr>
<tr><td rowspan="6">International</td><td colspan="2">Ore Minerals: Breithauptite NiSb, choanthite (white nickel) $NiAs_2$, garnierite $(Ni,Mg)_3Si_2O_5(OH)_4$ (nickel serpentine), gersdorffite NiAsS, millerite (yellow nickel) NiS, niccolite (red nickel, kupfernickel) NiAs, pentlandite (Fe,Ni)S, pyrrhotite (Fe,Ni)S and ullmannite NiSbS</td></tr>
<tr><td>World production in 2023 (USGS 2024)</td><td>3.6 Mt</td></tr>
<tr><td>Major world producers (% of 2023 total world production) (USGS 2024)</td><td>Indonesia (50%), Philippines (11%), New Caledonia (6%), Russia (6%), Canada (5%), Australia (4%), China (3%), Brazil (2%)</td></tr>
<tr><td>World reserves (USGS 2024)</td><td>>130 Mt</td></tr>
<tr><td>World resources (USGS 2024)</td><td>>350 Mt with 54% in laterites and 35% in magmatic sulfide deposits</td></tr>
<tr><td colspan="2">Uses: Most nickel is used in stainless steel, but its use in lithium-ion batteries for electric vehicles is growing rapidly.</td></tr>
</table>

3.14.2 New Zealand Occurrences of Nickel

Nickel occurrences are shown in Figures 3.26 and 3.27. Nickel is associated with mafic-ultramafic rocks in the South Island. The nickel and associated metals precipitated out during cooling and crystallisation of mafic-ultramafic magmas. Nickel occurs as pentlandite, along with accessory minerals pyrrhotite, chalcopyrite and magnetite. The relatively high density of the sulfur liquids and associated sulfide minerals results in these settling at the base of the magma chamber, potentially at ore-grade concentrations. In New Zealand, these types of deposits are classified as *Dunitic Ni-Cu* and *Gabbroid-associated Ni-Cu*. Weathering of these primary deposits may develop *Lateritic Ni*.

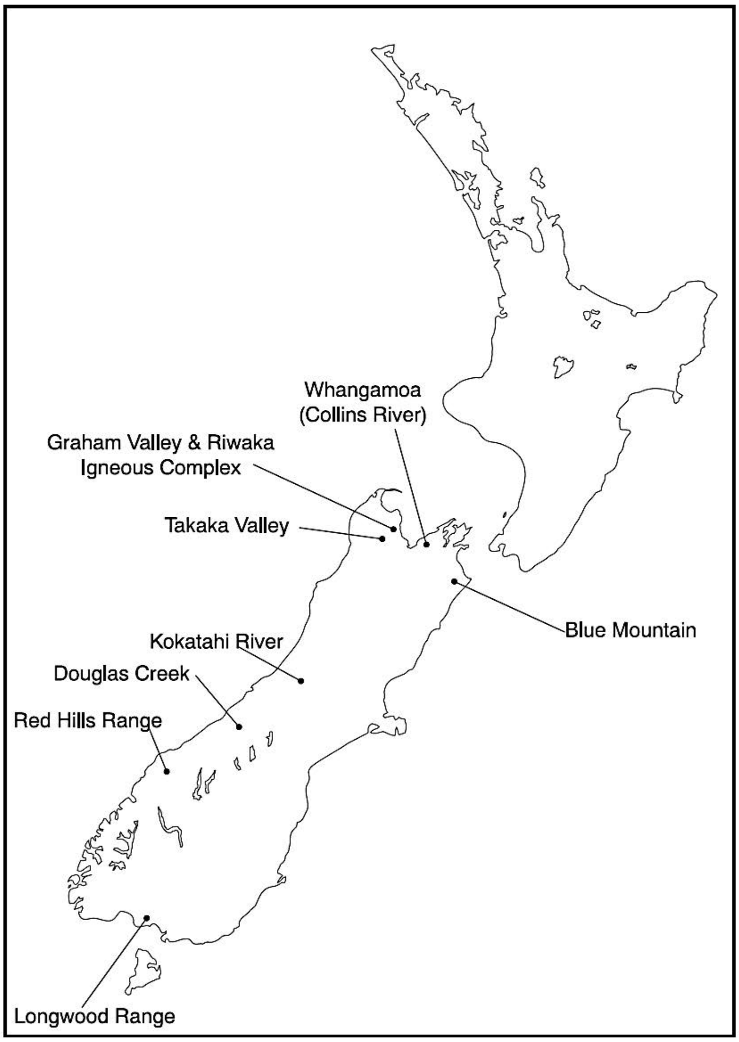

Figure 3.26 Location of nickel deposits in New Zealand (after Christie and Brathwaite [1995b]).

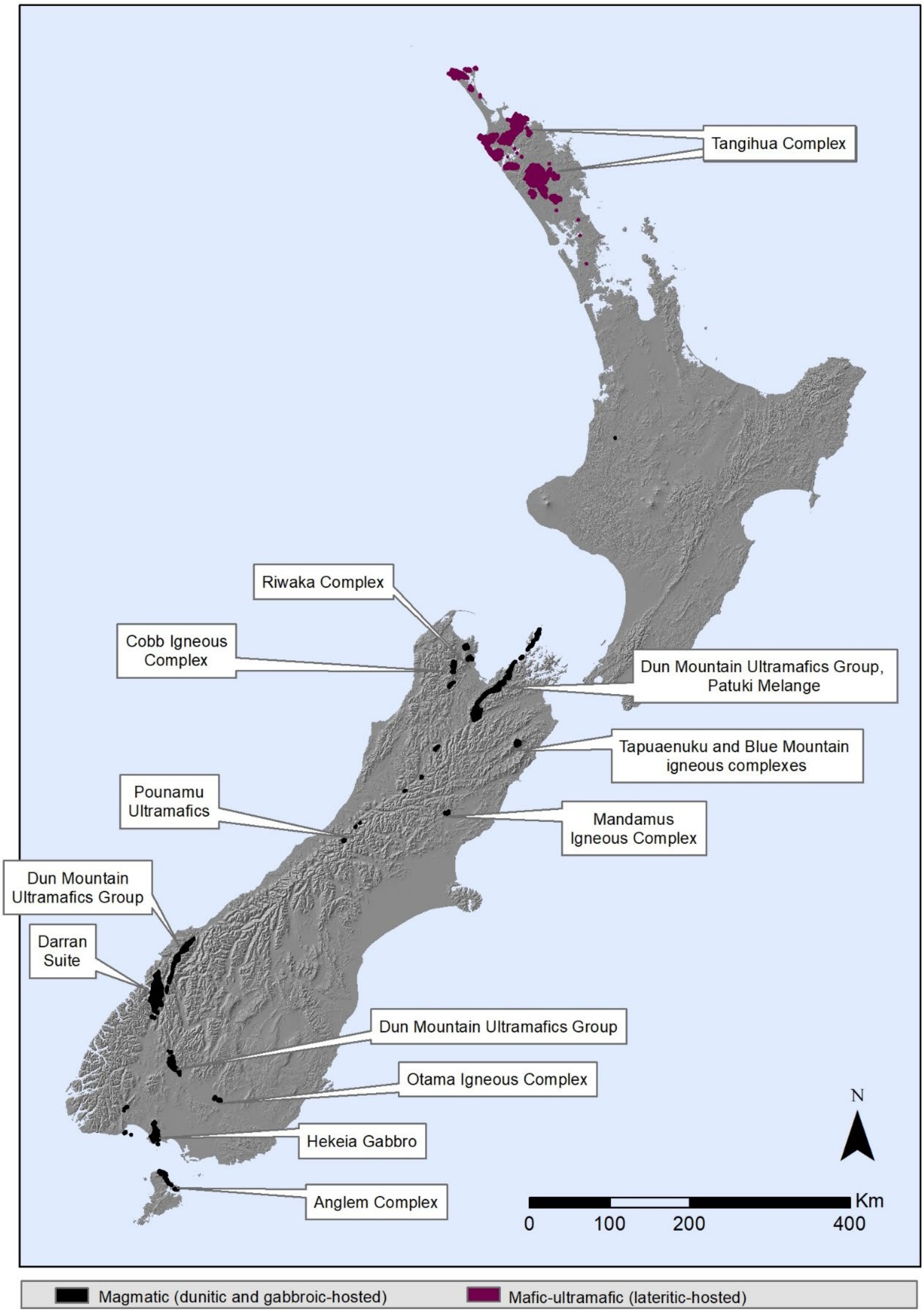

Figure 3.27 Location of mapped, ultramafic and mafic geology that could potentially host magmatic nickel and cobalt deposits in New Zealand (after Durance et al. [2018]).

Key References: Williams (1974); Brathwaite and Pirajno (1993); Christie and Brathwaite (1995d); Christie et al. (2010); Christie and Barker (2016); Christie and Turnbull (2016); Brathwaite et al. (2016, 2017a, 2017b); Turnbull et al. (2017); Durance et al. (2018).

3.14.3 Dunitic Ni-Cu

3.14.3.1 International Mineral Deposit Model

Features of the *Dunitic Ni-Cu* mineral deposit model are listed in Table 3.64. Note that there is overlap with the *Gabbroid-associated Ni-Cu* model.

Table 3.64 Features of international mineral deposit models equivalent to the *Dunitic Ni-Cu* model used in this report.

International Mineral Deposit Model – *Dunitic Ni-Cu*	
Reference	USGS model 6b Dunitic Ni-Cu (Cox and Singer 1986) and USGS model for magmatic sulfide-rich Ni-Cu-(platinum group elements) deposits related to mafic and ultramafic dike-sill complexes (Schulz et al. 2014)
Description	Disseminated sulfide mineralisation in intrusive dunites. Typically, dunitic and olivine peridotite lenses up to 1 km long and 100 m thick host lenticular shoots of massive, matrix and breccia sulfide. Ore minerals include pyrrhotite, pentlandite, magnetite, pyrite, chalcopyrite and chromite. Dunitic Ni-Cu deposits are analogous to the Ni-Cu deposits in basal ultramafic parts of greenstone belts with komatiitic, dunitic and picritic sub-types of Dill (2010)
International Examples	Jinchuan, Xiarihamu (China); Kabanga (Tanzania); Wellgreen, Yukon; Voisey's Bay, Newfoundland (Canada); Noril'sk and Pechanga (Russia); Agnew and Mt Keith, Western Australia (Australia)
Grade-Tonnage Model	USGS model 6b 50th percentile = 29 Mt at 1% Ni, possible by-product Cu, PGM, Au and Co (Cox and Singer 1986)

3.14.3.2 New Zealand Occurrences of Dunitic Ni-Cu *Deposits*

In New Zealand, this deposit type is associated with disseminated sulfide mineralisation in ultramafic and mafic intrusive rocks and has the potential to be hosted in the Permian serpentinite, dunite and peridotite of the Dun Mountain Ultramafic Group rocks (e.g. Serpentine-hosted Fe-Cu deposits; Table 3.20), as well as the Mesozoic lensoid schistose serpentinite of the Pounamu Ultramafics and in areas associated with other ultramafic igneous complexes. The occurrence of disseminated nickel mineralisation in the form of awaruite ± heazlewoodite ± pentlandite ± native copper in serpentinised peridotites in the Dun Mountain ultramafics in east Nelson (Brathwaite et al. 2016, 2017a) is similar to disseminated awaruite in serpentinised ophiolitic peridotites of the Cache Creek complex in British Columbia (Britten 2017) that have economic potential for nickel.

3.14.4 Gabbroid-Associated Ni-Cu

3.14.4.1 International Mineral Deposit Model

Features of the *Gabbroid-associated Ni-Cu* mineral deposit model are listed in Table 3.65.

Table 3.65 Features of the *Gabbroid-associated Ni-Cu* international mineral deposit model.

International Mineral Deposit Model – *Gabbroid-Associated Ni-Cu*	
Reference	USGS model 7a Synorogenic-synvolcanic Ni-Cu (Cox and Singer 1986). Gabbroid-associated Ni-Cu deposits are analogous to the Ni-Cu-(platinum group elements [PGE]) deposits in rift-related volcanic host rocks of Dill (2010). USGS model for magmatic sulfide-rich Ni-Cu-(PGE) deposits related to mafic and ultramafic dike-sill complexes (Schulz et al. 2014)
Description	Massive lenses, matrix and disseminated sulfide in small- to medium-sized gabbroic intrusions in greenstone belts. The sulfides are commonly in the more ultramafic parts of the complex and near the basal contacts of the intrusion. Host rocks are norite, gabbro-norite, pyroxenite, peridotite, troctolite and anorthosite, forming layered or composite igneous complexes. The main ore minerals are pyrrhotite, pentlandite and chalcopyrite, as well as local pyrite, Ti-magnetite, Cr-magnetite, graphite, by-product Co and PGE.
International Examples	Sudbury Igneous Complex (Canada); Stillwater Complex (USA); Bushveld Igneous Complex (South Africa); Great Dyke (Zimbabwe)
Grade-Tonnage Model	Model 7a 50th percentile = 2.1 Mt and 0.77% Ni and 0.47% Cu (for 16,170 t Ni and 9870 t Cu; using 16,000 t Ni and 10,000 t Cu), possible by-product Co, Au and platinum group metals (Cox and Singer 1986)

3.14.4.2 New Zealand Occurrences of Gabbroid-Associated Ni-Cu *Deposits*

The most significant occurrence is Ni-Cu sulfide mineralisation associated with the Riwaka mafic-ultramafic complex of Late Devonian age in the Graham Valley, Northwest Nelson (Table 3.66; Christie and Turnbull 2016; Turnbull et al. 2017). The complex is a series of layered intrusions emplaced along a fault zone in marble, phyllite and biotite schist (Bates 1989a). The Graham Valley Ni-Cu mineralisation occurs mainly within the cumulus gabbro between the Graham and Pearce valleys (e.g. Prospect, Field and Price’s creeks), where sulfide content ranges from 1 to 50%, characteristically with Ni>Cu. Nickel sulfide mineralisation is also associated with mafic-ultramafic rocks in the Cobb Valley (upper Takaka, e.g. Meter Creek) and at Blue Mountain in Marlborough. Minor occurrences are found in mafic-ultramafic rocks of the Red Hills range of Westland and Otago, the Darran Mountains of Fiordland (e.g. Camera Lake and Falls Creek), various locations in Southland, including West Dome, Otama Igneous Complex, Longwood Range and Takitimu Mountains, and in the Anglem Complex of Rakiura / Stewart Island.

Drilling at the Riwaka prospect in the 1970s was mainly to shallow depths and there is potential to expand on this exploration for Ni-Cu, along with associated platinum group elements (PGE).

Challenges: The Riwaka prospect lies on the margin of the Kahurangi National Park with part of the prospect within the park.

Key References: Bates (1989a); Christie and Brathwaite (1995d); Christie et al. (2010); Partington et al. (2001); Christie and Turnbull (2016); Turnbull et al. (2017); Durance et al. (2018).

Table 3.66 *Gabbroid-associated Ni-Cu* model occurrences (data modified after Brathwaite and Pirajno [1993]). Minerals: cp = chalcopyrite; il = ilmenite; mt = magnetite; pnt = pentlandite; po = pyrrhotite; py = pyrite.

Occurrence	**MM** [1]	**GERM** [2]	**Deposit Form**	**Minerals Major (Minor)**	**Host Rocks**
Riwaka Complex, Graham Valley	A18	M27/e569, 570, 519	Disseminated lenses	po, cp, pnt, py, mt	Pyroxenite, gabbro
Cobb Igneous Complex (e.g. Meter Creek)	-	M26/e43, 46	-	-	Diorite
Mt Solitary	A103	B44/e2	Disseminated	po, cp, pnt	Petadiorite, peridotite
Blue Mountain	D1	P29/e10	Disseminated	po, cp	Alkali gabbro, pyroxenite
Mt Tapuaenuku	D2	O30/e2	Disseminated	py, po, cp, mt, il, apatite	Pyroxenite, gabbro, anorthosite

[1] MM = Metallogenic map code (Brathwaite and Pirajno 1993).

[2] GERM = Geological Resource Map code.

3.14.5 Lateritic Ni

3.14.5.1 International Mineral Deposit Model

Features of the *Lateritic Ni* mineral deposit model are listed in Table 3.67.

Table 3.67 Features of the *Lateritic Ni* international mineral deposit model.

International Mineral Deposit Model – *Lateritic Ni*	
Reference	USGS model 38a Lateritic Ni (Cox and Singer 1986); Dill (2010); and Ni-Co laterites (Marsh et al. 2013)
Description	Nickel-rich *in situ* lateritic weathering products developed from ultramafic rocks, particularly peridotite, dunite and serpentinised peridotite. Nickel-rich iron oxides are most common. Some deposits are predominantly nickel silicates.
International Examples	Poro (New Caledonia); Cerro Matosa (Columbia); Nickel Mountain, Oregon (USA); Greenvale, Queensland (Australia)
Grade-Tonnage Model	USGS model 38a 50th percentile = 44 Mt at 1.4% Ni (616,000 t Ni, using 600,000 t Ni) (Cox and Singer 1986).

3.14.5.2 New Zealand Occurrences of Lateritic Ni *Deposits*

Traces of nickel have been found in the laterite developed on the serpentinite and gabbro at Surville Cliffs, North Cape (Bell and de C Clarke 1909). Durance et al. (2018) suggested that there was potential for lateritic nickel in the ultramafic components of the ophiolitic Tangihua Complex.

3.15 Platinum Group Metals (PGM)

3.15.1 International Description

International data for platinum group metals are listed in Table 3.68.

Table 3.68 Major minerals, world production, reserves and resources and major uses for platinum group metals.

Platinum Group Metals (PGM)						
International	**Ruthenium (Ru)**	**Rhodium (Rh)**	**Palladium (Pd)**	**Osmium (Os)**	**Iridium (Ir)**	**Platinum (Pt)**
	Ore Minerals: Braggite (Pt,Pd,Ni)S, cooperite (Pt,Pd)S, iridosmine OsIr, geversite $PtSb_2$, laurite RuS_2, monchelite $(Pt,Pd)(Te,Bi)_2$, native palladium Pd, native platinum Pt, native iridium Ir, osmiridium IrOs, rutheniridosmine RuOsIr, sperrylite $PtAs_2$, stabio-palladinite Pd_3Sb					
	Ruthenium Uses: Electronics, jewellery, medical and dental tools, mechanical bearings and parts					
	Rhodium Uses: Vehicle exhaust catalysts, crucibles, thermocouples, electrodes					
	Palladium Uses: Vehicle exhaust catalysts, jewellery, electronics, dentistry, chemical reagents					
	Osmium Uses: Jewellery, fountain pen nibs, medical and dental tools, mechanical bearings and parts					
	Iridium Uses: Crucibles, thermocouples, electrodes					
	Platinum Uses: Jewellery, vehicle-exhaust catalysts, dentistry, glass, crucibles, thermocouples, electrodes, coinage, chemicals manufacture					
	Trends: The use for PGMs is mainly for emissions-capping catalytic converters in diesel and petrol engines. Increasing electrification of vehicles has resulted in a decline in the demand and price for PGMs.					

3.15.2 Platinum Group Metals in New Zealand

PGM occur in three main geological environments: layered mafic igneous complexes, ophiolites, and in association with placer gold deposits (Figure 3.28). Past production of PGM has seen the recovery of small quantities in the late 1800s and early 1900s as a by-product of placer gold mining in Southland.

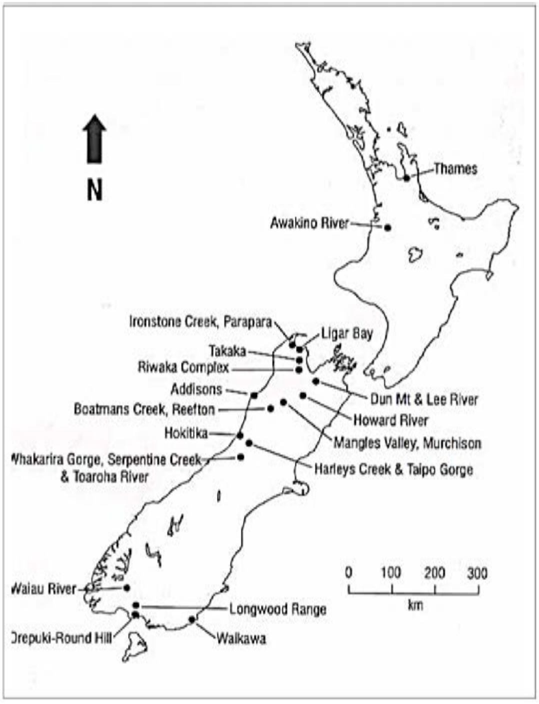

Figure 3.28 Location of platinum group metal occurrences (after Christie and Challis [1995]).

Key References: Williams (1974); Cowden et al. (1990); Brathwaite and Pirajno (1993); Christie and Challis (1995); Christie et al. (2006c); Ashley et al. (2012); Craw et al. (2016).

3.15.3 Magmatic PGM

3.15.3.1 International Mineral Deposit Model

Features of the *Magmatic PGM* mineral deposit model and *Alaskan-type* sub-model are listed in Table 3.69.

Table 3.69 Features of international mineral deposit models relevant to the *Magmatic PGM* model and *Alaskan-type* sub-model used in this report.

International Mineral Deposit Model – *Magmatic PGM*	
Reference	USGS model 2b Merensky Reef platinum group elements (Cox and Singer 1986); and USGS model for reef-type PGE and contact-type Cu-Ni-PGE deposits (Zientek 2012). ***Alaskan-type* sub-model** USGS model 9 Alaskan PGE (Cox and Singer 1986); and BCGS model M05 Alaskan-type Pt±Os±Rh±Ir (Lefebure and Höy 1996).
Description	Ultramafic intrusive complexes, commonly zoned, forming sills, stocks or intrusive. ***Alaskan-type* sub-model:** Ultramafic intrusive complexes, commonly zoned, forming sills, stocks or intrusive bodies with poorly known external geometry. Sub-economic platinum group elements (PGE) in lode occurrences are associated with: (1) thin (centimetre-scale), disrupted chromitite layers, (2) thick (metre-scale) concentrations of cumulus magnetite or (3) clinopyroxenite. Chromitite-hosted PGE occurrences are the main source of PGE for placer deposits. Lode occurrences of PGEs are primarily controlled by magmatic cumulate stratigraphy: (1) chromitites are restricted to dunites where they form thin discontinuous layers, or schlieren, pods and nodular masses seldom more than a metre in length; (2) magnetitites and concentrations of cumulus magnetite form well-bedded, locally continuous, layers up to 6 m thick, intercalated with hornblende clinopyroxenite; (3) lenses and vein-like bodies of relatively coarse-grained or 'pegmatoid', biotite and magnetite-poor, PGE-bearing clinopyroxenites are enclosed by finer-grained biotite and magnetite-rich PGE-poor clinopyroxenites.
International Examples	***Alaskan-type* sub-model** Red Mountain, Goodnews Bay, Alaska; Tin Cup Peak, Oregon (USA); Ural Mountains and Aldan Shield (Russia); Fifield district, New South Wales (Australia)
Grade-Tonnage Model	Major overseas deposits are in the tens of millions of tonnes and grade 10–20 g/t PGM, as well as associated nickel and copper. We suggest a model size of 5 Mt, grading 5 g/t PGM (~0.8 Moz PGM).

The *Alaskan-type* sub-model described in Table 3.70 is a sub-type of the *Magmatic PGM* model, and some *Magmatic PGM* deposits in New Zealand are similar to this model, particularly the Greenhills Complex at Bluff.

3.15.3.2 New Zealand Occurrences of Magmatic PGM *Deposits*

PGM are associated with magmatic nickel-copper sulfides in layered mafic complexes. Complexes that have been identified as prospective by the presence of *in situ* PGE, or nearby placer PGE with high Pt+Pd/Ru+Os+Ir ratios include the Riwaka, Rotoroa, Longwood and Greenhills (Bluff) complexes (Challis 1989; Mitchell 1995) These and other prospective intrusive complexes are listed in Table 3.70 and their locations shown in Part 1 (Figure 8.9). Exploration to date has been of a reconnaissance nature and consisted mostly of stream-sediment, soil and rock-chip geochemical surveys. The most advanced prospect, the Longwood Complex, has been tested by four drill holes totalling 2500 m (Figure 3.29) in 2024; this is being explored by Midway Resources.

Table 3.70 Prospects explored for *Magmatic PGM* (data modified after Brathwaite and Pirajno [1993]). Minerals: cp = chalcopyrite; il = ilmenite; mt = magnetite; pnt = pentlandite; po = pyrrhotite; py = pyrite; Pt = platinum.

Region	**Occurrence**	**MM** [1]	**GERM** [2]	**Deposit Form**	**Minerals Major (Minor)**	**Host Rocks**
West Nelson	Riwaka Complex	A18	M27/e519, 569, 570	Disseminated lenses	po, cp, pnt, py, mt	Pyroxenite, gabbro
	Rotoroa Complex	-	-	Disseminated	-	-
	Cobb Igneous Complex	-	-	Chromitite veins	-	Pyroxenite, peridotite
Marlborough	Blue Mountain	D1	P29/e10	Disseminated	po, cp	Alkali gabbro, pyroxenite
	Mt Tapuaenuku	D2	O30/e2	Disseminated	py, po, co, mt, il, apatite	Pyroxenite, gabbro, anorthosite
	Takitimu Mts	-	-	Disseminated	-	-
	Woodlaw	-	-	Disseminated	-	-
	Longwood Complex	B40	D46/e43, 46, 47	Disseminated	cp, Pt, gold	Anorthosite, troctolite
	Green Hills Complex, Bluff	B43	-	Disseminated in layers	chromite	Dunite

[1] MM = Metallogenic map code (Brathwaite and Pirajno 1993).

[2] GERM = Geological Resource Map code.

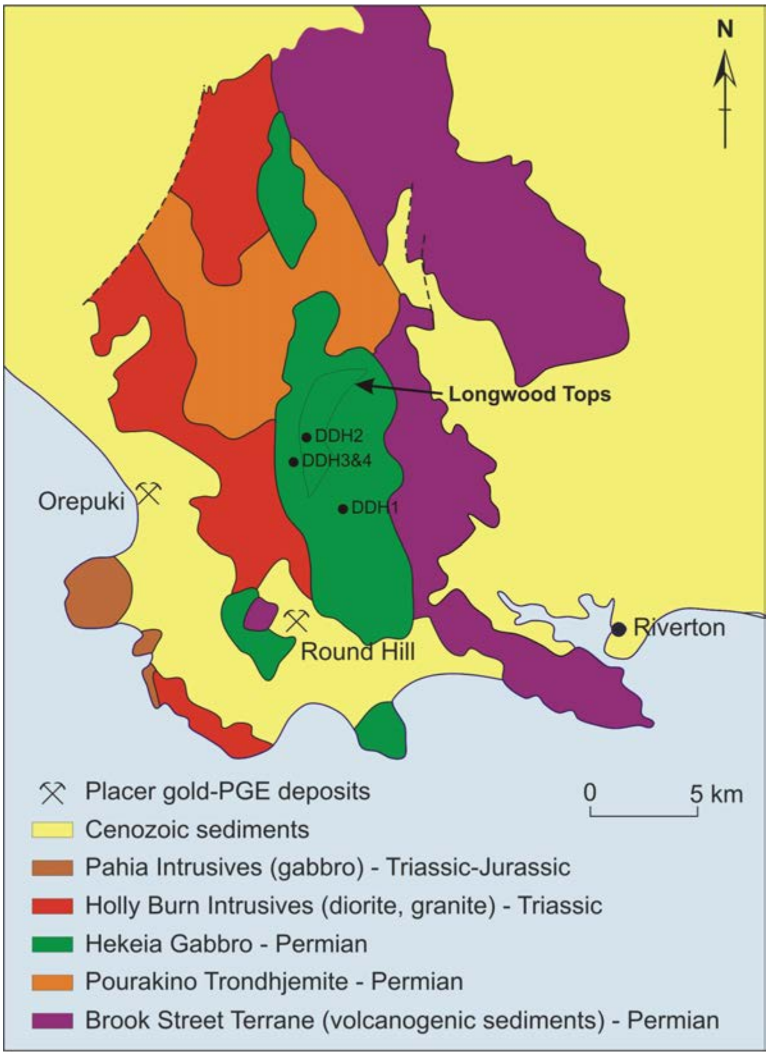

Figure 3.29 Geology of the Longwood Complex and environs, Southland (modified after Christie et al. [2006c]).

Except for Blue Mountain and Tapuaenuku, all of the gabbroic complexes with known associated PGE mineralisation lie within the Median Batholith, a narrow band of predominantly plutonic rocks separated into northern and southern sections by a 480 km offset across the Alpine Fault (Figure 3.30). The Devonian-Cretaceous Median Batholith (Mortimer et al. 1999) is a fundamental tectonic unit of the South Island separating the Western and Eastern Provinces, which consist of Paleozoic–Mesozoic meta-sedimentary terranes. The Western Province was part of the Gondwana supercontinent since at least the Permian. Rocks of the Eastern Province have been progressively accreted to the Western Province and Median Batholith since about 240 Ma (Early Triassic).

The Median Batholith comprises a variety of calc-alkaline plutons of gabbro, diorite and granite, with mostly Triassic–Cretaceous ages in the range 230–125 Ma, but some Permian gabbros and Devonian–Carboniferous plutons are also present. Genetically related metavolcanic and metasedimentary rocks make up about 10% by area of the Median Batholith.

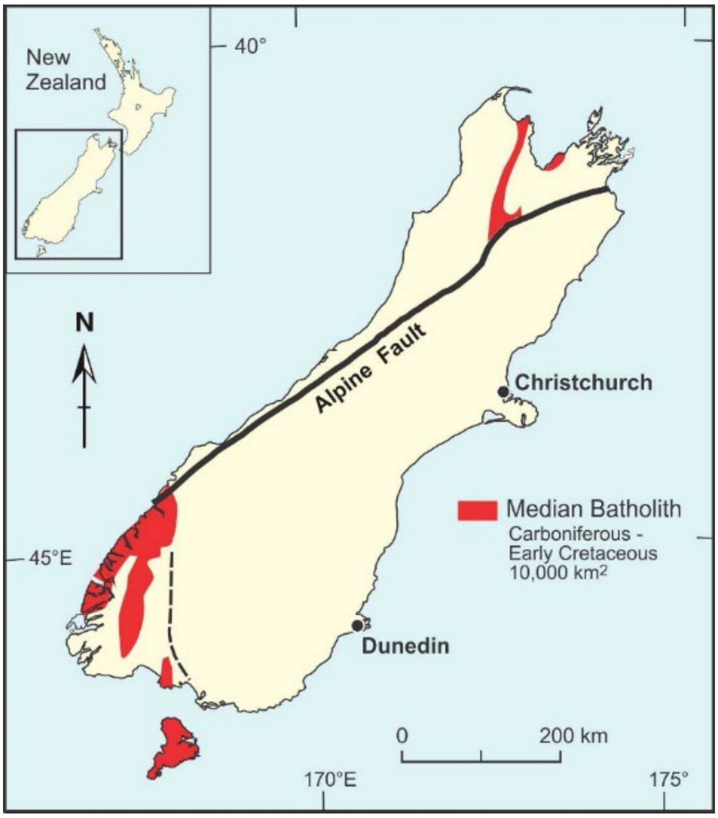

Figure 3.30 Location of the Median Batholith.

3.15.4 *Dunitic PGM* – Dun Mountain Ophiolite Belt

Several chromite occurrences in the Permian Dun Mountain Ophiolite Belt have been investigated for PGM potential. Locations of interest are listed in Table 3.71 and Figure 3.31. The Mount Baldy, Matakitaki, occurrence in east Nelson contains elevated Pt (717–1069 ppb) and Pd (287–531 ppb) in chromite (Brathwaite et al. 2012c, 2016, 2017a).

Table 3.71 Prospect explored for *Dunitic PGM*. Minerals: Pd = palladium; Pt = platinum.

Region	**Occurrence**	**MM** [1]	**GERM** [2]	**Production (t)**	**Deposit Form**	**Minerals Major (Minor)**	**Host Rocks**
West Nelson	Dun Mt	B15	O27/e573	~1400	Podiform lenses	Chromite	Serpentinised dunite and harzburgite
	Red Hills	B22	N29/e11	-	Podiform lenses	Chromite	Dunite and harzburgite
	Mount Baldy, Matakitaki	B23	-	-	Chromite segregations	Chromite, Pt, Pd	Gabbro, diorite
Otago – Southland	Red Mt	E39/e5	-	Podiform lenses	Chromite	Ultramafics	-

[1] MM = Metallogenic map code (Brathwaite and Pirajno 1993).

[2] GERM = Geological Resource Map code.

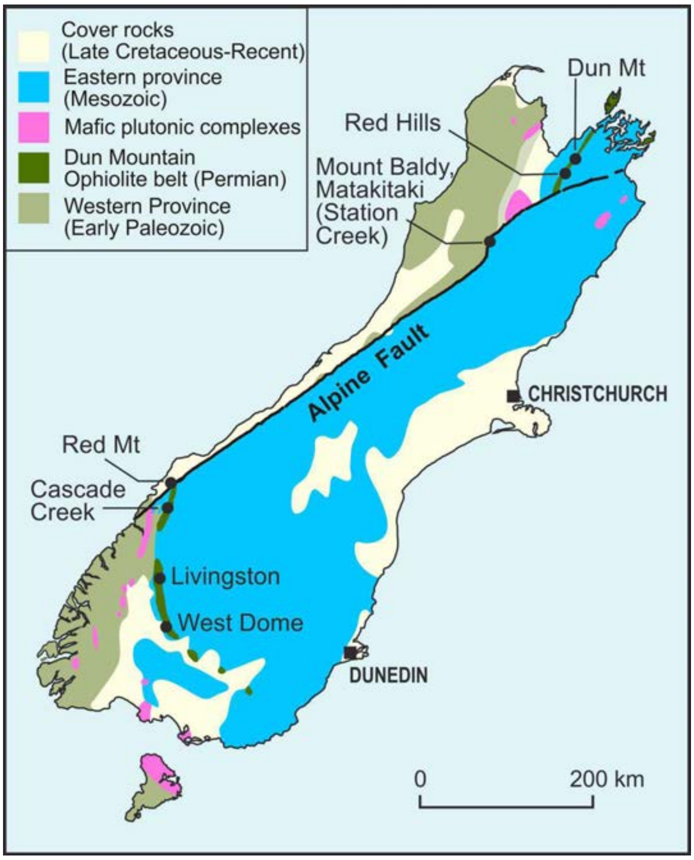

Figure 3.31 Location of the Dun Mountain Ophiolite Belt and prospects explored during the 1980s.

3.15.5 Placer PGM

3.15.5.1 International Mineral Deposit Model

Features of the *Placer PGM* mineral deposit model are listed in Table 3.72.

Table 3.72 Features of international mineral deposit models equivalent to the *Placer PGM* model used in this report.

International Mineral Deposit Model – *Placer PGM*	
Reference	USGS model 39a Placer Au-PGE (Cox and Singer 1986)
Description	Elemental gold and PGE alloys in grains and (rarely) nuggets in gravel, sand, silt and clay, and their consolidated equivalents, in alluvial, beach, eolian and (rarely) glacial deposits.
International Examples	Sierra Nevada, California (USA); Victoria (Australia)
Grade-Tonnage Model	Model 39a 50th percentile = 1.1 Mt and 0.2 g/t Au/PGM, possible by-product Ag (Cox and Singer 1986).

3.15.5.2 New Zealand Occurrences of Placer PGM *Deposits*

Detrital platinum has been recorded from several locations in the South Island, associated with placer gold (Figure 3.32; Challis 1989). The main alluvial prospects of economic interest are in Southland, principally the Waiau River and various prospects peripheral to the Longwood Complex (Table 3.73; Hay 1989; Stevens and Phillip 1992; Stevens 1992). Additionally, several beach-sand deposits may be prospective, including Te Wae Wae Bay and beaches on the southeast Catlins coast such as Waikawa (Graves 1987; Clark and Norton 1990; MacDonell 1992). These are primarily placer gold prospects with potential for by-product PGE.

Other occurrences of detrital PGM include Ironstone Creek near Parapara, Ligar Bay, near Collingwood, from alluvial gold workings around Takaka, in the Howard River in south Nelson, Lee River in the east Nelson Dun Mountain Ophiolite Belt and in alluvial and beach gold workings on the West Coast.

Challis (1989) noted that the mineralogy of the detrital PGE could be used to characterise the source, principally by using the ratio of Pt+Pd to Ru+Os+Ir. High ratios are indicative of a layered igneous complex source, whereas low ratios suggest derivation from the Dun Mountain Ophiolite Belt, Pounamu Ultramafics or similar sources. Therefore the Pt+Pd/Ru+Os+Ir ratio of detrital PGE occurrences can be used as a prospecting tool to highlight the PGE prospectivity of nearby igneous complexes.

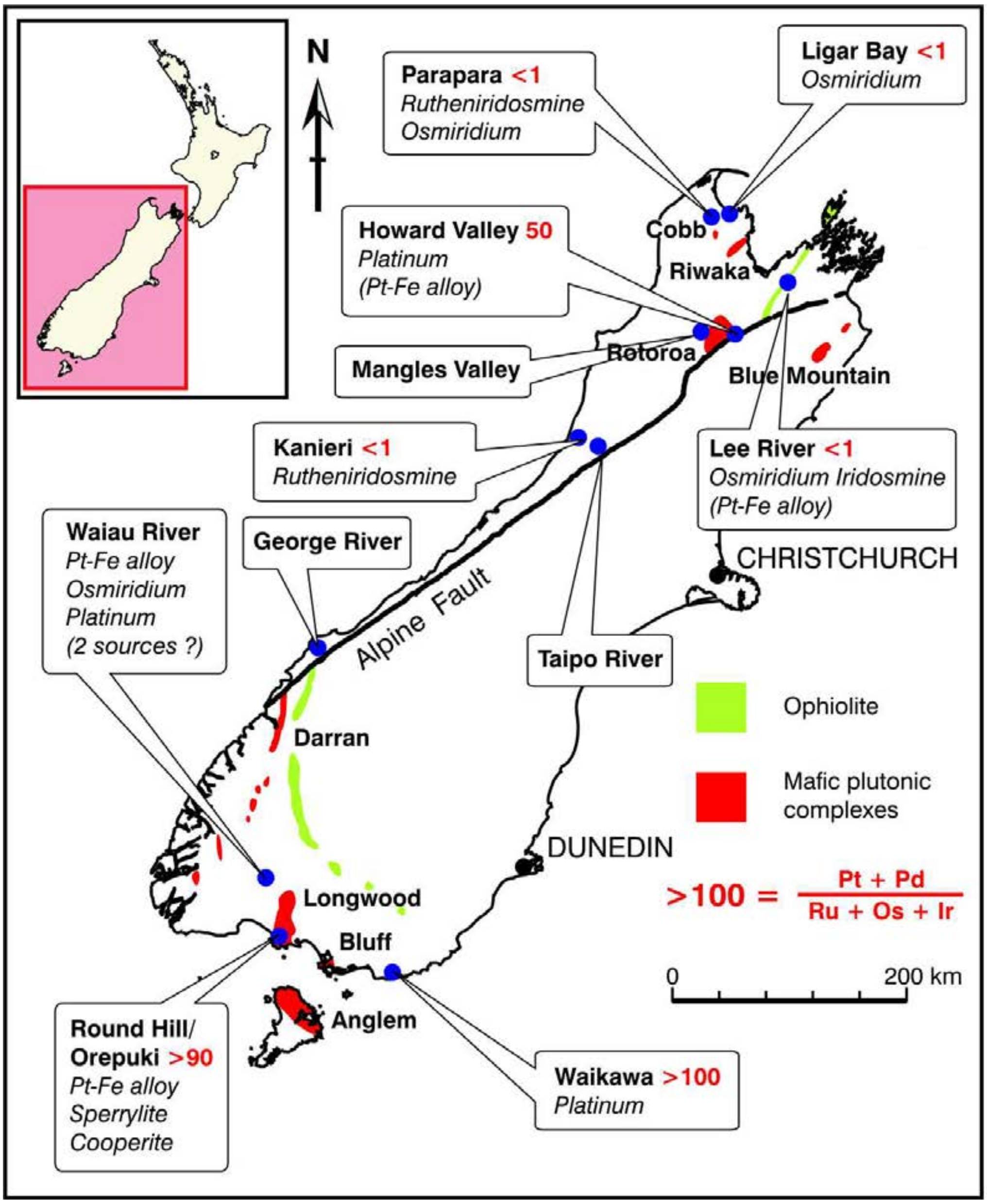

Figure 3.32 Locations of detrital platinum group metals (PGM) and *Placer PGM* where known (from data in Challis [1989]; Mitchell [1995]). Placer PGE from layered mafic complexes have high ratios of Pt+Pd/Ru+Os+Ir, whereas PGE sourced from ophiolites have low ratios (after Christie and Barker [2013]).

Production consists of 47 kg of PGM that was produced as a by-product of placer gold mining at Round Hill near Orepuki (1897–1907) and 13 kg of PGM concentrate that was produced from gold claims along the south coast of Southland (1907–1916) (Brathwaite and Pirajno 1993).

Occurrences of *Placer PGM* deposits are listed in Table 3.73.

Table 3.73 *Placer PGM* model occurrences. Minerals: il = ilmenite; mt = magnetite; mz = monazite; rt = rutile; Pt = platinum; th = thorite; zr = zircon.

Region	Occurrence	MM [1]	GERM [2]	Production (t)	Deposit Form	Minerals Major (Minor)	Host Rocks
West Nelson	Parapara-Collingwood	F10	M25/e591	Small	Alluvial placer	Gold	Quartz conglomerate
	Lee River	-	N28/e590	-	Alluvial placer	Pt	-
	Maud Creek	-	M29/e21	-	Alluvial placer	Pt	-
Southland	Tunnel Claim, Waiau Mouth	F190	D46/e31	Very small	Beach placer	Gold, mt, zr, rt, Pt, mz	Beach sand (black sand leads)
	Orepuki	F191	D46/e41	Very small	Alluvial and beach placers	Gold, mt, ze, rt, Pt, mz	Beach sand and terrace gravels
	Round Hill	F192	D46/e42	>2.5 Au >0.047 Pt	Alluvial placer	Gold, mt, il, mz, Pt	Gabbro gravels
	Waipapa Beach	F193	F47/e13	Very small	Beach placer	Gold, Pt, mt	Beach and dune sands (black sand leads)
	Haldane Bay	F194	F47/e10	Very small	Beach placer	Gold, Pt	Beach and dune sands (black sand leads)
	Porpoise Bay	F195	-	Very small	Beach and eolian placer	Gold, Pt	Beach and dune sands
	Wallace Beach	F196	D47/e12	Very small	Beach placer	Gold, Pt, il, zr	Beach sand
	Progress Valley Beach, Waikawa	F197	-	Very small	Beach placer	Gold, Pt, mz, th	Beach sand (black sand)

[1] MM = Metallogenic map code (Brathwaite and Pirajno 1993).

[2] GERM = Geological Resource Map code.

3.16 Rare Earth Elements

3.16.1 International Description

International data for rare earth elements (REE) are listed in Table 3.74.

Table 3.74 Major elements, ore minerals, world production, reserves and resources and major uses of rare earth elements, as well as associates scandium, yttrium and thorium.

<table>
<tr><th colspan="19">Platinum Group Metals (PGM)</th></tr>
<tr><td rowspan="6">International</td><td>Lanthium (La)</td><td>Cerium (Ce)</td><td>Praseodmium (Pr)</td><td>Neodymium (Nd)</td><td>Promethium (Pm)</td><td>Samarium (Sm)</td><td>Europium (Eu)</td><td>Gadolinium (Gd)</td><td>Terbium (Tb)</td><td>Dysprosium (Dy)</td><td>Holmium (Ho)</td><td>Erbium (Er)</td><td>Thulium (Tm)</td><td>Ytterbium (Yb)</td><td>Lutetium (Lu)</td><td rowspan="2">Scandium (Sc)</td><td rowspan="2">Yttrium (Y)</td><td rowspan="2">Thorium (Th)</td></tr>
<tr><td colspan="7">Light REE</td><td colspan="8">Heavy REE</td></tr>
<tr><td colspan="18">Ore Minerals: Allanite (epidote group) $CaCe(Fe^{2+}Al_2)(SiO_4)_3(OH)$ or $CaY(Fe^{2+}Al_2)(SiO_4)_3(OH)$, apatite $(Ca,Na,Ce,Th)_5(P,Si,S,Bi)_3O_{12}(F,OH,Cl,O)$, bastnaesite $(Ce,La)(CO_3)F$, brannerite $(U,Th,Ca,Y)(Ti,Fe)_2O_6$, cerite $Ce_9(Ca)Fe^{3+},Mg)(SiO_4)_6[SiO_3(OH)](OH)_3$, euxenite $(Y,Ca,Ce,U,Th)(Nb,Ta,Ti)_2O_6$, fergusonite $(Y,Ce,U,Th,Ca)(Nb,Ta,Ti)O_4$, florencite $REEAl_3(PO4)_2(OH)_6$, gadolinite $Be_2FeY_2Si_2O_{10}$, huttonite $ThSiO_4$, loparite (niobium perovskite) $(Ca,Ce,N)_2(Nb,Ti)_2O_6$, monazite $(Ce,La,Nd,Th)PO_4$, thorite $ThSiO_4$, uranthorite $(U,Th)SiO_4$, xenotime YPO_4 and zircon $ZrSiO_4$</td></tr>
<tr><td colspan="7">World production</td><td colspan="11">200,914 t (average 2015–2019)</td></tr>
<tr><td colspan="7">Major world producers
(% of average total 2015–2019)</td><td colspan="11">China (76%), Burma (9%), Australia (8%)</td></tr>
<tr><td colspan="18">Uses: High-strength magnets (e.g. electric vehicles and wind turbines), catalysts and polishing compounds</td></tr>
</table>

3.16.2 New Zealand Occurrences of Rare Earth Elements

The main locations of interest for PGM are shown in Figures 3.33 and 3.34. Monazite $(Ce,La,Y,Th)PO_4$ and xenotime YPO_4 occur as trace minerals in some granites, pegmatites and gneisses and are concentrated in placer-sand deposits derived from these source rocks. The main occurrences are in heavy-mineral-rich beach placers in Northwest Nelson, Westland and Southland and at Port Pegasus on Rakiura / Stewart Island. REE are also associated with carbonatite dikes and alkaline intrusive rocks in the South Island. REE may also be concentrated in clays produced by weathering of Late Miocene–Pliocene alkaline rhyolite domes.

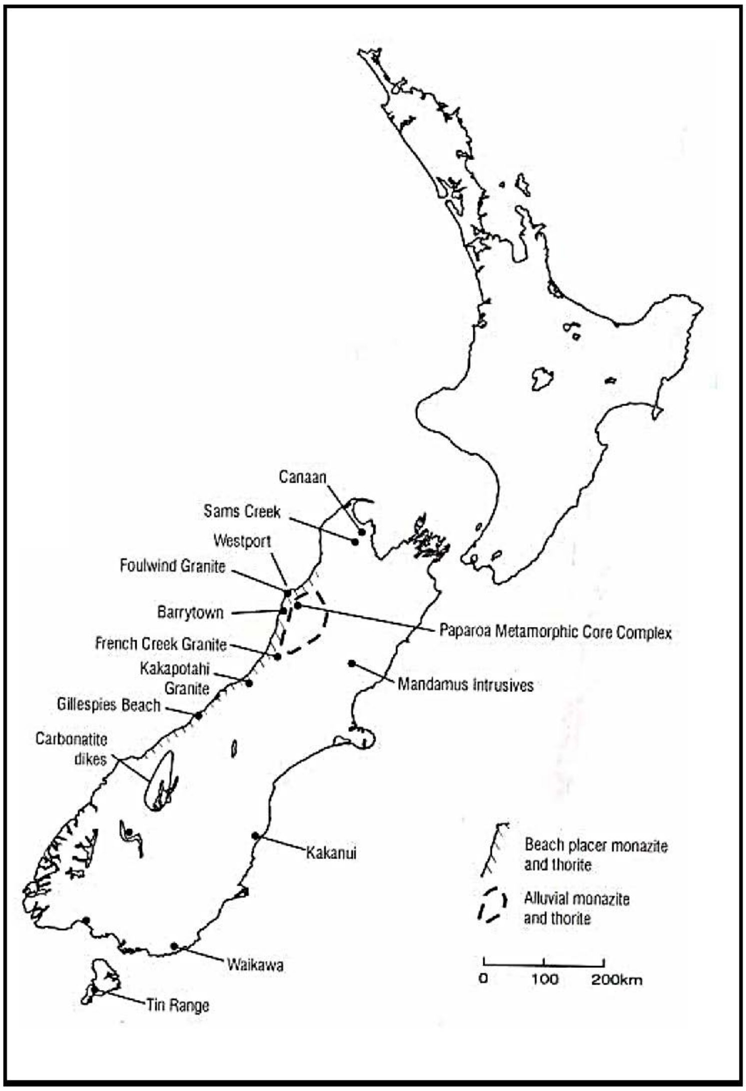

Figure 3.33 Location of rare earth element occurrences in New Zealand (after Christie et al. [1998]).

Key References: Williams (1974); Brathwaite and Pirajno (1993); Christie et al. (1998).

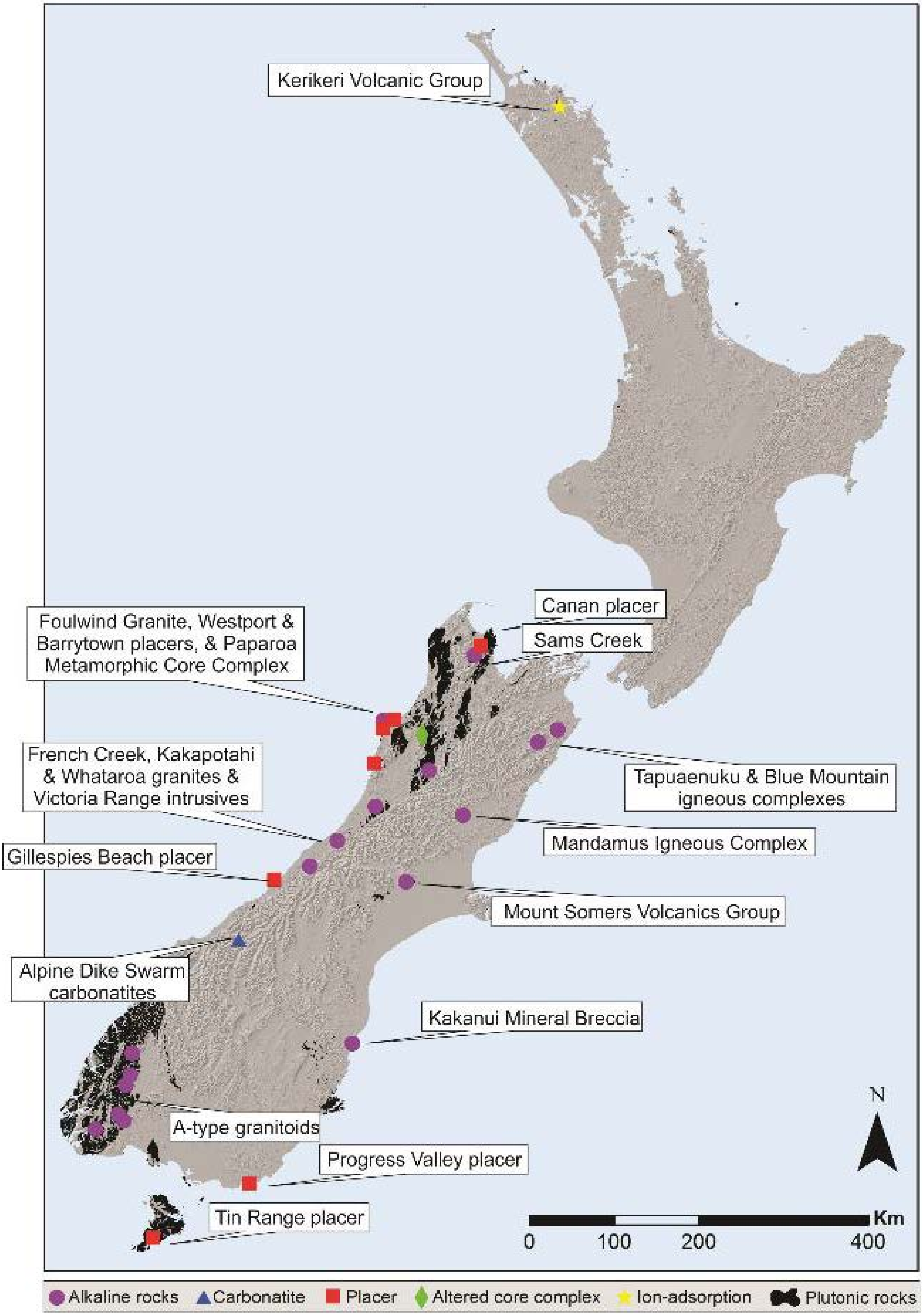

Figure 3.34 The location of plutonic rocks (black polygons) and lithologies with rare earth element potential in New Zealand (after Morgenstern et al. [2018]).

3.16.3 Carbonatite-Hosted REE (Rare Earth Elements)

3.16.3.1 International Mineral Deposit Model

Features of the *Carbonatite-hosted REE* mineral deposit model are listed in Table 3.75.

Table 3.75 Features of international mineral deposit models equivalent to the *Carbonatite-hosted REE* model used in this report.

International Mineral Deposit Model – *Carbonatite-Hosted REE*	
Reference	USGS model 10 Carbonatite deposits (Cox and Singer 1986); BCGS model N01 Carbonatite-hosted deposits (Simandl et al. 1999); and USGS Carbonatite and peralkaline intrusion-related REE deposits (Verplanck et al. 2014).
Description	Magmatic and metasomatic rare earth element mineralisations are found associated with some carbonatite and alkaline igneous intrusives.
International Examples	Bayan Obo, Inner Mongolia (China); Mountain Pass, California (USA)
Grade-Tonnage Model	USGS model 10 50th percentile = 6.3 Mt at 0.36% Nb_2O_5 and 0.009% Re_2O_5 for 22,680 t Nb_2O_5 and 567 t Re_2O_5 (Singer 1998). Deposits range in size up to 62.5 Mt at an average grade of 4.1% rare earth oxides (Bayan Obo in Inner Mongolia, People's Republic of China). The USGS model is biased toward Nb deposits.

3.16.3.2 New Zealand Occurrences of Carbonatite-Hosted REE *Deposits*

Carbonatitic lamprophyre rocks are associated with the Alpine Dike Swarm that intrude Haast Schist in south Westland and northwest Otago (Christie et al. 2010), as well as with the mafic-ultramafic Tapuaenuku Igneous Complex in Marlborough (Jongens et al. 2012). Carbonatite rocks in the Haast River, containing monazite, thorite, apatite, rutile, aegirine, albite, pyrite, sphalerite and galena, have recorded up to 12,560 ppm La+Ce+Y, or up to 8690 ppm Ce, 3810 ppm La and 2720 ppm Nd (Cooper and Paterson 2008). Analyses of carbonatite rocks in Marlborough have recorded up to 224 ppm Ce, 104 ppm La and 121 ppm Nd (Turner 2015).

In addition to dikes, the area of the South Westland dike swarm also has sills and a few diatreme-facies breccia pipes, similar to those exhibited by many kimberlites (Cooper 1986). The intrusives range in size from veinlets only a few centimetres wide to a sill 85 m thick. These are late Oligocene to Early Miocene in age and consist of a magmatic series ranging in composition from ultramafic peridotite, through dominant lamprophyre to subordinate tinguaite, trachyte and carbonatite (Cooper 1971, 1986, 1996). Fenitisation of immediately adjacent country rock is widespread. Carbonatite varieties make up only a small proportion of the intrusives. These are found in dikes and sills up to 1.2 m thick and carry accessory albite, titanian acmite, pyrite, sphalerite, galena, rutile, apatite, monazite and thorite.

3.16.4 Alkali Complex-Hosted REE

The USGS model for carbonatite and peralkaline intrusion-related REE deposits (Verplanck et al. 2014) describes magmatic and metasomatic REE mineralisations that are found associated with some alkaline igneous intrusives.

3.16.4.1 New Zealand Occurrences of Alkali Complex-Hosted REE Deposits

Alkaline igneous intrusive rocks are found on the West Coast (Foulwind, French Creek, Kakapotahi and Whataroa granites and Victoria Range intrusives), in Fiordland (Large, Clarke Hut, Electric, Jackson Peaks and Pomona Island granites, and Cozzete, Houseroof and Expedition plutons), on Rakiura / Stewart Island (Freds Camp Pluton), in Canterbury (Mandamus Igneous Complex and Mount Somers Volcanics Group), in northwest Nelson (Sams Creek) and in Marlborough (Tapuaenuku and Blue Mountain igneous complexes) (Morgenstern et al. 2018). Of these, the French Creek Granite (600 ppm) and the peralkaline Sams Creek granite (719 ppm) are notably enriched in REE. Reconnaissance exploration has been carried out on the French Creek Granite, and Mandamus and Tapuaenuku complexes (Price and Ryland 2011; Jongens et al. 2012; Price 2013; Strategic Materials 2013; Morgenstern et al. 2018). Morgenstern (2016) carried out a detailed REE mineralogical study of the French Creek Granite, reporting REE hosted in bastnäsite group minerals, allanite, zircon, fergusonite, (fluor)apatite, monazite, xenotime, florencite and perrierite-loparite.

3.16.5 REE-Bearing Monazite in Granitic and Metamorphic Rocks

3.16.5.1 International Mineral Deposit Model

Features of the *REE-bearing monazite in granitic and metamorphic rocks* mineral deposit model are listed in Table 3.76.

Table 3.76 Features of international mineral deposit models equivalent to the *REE-bearing monazite in granitic and metamorphic rocks* model used in this report.

International Mineral Deposit Model – *REE-Bearing Monazite in Granitic and Metamorphic Rocks*	
Description	Granites, pegmatites and gneisses enriched in monazite $(Ce,La,Y,Th)PO_4$ and xenotime YPO_4. The REE-bearing minerals may be concentrated in hydrothermal veins or by weathering (e.g. ion adsorbtion clay-type deposits).
International Examples	**Hydrothermal veins:** Steenkamstraal (South Africa) **Ion adsorbtion clay-type deposits:** Longnan and Xunwu, Jiangxi Province (China)
Grade-Tonnage Model	No published data. Grades (5–0.05% rare earth oxides) and tonnage of producers and prospects are highly variable with a large proportion of REE production as a by-product.

3.16.5.2 New Zealand Occurrences of **REE-Bearing Monazite in Granitic and Metamorphic Rocks**

Monazite is a common accessory mineral in many granitoid rocks of Westland. It is present in all of the main granitoid suites (Karamea, Rahu, Separation Point; Tulloch 1988a) but absent from Paleozoic Paringa (Cooper and Tulloch 1992) and Triassic to Early Cretaceous Median Suites. It is conspicuous in Foulwind and French Creek granites of the A-type Toropuhi Suite and French Creek Suites, respectively. Over the last ~15 years monazite has been used extensively for radiometric dating of igneous and metamorphic rocks, utilising both U-Pb and Th-Pb decay systems (Ireland and Gibson 1998). Xenotime accompanies monazite in Foulwind Granite and Kakapotahi granite.

Estimated monazite contents range from 0.005 wt% in Mt Murchison Granite (Separation Point Suite) to 0.015 wt% and 0.021 wt% in core and rim, respectively, of the Barrytown Pluton (Karamea Suite), to 0.029 wt% and 0.042 wt% in Foulwind Granite at Cape Foulwind and Tauranga Bay, respectively.

3.16.6 REE Associated with the Paparoa Metamorphic Core Complex

Hydrothermal systems formed when hot rocks from the deep crust were rapidly uplifted and juxtaposed under brittle, water-saturated upper crustal rocks along crustal-scale detachment faults. This led to the development of extensive alteration in the vicinity of these faults in the Paparoa Range (Tulloch 1995). In addition to traces of Au, Ag, Cu, Ba, F, Fe, carbonate and U mineralisation, Tennant and Sewell (1967) reported elevated levels of REE in Paparoa Range stream sediment samples. REE abundances in Otututu and Ohikanui rivers are about four times greater than those in the Karamea area. Tulloch and Christie (2000) suggested that this mineralisation in the northern Paparoa Range, with its clear relationship to major continental rifting, has much in common with the Olympic Dam style of mineralisation, albeit the latter being much larger and generally of Proterozoic age.

3.16.7 Clay-Bearing REE

In Northland, halloysite clays associated with sub-tropically weathered alkaline rhyolite domes of the Kerikeri Volcanic Group record anomalously high REE concentrations, representing an ion-adsorption mineralisation style. Maximum Ce+La+Y anomalies of 678 ppm occur at Matauri Bay (Brathwaite et al. 2012a), 647 ppm at Pungaere (Smith et al. 1977) and 320 ppm at Maungparerua (Brathwaite et al. 2014). Another volumetrically minor occurrence of halloysite containing anomalously high REE concentrations (La+Ce+Y up to 527 ppm) is within the hydrothermally altered French Creek Granite (Morgenstern 2016).

3.16.8 Placer REE

Detrital REE minerals such as monazite, thorite, uranothorite, and xenotime occur in the heavy-mineral fraction of beach and river sand.

3.16.8.1 New Zealand Occurrences of Placer REE Deposits

Monazite and xenotime have been identified in ilmenite-rich, heavy-mineral beach sands in Fiordland, Southland, Rakiura / Stewart Island, West Coast and northwest Nelson, as well as in West Coast alluvial deposits (Hutton 1950; Christie and Brathwaite 1999b; Christie et al. 2010; Tay et al. 2021). The largest known concentrations of detrital monazite occur at Westport and Barrytown (0.005–0.12 volume percentage). Smaller deposits occur at Cape Foulwind, Nine Mile Beach, Waitakere / Nile River and Constant Bay (0.001–0.02 volume percentage). A recent, scanning electron microscope (SEM) study by Ritchie (2017) found that allanite was the most abundant REE-bearing mineral in the beach sands of Westland, with abundance increasing northwards. It is sourced from both Alpine Schist rocks and Western Province granitoids (particularly those in the Paparoa and Victoria ranges). The richest concentrations of detrital allanite are at Rapahoe Beach (0.83 volume percentage), and allanite could potentially be an economic by-product of garnet processing in Westland (Ritchie 2017; Ritchie et al. 2019). Tay et al. (2021) documented the abundance and geochemistry of REE-bearing minerals from beaches in North Westland and found that concentrations of REE in allanite, monazite and xenotime were highest in terraces at Waimangaroa, Little Wanganui and Barrytown.

Monazite is a by-product of ilmenite heavy-mineral sand mining at Westport and is planned to be recovered in the proposed mining at Barrytown.

Monazite has been found in alluvial deposits of the Tin Range on Rakiura / Stewart Island and at Canaan in northwest Nelson. Monazite and xenotime have also been reported in West Coast gold-dredge concentrates (Arahura, Atarau, Barrytown, Blackball, Grey River, Kaniere, Ngahere, Rimu, Slab Hutt and Snowy River). Monazite has been found in quartz conglomerates in Otago (Christie et al. 1998), and granitic clasts with elevated REE concentrations occur in the Kekerengu, Murihiku and Mt Saul conglomerates (Christie et al. 2011).

Key References: Cooper and Paterson (2008).

3.17 Silver (Ag)

3.17.1 International Description

International data for silver are listed in Table 3.77.

Table 3.77 Major minerals, world production, reserves and resources and major uses for silver.

Silver (Ag)		
International	**Ore Minerals:** Argentite/acanthite Ag_2S; cerargyrite (horn silver) AgCl; electrum AuAg; miargyrite $AgSbS_2$; petzite $(Au,Ag)_2Te$; polybasite $(Ag,Cu)_{16}Sb_2S_{11}$; proustite (light ruby silver) Ag_3AsS_3; pyrargyrite (ruby silver) Ag_3SbS_4; silver (native) Ag; stephanite Ag_5SbS_4; sylvanite $(Au,Ag)Te_2$; and tetrahedrite $(Cu,Fe,Zn,Ag)_{12}Sb_4S_{13}$	
	World mine production 2023 (USGS 2024)	26,000 t
	Major world producers (% of 2023 total world mine production)	Mexico (25%), China (13%), Peru (12%), Poland (5%), Chile (5%), Russia (5%), Bolivia (5%), Australia (5%), USA (4%), Argentina (4%)
	World reserves (USGS 2024)	720,000 t
	World resources (USGS 2024)	N/A
	Uses: Solar panels, water filtration, jewellery, ornaments, high-value tableware and utensils (hence the term 'silverware'), coinage, electrical contacts and conductors, specialised mirrors, window coatings, catalysis of chemical reactions, as a colorant in stained glass and in specialised confectionery. Its compounds are used in photographic and X-ray film.	

3.17.2 New Zealand Occurrences of Silver

The main occurrences of silver are in epithermal Au–Ag deposits in Late Cenozoic rocks of Northland, the Coromandel Peninsula (Hauraki Goldfield) and the Taupō Volcanic Zone, listed in Section 3.8 (Figure 3.35; Table 3.78). Silver also occurs in polymetallic veins described in the Zinc-lead section (Section 3.22).

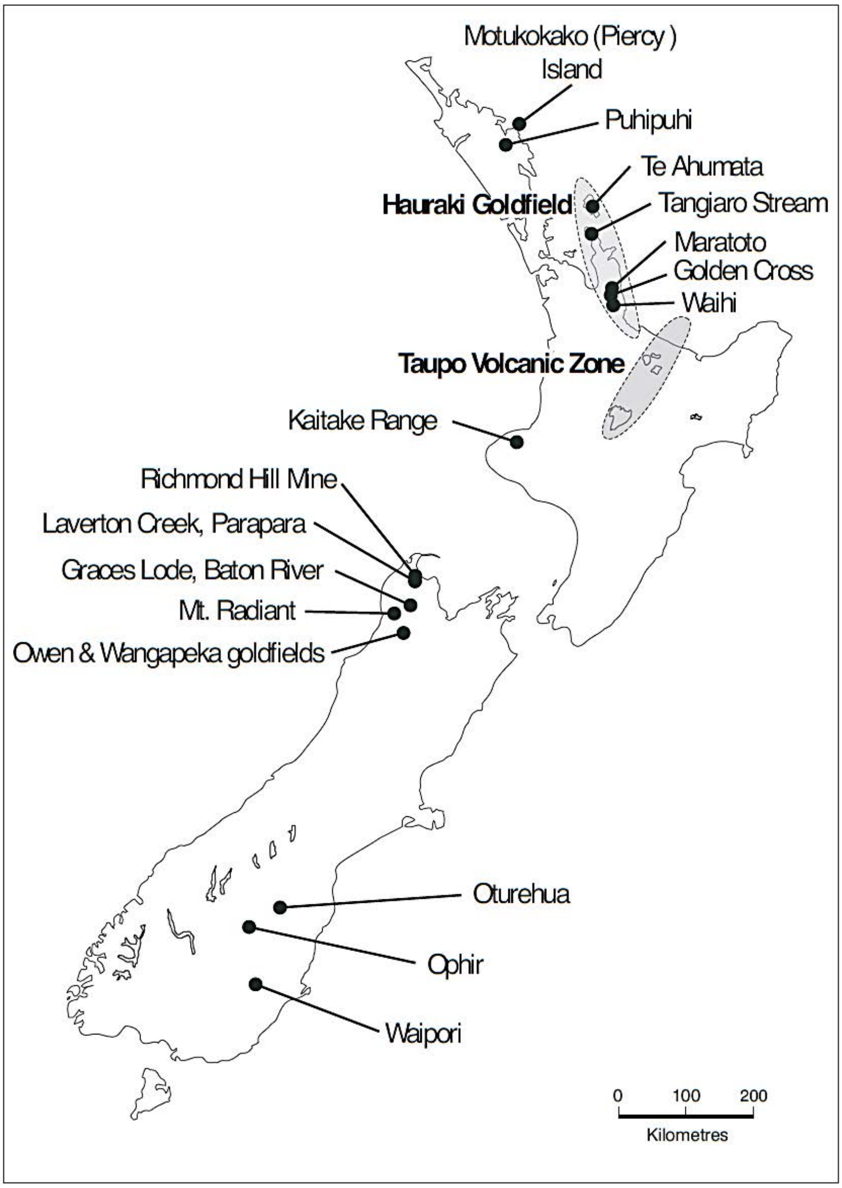

Figure 3.35 Location of silver deposits in New Zealand (after Christie and Brathwaite [1996c]).

Key References: Williams (1974); Brathwaite and Pirajno (1993); Christie et al. (2007).

Table 3.78 Silver occurrences. Minerals: ac = acanthite; Ag sulfoslats = silver sulfosalts; cp = chalcopyrite; el = electrum; gn = galena; hes = hessite; marc = marcasite; proust = proustite; py = pyrite; pyrarg = pyrargyrite; sp = sphalerite; td = tetrahedrite.

Occurrence	MM [1]	GERM [2]	Production (t)	Deposit Form	Minerals Major (Minor)	Host Rocks	Genesis
Richmond Hill	A6	M25/e520	-	Quartz veins	td, gn, py, cp, sp	Granite porphyry	Hydrothermal – magmatic
Parapara prospect	A7	M26/e595	-	Quartz veins	gn, sp, py	Quartzite, diorite	Hydrothermal – magmatic
Mt Rangitoto	A87	I34/e24	-	Quartz-sulfide veins	py, sp, gn, aspy, cp, (el)	Greywacke, argillite, granite	Hydrothermal – magmatic
Puhipuhi	I14	-	0.042 Ag	Quartz veins	marc, py, proust, (td, cp)	Silicified greywacke	Hydrothermal – hot spring
Te Ahumata	I22	S09/e1	1.295 Ag–Au	Quartz veins	py, pyrarg. El, sb, Ag sulfosalts	Andesite and porphyry, rhyolite	Hydrothermal – epithermal
Tangiaro Stream	I26	T10/e12	-	Quartz veins	py, aspy, (td, cp, sp, el)	Andesite	Hydrothermal – epithermal
Maratoto	I69	T13/e29, 34, 43–46	5.972 Au–Ag	Quartz veins	py, marc, gl, sp, cp, ac, hes, el	Andesite breccias and flows	Hydrothermal – epithermal
Tui	I81	T13/e53	-	Quartz veins	sp, gn, cp, py, (marc, td, cin)	Andesite flows and pyroclastics	Hydrothermal – epithermal

[1] MM = Metallogenic map code (Brathwaite and Pirajno 1993).

[2] GERM = Geological Resource Map code.

3.18 Tin (Sn)

3.18.1 International Description

International data for tin are listed in Table 3.79.

Table 3.79 Major minerals, world production, reserves and resources and major uses for tin.

Tin (Sn)		
International	**Ore Minerals:** Cassiterite (or tinstone) SnO_2, stannite Cu_2FeSnS_4 and teallite $PbSnS_2$	
	World mine production in 2023	290,000 t
	Major world producers (% of 2023 total world mine production)	China (23%), Burma (19%), Indonesia (18%), Peru (8%), Congo (7%), Bolivia (6%), Brazil (6%), Australia (3%), Nigeria (3%), Malaysia (2%), Vietnam (2%)
	World reserves (USGS 2024)	4.3 Mt
	World resources (USGS 2024)	Principally in western Africa, southeastern Asia, Australia, Bolivia, Brazil, Indonesia and Russia.
	Uses: Solders, chemicals and tinplate. **Future trends:** Tin use in solders for a wide range of new technologies is expected to grow as decarbonisation proceeds.	

3.18.2 New Zealand Occurrences of Tin

The main occurrences of the tin mineral cassiterite in New Zealand are in greisen and placer deposits on the West Coast and in southern Rakiura / Stewart Island, in association with scheelite in hydrothermal vein deposits in Westland and in pegmatites at Wilmot Pass in Fiordland and at Wakaputa Point in the Longwood Complex (Figure 3.36).

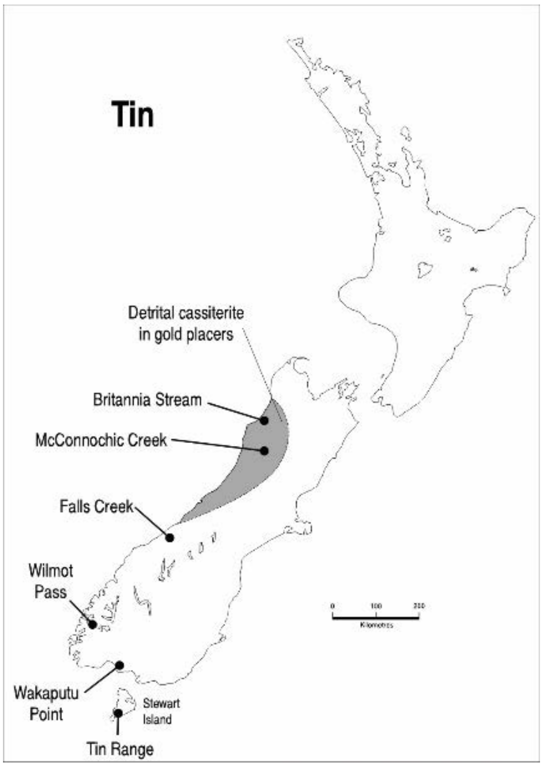

Figure 3.36 Location of tin occurrences in New Zealand (after Christie and Brathwaite [1996a]).

Key References: Williams (1974); Brathwaite and Pirajno (1993); Christie and Brathwaite (1996a, 1998).

3.18.3 Greisen Sn

3.18.3.1 International Mineral Deposit Model

Features of the *Greisen Sn* mineral deposit model are listed in Table 3.80.

Table 3.80 Features of international mineral deposit models equivalent to the *Greisen Sn* model used in this report.

International Mineral Deposit Model – *Greisen Sn*	
Reference	USGS model 15c Sn greisen deposits (Cox and Singer 1986); and BCGS model I13 Sn veins and greisens
Description	Disseminated cassiterite and cassiterite-bearing veinlets, stockworks, lenses, pipes and breccia in greisenised granite.
International Examples	Lost River, Alaska (USA); Anchor Mine, Tasmania (Australia); Erzgebirge (Czech Republic)
Grade-Tonnage Model	USGS model 15c 50th percentile = 7.2 Mt at 0.28% Sn (Cox and Singer 1986) for 20,160 (20,000) t Sn

3.18.3.2 New Zealand Occurrences of Greisen Sn *Deposits*

The main occurrence is on the Tin Range in the Port Pegasus area of southern Rakiura / Stewart Island (Table 3.81). Cassiterite is also present in several hydrothermal vein and greisen type W-Sn occurrences along the western side of the Karamea Batholith in southwest Nelson and Westland (Pirajno 1985; Tulloch and Mackenzie 1986; Kutsukake 1988; Brathwaite and Pirajno 1993). The mineralisation is localised in the apical (cupola) zones of structurally controlled granitic sheets or stocks and in their contact zones with Greenland Group greywacke or earlier granitoid rocks. In contrast to classic Sn-W granite provinces (e.g. northeast Tasmania), the mineralisation is unusual in containing scheelite with little wolframite, cassiterite, fluorite and topaz (Tulloch and Brathwaite 1986). Occurrences where cassiterite is the main mineral of economic interest are Britannia Stream, Falls Creek and Tin Range. Other occurrences where traces of cassiterite accompany scheelite are Bateman Creek, Kirwans Hill, Barrytown and Doctor Hill. At McConnochie Creek, cassiterite occurs with chalcopyrite and molybdenite (Pirajno 1982). These deposits are described in Section 3.20.

Table 3.81 *Greisen Sn* model occurrence (data modified after Brathwaite and Pirajno [1993]). Minerals: bis = bismuthinite; bn = bornite; cas = cassiterite; cp = chalcopyrite; marc = marcasite, mo = molybdenite; py = pyrite; sch = scheelite; tm = tourmaline; wf = wolframite.

Occurrence	MM [1]	GERM [2]	Production (t)	Deposit Form	Minerals Major (Minor)	Host Rocks
Waimangaroa (Britannia Stream)	A42	L29/e149	0.203 Au	Quartz veins, disseminated	cas, py, cp, bn	Granite
Farmer Creek	A54	L30/e294	-	Quartz veins	cas, py	Greywacke, granite
McConnochie Creek	A66	L30/e252	-	Quartz veins	cp, mo, py, marc, sp, bis	Greywacke and granite
Barrytown (W-Sn)	-	K31/e63	-	Veins and greisen	sch, wf, py, cp, cas, bis, rutile, tm, mo, topaz	Biotite granite

Occurrence	MM [1]	GERM [2]	Production (t)	Deposit Form	Minerals Major (Minor)	Host Rocks
Doctor Hill	A84	J33/e79	-	Quartz veins	sch, cas, tm	Biotite granite
Falls Creek (W-Sn)	-	J33/e68	-	Veins and greisen	sch, wf, py, cp, cas, bis, rutile, tm, mo, topaz	Biotite granite
Tin Range	A111	D49/e4	1.0 Sn	Veins and greisen	wf, cas	Granite, mica schist

[1] MM = Metallogenic map code (Brathwaite and Pirajno 1993).

[2] GERM = Geological Resource Map code.

3.18.4 Placer Sn

3.18.4.1 International Mineral Deposit Model

Features of the *Placer Sn* mineral deposit model are listed in Table 3.82.

Table 3.82 Features of international mineral deposit models equivalent to the *Placer Sn* model used in this report.

International Mineral Deposit Model – *Placer Sn*	
Reference	USGS model 39e Alluvial placer Sn (Cox and Singer 1986); and BCGS model C01 Surfical placers (Lefebure and Ray 1995).
Description	Detrital cassiterite grains in gravel, sand, silt and clay, in alluvial deposits
International Examples	Lost River, Alaska (USA); Anchor Mine, Tasmania (Australia); Erzgebirge (Czech Republic)
Grade-Tonnage Model	Deposits are typically large tonnage (0.1–100 Mt) but low-grade (50–200 g/t Sn).

3.18.4.2 New Zealand Occurrences of Placer Sn *Deposits*

Detrital cassiterite has been reported from alluvial gold operations on the West Coast and Rakiura / Stewart Island (e.g. Hutton 1950). The West Coast occurrences are mainly in dredge concentrates.

In the Port Pegasus area of Rakiura / Stewart Island, cassiterite is associated with gold in small stream and eluvial gravel deposits on the flanks of the Tin Range (McKay 1890; Williams 1934; Howard 1940; Williams and Mackie 1959). The main localities are Pegasus Creek (D49/e6, 9), McArthurs Creek (D49/e5) and Robertson River (D49/e2, 3). The cassiterite is derived from the greisen zone on the crest of the Tin Range. Heavy mineral concentrates of the alluvial deposits contain magnetite, cassiterite, garnet, wolframite, monazite, gahnite, epidote, topaz, zircon, rutile and gold (Williams 1934). The placers were worked intermittently from 1888 until 1914, producing 1 t of tin concentrate and small quantities of gold.

3.19 Titanium (Ti)

3.19.1 International Description

International data for titanium are listed in Table 3.83.

Table 3.83 Major minerals, world production, reserves and resources and major uses for titanium.

Titanium (Ti)		
International	**Ore Minerals:** Ilmenite $FeTiO_3$; perovskite $CaTiO_3$; rutile, anatase and brookite TiO_2; and titanite (sphene) $CaTiSiO_5$	
	World mine production for 2023	8.6 Mt ilmenite and 560,000 t rutile
	Major world producers (% of 2023 total world mine production)	**Ilmenite:** China (36%), Mozambique (19%), South Africa (12%), Canada (6%), Norway (5%), Australia (5%), Senegal (4%) **Rutile:** Australia (36%), Sierra Leone (20%), South Africa (18%), Kenya (10%), Ukraine (9%), India (2%)
	World reserves (USGS 2024)	750 Mt TiO_2
	World resources (USGS 2024)	2 Bt collectively of anatase, ilmenite and rutile
	Uses: Paints, polymers and aerospace. **Future trends:** The role of titanium in light-weighting transport, especially aerospace, is expected to grow.	

3.19.2 New Zealand Occurrences of Ilmenite

Ilmenite $FeTiO_3$ occurs in beach sand placers on the West Coast, Southland and Coromandel Peninsula and as stratiform segregations with magnetite in gabbro at Mt George in Fiordland, in anorthosite on Mt Tapuaenuku in the Kaikoura Ranges and in diorite at Mt Pisgah in Northwest Nelson (Figure 3.37).

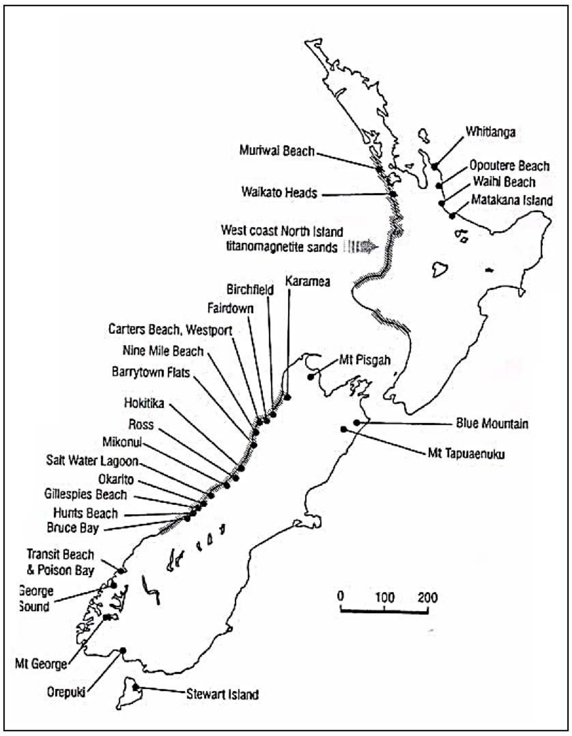

Figure 3.37 Location of titanium deposits in New Zealand (after Christie and Brathwaite [1998]).

Key References: Nicholson et al. (1958); Williams (1974); Brathwaite and Pirajno (1993); Christie and Brathwaite (1998); Brathwaite and Christie (2006).

3.19.3 Magmatic Fe-Ti-V

3.19.3.1 International Mineral Deposit Model

Features of the *Magmatic Fe-Ti-V* mineral deposit model are listed in Table 3.84.

Table 3.84 Features of international mineral deposit models equivalent to the *Magmatic Fe-Ti-V* deposit model used in this report.

International Mineral Deposit Model – *Magmatic Fe-Ti-V* Deposits	
Reference	USGS Model 3 Bushveld Fe-Ti-V (Cox and Singer 1986); and USGS magmatic Fe-Ti-oxide deposits related to Proterozoic massif anorthosite plutonic suites (Woodruff et al. 2013).
Description	Layers of Ti-V-rich magnetite in the upper parts of large repetitively layered mafic-ultramafic intrusions.
International Examples	Bushveld Complex (South Africa); Egersund (Norway); Allard Lake, Quebec (Canada); Tahawus, New York (USA); as well as Duluth gabbro in Minnesota (USA).
Grade-Tonnage Model	Deposits range from 1 to 300 Mt, containing 10–45% TiO_2, 32–45% Fe and 0.2% or less V. 50th percentile is 50 Mt at 15% TiO_2, 35% Fe and 0.1% V for 7.5 Mt TiO_2, 17.5 Mt Fe and 50,000 t V.

3.19.3.2 New Zealand Occurrences of Magmatic Fe-Ti-V *Deposits*

Ilmenite occurs as stratiform segregations with magnetite in diorite at Mt Pisgah in Northwest Nelson, in gabbroic rocks on Mt Tapuaenuku and Blue Mountain in the Kaikōura Ranges and in gabbro at Mt George in Fiordland (Figure 3.26; Table 3.85).

In central Fiordland, stratiform bands of massive ilmenite and magnetite are present in a northerly trending discontinuous band of gabbroic to dioritic intrusions that extends over a distance of about 90 km, from Mt Soaker south to Lake Poteriteri. The intrusions are lenses and tabular bodies representing remnants of sills deformed during metamorphism and folding. Gabbroic phases attain a thickness of over 200 m and, in places, contain magmatic segregations of magnetite and ilmenite. The magnetite-ilmenite-rich layers contain from 3% to 25% magnetite, slightly lesser ilmenite and up to 2% sulfide (pyrite, pyrrhotite and minor chalcopyrite). The magnetite concentrates contain 1.2–1.4% V_2O_5. Mt George is the best-known example, although several others have been described, including Howitt Peaks, Mt Troup near Doubtful Sound, Wilmot Pass, Lake Roe and Bow Lake in the Lake Hauroko area, as well as the Northwest Arm of Lake Te Anau.

At Mt George, a 180-m-thick gabbro orthogneiss sill strikes north/south and dips steeply west (Figure 3.38). It contains 2–50-cm-thick segregation layers of magnetite-ilmenite in a 5–50-m-thick oxide zone immediately overlying a generally less than 10-m-thick basal layer (east) of coarse-grained hornblende, plagioclase, magnetite and ilmenite with minor clots of sulfide minerals (pyrite, pyrrhotite and chalcopyrite). Magnetite concentrates contain an average of 1.2% V_2O_5.

Figure 3.38 Mount George Gabbro of Cretaceous age at Mount George (the nearer rocky peak at left). Primary mamatic layering, including bands rich in magnetite and ilmenite, runs diagonally across the tussock face towards the lake (centre right) and dips to the west (left). The prominent scree ledge with a small tarn (centre left) separates the mineralised gabbro from overlying diorite. The entrance to Doubtful Sound lies at the far upper left, directly above Mt George (after Figure 33 of Turnbull et al. [2010]). Photo CN48264B: DL Homer.

Table 3.85 *Magmatic Fe-Ti-V* model occurrences (data modified after Brathwaite and Pirajno [1993]). Minerals: cp = chalcopyrite; hm = hematite; il = ilmenite; mt = magnetite; po = pyrrhotite; py = pyrite; rt = rutile.

Region	Occurrence	MM [1]	GERM [2]	Deposit Form	Minerals Major (Minor)	Host Rocks
Marlborough	Blue Mountain	D1	P29/e9	Disseminated	po, cp	Alkali gabbro, pyroxenite
	Mt Tapuaenuku	D2	O30/e2	Disseminated	py, po, cp, mt, il, apatite	Pyroxenite, gabbro, anorthosite
West Nelson	Mt Pisgah	A10	N26/e586	Magnetite-ilmenite layer	mt, Il, (hm, rt)	Diorite
Fiordland	Mt George	A98	C43/e4	Layered zone	Il, mt	Metagabbro
	Howitt Peaks	-	C42/e4	-	mt, il, py, po,	Hornblendite
	Lake Roe near Lake Hauroko	-	C44/e1	Stratiform	mt, il	Gabbro sill
	Bow Lake near Lake Hauroko	-	C44/e2	Stratiform	mt, il	Gabbro sill
	Northwest Arm of Lake Te Anau	-	C42/e2	Stratiform	mt, il, sulfides	Hornblende gneiss

[1] MM = Metallogenic map code (Brathwaite and Pirajno 1993).

[2] GERM = Geological Resource Map code.

3.19.4 By-Product Ti

The very large resources of titanomagnetite in the west coast North Island ironsands contain 7–8% TiO_2. Investigations on the recovery of a titanium mineral-rich concentrate from titanomagnetite ironsands of the west coast of the North Island have so far been unsuccessful. However, New Zealand Steel has investigated methods of producing a 40–45% TiO_2 concentrate by-product by separating the titanium minerals ilmenite, leucoxene and rutile from ironsand at the Waikato North Head mine. The concentrate would be used in the manufacture of ferrotitania, which is used in steel alloys.

3.19.5 Shoreline Placer Ti

3.19.5.1 International Mineral Deposit Model

Features of the *Shoreline placer Ti* mineral deposit model are listed in Table 3.86.

Table 3.86 Features of the *Shoreline placer Ti* international mineral deposit model.

International Mineral Deposit Model – *Shoreline Placer Ti*	
Reference	USGS model 39c Shoreline placer Ti (Cox and Singer 1986); and USGS model for heavy-mineral sands in coastal environments (Van Gosen et al. 2014)
Description	Detrital ilmenite and other heavy minerals concentrated by beach processes. Elongate 'shoestring' ore bodies parallel to coastal beaches and dunes.
International Examples	Green Cove and Trail Ridge, Florida; Lakehurst, New Jersey; Concord and Brink, Virginia (USA); Eneabba (Western Australia); Erasama, Chhatrapur, Srikakulam, Visakhapatnam, Ratnagiri, Kollam and Manavalakurichi areas (India); Pulmoddai (Sri Lanka); Ranobe and Fort Dauphin (Madagascar); Mokaba (Sierra Leone); Beihai, Haikanng, Dianbai, Nanshanhai, Sai-Lao, Wuzhaung and Xinglong districts (China)
Grade-Tonnage Model	USGS model 39c 50th percentile = 100 Mt at 1.3% TiO_2 (Cox and Singer 1986).

3.19.5.2 New Zealand Occurrences of Shoreline Placer Ti *Deposits*

Ilmenite beach placers are found in the Coromandel Peninsula, along the west coast of the South Island and in Southland. In the Coromandel Peninsula, ilmenite occurs in significant concentrations in some Holocene beach and dune sands on the east coast (Wharekaho Bay at Whitianga, Opoutere Beach and Waihi Beach) and on Matakana Island (Table 3.87).

Table 3.87 *Shoreline placer Ti* model occurrences in the eastern Coromandel Peninsula, North Island. Minerals: il = ilmenite; hm = hematite; mt = magnetite; zr = zircon.

Occurrence	**MM** [1]	**GERM** [2]	**Deposit Form**	**Minerals Major (Minor)**	**Host Rocks**
Wharekaho Beach, Whitianga	I40	T11/e48	Stratiform	il, mt, hm	Beach sand
Oputere Beach	I58	T12/e52	Stratiform	il, mt, hm, zr	Dune sand
Waihi Beach	I79	U13/e2	Stratiform	il	Dune sand
Matakana Island	I80	U14/e23	Stratiform	il	Dune and beach sand

[1] MM = Metallogenic map code (Brathwaite and Pirajno 1993).

[2] GERM = Geological Resource Map code.

In the South Island, ilmenite is present in coastal sand deposits along 320 km of coastline between Karamea River in the north and Bruce Bay in the south (Figure 3.37 and Table 3.88). The deposits consist of narrow, elongate Holocene beach and dune deposits, generally parallel to and backing the modern storm beach (e.g. Barrytown). In some areas, ilmenite is present in a succession of raised (interglacial) beach deposits, which may be cemented to varying degrees. In the beach sands, ilmenite has been concentrated by wave action into blacksand leads with grades of 10–25% ilmenite. In the dune sands, ilmenite occurs in concentrations generally less than 6%. Other associated heavy minerals include garnet, magnetite, zircon, and rutile, as well as traces of gold, monazite, beryl, uranothorite, scheelite, cassiterite and xenotime.

Ilmenite is also found in Southland beaches at Coal River, Grace Burn, Te Wae Wae Bay, Orepuki and Riverton, as well as on several beaches on the northeast coast of Rakiura / Stewart Island.

Ilmenite beach-sand deposits on the West Coast are a potentially large resource. Ilmenite makes up 5–25% of the sands, but the titanium oxide content of the ilmenite is low (45–47% TiO_2) by world standards due to inclusions of garnet and other silicate minerals. The largest deposits are at Westport and Barrytown. Westport has a resource of 122 Mt of sand with an average grade of 4.5% ilmenite, equivalent to 5.5 Mt of contained ilmenite. Barrytown has 50 Mt of potentially mineable sand at an average grade of 13.8% ilmenite (6.9 Mt), 0.2% zircon, 100 mg/m^3 gold and less than 0.1% each of monazite and rutile. These and other identified deposits make up a total resource of about 30 Mt of ilmenite.

Production of a heavy-mineral sand concentrate commenced at Westport in 2023 and may commence at Barrytown in late 2024. The concentrate is shipped overseas for processing and separation of ilmenite, garnet, zircon, monazite and gold.

Table 3.88 South Island shoreline placer titanium ilmenite resources (data modified after NZGS [1970a]; Brathwaite and Pirajno [1993]; Christie and Brathwaite [1999b]; Brathwaite and Christie [2006]; Christie et al. [2009]).

Location	MM [1]	GERM [2]	Ilmenite (Mt)	Grade (% Ilmenite)	Other Recoverable Minerals
West Coast					
Karamea North	H1	L27/e593	2.5	6%	Zircon, monazite
Karamea South	H2	L27/e594	0.65	3.6%	Zircon, monazite
Birchfield	H3	K29/e44	1.0	5.8%	Zircon, monazite
Fairdown	H4	K29/e45	No estimate	-	-
Carters Beach	H5	K29/e46	6.5–9.6	7.6–15%	Zircon, monazite, gold
Nine Mile Beach North	H6	K29/e70	1.8–2.4	5.4–7.4%	Zircon, monazite, gold
Nine Mile Beach South	H7	K29/e82	0.45–0.58	10–13%	Zircon, monazite, gold
Barrytown Flats	H8	K30/e14, K31/e42	6.9	13.8%	Zircon, monazite, gold
New River	H9	J32/e46	No estimate	-	-
Hokitika North (Awatuna)	H10	-	0.42	6.0%	Zircon, monazite, gold

Location	MM [1]	GERM [2]	Ilmenite (Mt)	Grade (% Ilmenite)	Other Recoverable Minerals
Hokitika	H11	-	0.65	5.9%	Zircon, monazite, gold
Hokitika South	H12	-	3.0	6.4%	Zircon, monazite, gold
Ross	H13	I33/e2	0.56	5.5%	Zircon, monazite, gold
Mikonui	H14	-	0.17	5.2%	Zircon, monazite, gold
Ounatai	H15	I33/e4	Small	-	-
Saltwater Lagoon	H16	I34/e20	0.51	10.1%	Zircon, monazite, gold
Five Mile Beach Okarito	H17	H34/e1, H35/e16	0.47	5.6%	Zircon, monazite, gold
Omoeroa	H18	H35/e19	No estimate	1.6%	-
Gillespies Beach	H19	H35/e14	0.44	3.2%	Gold
Hunts Beach	H20	-	0.31	11.0%	Zircon, monazite
Bruce Bay	H21	-	0.12	6.0%	Zircon, monazite
Fiordland					
Transit Beach	H22	D40/e3	-	-	Garnet, zircon, monazite
Poison Bay	H23	C40/e1	-	-	Garnet, zircon, monazite
Southland					
Orpuki Beach	-	D46/e56	-	-	Garnet, rutile, zircon, monazite
Riverton Beach	-	D46/e67	-	-	Garnet, zircon, monazite
Rakiura / Stewart Island					
Ringaringa Beach	-	E48/e2	-	-	-
Doughboy Bay	-	D49/e8	-	-	-
Lonnekers Beach	-	E48/e5	-	-	-

[1] MM = Metallogenic map code (Brathwaite and Pirajno 1993).

[2] GERM = Geological Resource Map code.

3.20 Tungsten (W)

3.20.1 International Description

International data for tungsten are listed in Table 3.89.

Table 3.89 Major minerals, world production, reserves and resources and major uses for tungsten.

	Tungsten (W)	
International	**Ore Minerals:** Scheelite which is a solid solution mixture of scheelite $CaWO_4$ and powellite $CaMoO_4$. Wolframite which is solid solution mixture series between of ferberite $FeWO_4$ and huebnerite $MnWO_4$	
	World mine production in 2023 (USGS 2024)	78,000 t
	Major world producers (% of 2023 total world mine production)	China (81%), Vietnam (4%), Russia (3%), North Korea (2%), Bolivia (2%), Spain (2%), Rawanda (2%)
	World reserves (USGS 2024)	4.4 Mt
	World resources (USGS 2024)	N/A
	Uses: Milling/cutting tools, construction/mining tools and other wear tools.	

3.20.2 New Zealand Occurrences of Tungsten

Orogenic schist-hosted quartz-scheelite ± gold lodes in Otago and Marlborough form the most abundant type of tungsten deposit in New Zealand (Figure 3.39). Glenorchy, Macraes and Wakamarina are the largest of these. Scheelite also occurs in quartz veins associated with granite in Northwest Nelson, Buller and Westland. Wolframite accompanies cassiterite in greisen on the Tin Range in southern Rakiura / Stewart Island.

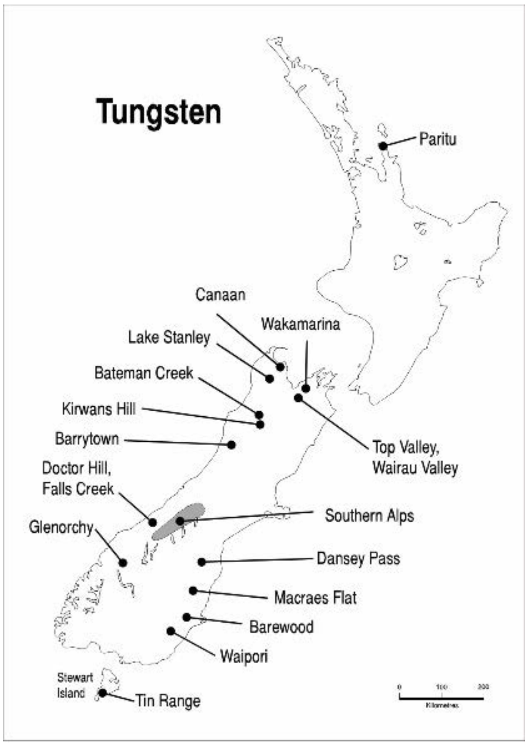

Figure 3.39 Location of tungsten occurrences in New Zealand (after Christie and Brathwaite [1996b]).

Key References: Williams (1974); Brathwaite and Pirajno (1993); Christie and Brathwaite (1996b); Durance and Polette (2016).

3.20.3 Orogenic Scheelite-Bearing Quartz Veins

Orogenic *Vein W* quartz lodes within the Marlborough, Alpine and Otago schists contain scheelite, gold-scheelite, gold, gold-stibnite, stibnite or cinnabar (Table 3.90). Most were mined for their gold content, but several produced significant tungsten. The lodes are developed along shear zones that are generally discordant to the foliation of the host schist.

The Wakamarina field in Marlborough produced 475 t of concentrate containing 65% WO_3 (1874–1944), mainly from the Golden Bar lode (Skinner and Brathwaite 1999). Scheelite is present in many of the quartz lodes on the northern side of the Wairau valley in Marlborough (Johnston 1993), such as the Sylvia lode on the Junction Spur in Top Valley. The most important prospect outside of the Junction Spur was the King John on the west side of Staircase Creek, a tributary of Top Valley Stream.

In the Glenorchy area, west Otago, the schists contain metavolcanic greenschist, Fe-Mn-bearing metachert and sulfide-rich pelitic schist, as well as quartzofeldspathic and pelitic schist of the Caples Terrane. The lodes consist of lensoid shear zones containing crushed schists and irregular quartz lodes. The lodes are gently dipping and cross-cut schistosity in the enclosing schists at a high angle.

Exploration data and mine plans were compiled in a GIS and re-assessed by New Zealand Antimony (Fulton 2001; Yardley 2002) to estimate prospective resources of 143,000 t at 1.7% WO_3 (Table 3.90).

The main minerals present in the lodes are quartz, scheelite, pyrite, arsenopyrite, calcite and magnetite. The total estimated production from 1881 to 1965 from the five main producing lodes on the Glenorchy Field was 2188 t of scheelite concentrate.

Scheelite is associated with gold mineralisation at Barewood, where three parallel, well-defined vein systems, about 1 km apart, are traceable for several kilometres.

New Zealand’s total recorded production of tungsten is 3828 t of tungsten concentrate, of which 475 t was from Wakamarina (1874–1944), 2353 t from the Glenorchy field (1881–1988) 1000 t from Macraes Flat (1875–1936) and 19 t from Barewood (1907–1917 and 1943).

Key References: Williams (1974); Brathwaite and Pirajno (1993); Christie and Brathwaite (1996b).

Table 3.90 *Vein W* model occurrences. Minerals: aspy = arsenopyrite; cp = chalcopyrite; gn = galena; py = pyrite; mo = molybdenite; mt = magnetite; sb = stibnite; sch = scheelite.

Region	Occurrence	MM [1]	GERM [2]	Production (t)	Deposit Form	Minerals Major (Minor)	Host Rocks
Marlborough	Wakamarina	C33	O27/e592	243 W 0.525 Au	W-Au quartz veins	sch, py, gold	Quartzofeldspathic schist
	Top Valley	C37	O28/e18	2 W	W-Au quartz veins	sch, (aspy, py, sb)	Quartzofelspthic chlorite schist
West Coast	Ngakawau	-	L29/e9	-	Quartz veins	sch, py, aspy, cp, mo	Metagreywacke and metapelite
	Kirwan Hill Extension	-	L30/e253	-	Quartz veins	sch, py, po, sp	Metagreywacke and metapelite
	Lake Stream	-	L31/e43	-	Quartz veins	py, sch, mt, mo, cp	Metagabbro/ porphyritic granite
Southern Alps	Dechen Creek	C49	G37/e8	-	Quartz veinlets	sch	Pelitic and quartzofelspathic chlorite schist
	Mt Ward-Baker Creek	C50	H37/e3, e4	-	Quartz veinlets	sch	Pelitic and quartzofelspathic chlorite schist
	Dodger Stream	C51	H37/e1	-	Quartz-carbonate veinlets	sch	Quartzofelspthic chlorite schist
	Boanerges	C52	H37/e2	-	Quartz-carbonate veinlets	sch	Quartzofelspthic chlorite schist
	Fergusson Creek	C53	G38/e5	-	Quartz veinlets	sch	Quartzofelspathic and pelitic schist
	Long Flat Creek	C54	G38/e6	-	Quartz veinlets and bedding laminae	sch	Quartzofelspathic and pelitic schist
	Scrubby Flat Creek	C55	G38/e7	-	Quartz veinlets and bedding laminae	sch	Pelitic and chloritic schist
	Lake Creek	C56	L31/e43	-	Quartz veins	sch	Chloritic argillite

Region	Occurrence	MM [1]	GERM [2]	Production (t)	Deposit Form	Minerals Major (Minor)	Host Rocks
Otago	Nunns (Mareburn)	C82	I42/e76	0.020 Au 18 W	Au-W quartz veins	sch, gold	Quartzofelspathic chlorite schist
	Macraes field	C83	I42/e27 (e28, 29, 33, 47, 48, 50, 53, 54, 55, 56, 76	~640 W 3,331 Au	Au-W quartz veins	py, aspy, sch, gold	Quartzofelspathic and pelitic (graphitic) chlorite schist
	Mt Alfred Lode, Paradise	C57	E40/e13, e14	Small	W-quartz veins	sch, py	Pelitic schist and greenschist
	Invincible Lode	C58	E40/e35	0.146 Au	Au-W quartz veins	py, sch, gold	Pelitic schist and greenschist
	Twelve Mile Creek Lode	C59	E40/e16	Very small	W-quartz veins	sch	Pelitic schist and greenschist
	Glenorchy field	C60	GERM has ~90 localities, e.g. E41/e24	~1000 W	W-Au quartz veins	sch, py, aspy, gold	Pelitic schist and greenschist
	Barewood	C86	I43/e25, e36	0.420 Au 12 W	Au-W quartz veins	py, sch, sb, gold, (gn)	Quartzofelspathic chlorite schist
	Stony Creek, Waipori	C90	H44/e6	~22 Sb	Sb-W quartz veins	sb, sch	Quartzofelspathic chlorite schist
	Russells, Waipori	C91	H44/e41	-	W quartz veins	sch	Quartzofelspathic chlorite schist
	Lammerlaw Creek	C93	H44/e9	8 W	W quartz veins	sch	Quartzofelspathic chlorite schist
	Bella Point	C94	H44/e8	Very small	Au-W quartz veins	gold, sch	Quartzofelspathic chlorite schist

[1] MM = Metallogenic map code (Brathwaite and Pirajno 1993).

[2] GERM = Geological Resource Map code.

Resources estimated by Yardley (2002) from historic data are listed in Table 3.91.

Table 3.91 Prospective resources at Glenorchy calculated from a GIS compilation of historic data (after Yardley [2002]).

Grade Range	Estimated Tonnage within Grade Range (t)				
	0–0.5% WO_3	0.5–1.0% WO_3	1.0–1.5% WO_3	1.5–4.0% WO_3	+4.0% WO_3
Kelly Reef (Mt Judah)	16,419	3305	1794	4159	5469
Glenorchy Reef (Mt Judah)	10,526	2256	1225	2830	3734
Mt McIntosh	1,202,000	96,800	21,500	22,200	-2
Total	**1,228,945**	**102,361**	**24,519**	**29,189**	**9203**

3.20.4 Greisen W-Sn

3.20.4.1 International Mineral Deposit Model

Features of the *Greisen W-Sn* mineral deposit model are listed in Table 3.92.

Table 3.92 Features of international mineral deposit models equivalent to the *Greisen W-Sn* model used in this report.

International Mineral Deposit Model – *Greisen W-Sn*	
Reference	USGS model 15a W veins (Cox and Singer 1986); and USGS model 15c Sn greisen deposits (Cox and Singer 1986)
Description	Scheelite (± cassiterite) in sheeted quartz veins, stockwork quartz veins and disseminations in greisenised granitic rocks and adjacent metasedimentary rocks.
International Examples	Erzgebirge on both sides of the Czech-German border (e.g. Cinovec [Czech Republic]; Sadisdorf [Germany]); Panasqueira (Portugal); Lost River, Alaska (USA); Wolfram Camp (Australia); Xihuashan (China); Mawchi (Myanmar); Yugodzyr (Mongolia). Note that most of these are wolframite deposits.
Grade-Tonnage Model	Model 15a 50th percentile = 0.56 Mt and 0.9% W (Cox and Singer 1986) (These are for wolframite deposits)

3.20.4.2 New Zealand Occurrences of Greisen W-Sn *Deposits*

A number of hydrothermal vein and *Greisen W-Sn* occurrences have been discovered along the western side of the Karamea Batholith in southwest Nelson and Westland, including Bateman Creek, Kirwin Hill, Barrytown, Doctor Hill and Falls Creek (Table 3.93; MacKenzie 1983; Pirajno 1985; Maxwell 1989; Pirajno and Bentley 1995; Tulloch and Mackenzie 1986; Brathwaite and Pirajno 1993; Durance and Polette 2016). In contrast to classic Sn-W granite provinces (e.g. northeast Tasmania), the mineralisation is unusual in having scheelite dominant over wolframite and cassiterite, together with a paucity of fluorite and topaz (Tulloch and Brathwaite 1986). The greisen of the Tin Range on Rakiura / Stewart Island is more typical of the classic type in containing cassiterite and wolframite and no scheelite.

Table 3.93 *Greisen W-Sn* model occurrences. Minerals: aspy = arsenopyrite; cas = cassiterite; cp = chalcopyrite; gn = galena; mo = molybdenite; mt = magnetite; po = pyrrhotite; py = pyrite; sch = scheelite.

Occurrence	MM [1]	GERM [2]	Deposit Form	Minerals Major (Minor)	Host Rocks
Canaan	A11	N26/e510	Quartz veins	Sch, (py, cp, gn, mo)	Marble, granodiorite
Ngakawau	A43	L29/e9	Quartz vein stockwork	sch, py, (aspy, gold)	Hornfelsed greywacke, quartz porphyry
Bateman Creek	A55	L30/e295	Quartz veins	sch, py, (cp, mo)	Greywacke, granite
Kirwan Hill	A59	L30/e253	W quartz veins	sch, po, (cp)	Greywacke, argillite
Barrytown	A76	K31/e63	W quartz veins, greisen	sch	Chert, argillite, biotite granite
Lake Stream	A74	L31/e43	Concordant quartz veins	py, mt, sch, (mo, cpy)	Metagabbro, porphyritic granite
Doctor Hill	A84	J33/e79	Quartz veins	sch, cas, tm	Biotite granite
Falls Creek	-	J33/e68	Veins & greisen	tm, sch, cas, py	Biotite granite

[1] MM = Metallogenic map code (Brathwaite and Pirajno 1993); [2] GERM = Geological Resource Map code.

3.20.5 Tungsten Skarn

3.20.5.1 International Mineral Deposit Model

Features of the *Tungsten skarn* mineral deposit model are listed in Table 3.94.

Table 3.94 Features of international mineral deposit models equivalent to the *Tungsten skarn* model used in this report.

International Mineral Deposit Model – *Tungsten Skarn*	
Reference	USGS model 14a tungsten skarn deposits (Cox 1986)
Description	Skarns formed in the contact zones and roof pendants of granitoid batholiths and thermal aureoles of apical zones of stocks that intrude carbonate rocks. The intrusive rocks are typically tonalite, granodiorite and/or quartz monzonite. The ore mineralogy consists of scheelite ± molybdenite ± pyrrhotite ± sphalerite ± chalcopyrite ± bornite ± arsenopyrite ± pyrite ± magnetite ± traces of wolframite, fluorite, cassiterite and native bismuth. Alteration mineralogy consists of diopside-hedenbergite + grossular-andradite. Late-stage spessartine + almandine. Outer barren wollastonite zone. Inner zone of massive quartz may be present.
International Examples	Pine Creek and Strawberry, California (USA); MacTung, British Columbia; Cantung Northwest Territories; Dublin Gulch, Yukon (Canada); King Island, Tasmania (Australia); Sangdong (South Korea); Xianglushan, Jiangxi; Xintianling, Hunan (China)
Grade-Tonnage Model	USGS model 14a 50th percentile = 6 Mt at 0.44% WO_3 (Green et al. 2020)

3.20.5.2 New Zealand Occurrences of Tungsten Skarn *Deposits*

No true tungsten skarn deposits are known, although quartz-scheelite veins are associated with garnet-hedenbergite skarn at Canaan (Table 3.93), and suitable geological environments exist in Northwest Nelson where granodiorite of the Cretaceous Separation Point Batholith intrudes Paleozoic calcareous metasedimentary rocks in the Pikikiruna and Mt Arthur ranges.

During the 1970s, Carpentaria Exploration carried out regional exploration for tungsten skarns in seven areas along the Separation Point Granite / Arthur Marble contact zone. Although no areas for follow-up work were located, the potential for tungsten was not fully tested because of analytical problems, as well as the use of standard stream-sediment samples instead of the pan-concentrate sampling methods now commonly used (Zuckerman 1972b, 1972c).

3.20.6 Stratabound W

3.20.6.1 International Mineral Deposit Model

Features of the *Stratabound W* mineral deposit model are listed in Table 3.95.

Table 3.95 Features of international mineral deposit models equivalent to the *Stratabound W* model used in this report.

International Mineral Deposit Model – *Stratabound W*	
Reference	Tungsten, stratabound deposits in NERC (2011).
Description	Concordant lenses of stratiform scheelite in submarine volcano-sedimentary sequences. Tungsten is syngenetically deposited in sediments from submarine hydrothermal solutions. Stratiform scheelite mineralisation, commonly with stibnite and cinnabar in some metavolcanic sequences, was considered to be volcanogenic exhalative in origin by Höll and Maucher (1976). A possible modern analogue is Frying Pan Lake at Waimangu Geothermal Field (Seward and Sheppard 1986).
International Examples	Examples occur in Austria (Kleinarltal and Mitersill), Sardinia (Turkey), Spain, Argentina, Broken Hill district (Australia), New Mexico (USA) and China (Damingshan, Guangxi Zhuang).
Grade-Tonnage Model	The type deposit, Felbertal in Austria, had pre-mining resources of about 12 Mt at 0.5% WO_3 for 60,000 t WO_3.

3.20.6.2 New Zealand Occurrences of Stratabound W *Deposits*

Stratabound scheelite mineralisation of possible synsedimentary-exhalative origin occurs near Lake Stanley (Northwest Nelson (M26/e902), hosted in marble lenses within the Cambrian Balloon Formation (Maxwell 1983; Brathwaite and Pirajno 1993). Scheelite is in streaks and lenses, each a few millimetres thick, within carbonate laminae that are interbedded with carbonaceous or siliceous laminae. Stockworks of scheelite-bearing quartz veinlets are also present in some places and were probably formed by metamorphic re-mobilisation of the synsedimentary mineralisation.

Reconnaissance exploration in the Southern Alps by CRA Exploration Pty Ltd outlined an extensive zone containing weak scheelite mineralisation in a belt about 8 km wide and 60 km long from Lake Hawea north to Mount Cook National Park (Purvis et al. 1982; Hawke and Price 1983, 1989; Price et at. 1985). Scheelite is in quartz veins and segregations and is regionally localised to the vicinity of the pumpellyite-actinolite/greenschist facies boundary. It is commonly associated with calc-silicate and carbonate minerals. Occurrences of disseminated and bedding laminae-bound scheelite in chert and carbonaceous pelite were found in Long Flat and Scrubby Flat creeks, Hunter River area (Purvis et al. 1982). Wood (1983) also recognised widespread scheelite occurrences over a distance of 360 km in greenschist facies schist along the Southern Alps. He described the scheelite as occurring in disseminated spots, as well as in fine quartz veins. Craw and Norris (1991) considered that scheelite-quartz vein formation at Lake Hawea was synmetamorphic and represented tungsten mobilisation during metamorphism of the greywackes.

Stratabound scheelite mineralisation is also present at Dansey Pass, North Otago, in rocks of the Permian Dansey Metavolcanic Formation. Exploration by a Lime & Marble Ltd – Kennecott Explorations (Australia) Ltd joint venture (McClelland 1981a, 1981b), and later by BP (Rutherford and MacKay 1984), located two zones of scheelite vein mineralisation grading up to 1.3% WO_3 in shear zones in metavolcanics. Exploration by BP of the metavolcanic units interbedded with Haast Schist of the Kakanui Mountains, southeast of Dansey Pass, located rare scheelite mineralisation restricted to small scale quartz veining, quartz segregations and coatings on joint planes (MacKay 1984).

3.21 Vanadium (V)

3.21.1 International Description

International data for vanadium are listed in Table 3.96.

Table 3.96 Major minerals, world production, reserves and resources and major uses for vanadium.

Vanadium (V)		
International	**Ore Minerals:** Vanadiferous minerals such as titanomagnetite, magnomagnetite, magnetite, rutile and ilmenite; vanadinitie; carnotite; patronite; roscoelite	
	World 2023 production (USGS 2024)	100,000 t
	Major world producers (% of 2023 total world mine production) (USGS 2024)	China (68%), Russia (20%), South Africa (9%), Brazil (6%)
	World reserves (USGS 2024)	19 Mt
	World resources (USGS 2024)	More than 63 Mt
	Uses: High-strength low-alloy steel, special steel and super-alloys. **Future trends:** Vanadium redox flow batteries may become increasingly important for stationary energy storage.	

3.21.2 Occurrence of Vanadium in New Zealand

Vanadium occurs in association with iron and titanium in placer titanomagnetite deposits of the west coast of the North Island and magnetite-ilmenite deposits in Fiordland (see iron and titanium; Sections 3.9 and 3.19, respectively).

A vanadium-rich slag is produced by BHP New Zealand Steel during steel manufacture at the Glenbrook Steel mill. Currently 12,000 t/yr is produced and exported to China, representing 10% of the world's vanadium production. The slag is processed to enrich V_2O_5 with the product used to make ferrovanadium, which is used as an additive in steel.

Key References: Williams (1974); Brathwaite and Pirajno (1993).

3.22 Zinc (Zn) – Lead (Pb)

3.22.1 International Description

International data for zinc and lead are listed in Table 3.97.

Table 3.97 Major minerals, world production, reserves and resources and major uses for lead and zinc.

International		Zinc (Zn)	Lead (Pb)
	Ore Minerals	Smithsonite $ZnCO_3$ and sphalerite ZnS	Anglesite $PbSO_4$, bournonite $PbCuSbS_3$, cerussite $PbCO_3$, galena PbS and jamesonite $Pb_4FeSb_6S_{14}$
	World mine production in 2023 (USGS 2024)	4.5 Mt	12.43 Mt
	Major world producers (% of total 2023 world production) (USGS 2024)	China (42%), Australia (10%), USA (6%), Mexico (6%), Peru (6%), Russia (4%), Bolivia (2%), Sweden (2%), Turkey (2%), Iran (1%), Tajikistan (1%)	China (33%), Peru (12%), Australia (9%), India (7%), USA (6%), Mexico (6%), Bolivia (4%), Kazakhstan (3%), Russia (3%)
	World reserves (USGS 2024)	95 Mt	220 Mt
	World resources (USGS 2024)	More than 2 Bt	1.9 Bt
	Uses:	Building and construction (e.g. roofing material, cladding, flashing, gutters and gutter joints), sculptures, ballast, ammunition, radiation shielding, alloys (e.g. brass)	As an anti-corrosion agent (e.g. galvanisation coating of iron and steel), sacrificial anode, batteries and alloys

3.22.2 New Zealand Occurrences of Zinc and Lead

Zinc (sphalerite ZnS) and lead (galena PbS) usually occur together in their main types of ore deposits. In New Zealand, most of the known lead-zinc deposits are in hydrothermal veins, commonly associated with gold and silver, as in the Coromandel Peninsula. The only deposit mined specifically for zinc and lead was the Tui Mine near Te Aroha between 1967 and 1973, having produced 13,159 t of zinc concentrate and 7755 t of copper-lead concentrate, with remaining resources estimated at 140,000 t of ore grading approximately 5.5% Zn, 4% Pb and 0.5% Cu (Bates 1989b) (Figure 3.40). Other small Au–Ag deposits containing potentially economic Zn and Pb mineralisation are Monowai and Sylvia near Thames and Waiorongomai near Te Aroha.

In the South Island, there are a number of hydrothermal lead-zinc-quartz vein occurrences related to granite intrusions, as at Parapara Peak, Richmond Hill and Rolling River in Northwest Nelson and Bradshaws Reef in Fiordland (Figure 3.40).

A sphalerite-galena bearing pyroxene-garnet skarn has been found in Oligocene-age limestone at Motukokako (Piercy) Island in the Bay of Islands (Figure 3.40) (Brathwaite et al. 1990).

Massive sulfide sphalerite-galena-pyrite-gold ore in quartz-sericite schist at Johnstons United Mine in Northwest Nelson (Figure 3.40), was formerly worked for gold (1866–1897) and is a likely example of a metamorphosed volcanogenic massive sulfide deposit. Bedded sphalerite-pyrite mineralisation associated with graphitic schist at Mt Irene in Fiordland is interpreted as a metamorphosed shale-hosted lead-zinc deposit.

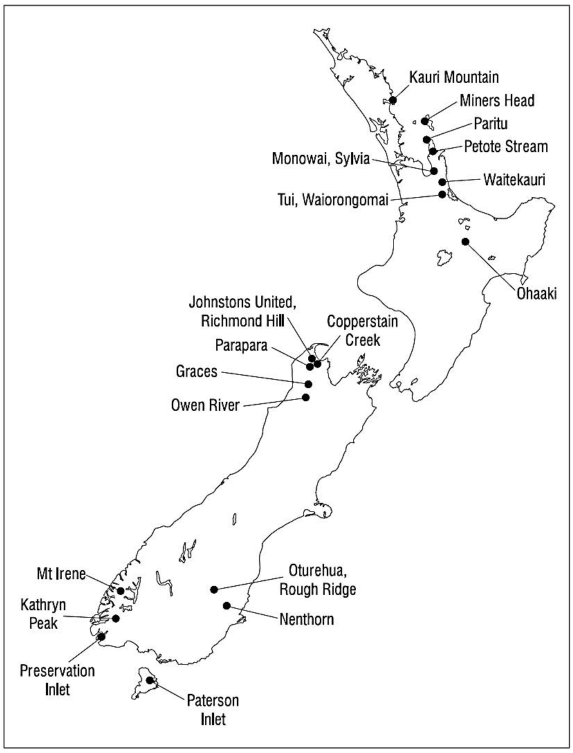

Figure 3.40 Location of lead and zinc deposits in New Zealand (after Christie and Brathwaite [1995a]).

Key References: Williams (1974); Bates (1989b); Brathwaite and Pirajno (1993); Christie and Brathwaite (1995a),

3.22.3 Zinc-Lead Skarn

3.22.3.1 International Mineral Deposit Model

Features of the *Zinc-lead skarn* mineral deposit model are listed in Table 3.98.

Table 3.98 Features of the *Zinc-lead skarn* international mineral deposit model.

International Mineral Deposit Model – *Zinc-Lead Skarn*	
Reference	USGS model 18c zinc-lead skarn (Cox and Singer 1986); and BCGS model K02 zinc-lead skarns (Lefebure and Ray 1995).
Description	Deposits consist of Zn-Pb-Ag sulfide minerals as replacement bodies in limestone proximal or distal to quartz diorite stocks. They contain disseminated sphalerite, galena and pyrite.
International Examples	San Antonio and Santa Eulalia (Mexico); Yeonhua (South Korea); Ban Ban (Australia); El Sapo (Columbia)
Grade-Tonnage Model	USGS model 18c 50th percentile = 1.4 Mt, and 5.9% Zn and 2.8% Pb, possible by-product Ag, Au and/or Cu (Cox and Singer 1986). See also Lefebure and Höy (1996, Table 15) BCGS model K02. Worldwide, skarn deposits range from <1 to 30 Mt and grade 10–20% Zn + Pb and 30–300 g/t Ag.

3.22.3.2 New Zealand Occurrences of Zinc-Lead Skarn *Deposits*

Zinc-lead skarn mineralisation is present in Oligocene Whangārei Limestone at Motukokako (Piercy) Island (MM I10; GERM Q05/e25) (Brathwaite et al. 1990). The skarn is composed of the calc-silicate minerals hedenbergite, garnet, epidote, axinite, ilvaite and babingtonite, which are enriched to varying degrees in manganese and iron. Sphalerite and galena are disseminated in the skarn, the adjacent re-crystallised limestone and in quartz veins that cut the limestone and the unconformably underlying greywacke. The skarn mineralisation was formed by hydrothermal fluids generated by an unexposed intrusion. The grade of the skarn mineralisation is of the order of 1–6% Zn and 0.2–1% Pb, with up to 100 ppm Ag (Brathwaite et al. 1990).

3.22.4 Polymetallic Veins

3.22.4.1 International Mineral Deposit Model

Features of the *Polymetallic veins* mineral deposit model are listed in Table 3.99.

Table 3.99 Features of the *Polymetallic veins* international mineral deposit model.

International Mineral Deposit Model – *Polymetallic Veins*	
Reference	USGS model 22c Polymetallic veins (Cox and Singer 1986) USGS model 25b Creede epithermal veins (Cox and Singer 1986); and BCGS model I05 Polymetallic veins Ag-Pb-Zn±Au (Lefebure and Höy 1996).
Description	Sulfide-rich veins containing sphalerite, galena, silver and sulfosalt minerals in a carbonate and quartz gangue. These veins can be sub-divided into those hosted by metasediments and another group hosted by volcanic or intrusive rocks. The latter type of mineralisation is typically contemporaneous with emplacement of a nearby intrusion. The veins are typically steeply dipping, narrow, tabular or splayed. They commonly occur as sets of parallel and offset veins. Individual veins vary from centimetres up to more than 3 m wide and can be followed from a few hundred to more than 1000 m in length and depth. Veins may grade into broad zones of stockwork or breccia.
International Examples	**Metasediment host:** Coeur d'Alene district, Idaho (USA); Harz Mountains and Freiberg district (Germany); Příbram district (Czechoslovakia). **Igneous host:** Sunnyside and Idorado, Silverton district and Creede, Colorado (USA); Pachuca (Mexico).
Grade-Tonnage Model	Individual vein systems range from several hundred to several million tonnes, grading from 5 to 1500 g/t Ag, 0.5 to 20% Pb and 0.5 to 8% Zn. The 50th percentile for polymetallic veins given by Cox and Singer (1986) is 7600 t at 820 g/t Ag, 0.13 g/t Au, 9% Pb and 2.1% Zn for 684 t Pb, 160 t Zn, 200,390 oz Ag and 32 oz Au.

3.22.4.2 New Zealand Occurrences of Polymetallic Vein *Deposits*

These are quartz-vein deposits that contain base metal and silver mineralisation. Their origin is poorly known, although most are generally considered to be mesothermal and granite-related. The intermediate-sulfidation epithermal Zn-Pb-Cu-Ag-Au deposits described in Section 3.8 and associated with Miocene–Pliocene volcanic rocks have many similarities with this class.

Occurrences of *Polymetallic vein* deposits are listed in Table 3.100.

Table 3.100 *Polymetallic vein* model occurrences (data modified after Brathwaite and Pirajno [1993]). Minerals: aspy = arsenopyrite; bourn = bournonite; cp = chalcopyrite; el = electrum; gn = galena; py = pyrite; sb = stibnite; sp = sphalerite; td = tetrahedrite.

Region	**Occurrence**	**MM**[1]	**GERM**[2]	**Production (t)**	**Deposit Form**	**Minerals Major (Minor)**	**Host Rocks**
Northland	Tupou Bay	I3	-	-	Quartz veins	py, sp, gn, cp	Sandstone
	Reef Bay	I17	-	-	Sulfide vein	py, sp, gn, cp	Andesite porphyry, siltstone
South Island	Richmond Hill	A6	M25/e520	-	Quartz veins	td, gn, py, cp, sp	Granite porphyry
	Parapara	A7	M26/e595	-	Quartz veins	gn, sp, py	Quartzite, diorite
	Rolling River	A36	M26/e634	-	Quartz-sulfide veins	py, gn, sp, gold	Sandstone, marble
	Beilbys Reef	A37	M28/e552	0.002 Au	Quartz-sulfide veins	py, gn, sp, gold	Marble, slate
	Owen River	A38	M28/e553–555	-	Quartz veins	py, sp, gn, gold	Marble, slate
	Aynsley Creek	-	K31/e72	-	Quartz veins	-	-
	Croesus Knob	-	K31/366	-	Quartz veins	Au, py, sp, gn, cp, sb, bourn	Greywacke, argillite
	Seventeen Mile Bluff	-	J31/e26	-	Quartz veins	cp, mo, py	Greywacke intruded by granite
	Mt Rangitoto	A87	I34/e24	-	Quartz-sulfide veins	py, sp, gn, aspy, cp, (el)	Greywacke, argillite, gneiss
	Galena Creek	-	G36/e17	-	Quartz veins	-	Schist, gneiss
	Cowan Creek	-	F37/e8	-	-	gn, Au	Carbonatite

[1] MM = Metallogenic map code (Brathwaite and Pirajno 1993).

[2] GERM = Geological Resource Map code.

3.22.5 Sediment-Hosted Zn-Pb

3.22.5.1 International Mineral Deposit Model

Features of the *Sediment-hosted Zn-Pb* mineral deposit model are listed in Table 3.101.

Table 3.101 Features of international mineral deposit models equivalent to the *Sediment-hosted Zn-Pb* model used in this report.

International Mineral Deposit Model – *Sediment-Hosted Zn-Pb*	
Reference	USGS model 31a Sediment exhalative zinc-lead (Cox and Singer 1986); and USGS model for Sedimentary exhalative Zn-Pb-Ag deposits (Emsbo et al. 2016)
Description	These are synsedimentary deposits formed by submarine exhalations of hydrothermal fluid. The ores are concordantly interbedded within marine black shale, siltstone, sandstone, chert, dolomite and limestone. There is no apparent volcanic association.
International Examples	Hilton-George Fischer, Mount Isa, Century and Cannington, Queensland (Australia); Red Dog, Alaska (USA); McArthur River HYC, Northern Territory (Australia); Howards Pass, Yukon (Canada); Kholodninskoye (Russia); Sullivan, British Columbia (Canada); Broken Hill, New South Wales (Australia)
Grade-Tonnage Model	Deposits contain 4–550 Mt of ore (the average of 38 worldwide examples is 60 Mt) and have grades of 0.6–18% (av. 7.3%) Zn, 0.3–13% (av. 4%) Pb, nil–1.0% (av. 0.1%) Cu, and trace to 180 g/t Ag (av. 48 g/t). Model 31a 50th percentile = 15 Mt and 5.6% Zn, 2.8% Pb and 30 g/t Ag (Cox and Singer 1986). See also Lefebure and Höy (1996), model E14.

3.22.5.2 New Zealand Occurrences of Sediment-Hosted Zn-Pb *Deposits*

Corner and Jennings (1994) noted that zinc and lead anomalies in geochemical surveys of the Burgoo Stream, Hodge Creek, Crow River, Island Stream-Roaring Lion and Sputnik Creek, in Northwest Nelson, indicated the potential for sediment-hosted zinc mineralisation. Zinc anomalies in stream sediments are discussed by Carver (2009) and are particularly common in the Takaka volcanic-volcaniclastics.

Occurrences of *Sediment-hosted Zn-Pb* deposits are listed in Table 3.102.

Table 3.102 Occurrence of *Sediment-hosted Zn-Pb* deposits (data modified after Brathwaite and Pirajno [1993]). Minerals: cp = chalcopyrite; po = pyrrhotite; py = pyrite; sp = sphalerite.

Occurrence	MM [1]	GERM [2]	Deposit Form	Minerals Major (Minor)	Host Rocks	Genesis
Mt Irene	A96	C42/e3	Stratiform	py, sp, po, cp	Calc-schist, marble	Hydrothermal – seafloor
Kathryn Peak	A104	B44/e6	Stratiform	py, sp	Quartzofelspathic schist	Hydrothermal seafloor

[1] MM = Metallogenic map code (Brathwaite and Pirajno 1993).

[2] GERM = Geological Resource Map code.

3.22.6 Volcanogenic Massive Sulfide (VMS) Zn-Pb

3.22.6.1 International Mineral Deposit Model

Features of the *VMS Zn-Pb* mineral deposit model are listed in Table 3.103.

Table 3.103 Features of international mineral deposit models equivalent to the *VMS Zn-Pb* deposits model used in this report.

International Mineral Deposit Model – *Volcanogenic Massive Sulfide (VMS) Zn-Pb*	
Reference	USGS model 24a Cyprus massive sulfide (Cox and Singer 1986); USGS model 24b Besshi massive sulfide (Cox and Singer 1986) USGS Volcanogenic massive sulfide (Shanks et al. 2012)
Description	VMS deposits are polymetallic seafloor deposits formed by hydrothermal systems that were generated by submarine volcanic activity and are partly syngenetic and partly epigenetic in origin. These typically occur as multiple stratiform lenses within rhyolitic to basaltic submarine volcanic and associated rocks, commonly overlying, or adjacent to, discordant feeder zones containing low-grade stringer and disseminated mineralisation.
International Examples	Buchans, Newfoundland; Perseverence, Quebec; Kidd Creek, Ontario (Canada); Hellyer, Tasmania (Australia); Laochang (China)
Grade-Tonnage Model	Most VMS ore bodies contain between 0.1 and 10 Mt of ore, although groups of related deposits commonly aggregate more than 100 Mt. Kuroko deposits typically contain 4–5% Zn, 1–2% Cu and 1–1.5% Pb. Rosebery-type deposits are higher grade with up to 30% Zn+Pb+Cu, and up to 200 g/t Ag and 3 g/t Au. Major deposits include the Kuroko deposits of Japan; Rosebery, Hellyer and Woodlawn in Australia; and Kidd Creek in Ontario, Canada.

3.22.6.2 New Zealand Occurrences of VMS Zn-Pb *Deposits*

Lead-zinc mineralisation occurs as small lenses of massive sulfide in quartz-sericite schist at Johnston’s United Mine (MM A2; GERM M25/e539) in the Aorere goldfield. Although originally mined for gold between 1866 and 1897, the style of mineralisation attracted some exploration for VMS deposits (Roberts 1975; Canyon Resources Pty Ltd 1984; Brathwaite and Pirajno 1993). Minerals present include: pyrite, arsenopyrite, pyrrhotite, galena, sphalerite, chalcopyrite and tetrahedrite (Grindley and Wodzicki 1960).

In the early 1990s, Westland Ilmenite Ltd carried out reconnaissance prospecting for VMS deposits associated with the volcanic rocks of the Haupiri Group in Northwest Nelson (Mathison et al. 1992; Jones and Savory 1993). Several anomalies were identified in an airborne electromagnetic and magnetic survey and were followed up by geochemical surveys, mapping and ground electromagnetic surveys. This work outlined a few areas of VMS-style alteration and massive pyrite mineralisation, with low concentrations of copper, lead and/or zinc located in tributaries of the Anatoki and Waingaro rivers.

3.23 Zirconium (Zr)

3.23.1 International Description

International data for zirconium are listed in Table 3.104.

Table 3.104 Major minerals, world production, reserves and resources and major uses for zirconium.

Zirconium (Zr)		
International	**Ore Minerals: B**addeleyite ZrO_2 and zircon $ZrSiO_4$	
	World mine production in 2023 (USGS 2024)	1.6 Mt of Zr mineral concentrates
	Major world producers (% of total 2023 world production) (USGS 2024)	Australia (31%), China (9%), South Africa (9%), USA (6%), Indonesia (6%), Mozambique (6%), Sengal (3%), Kenya (2%), Madagascar (2%), Sierra Leone (2%)
	World reserves (USGS 2024)	74 Mt Zr concentrates
	World resources (USGS 2024)	N/A
	Uses: As a refractory and opacifier, although small amounts are used as an alloying agent for its strong resistance to corrosion.	

3.23.2 New Zealand Occurrences of Zircon

Zircon is widely distributed as an accessory detrital mineral in titanomagnetite and ilmenite beach-sand deposits of the North and South Islands (Figure 3.41). Detrital zircon also occurs in alluvial placers in Westland, Otago and Southland.

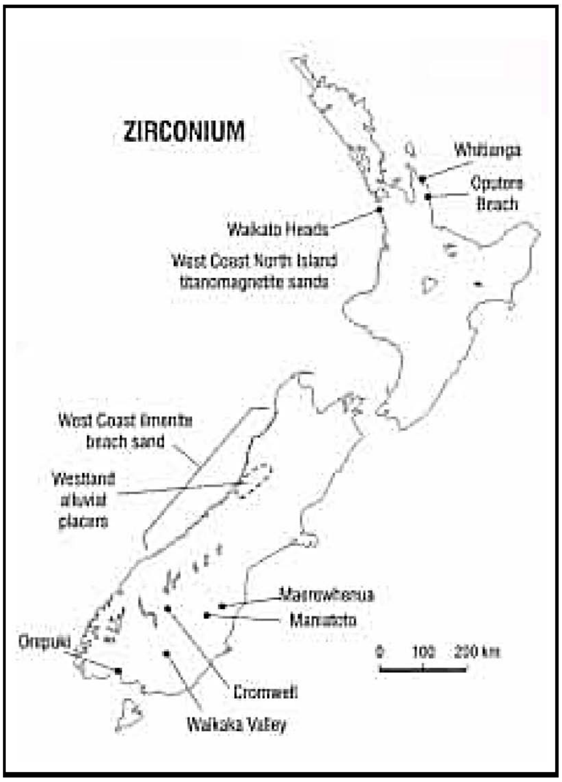

Figure 3.41 Location of zirconium deposits in New Zealand (after Christie and Brathwaite [1999a]).

Key References: Williams (1974); Brathwaite and Pirajno (1993); Christie and Brathwaite (1999a).

3.23.3 Placer Zircon

3.23.3.1 International Mineral Deposit Model

Features of the *Placer zircon* mineral deposit model are listed in Table 3.105.

Table 3.105 Features of international mineral deposit models equivalent to the *Placer zircon* model used in this report.

International Mineral Deposit Model – *Placer Zircon*	
Reference	USGS Deposit model for heavy-mineral sands in coastal environments (Van Gosen et al. 2014)
Description	Detrital zircon in the heavy-mineral fraction of beach sands. Zircon occurs as an accessory mineral in all types of igneous rocks and is abundant in silica-rich rocks. It is extremely resistant to weathering and concentrates along with some other heavy minerals in beach- and alluvial-sand deposits that may contain up to 3% zircon. Zircon is mined as a co-product of beach-sand mining for titanium ores (see Section 3.19). The main deposits are the relatively young beach sands found on or near active coast lines of Australia, South Africa, the USA, India, Sri Lanka, Malaysia, China, Thailand and Tanzania.
International Examples	Jacinth and Ambrosia in Eucla Basin, Western Australia – South Australia; Eneabba, Cataby and Mindarie, Western Australia; Balranald, Ginkgo and Snapper in the Murray Basin, New South Wales; North Stradbroke Island and Fraser Island, Queensland (Australia); Geelwai Karoo and Richards Bay (South Africa); Moebase and Naburi (Mozambique); Trail Ridge, Florida; Brunswick, Georgia (USA)
Grade-Tonnage Model	Individual economic deposits typically have 10 Mt of sand at >2% heavy minerals and may occur in districts with >1 Bt of sand averaging 5% heavy minerals (Van Gosen et al. 2014). Zircon contents of the heavy-mineral-sand fraction are variable between deposits.

3.23.3.2 New Zealand Occurrences of Placer Zircon *Deposits*

Ilmenite beach-sand deposits near Whitianga and at Wharekawa on the east coast of the Coromandel Peninsula are reported to average 1% zircon (McLaughlin 1973). If these deposits are ever mined for ilmenite, the zircon would be a potentially recoverable by-product.

The titanomagnetite beach sands on the west coast of the North Island contain trace zircon, but few details are known. The Waikato North Head deposit, currently mined for iron ore, contains about 0.1% zircon that is potentially recoverable (Shannon et al. 1965).

The ilmenite beach sands of the West Coast, South Island, typically contain 0.1–0.39% zircon, with locally higher concentrations up to 0.5% zircon (McPherson 1978; Nicholson et al. 1966; Nicholson 1967; Minehan 1989). Beach sand at Orepuki, Southland, contains 0.1–1.1% zircon (Martin and Long 1960). Zircon is a by-product of ilmenite heavy mineral sand mining at Westport and is expected to be recovered at the proposed heavy-mineral sand mining operation at Barrytown.

In Otago and Southland, zircon was identified in alluvial gold workings, for example, Maniototo, Maerewhenua, Lowburn and Waikaka Valley. The grade of the zircon in the alluvial gravels is unknown but is probably well below 0.1%. However, it may be worth recovering as a by-product in any future large alluvial gold mining operation.

4.0 ONSHORE NON-METALLIC MINERALS

4.1 Aggregate and Sand

Aggregate is hard inert material used for making roads and for construction of buildings, bridges and other structures (mainly as concrete), with lesser quantities used for reclamation, harbour protection and railway ballast (Figure 4.1). Sand has similar applications in building, as well as several industrial uses, such as moulding sand. Aggregate suitability is determined by its physical properties (strength, durability, cohesiveness, size), chemical properties, few or no deleterious minerals and good homogeneity and volume of material at a quarry site. Naturally occuring rocks, sand and gravel are the most widely used aggregate materials and can be produced from a range of rock types, including greywacke, basalt, andesite, limestone, schist and granite. These can be produced by quarries working hard-rock deposits and from sand and gravel transported by rivers and glaciers (Figure 4.2). The latter are extracted from river channels and alluvial terraces where natural transport processes have upgraded their quality through the breakdown of weaker material. Quarried rock is crushed and screened to make various sized products (Figures 4.3 and 4.4). River gravels may not require crushing before screening.

This section briefly reviews aggregate production, issues and opportunities, and the reader is referred to descriptions by MacFarlan and Barry (1991), Christie et al. (2001b), Black (2009, 2014), Hill (2021) and Hill and Chilton (2024a–e) for additional information.

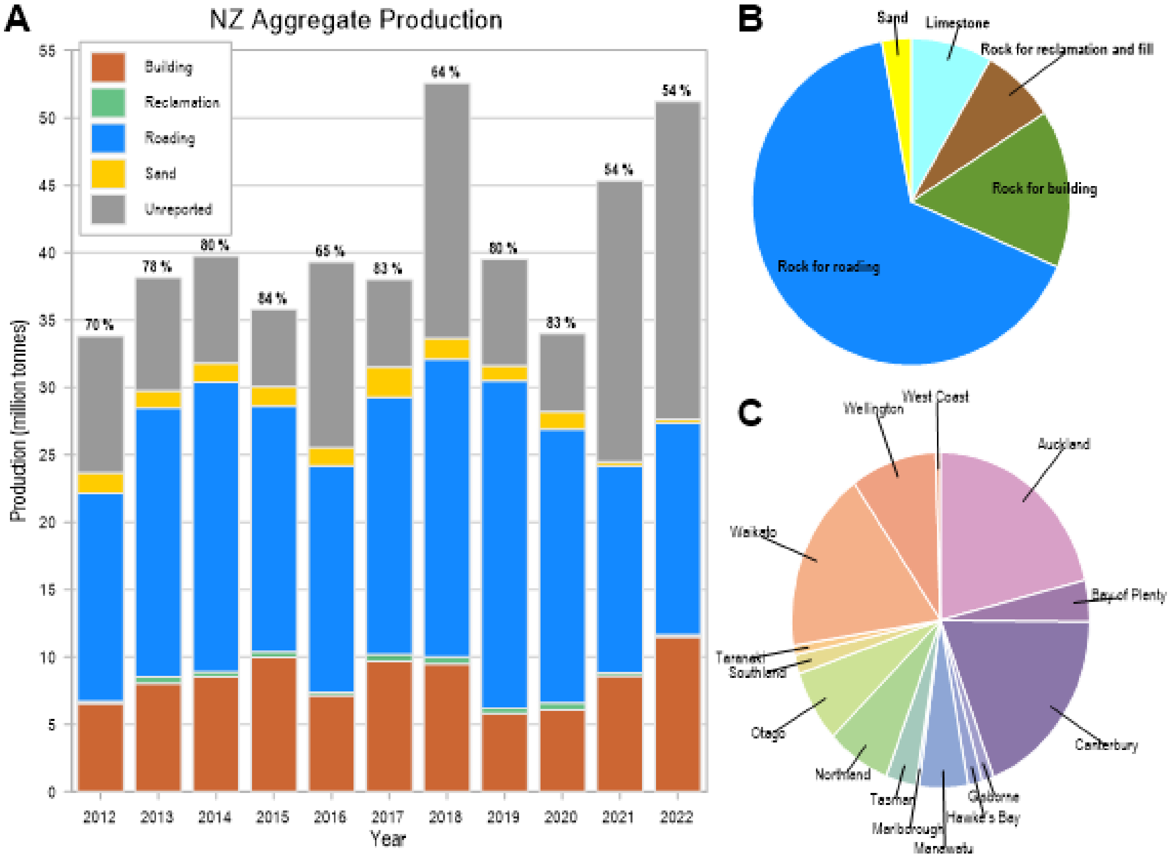

Figure 4.1 New Zealand aggregate production statistics. (a) annual production for aggregate for building, reclamation and fill and for roading, as well as industrial sand end uses for the last 10 years. Significant under-reporting of production values in New Zealand (reporting percent labelled) limits total production value statistics (unreported sections shown here in grey are estimated from missing percentage). (b) Ratio of rock, sand and limestone aggregate extracted for the 2019 production year. (c) Regional distribution of industrial minerals extracted for the 2019 production year (Source: New Zealand & Petroleum and Minerals).

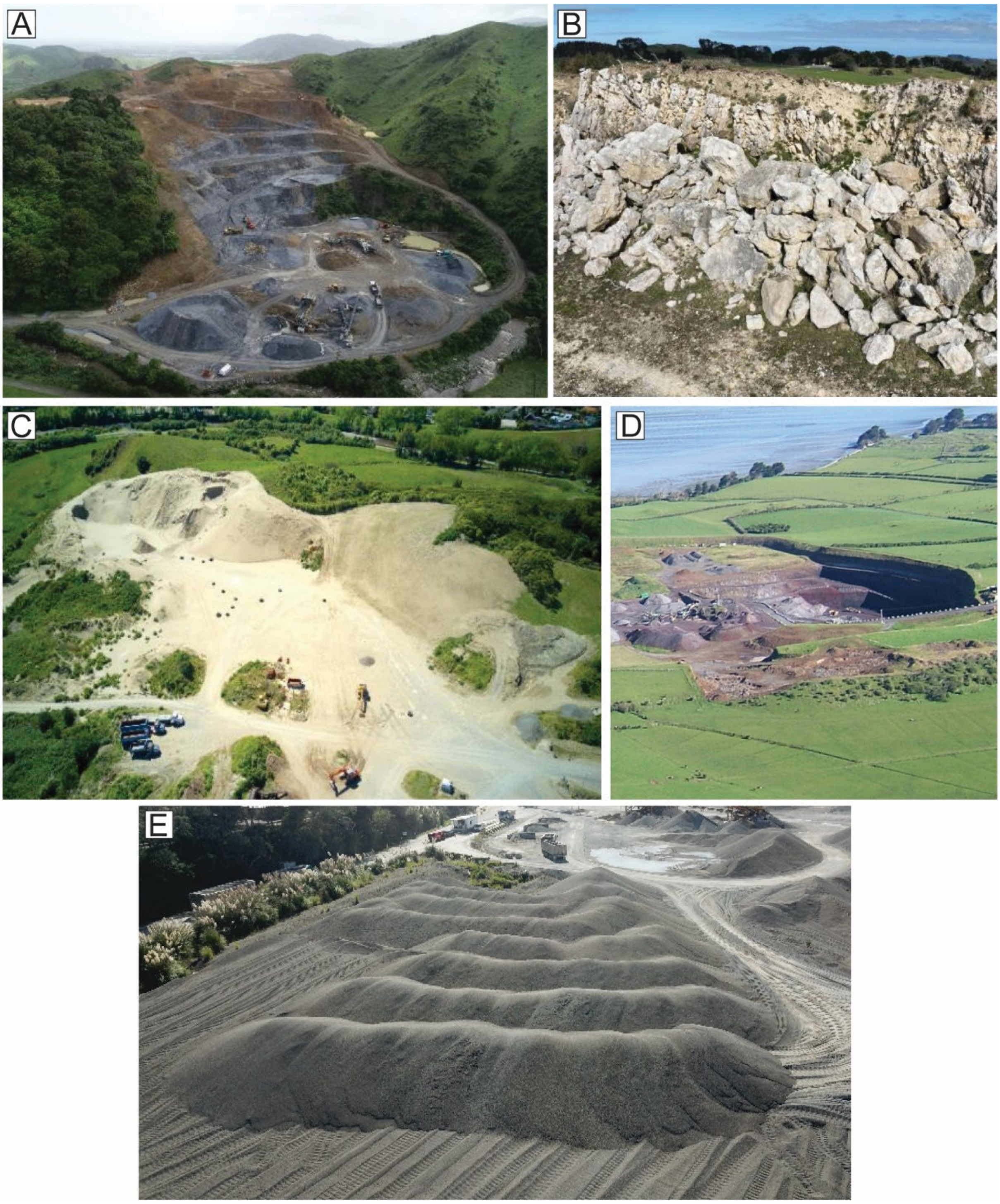

Figure 4.2 Examples of extractive quarrying activity in New Zealand. (a) A hard-rock greywacke (sandstone and siltstone) quarry in Otaki; (b) limestone armour rock (rip-rap) stockpile in southern Hawkes Bay; (c) sand quarried from an inland dune deposit on the Kāpiti Coast; (d) basalt quarry in Auckland City; and (e) gravel and sand stock piles at a processing site in the Manawatū. Photographs A–C, E by Matt Hill; photograph D by Bruce Hayward.

Figure 4.3 Aggregate processing plant at Belmont quarry in Lower Hutt. Greywacke rock is quarried and then crushed and screened into various-sized products.

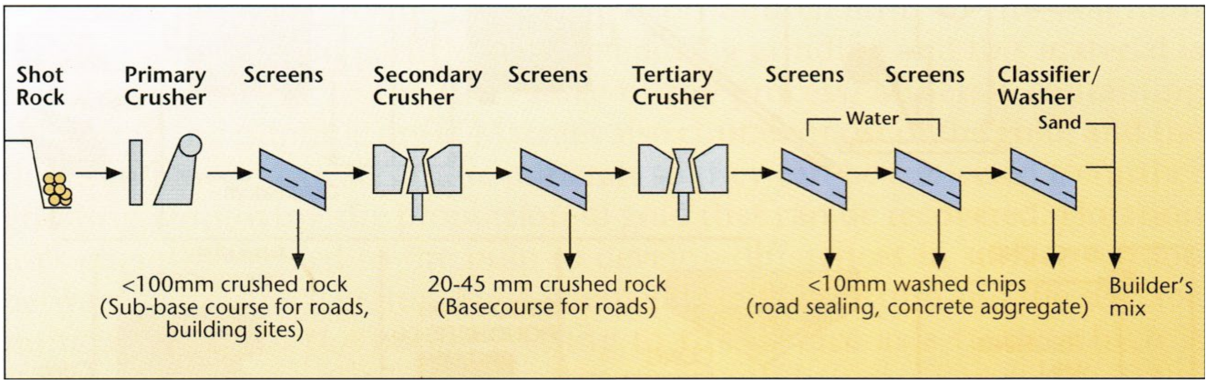

Figure 4.4 Aggregate rock is crushed and screend to make various-sized products.

New Zealand is fortunate to have large areas of accessible rock and gravel deposits throughout most of the country that can be utilised for aggregate. However, resources that are economic to develop need to be accessible, of suitable quality for their end use and close to the point of demand to control costs and the effects of transport (Figure 4.5). As a result, economic aggregate resources near cities are scarce commodities that need to be managed to ensure that supplies are available for the future. As their location is determined by natural processes, the location of quarries is restricted to very few potential locations, unlike many other land uses.

The main source rock for aggregate is greywacke (a layered sandstone and siltstone rock), which occurs in many parts of New Zealand. Hard-rock quarries are the main source of supply in the North Island. Gravel deposits are significant producers in Canterbury, the West Coast and Southland in the South Island, and the Kāpiti Coast and Hawke's Bay in the North Island. Volcanic rocks, mainly andesite and basalt, are worked locally, particularly in the North Island.

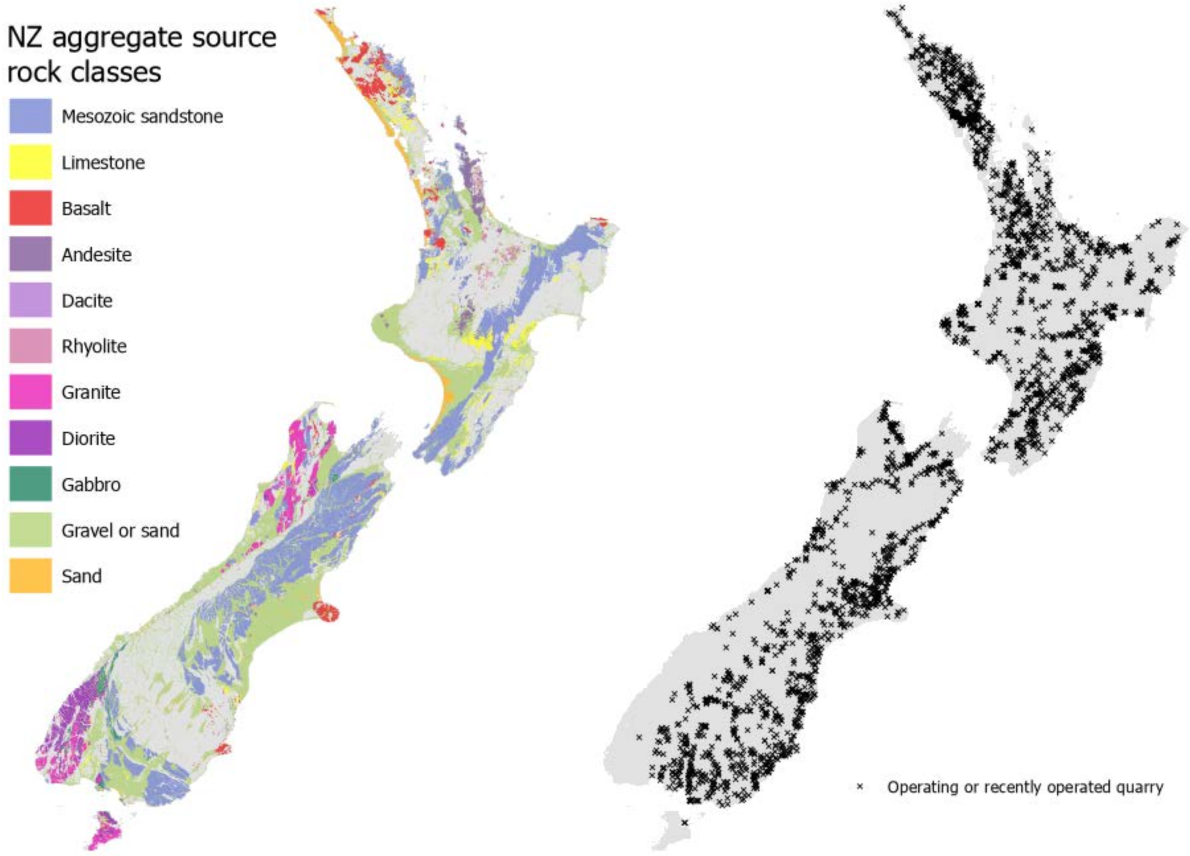

Figure 4.5 The occurrence of main aggregate source rocks in New Zealand divided into their major resource classes (left; derived from Heron [2024] geological map data and interpretation by Hill and Chilton [2024a–e]) and distribution of quarries around New Zealand (right; based on AQA [2024]).

The total annual production of aggregates in 2022 reported to the Ministry of Business, Innovation & Employment (MBIE) was about 28 Mt (Table 4.1); however, Market Economics (McIlrath and Harris 2024) estimated the true total at about 47.9 Mt as only 54% of surveyed quarries reported data. The production is from several hundred quarries and pits located throughout the country. The aggregates industry is dominated by the activities of a small number of major companies, whereas there are a large number of smaller producers who cater primarily for very localised demand (Table 4.1). Most of the large quarries in New Zealand have been operating for many years.

Table 4.1 Size of aggregate operations (after Happy [1993]; Happy and Ashby [1993]).

Size of Production		Percentage of Production
Large scale	More than 500,000 tpa	About 20% of production
Medium scale	50,000–500,000 tpa	About 65% of production and about 20% of the operations
Small scale	Less than 50,000 tpa	About 15% of production

Aggregate is a major component of infrastructure (NZIC 2021; Wilson et al. 2022; McIlrath and Harris 2024). Demand for it is driven by the level of economic activity, which in turn is related to total population and the rate of population and economic growth. The re-building of Christchurch following the earthquakes in 2010 and 2011 and urban expansion in Auckland have increased the demand for building aggregate and concrete.

Road construction and maintenance accounts for more than half of the aggregate being used in New Zealand. While some of our high-traffic roads have a smooth asphaltic concrete (‘bitumen hotmix’) surface, most have a chipseal (sprayed bitumen film with a coating of stones on top). High-quality aggregate is used for these surface layers, but most of the aggregate used in road making goes into the base course and sub-base layers that support the road surface (Figure 4.6).

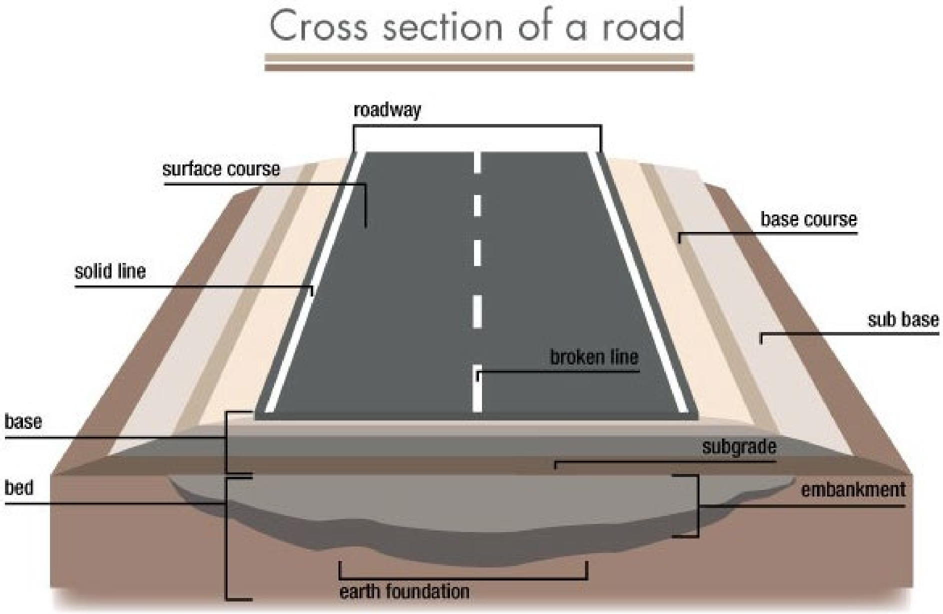

Figure 4.6 Profile of the construction materials in a road (Source: AQA).

Aggregate used for sub-base and base-course layers under roads can be upgraded by using additives such as lime, cement, bitumen or slag that helps bind the finer aggregate particles, increasing its strength (Figure 4.7). This allows lower-quality material to be used for road building. Recycling of some aggregate materials, such as road aggregate and concrete, reduces waste. Asphalt pavement is now recycled and re-used for sealing roads.

Figure 4.7 Stabilisation of road aggregate to bond particles.

4.1.1 Resources

There are no detailed resource estimates, although, on a national basis, there are very extensive deposits of greywacke and volcanic rocks to meet future demand for aggregates. However, the quantity of rock available for any specific purpose is variable from area to area. Generally there are adequate local sources, although two notable exceptions are the Taranaki and Gisborne areas, which lack high-grade rock materials. Also, the Auckland area, with its large population and consequent high volume of use, is having to transport aggregate from farther afield as existing quarries are being worked out.

4.1.2 Challenges

Finding sites for new quarries is difficult because workable aggregate resources need to be located near major transport routes and, predominantly, close to towns and cities to minimise transport impacts and costs. In general, transporting aggregate a distance of 30 km doubles its cost at the quarry (NZIC 2021).

Because of the high demand in urban areas, the potential for new aggregate production is usually greatest in urban-fringe areas where competing land uses, particularly urban expansion, may cause the closure of existing quarries and prevent the opening of new ones, effectively sterilising the resource.

AQA (2020) suggested that adequate provision must be made in planning documents to protect existing and potential aggregate and sand deposits and provide for their extraction. Without planning to secure adequate access to resources at workable locations, and protect them from encroachment, there is the real risk of losing access to such proximate resources.

As for all extractive activities, cultural sensitivity and social licence to operate are important considerations. Ideally, quarries should be located close to their markets, but the sensitivity of residents to quarrying can place significant constraints on operators. Developing a new quarry near a built-up area can generate considerable opposition because of truck movements, dust, noise and visual appearance of the operation. This is also reflected in reverse sensitivity – as communities encroach upon existing operations, they are affected by, and frequently negatively respond to, the quarrying and associated activities.

These factors have resulted in the trend toward fewer and larger aggregate quarries and pits, generally involving longer transport distances, increasing the costs of aggregate.

Sand has been mined at several locations offshore; however, local concern over perceived environmental risk, particularly the potential for beach erosion, has terminated most of these operations and alternative sources of sand have been sought, such as obtaining the sand-sized fraction from crushed rock.

4.1.3 Opportunities

Hill (2021) and Hill and Chilton (2024a–e) have carried out GIS modelling to map ‘aggregate opportunity’ in New Zealand by considering a number of factors in addition to geological source material, including:

- Land use (e.g. conservation land, Department of Conservation land and land cover).
- Future demand (e.g. roading and construction).

- Supporting infrastructure (e.g. access to roads, railway, electricity supply and labour market).
- Cultural sensitivity (e.g. visibility, residential areas, population density and mapped community sites and features).

The resulting maps shown in Figures 4.8 and 4.9 can be used to:

1. Manage aggregate resources to ensure that infrastructure providers have a reliable and affordable supply.
2. Determine regional import demand or export potential.
3. Identify land for protection from urbanisation, ensuring availability of aggregate resources for future production.
4. Generate targets for exploration activities.
5. Provide insight into future resource availability (Hill 2021).

More detailed modelling has been carried out for the Auckland, Bay of Plenty, Wellington and Otago regions (Hill and Chilton 2024a–e) to help councils and the local industry understand the regional aggregate opportunity and protect resources before other land use prevents access. However, New Zealand requires more detailed geological mapping of advanced rock and engineering parameters to fully understand aggregate resources.

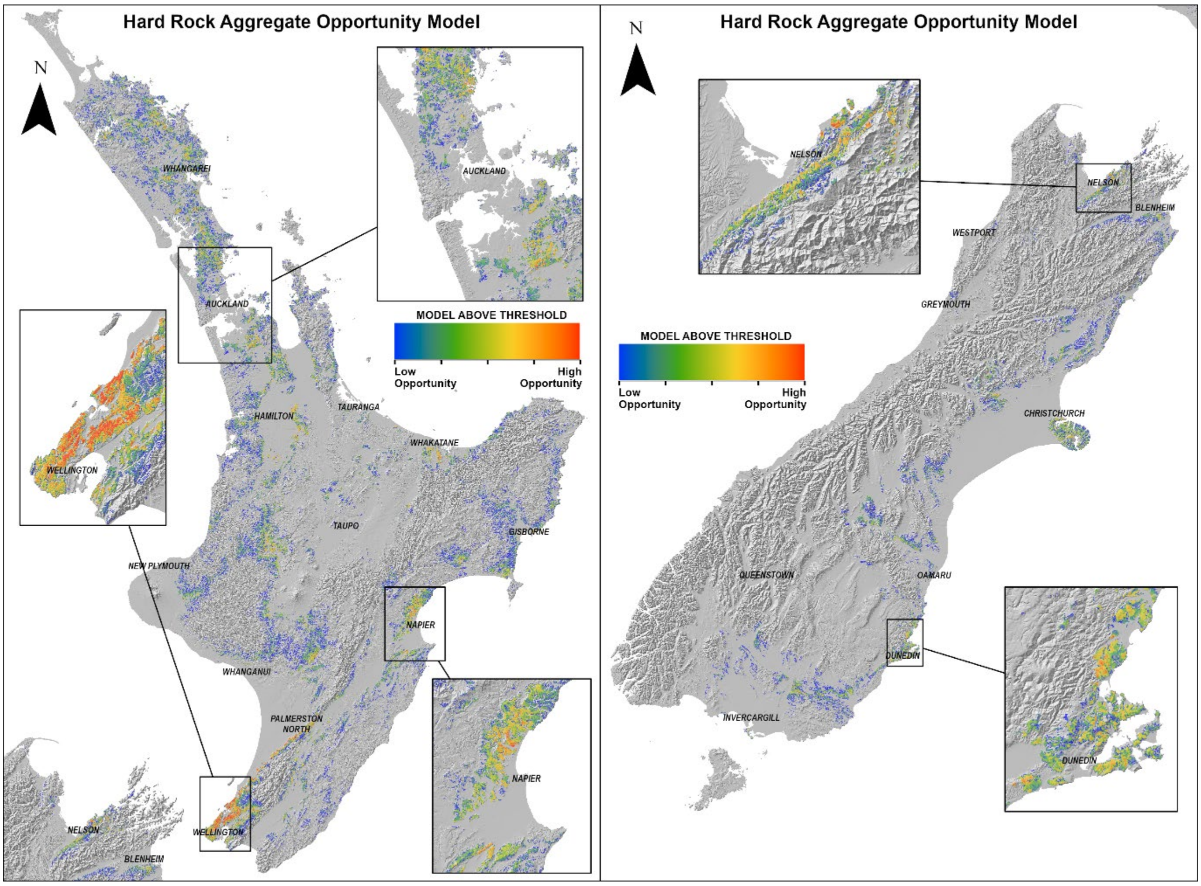

Figure 4.8 Maps of the aggregate opportunity hard-rock model for the North Island (left) and South Island (right) from Hill (2021). Colours represent the level of aggregate opportunity determined from modelling of geology, land use, demand, infrastructure and cultural sensitivity.

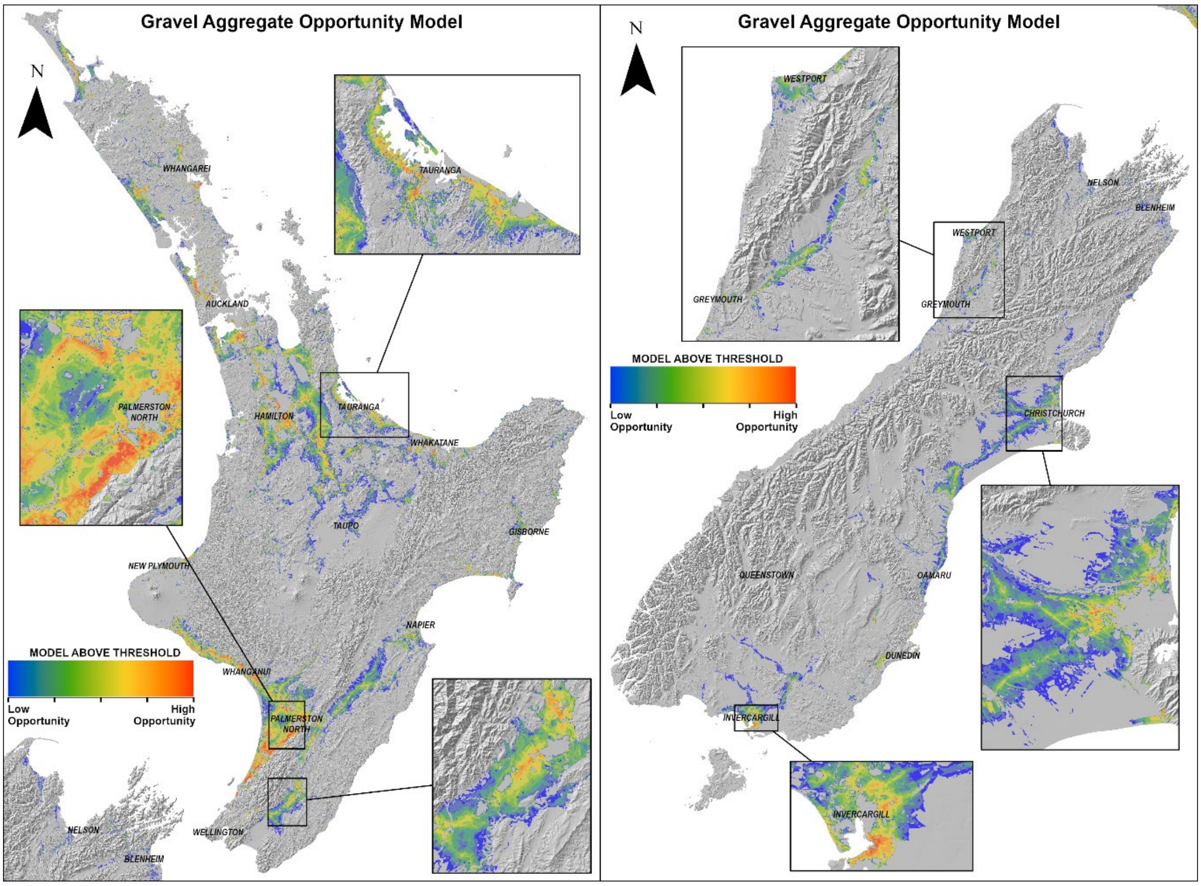

Figure 4.9 Maps of the aggregate opportunity gravel model for the North Island (left) and South Island (right) from Hill (2021). Colours represent the level of aggregate opportunity determined from modelling of geology, land use, demand, infrastructure and cultural sensitivity.

Key References: MacFarlan and Barry (1991); Happy (1993); Christie et al. (2001b); Black (2009, 2014); Hill (2021); Hill and Chilton (2024a–e).

4.2 Barium (Ba)

4.2.1 International Description

International data for barite are listed in Table 4.2.

Table 4.2 World production, reserves and resources and major uses of barite.

Barium (Ba)		
International	**Major Minerals:** Barite $BaSO_4$	
	World mine production of barite in 2023 (USGS 2024)	8,500,000 t barite
	Major world producers of barite (% of total 2023 world production) (USGS 2024)	India (32%), China (22%), Morocco ((14%), Kazakhstan (7%), Laos (7%), Iran (4%), Mexico (3%), Russia (3%), Turkey (3%)
	World reserves of barite (USGS 2024)	>278,000,000 t
	World resources of barite (USGS 2024)	2 Bt; only 740 Mt are identified resources
	Uses: Weighting agent in oil and gas well-drilling muds; preparation of barium compounds; pigment in paints and weighted filler for paper, cloth and rubber.	

4.2.2 New Zealand Occurrences of Barite

Six occurrences of barite mineralisation have been reported from Thomson Hill (MM A34), between the Wangapeka and Baton valleys in Northwest Nelson. The mineralisation consists of hydrothermal barite-fluorite-quartz-adularia veins, up to 30 cm thick, cutting Arthur Marble near the contact with hydrothermally altered Separation Point Suite granitoid. The barite is near pure $BaSO_4$ end-member composition and locally constitutes up to 95% of the veins. The largest occurrence of barite has an estimated resource of <3000 t of crude ore. Grades of 45.6–59.5% $BaSO_4$ were obtained from grab samples.

Key References: NZGS (1970b); Williams (1974).

4.3 Building Stone

Although few buildings in New Zealand are constructed entirely of building stone, there is a widespread use of building stone for decorative walls and general paving. Many rock types are suitable for use as a dimension stone, including (Hayward 1987):

- **Limestone:** Oamaru; Whangārei; Hanmer; Te Kūiti; various localities in Hawke’s Bay, Canterbury and north Otago.
- **Sandstone:** Dobson near Greymouth; Charteris Bay on Lyttelton Harbour.
- **Dolomite:** Mt Burnett in west Nelson.
- **Marble:** Takaka Hill, Canaan Valley, Riwaka Valley, Takaka Valley, as well as in west Nelson and Caswell Sound and Malaspina Sound in Fiordland.
- **Schist:** Otago.
- **Serpentine:** Griffin Range near Taramakau.
- **Tonalite:** Paritu in the northern Coromandel Peninsula.
- **Granite:** Tonga Bay.
- **Norite:** Bluff Hill.
- **Ignimbrite:** Hinuera Valley, Putaruru.
- **Basalt:** Northland, Auckland, Port Hills on Banks Peninsula and around Dunedin.

However, only dolomite from Mt Burnett, Takaka marble, schist from Otago, Oamaru limestone and Hinuera stone have recently produced in quantity.

Key References: Hayward (1987).

4.4 Bentonite Clay

4.4.1 International Description

International data for bentonite clay are listed in Table 4.3.

Table 4.3 World production, reserves and resources and major uses of bentonite clay.

Bentonite $[(Ca,Na)_{0,3}(Al,Mg)_2Si_4O_{10}(OH)_2\cdot n\ H_2O]$		
International	**Alternative Name:** Calcium bentonite is also known as fuller’s earth.	
	World mine production in 2023 (USGS 2024)	**Bentonite:** 20,000,000 t **Fuller’s earth:** 4,300,000 t
	Major world producers (% of total 2023 world production) (USGS 2024)	**Bentonite:** USA (24%), India (19%), Turkey (12%), China (11%), Greece (7%), Denmark (5), Iran (4%), Czechia (1%) **Fuller’s earth:** USA (53%), India (17%), Spain (13%), Mexico (3%), Senegal (3%), Turkey (1%)
	World resources (USGS 2024)	Extremely large
	Uses: Drilling mud (50% of world consumption) and as a binder, purifier, absorbent and carrier for fertilisers and pesticides, filler, sealant, catalyst in petroleum refining and in medicine.	

4.4.2 New Zealand Occurrences of Bentonite Clay

Bentonite, deposited in a freshwater environment during the Late Cenozoic, is mined by Transform Minerals (NZ) Limited in the Harper Hills near Coalgate, 65 km west of Christchurch (Figure 4.10). Non-swelling calcium bentonite occurs in a main bed up to 62 m thick, separated from a lower, carbonaceous, bentonite bed by 3–4 m of quartz sand and gravel. It is processed by treatment with soda ash to impart swelling properties. In the 1980s, resources totalled around 10 Mt (Mintech [NZ] Ltd in MacFarlan and Barry [1991]). Coalgate bentonite is used for paper-making, as a drilling mud, as a growing medium, a stock feed additive, for sealing ponds and reservoirs and for treating wastewater and effluent.

Marine bentonitic beds are widespread along the east coast of both the North and South Islands. They have been worked in the past at Mangatu, north of Gisborne and at Porangahau, where there is a resource of about 1 Mt (Mintech [NZ] Ltd in MacFarlan and Barry [1991]).

The main uses are as a binder in foundry sand, for drilling muds, for sealing drillholes, for sealing dams and diaphragm walls in construction projects, as a bitumen emulsifier, in fibre cement and as pellet hardener in stockfood.

Key References: Williams (1974); MacFarlan and Barry (1991); Christie et al. (2000).

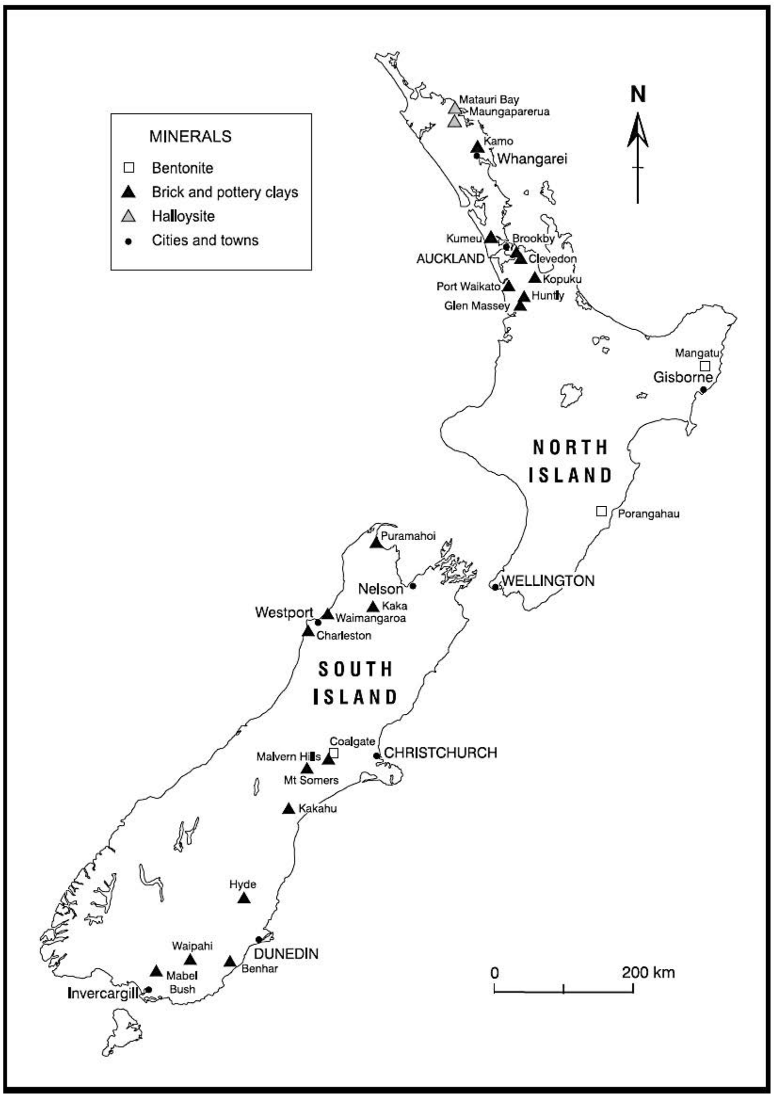

Figure 4.10 Location of selected clay deposits in New Zealand (after Christie et al. [2000]).

4.5 Halloysite Clay [$Al_2SiO_5(OH)_4 \cdot nH_2O$]

Halloysite clay is produced from deposits at Matauri Bay, 100 km north of Whangārei in Northland (Figure 4.10) by Imerys Ceramics (Townsend 1989; Harvey et al. 1990; Luke 1997; Brathwaite et al. 2014; Brathwaite and Christie 2016). Two pits are worked on the Matauri Bay and Mahimahi rhyolite domes, located 2 km apart. The company also has deposits at Shepherds Hill to the west of Matauri Bay and Maungaparerua, 8 km west of Kerikeri.

The high-purity halloysite possesses exceptional whiteness and brightness, as well as an overall fine particle size. Iron oxides average 0.28% and titania averages 0.08%. The inherent brightness of the raw material, coupled with low iron and titania levels, imparts whiteness and translucency to the finished product.

The processed halloysite is exported for the manufacture of high-quality ceramics, principally porcelain but also fine bone china and technical ceramics. There are two main applications in the technical ceramics sector.

The deposits have been worked since 1969. Annual production data for recent years has been withheld and was last reported in 2019 as 50,569 t of raw clay mined from the Matauri Bay and Mahimahi pits (61,650 t in 2016). Plant capacity is about 25,000 tpa of processed halloysite.

Sufficient resources exist at the Matauri Bay and nearby Mahimahi deposits to sustain production for over 30 years at current rates. Potential resources are present in other deposits at Shepherds Hill west of Matauri Bay and at Maungaparerua near Kerikeri.

Key References: Townsend (1989); Luke (1997); Brathwaite et al. (2014); Brathwaite and Christie (2015, 2016).

4.6 Kaolinite Clay for Bricks, Pottery and Industry

4.6.1 International Description

International data for kaolinite clay are listed in Table 4.4.

Table 4.4 World production, reserves and resources and major uses of kaolinite clay.

Kaolinite Clay [$Al_2Si_2O_5(OH)_4$]		
International	**Alternative Name:** Kaolin	
	World mine production in 2023 (USGS 2024)	51,000,000 t
	Major world producers (% of total 2023 world production) (USGS 2024)	Uzbekistan (17%), China (16%), India (16%), USA (9%), Czechia (6%), Russia (5%), Turkey (4%), Iran (4%), Brazil (2%)
	World reserves (USGS 2024)	Large
	World resources (USGS 2024)	Extremely large
	Uses: Filler and whitener in paper, ceramics and paint. It also has other industrial uses, as well as in medicines and cosmetics.	

4.6.2 New Zealand Occurrences of Kaolinite Clays

In New Zealand, kaolinite clays are formed mainly by:

1. Surface weathering of clay-rich rocks such as argillite and greywacke in several locations near Auckland, for example, Port Waikato, Brookby and Glen Massey.
2. Acid leaching of mudstone to produce fireclays associated with coal measures (e.g. Kamo, Maramarua and Huntly in the North Island, and Puramahoi, Malvern Hills, Kakahu, Hyde, Benhar, Waipahi and Mabel Bush in the South Island).
3. Weathering of mudstone and siltstone at West Auckland and near Nelson.
4. Hydrothermal alteration of rhyolite in the Coromandel Peninsula and Canterbury.

Recent production statistics for clay for bricks, tiles, etc., are withheld and were last reported in 2014 as 125,508 t. Production has mainly been from clay pits in West Auckland, Brookby, Port Waikato, Maramarua, Malvern Hills, Mt Somers and Waipahi. Kaolinite clays for pottery are produced at Kaka, Malvern Hills, Hyde and Mabel Bush.

Kaolinite clays are used widely for domestic brick, tile, pipe, ceramics and pottery manufacture. Some kaolinite is also used as a filler in rubber, bitumen and adhesives. High-purity kaolinite is used by the New Zealand paper industry for paper coating and filling.

The quantity of clay present in most areas is poorly defined but known to be large, especially in weathered argillite and greywacke and coal measure clay deposits.

Key References: Thompson (1989); MacFarlan and Barry (1991); Christie et al. (2000).

4.7 Diatomite

4.7.1 International Description

International data for diatomite are listed in Table 4.5.

Table 4.5 World mine production, reserves and resources and major uses of diatomite.

Diatomite / Diatomaceous Earth (SiO_2)		
International	**Name:** Diatomaceous earth is the commercial name for diatomite.	
	World mine production in 2023 (USGS 2024)	2.6 Mt
	Major world producers (% of total 2023 world production) (USGS 2024)	USA (32%), Denmark (17%), China (10%), Turkey (8%), Argentina (4%), Mexico (4%), France (4%), Mozambique (3%); Spain (2%), Czechia (2%), Germany (2%), South Korea (2%), Russia (2%)
	World reserves (USGS 2024)	Large (521 Mt for USA, China, Spain and Turkey only)
	World resources (USGS 2024)	N/A
	Uses: Filtration material, sorbents, fillers, heat-insulation materials, pet litter, agriculture and a soil for potted plants.	

4.7.2 New Zealand Occurrences of Diatomite

Diatomite is used as a pozzolan cement, mild abrasive, filtration medium, filler in insulating material and as pet litter. Recent annual production data is withheld and was last reported in 2013 as 4 t (95 t in 2010). Most production has been from Whirinaki, Middlemarch and Oamaru, with minor production at Kingsland and Papakaio (Williams 1974).

The lacustrine deposit at Mercer contains about 180,000 t of extractable diatomite and pumicite (Waterhouse 1967; Thompson 1989). In the Rotorua basin, there are considerable quantities of lacustrine diatomite between Ngongotaha and Hamurana. Resources at Whirinaki (Ngakuru) are estimated at 2 Mt, containing more than 50% high-grade material with more than 50% diatoms (NZGS 1970b). At Middlemarch, diatomite lake beds are more than 35 m thick and approximately 5 Mt are present (Gordon 1959; Williams 1974). Near Oamaru, marine diatomite beds cover an area of about 26 km^2 and vary in thickness from a few centimetres to 9 m. A cave valley near Oamaru was estimated to have 140,000 t of diatomite (Edwards 1991); however, this is one of many occurrences in the area, suggesting a much larger resource.

Key References: Ritchie (1962); Williams (1974); Thompson (1989); MacFarlan and Barry (1991).

4.8 Dolomite

4.8.1 International Description

International data for dolomite are listed in Table 4.6.

Table 4.6 World mine production, reserves and resources and major uses of dolomite.

Dolomite [$CaMg(CO_3)_2$]		
International	**Major world exporters in 2021**	China (9.1 Mt), United Arab Emirates (2.1 Mt), Canada (1.6 Mt), Belgium (1.1 Mt), Philippines (1.1 Mt), Slovakia (1 Mt)
	Major world importers in 2021	India (4.6 Mt), Japan (2.4 Mt), USA (1.9 Mt), Taiwan (0.7 Mt), China (0.6 Mt), the Netherlands (0.6 Mt)
	World reserves and resources	Very large
	Uses: Agricultural and horticultural fertiliser, ornamental stone, concrete aggregate and a source of magnesium oxide, as well as in the Pidgeon process for the production of magnesium and a marine aquarium substrate. Calcined dolomite is used as a catalyst in industrial processes.	

Dolomite is formed as a magnesium replacement of limestone or of lime mud before lithification. The dolomitisation process may be assisted by microbial activity.

4.8.2 New Zealand Occurrences of Dolomite

The main occurrence of dolomite is on Mt Burnett in Northwest Nelson (Figure 4.11), where it is present in discontinuous lenses in a folded dolomite-marble sequence of Paleozoic age. The dolomite is 60–70% $CaCO_3$ and 28–39% $MgCO_3$, with up to 3% SiO_2 and up to 0.66% Fe_2O_3 (Bishop and Braithwaite 1969). The main lens of dolomite contains about 70 Mt. Other lenses each contain up to 1 Mt (Williams and Katz 1974).

The Mt Burnett quarry is operated by Golden Bay Dolomite. The plant at the quarry has a capacity of around 100,000 tpa, although current output is of the order of 25,000–40,000 tpa.

About 80% of the product is used as an additive to phosphatic fertilisers for spreading on magnesium-deficient soils, and the balance is used for aggregate and rip rap, with large blocks used for river and coastal protection in the Wellington region. The dolomite has formerly been used in glass manufacture and in the steel industry.

Recent production statistics are withheld and were last reported as:

- **Agriculture (2018):** 25,297 t (298,948 t in 2010).
- **Industry (2014):** 43,624 t (86,399 t in 2010).

Key References: Bishop and Braithwaite (1969); Williams (1974); Thompson (1989); MacFarlan and Barry (1991); Thompson et al. (1995).

4.9 Feldspar

4.9.1 International Description

International data for feldspar are listed in Table 4.7.

Table 4.7 Major minerals, world production, reserves and resources and major uses of feldspar.

Feldspar		
International	**Major Minerals:** Plagioclase group with end members albite ($\mathrm{NaAlSi_3O_8}$) and anorthite ($\mathrm{CaAl_2Si_2O_8}$), as well as potassium feldspar (K-spar) end member ($\mathrm{KAlSi_3O_8}$)	
	World mine production in 2023 (USGS 2024)	27 Mt
	Major world producers (% of total 2023 world production) (USGS 2024)	Turkey (23%), India (19%), China (9%), Italy (8%), Iran (7%), Republic of Korea (3%), Spain (3%), Brazil (3%), Saudi Arabia (2%), Mexico (2%), Czechia (2%), Pakistan (2%)
	World reserves (USGS 2024)	>2.294 Bt with most in China and Turkey
	World resources (USGS 2024)	Very large
	Uses: As a raw material in glassmaking and ceramics, and as a filler and extender in paint, plastics and rubber.	

4.9.2 New Zealand Occurrences of Feldspar

Feldspar deposits of possible economic potential occur in four main geological environments:

1. Pegmatite and aplite dikes in granites of Paleozoic and Mesozoic age along the western side of the South Island (e.g. Separation Point Granite, Deep Creek, Charleston).
2. In the weathered zone of granite plutons in Northwest Nelson.
3. Weathered feldspar-rich volcanic rocks in Northland, Rotorua-Taupō, Malvern Hills and Dunedin.
4. Dune, beach and marine sands of Quaternary age at Ruakaka Flat south of Whangārei and near Kaipara Harbour are rich in calcium feldspar.

Feldspar-rich sand (50–75% feldspar) has been dredged about 200 m offshore between Mangawhai and Pakiri on the east coast of Northland. This material is mined for use as sand rather than for production of feldspar.

Sand dunes at Ruakaka Flats, south of Marsden Point in Northland, contain more than 400 Mt of sand that could yield, at 60% recovery, 240 Mt of feldspar (see Thompson [1989]).

Key References: Williams (1974); Thompson (1989).

4.10 Fluorite / Fluorspar (CaF_2)

4.10.1 International Description

International data for fluorite are listed in Table 4.8.

Table 4.8 World mine production, reserves and resources and major uses of fluorspar.

Fluorite / Fluorspar (CaF_2)		
International	**Name:** Fluorspar is the commercial name for fluorite.	
	Major Minerals: Fluorite (CaF_2), bastnaesite, cryolite, sellaite, villiaumite, fluorite, fluorapatite, various phyllosilicates and topaz	
	World mine production in 2023 (USGS 2024)	8.8 Mt
	Major world producers (% of total 2023 world production) (USGS 2024)	China (65%), Mexico (11%), Mongolia (11%), South Africa (5%), Vietnam (2%), Spain (2%), Iran (1%)
	World reserves (USGS 2024)	280 Mt mostly in China and Mexico
	World resources (USGS 2024)	5 Bt of fluorspar in 74 Bt of phosphate rock
	Uses: Fluorspar is used directly as a fluxing material and as an additive in different manufacturing processes. It is the source of fluorine in the production of hydrogen fluoride or hydrofluoric acid, which is used as the feedstock for numerous organic and inorganic chemical compounds.	

4.10.2 New Zealand Occurrences of Fluorite

Fluorite occurs in veins associated with barite at Thomson Hill (MM A34), with grades from 7.8 to 19.5% CaF_2. At Wekakura (MM A19), near the mouth of the Heaphy River, thin veins, clusters and lenticular patches of fluorite occur within granite of the Karamea Suite. Chip sampling at the most mineralised sites gave CaF_2 content in the range 0.16–0.36%, with the best channel sample at 5.4% over 3 m (Riley and Hume 1973).

In the headwaters of Kehu Stream (MM A47), green fluorite veins, less than 0.3 m thick, cut Berlins Porphyry (Nathan 1978), and a breccia pipe containing up to 30% fluorite was located in the Kehu pluton by AHI Minerals (Leach 1976).

Numerous minor occurrences of fluorite veining have been reported throughout the Sinclairs Castle area (MM A50), including sparse small veins in pink porphyry in Fluorite Creek and fluorite-bearing float in the Cascade, V37 and Rochfort creeks (Bates 1978).

Key References: NZGS (1970b).

4.11 Garnet

4.11.1 International Description

International data for garnet are listed in Table 4.9.

Table 4.9 World mine production, reserves and resources and major uses of garnet.

Garnet $[(Mg,Fe,Mn)_3Al_2(SiO_4)_3]$		
	World mine production in 2023 (USGS 2024)	970,000 t
	Major world producers (% of total 2023 world production) (USGS 2024)	Australia (40%), China (32%), South Africa (19%), USA (7%), India (2%), Pakistan (0.2%)
	World reserves (USGS 2024)	Moderate to large (e.g. 51 Mt in China, India, USA and South Africa)
	World resources (USGS 2024)	Large
	Uses: Garnet is mainly used as an abrasive for industrial blast-cleaning, polishing, sand papering and water-jet cutting. It is starting to replace silica in abrasives because silica is dangerous to worker health (i.e. silicosis). Garnet is also used for filtration and in jewellery.	

4.11.2 New Zealand Occurrences of Garnet

Garnet is a minor constituent in most Quaternary fluvial and ilmenite beach-sand deposits on the West Coast, but, in the Westport area, it is a major constituent and is typically twice as abundant as ilmenite. Composition is typically in the pyrope-almandine field, with minor andradite (Hutton 1950). Grain morphology is either angular or sub-rounded, suggesting two sources (McPherson 1978). The presence of angular grains in the Fox, Four Mile and Totara rivers suggests local sources, likely from the Charleston Metamorphic Group gneiss. The well-rounded garnet is derived from the extensive garnet-zone schists in the Southern Alps and has been transported northwards by longshore drift. Also, some garnet may have been re-worked through intermediate deposits, perhaps Tertiary or Quaternary in age.

In 2023, Westland Mineral Sands started mining mineral sands near Westport for export and processing to produce ilmenite, garnet and other mineral products. Garnet is also likely to be produced from mineral sand mining at Barrytown.

Ritchie et al. (2019) estimated garnet resources at several West Coast locations listed in Part 1 (Table 7.2).

Key References: Williams (1974); Ritchie (2017); Ritchie and Scott (2019); Ritchie et al. (2019).

4.12 Glauconite $(K,Na)(Fe,Al,Mg)_2(Si,Al)_4O_{10}(OH)_2$

4.12.1 International Description

Glauconite is an iron-potassium silicate that contains up to 9% K_2O and can be used as a potential feedstock for production of potash, a potassium fertiliser and soil conditioner (e.g. in Brazil). Glauconite forms exclusively in marine settings, typically on the continental shelf in areas with slow rates of sediment accumulation. In concentration, this green mineral imparts a green colour to the sand and hence the name ‘greensands’.

4.12.2 New Zealand Occurrences of Glauconite

Glauconite occurs as greensand in Cretaceous–Miocene-age sedimentary sequences on the eastern parts of the North and South Islands and Chatham Islands. Eocene-age Wanstead Formation greensand has recently been explored at Otaka, East Cape, for use in manufacturing potash fertiliser (Merchant 2012, 2013; Bridson 2014, 2015a, 2015b). The greensands are contained within folded sediments that lie in fault-bound zones. In a western zone, grades of are typically 5.4–5.8% K_2O, whereas, in the eastern zone, the rocks average about 7.2%. Gangue minerals are quartz, lesser feldspar and locally calcite. The beds are east-dipping and post-dated by glauconitic Oligocene-age Weber Formation limestones that locally contain up to 45% glauconite and have associated phosphate. Exploration was abandoned in 2015.

Similar greensand units in the Wairarapa, south of Waipukerau, were also prospected by Glauconite NZ and later NZ Potash (Drew 2014), but the units were found to be thin and had insufficient glauconite (20–50%).

Reconnaissance exploration has also been carried out on the greensands in the Castle Hill basin in northern Canterbury by Middle Island (2013), where glauconites had been described previously by McConchie and Lewis (1978, 1980). Middle Island also carried out reconnaissance exploration of the Otepopo Greensand in the Herbert to Moeraki area, southwest of Oamaru (Middle Island 2015, 2020) but found the glauconite content to be low grade at around 5% K_2O equivalent.

Glauconitic greensands have potential uses as soil conditioners/fertilisers, substituting for potash (Lefond 1975) and for water purification by filtration and ion exchange.

Merchant (2012) suggested that Otaka and similar deposits have potential for hundreds of millions of tonnes with grades in the range of 7–7.5% K_2O.

Opportunities: Glauconite offers a potential substitute for imported potash used to make fertiliser.

Key References: Merchant (2012, 2013).

4.13 Limestone

4.13.1 International Description

International data for limestone are listed in Table 4.10.

Table 4.10 World production, reserves and resources and major uses of limestone.

Limestone ($CaCO_3$)		
International	**Major Minerals:** Calcite and aragonite, both $CaCO_3$, and dolomite $CaMg(CO_3)_2$ Limestone may be converted to: • Agricultural lime by crushing to a fine size. • Burnt lime, also known as unslaked lime or quicklime, by burning (calcination) limestone in a lime kiln above 900°C, producing calcium oxide CaO. • Hydrated lime, also known as slaked lime, by adding water to burnt lime, producing calcium hydroxide $Ca(OH)_2$.	
	World quicklime and hydrated lime production in 2023 (USGS 2024)	430 Mt
	Major world producers of quicklime and hydrated lime (% of total 2023 world production) (USGS 2024)	China (72%), India (4%), USA (4%), Russia (3%), Brazil (2%), Japan (1%), Germany (1%), Republic of Korea (1%), Turkey (1%), Iran (1%), Italy (1%), France <1%)(), Australia (<1%), Ukraine (<1%)
	World reserves (USGS 2024)	Adequate for many years of demand
	World resources (USGS 2024)	Very large
	Uses: Limestone is mostly used as a raw material in the production of lime, primarily for treating soils, purifying water and smelting ores. It is also used in cement production, as aggregate, in chemical industries, as an acid buffer and as an additive in toothpaste, paper, plastics, paint, tiles and other materials as both a white pigment and a filler.	

4.13.2 New Zealand Occurrences of Limestone

Limestone deposits are widespread throughout New Zealand (Figure 4.11). Mortimer and Strong (2014) and Thomson et al. (2021) reported analyses of limestone and agricultural lime with an overall average of 84% calcium carbonate ($CaCO_3$).

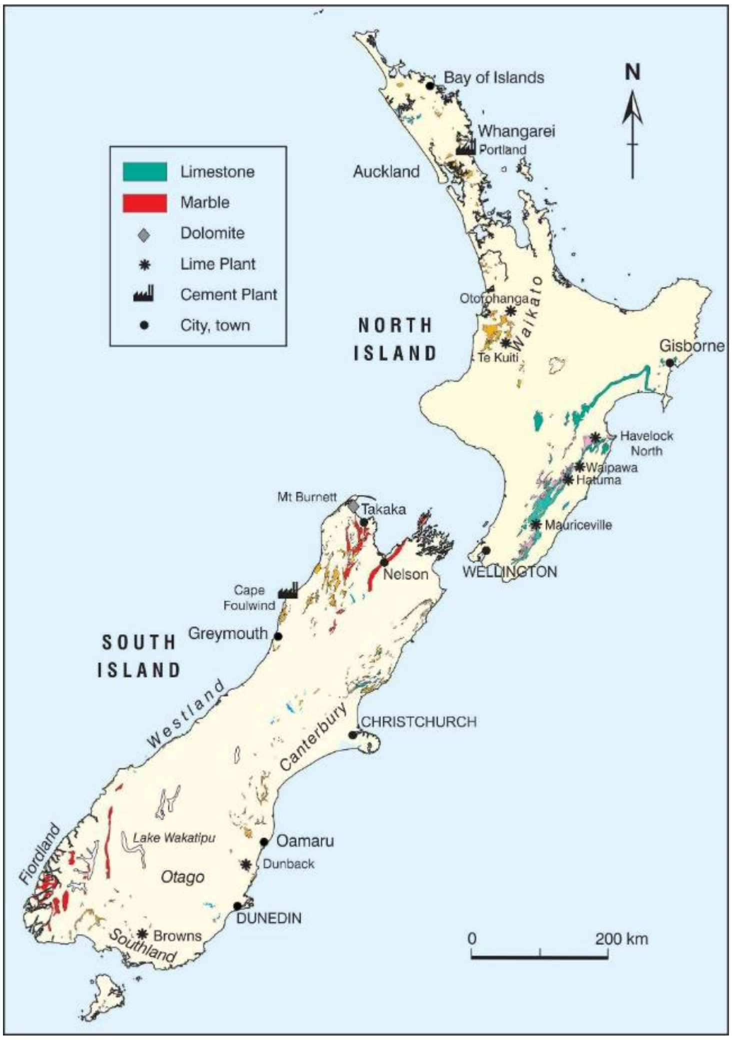

Figure 4.11 Locations of limestone, marble and dolomite deposits (after Christie and Barker [2013]).

Limestone containing more than 70% $CaCO_3$ is used for agricultural fertiliser (Morton 2019) for roading aggregate. High-grade limestone and marble suitable for domestic and export industrial use are widespread. The best-quality large tonnage deposits, containing 97.4–99.5% $CaCO_3$, are present in the south Waikato near Te Kūiti, where limestone is produced for a wide range of industrial uses and for making burnt lime. High-quality limestone is used domestically as a filler in paper, plastics, paint and rubber, for paper surface coatings and in glass making.

Uses of burnt lime (calcium oxide, CaO) include steelmaking at the Glenbrook mill, in processing gold ore at the Martha Hill gold mine at Waihi, at Macraes in Otago and offshore at Lihir (Papua New Guinea) and at Gold Ridge (Solomon Islands). Domestic uses also include pulp and paper manufacture at the Tasman and Carter Holt Harvey paper mills, in the sugar industry, in soil stabilisation and in sewage sludge and wastewater treatment.

Limestone and marl (calcite-bearing mudstone) are used in cement manufacture at Portland, near Whangārei, operated by Golden Bay Cement Company Limited. The domestic market is the principal consumer of the cement products, although some is exported to the Pacific Islands.

Production statistics for 2022 are presented for three uses:

- **Marl and cement:** Currently withheld.
- **Agriculture:** 625,832 t in 2022.
- **Industry:** 628,176 t in 2022.

Limestone for agricultural use is produced at more than 68 quarries throughout New Zealand (Thompson et al. 2021). There are extensive deposits, mostly in the tens of millions of tonnes and more, in the known limestone areas.

Key References: Williams (1974); MacFarlan and Barry (1991); Turnbull and Smith Lyttle (1999); Christie et al. (2001a); Mortimer and Strong (2014).

4.14 Magnesite

See Magnesium (Section 3.11).

4.15 Marble

4.15.1 International Description

International data for marble are listed in Table 4.11.

Table 4.11 World production, reserves and resources and major uses of marble.

Marble		
International	**Major Minerals:** Calcite ($CaCO_3$), dolomite [$CaMg(CO_3)_2$]	
	Top five countries for high-quality marble	Turkey, Italy, Greece, Iran and Spain
	Major world exporters in 2018 (percentage of the world market)	Turkey (42%), Italy (18%), Greece (10%)
	Major world importers in 2018 (percentage of the world market)	China (64%), India (11%), Italy (5%)
	World resources (USGS 2024)	Very large
	Uses: Sculpture and building stone (construction or dimension stone), for example, wall and floor tiles, kitchen benches, baths and hand basins, furniture (e.g. tables).	

Marble is a metamorphic rock consisting of carbonate minerals, most commonly calcite $CaCO_3$ or dolomite $CaMg(CO_3)_2$. It has a crystalline texture, and is generally not foliated (layered).

4.15.2 New Zealand Occurrences of Marble

Marble occurs mainly in Ordovician sedimentary sequences in Northwest Nelson (e.g. Takaka Hill and Pikikiruna Range) and Fiordland (e.g. Caswell, Doubtful and Breaksea sounds) (Figure 4.11). Marble is used as building stone, in industry as a filler and for surface coating, as well as for agricultural lime. The main production has been from quarries on Takaka Hill in Northwest Nelson, particularly the Ngarua quarry operated by Ravensdown that has been producing marble with a calcium carbonate content greater than 98.6%. The deposits of marble are very large, particularly in the Pikikiruna and Arthur ranges and Takaka Hill deposits in Northwest Nelson.

Key References: Thompson (1989); MacFarlan and Barry (1991); Christie et al. (2001a).

4.16 Perlite

4.16.1 International Description

International data for perlite are listed in Table 4.12.

Table 4.12 World mine production, reserves and resources and major uses of perlite.

Perlite	
World mine production in 2023 (USGS 2024)	4.9 Mt
Major world producers (% of total 2023 world production) (USGS 2024)	China (31%), Turkey (29%), Greece (22%), USA (9%), Armenia (4%), Hungary (2%), Iran (2%)
World reserves (USGS 2024)	NA (307 Mt in Greece, the USA, China, Slovakia and Iran)
World resources (USGS 2024)	Large with significant resources in China, Greece, Turkey and the USA
Uses: Construction and manufacturing application using lightweight plasters, concrete and mortar, insulation and ceiling tiles. Other application include filtering beer and uses in foundries, cryogenic insulation and ceramics (as a clay additive).	

4.16.2 New Zealand Occurrences of Perlite

Perlite is an expanded material made from perlitic rhyolite, a volcanic glass that occurs as near-surface layers on rhyolite domes and as perlitic flows of glassy rhyolite lava. The main localities for the surface layer type are in the Rotorua–Taupō area, particularly at Earthquake Flat, and for the lava flow type at Maungaiti Dome (Atiamuri) and on Great Barrier Island. Other localities include Mokohinau Island, Paku Island and Gebbies Pass.

Perlite is used in the domestic market as an inert insulator and filler, as well as for horticultural/ pot-plant mixes.

No annual production statistics have been reported recently, with the last reported in 2012 at 3598 t. Perlite is quarried intermittently at Cashmores Perlite quarry near Atiamuri, southwest of Rotorua, by Industrial Processors Limited, producing about 9000 t of ore per year. The material is processed in Auckland by crushing, screening and heating to 900°C to expand the perlite by 7–20 times.

Inferred resources of perlitic rhyolite are 100 Mt at Awana on Great Barrier Island and 20 Mt at Maungaiti Dome south of Rotorua. Small quantities are also present in the Whitianga–Tairua area and around the Rotorua–Taupō area (Thompson 1989).

Opportunities: The high expansion capacity of perlite from the Taupō Volcanic Zone, which results partly from its young age, makes it particularly good for filtration applications. There is potential for developing this market.

Key References: Thompson et al. (1954); Thompson (1989); MacFarlan and Barry (1991).

4.17 Phosphate

4.17.1 International Description

International data for phosphate are listed in Table 4.13.

Table 4.13 World mine production, reserves and resources and major uses of phosphate.

Phosphate Rock ($(PO_4^{3})^{-}$)		
International	**World mine production in 2023 (USGS 2024)**	220 Mt of phosphate rock containing 63.6 Mt of P_2O_5
	Major world producers (% of total 2023 world production) (USGS 2024)	China (41%), Morocco (16%), USA (9%), Russia (6%), Jordon (5%), Saudi Arabia (4%), Brazil (2%), Egypt (2%), Peru (2%), Tunisia (2%), Australia (1%), Israel (1%, Senegal (1%)
	World reserves (USGS 2024)	74 Bt of phosphate rock
	World resources (USGS 2024)	More than 300 Bt of phosphate rock
	Uses: Mostly in agriculture as a fertiliser. For other applications, phosphate is typically turned into phosphoric acid, which is used in a wide variety of products, such as food, cosmetics, animal feed and electronics.	

4.17.2 New Zealand Occurrences of Phosphate

At Clarendon, south of Dunedin, the 40-m-thick glauconitic Clarendon Sand of Early Miocene age contains phosphate-rich beds near both its base and top. L&M Mining is currently exploring the Clarendon deposit and also other prospects in North Canterbury, South Canterbury and Waitaki (Manhire et al. 2024). Clarendon produced about 140,000 t (25% P_2O_5) during 1920–1924, and a further 53,000 t between 1942 and 1944, for use as a fertiliser. There has been no production since 1944.

Phosphate is used to make superphosphate fertiliser by dissolving phosphate rock in sulfuric acid. New Zealand has two superphosphate manufacturing companies, Ballance Agri-Nutrients and Ravensdown Fertiliser Co-op, which operate a total of four plants across them.

Douglas (1989) estimated that Clarendon has a possible resource of 5 Mt of phosphate rock, averaging 11% P_2O_5. Recent exploration by L&M Mining has indicated that the drilled areas (1/25th of the deposit) contain a resource of 1.6 Mt of phosphate ore, with an average grade of 18% P_2O_5 (Manhire et al. 2024).

Opportunities: New Zealand imports about 680,000 t of phosphate annually, mostly (~60%) from Morocco. These imports could potentially be substituted by local production from onshore phosphate deposits (e.g. Clarendon; Manhire et al. 2024) or Chatham Rise phosphorite nodules (see Section 7.1). There is potential for a combined phosphate and glauconite operation at Clarendon, provided suitable processes and markets can be developed.

Key References: Thompson (1989); MacFarlan and Barry (1991).

4.18 Pounamu (Greenstone)

Pounamu, also known as New Zealand greenstone and New Zealand jade, is the Māori term for nephrite, an amphibole group mineral with a composition within the tremolite ($Ca_2Mg_5Si_8O_{22}(OH)_2$) -actinolite ($Ca_2(Mg,Fe)_5Si_8O_{22}(OH)_2$) series. Pounamu includes a wide variety of rocks; both nephrite and bowenite (a serpentine mineral). Jade is generally either nephrite or jadeite (pyroxene group). For example, Chinese jade is jadeite and therefore not strictly equivalent to the New Zealand nephrite jade.

Pounamu is found in western South Island and formed by the metamorphism of the contact zone between schist and ultramafic rocks or magnesium-rich carbonates (Figure 4.12).

Most pounamu has been recovered as river boulders from the West Coast, especially from the Arahura, Taramakau and Hokitika rivers and their tributaries, although some has also been recovered from glacial boulders (e.g. Cascade Plateau). However, in several localities, nephrite has been located in outcrop within the Pounamu Ultramafics belt.

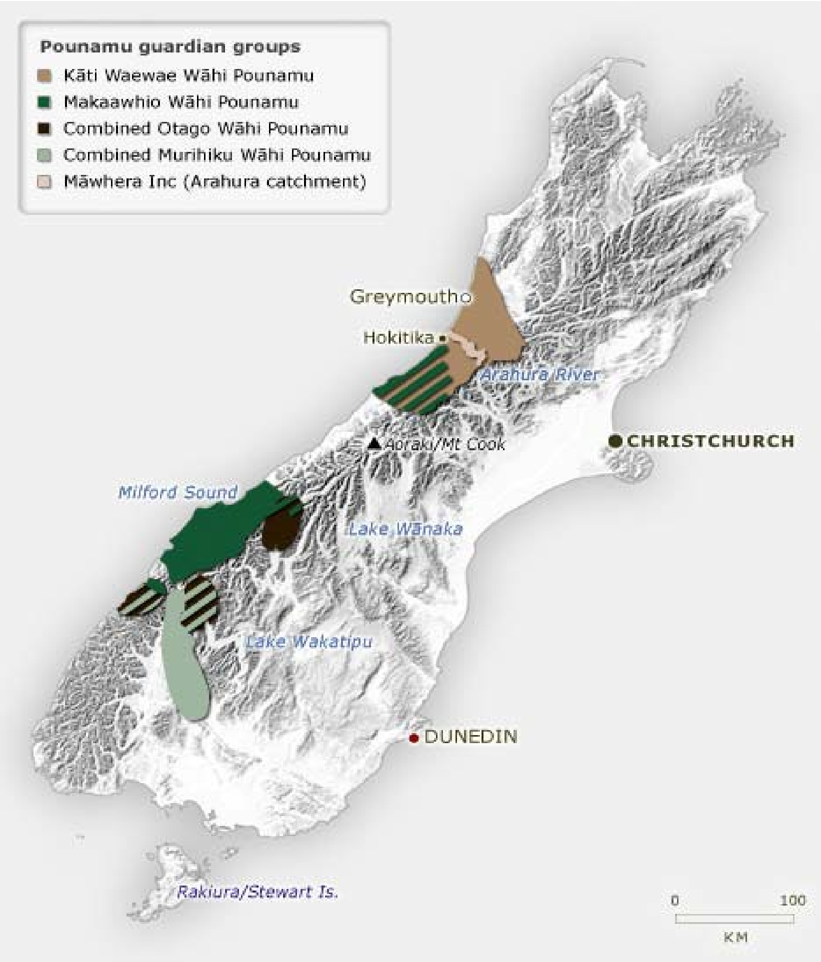

Figure 4.12 Pounamu resources of New Zealand, most of which are owned and managed by Te Rūnanga o Ngāi Tahu. The resource is managed by local rūnanga or kaitiaki (guardians) who have authority over their respective fields, depending on historical interests (Source: Te Rūnanga o Ngāi Tahu, Pounamu Management Plan).

Pounamu has been used by Māori for jewellery, tools (e.g. adzes, chisels gouges and knives for carving and cutting wood, fish hooks) and weapons (e.g. clubs and points for spears) and has strong cultural and spiritual significance. Modern use is mainly for jewellery and ornaments. Ownership of pounamu was vested with Ngāi Tahu in September 1997 as part of their Tiriti o Waitangi claim.

Studies have been carried out to assess pounamu resources (Cox et al. 2005; Cox and Nibourel 2015) and to fingerprint their source (Adams et al. 2007; Campbell et al. 2008). Resource estimates made to date are confidential. Because pounamu has significant spiritual value to Māori, the value of the resources may be far greater to the owners, Ngāi Tahu, than can be estimated as a mineable mineral commodity.

Key References: Beck (1984); Beck and Mason (2002); Adams et al. (2005, 2007); Cox et al. (2005); Cox and Nibourel (2015); Campbell et al. (2008).

4.19 Potassium (K) – Potash (KCl, K_2O)

4.19.1 International Description

International data for potash are listed in Table 4.14.

Table 4.14 World production, reserves and resources and major uses of potash.

Potash (KCl, K_2O or $K_2Mg_2O_{12}S_3$)		
International	**Terminology and composition:** Potash denotes a variety of mined and manufactured salts that contain the element potassium in water-soluble form. In agriculture, the term ‘potash’ refers to potassic fertilisers, which are potassium chloride (KCl), sulfate of potash and potassium magnesium sulfate (SOPM) or langbeinite. MOP (muriate of potash) is an agriculturally acceptable mix of KCl (95% pure or greater) and sodium chloride for fertiliser use.	
	World mine production in 2023 (USGS 2024)	970,000 t (K_2O equivalent)
	Major world producers (% of total 2023 world production) (USGS 2024)	Canada (33%), Russia (17%), China (15%), Belarus (10%), Germany (7%), Israel (6%), Jordon (0.5%), Laos (0.5%)
	World reserves (USGS 2024)	>11 Bt of recoverable ore and 3.6 Bt of K_2O equivalent
	World resources (USGS 2024)	7 Bt
	Uses: The main use is for fertiliser.	

4.19.2 New Zealand Occurrences of Potash

Exploration for minerals that might be used to make potash has included glauconite (see Section 4.12) and feldspar. NZ Potash inspected a regolith of feldspar, mostly orthoclase, in weathered Separation Point Granite southwest of Motueka and east of the Arthur Range (Bridson 2015c). This material had been previously trialled as a source of feldspar for ceramics, but the high iron content made it unsatisfactory. Williams (1974) noted that the feldspar assayed 11–12% K_2O. The Ngakuru zeolitic tuff deposits contain 10–25% K-feldspar and average 4% K_2O (Brathwaite 2003)

New Zealand imports about 25,000 t of potash annually, which is mostly potassium chloride from Canada, representing about 65% of potash imports.

Opportunities: East Cape glauconite is a possible substitute potassium fertiliser.

Key References: Williams (1974); Douglas (1989); MacFarlan and Barry (1991).

4.20 Pumice

4.20.1 International Description

International data for pumice are listed in Table 4.15.

Table 4.15 World production, reserves and resources and major uses of pumice.

Pumice		
International	**World mine production in 2023 (USGS 2024)**	18 Mt of pumice and pumicite
	Major world producers (% of total 2023 world production) (USGS 2024)	Turkey (48%), Uganda (8%), Greece (6%), Saudi Arabia (5%), Algeria (5%), Ecuador (4%), Chile (4%), Ethiopia (3%), Guatemala (3%)
	World reserves (USGS 2024)	Large
	World resources (USGS 2024)	Large
	Uses: Pumice is used an abrasive, especially in polishes, pencil erasers and the production of stone-washed jeans. It is also used in water filtration, chemical spill containment, cement manufacturing, horticulture and the pet industry.	

Pumice is a pyroclastic volcanic rock that was molten when erupted but cooled quickly, with the dissolved gasses released causing a froth that consolidated into a highly vesicular, porous and rough-textured rock of volcanic glass.

4.20.2 New Zealand Occurrences of Pumice

Primary pumice deposits are found in the Taupō-Bay of Plenty area and include Haparangi Rhyolitic Pumice and Waitahanui, Mihi and Rotoiti breccias. Secondary deposits consist of alluvial and slope-wash deposits found near Hamilton and on the Hauraki Plains, as well as alluvial pumice deposits along the Waikato and Wanganui rivers.

Pumice is used as fill in road construction, for sand in concrete block manufacture, in wallboard manufacture, for foundations and drainage ditches, for horticultural soil mixes and for stone-washing of denim clothing.

Recent annual production statistics are withheld, with the last reported in 2020 at 37,034 t (233,888 t in 2018) mainly produced from the Bay of Plenty area. The main recent producers are the Atiamuri sand and pumice quarry operated by Industrial Processors, and Bakers Pumice located in Awakeri, near Whakatāne, which is closing down. Other operations include Okareka pumice (Moore TW) at Okareka, Taupō Pumice pit (Jaks Haulage) near Rotokawa, and Tauhara pumice pit (Robert Glenn) (Inside Resources[2]).

Large resources are available in the Taupō – Bay of Plenty area, along the Waikato River valley, on the Hauraki Plains, along the Wanganui River at Taumarunui and at Wanganui.

Key References: NZGS (1970b); MacFarlan and Barry (1991).

---

[2] https://www.insideresources.co.nz/

4.21 Salt

4.21.1 International Description

International data for salt are listed in Table 4.16.

Table 4.16 World mine production, reserves and resources and major uses of salt.

Salt (NaCl)		
International	**World mine production in 2023 (USGS 2024)**	270 Mt
	Major world producers (% of total 2023 world production) (USGS 2024)	China (20%), USA (16%), India (11%), Germany (6%), Australia (5%), Canada (4%), Chile (3%), Russia (3%), Mexico (3%), Turkey (3%), the Netherlands (2%)
	World reserves (USGS 2024)	Large
	World resources (USGS 2024)	Large
	Uses: As a feedstock for the production of chemicals, plastics and paper pulp, water conditioning, de-icing highways, agricultural uses and as edible salt.	

4.21.2 New Zealand Occurrences of Salt

There are no known natural-bedded salt deposits in New Zealand. Salt is produced by Dominion Salt Limited at Grassmere, south of Blenheim, by solar evaporation of sea water. The evaporation ponds are constructed in a low-lying area close to the sea. They are separated into paddocks with gates to admit and retain sea water. Low rainfall, high sunshine hours and adequate wind assist in the evaporation of the sea water. The final processing includes washing, crushing, drying and screening before packing. The company supplies raw solar- and vacuum-dried salt to the domestic market for use in chlorine manufacture, edible salt, water treatment, tanning, dairy and agricultural usage and commercial and industrial applications, such as pharmaceuticals.

Recent annual production statistics are withheld, last reported in 2013 at 52,343 t. Annual production is probably about 60,000 t of salt.

Potential import substitution: New Zealand imports about 75,000 t annually, mainly from Australia, the Bahamas and Netherlands Antilles. It may be possible to substitute some of the imported salt by increased local production at Lake Grassmere.

4.22 Serpentinite

4.22.1 International Description

International data for serpentinite are listed in Table 4.17.

Table 4.17 World production, reserves and resources and major uses of serpentinite.

Serpentinite [$(Mg, Fe)_3Si_2O_5(OH)_4$]		
International	**Major Minerals:** Antigorite [$(Mg, Fe)_3Si_2O_5(OH)_4$], lizardite [$Mg_3(Si_2O_5)(OH)_4$], chrysotile [$Mg_3(Si_2O_5)(OH)_4$]	
	Main occurrences	Australia, Armenia, Italy, Russia, the USA, Canada, Paraguay, New Zealand, and Brazil
	World mine production in 2022	>3 Mt
	Major world producers 2002	China, Brazil
	World resources	200 Mt
	Uses: Decorative stone in building, particularly counter- and table-tops, flooring and wall cladding; concrete aggregate; fertiliser; refractory applications such as linings for furnaces and kilns; in metallurgy for addition of magnesium and as a flux in steelmaking; medicines; and ornamental purposes such as jewellery and carvings; decorative stones in gardens and landscaping.	

Serpentinite is a metamorphic rock composed predominantly of one or more serpentine group minerals formed by near to complete serpentinisation of mafic to ultramafic rocks.

4.22.2 New Zealand Occurrences of Serpentinite

The serpentinite used in the New Zealand industry has been mined from deposits formed in four main geological settings:

1. As part of the ultramafic rock sequence of the Dun Mountain Ophiolite Belt (Permian) in the South Island. The main deposits are on D'Urville Island, from Whangamoa to Red Hills in east Nelson and at Mossburn in Southland.
2. Layered bodies of serpentinised gabbro and peridotite of Permian age at Greenhills in Southland.
3. Lenses of metamorphosed ultramafic rock (Pounamu Ultramafics) occurring within medium-grade metamorphic rocks of the Alpine Schist in Westland.
4. Diapiric serpentine bodies, up to 1 km in length and 60 m in width, emplaced vertically along a fault separating rocks of Mesozoic age from those of Oligocene age at Piopio in Waikato. Serpentine bodies in the Silverdale-Brynderwyn area have likely been re-deposited within a large landslide rather than intruded along fault planes.

The main use is as an additive to superphosphate fertiliser to supply magnesium and assist in the free-running properties of fertiliser required for aerial topdressing. The development of granulated, free-running superphosphate has reduced this market.

Some serpentine is also used as ornamental stone.

Some former quarries closed for health reasons because their serpentine was found to contain asbestos fibres.

Recent annual production statistics have been withheld, with the last reported in 2013 at 52,343 t. The production is from three quarries: Aria, 10 km south of Piopio, near Te Kūiti (Part 1, Figure 9.1), Mossburn (E44/e11; Reed 1950; Coleman 1966), at Black Ridge in Southland and Greenhills, near Bluff in Southland. The Aria quarry is operated by Rorisons RMD and in the past has produced between 40,000 and 50,000 t of serpentine annually (Inside Resources). The Mossburn quarry was active from the 1940s but closed in 1984 after the closure of the Mossburn to Lumsden railway line. Southland Serpentine re-opened the quarry in 2006. The product is distributed from a processing plant in Lumsden. At Greenhills, layered bodies of serpentinised gabbro and peridotite are present in the Bluff Complex.

Although most of the serpentinite bodies around Silverdale-Brynderwyn and Piopio have been largely worked out, there are unmeasured but large quantities still present at Whangamoa and Lee River in Nelson, and at Mossburn in Southland. A resource of 18 Mt is present at Greenhills (Richards 1978).

Key References: Coleman (1966); Williams (1974); MacFarlan and Barry (1991).

4.23 Silica

4.23.1 International Description

International data for silica are listed in Table 4.18.

Table 4.18 Element properties, major minerals, world production, reserves and resources and major uses of silicon/silica.

Silicon (Si) and Silica (SiO_2)		
International	**Ore Minerals:** Quartz and other forms of (SiO_2) such as tridymite, cristobalite, coesite, stishovite, lechatelierite and chalcedony	
	World production	2,786,994 t (average 2015–2019)
	Major world producers (% of average total 2015–2019)	China (79%), Brazil (5%), Norway (5%)
	Uses: Chemicals, aluminium alloys and solar panels. It is a key constituent of most solar photovoltaic cells. Widely used in semi-conductors for numerous applications.	

4.23.2 New Zealand Occurrences of Silica

4.23.2.1 Quartz-Rich Sand (Silica Sand) in Dune, Beach and Shallow Offshore Marine Environments

Quartz-rich (silica) sand of Quaternary age forms dune, beach and shallow offshore marine sand deposits along the present-day coastline. The main localities are all in Northland, at Parengarenga Harbour on the east coast and around Kaipara Harbour on the west coast (Part 1, Figure 9.1). Previously, about 40,000 tpa of sand were dredged from Parengarenga Harbour and processed into glass at a plant in Auckland. There is about 120 Mt at the northern Kokota Spit and regional resource of about 1500 Mt (Williams 1974).

On the Kaipara Harbour, the Glorit silica sand quarry is operated by James Hardie. The extracted sand is transported to a plant in Penrose, Auckland, to make fibre-cement building materials, including exterior claddings, internal linings and fire-resistant and acoustic wall panels. The quarry is near the end of its life, so operations are moving to McLachlan Road, Kaukapakapa, about 16 km south of Glorit (Inside Resources). Tapora Sands quarry in Tapora is operated by ISL (Industrial Sands Ltd) and the high-purity silica sand is processed at a plant in Glorit for use in foundry casting and mould making. Other applications include specialised flooring, resin and grout fillers, glass manufacturing and anti-slip surfaces. There is possibly silica sand resources of 10 Mt in the Kaipara Harbour area (Williams 1974).

4.23.2.2 Quartz-Rich Sand Concentrated on Erosional Land Surfaces and Associated with Coal Measures

Quartz-rich (silica) sands are concentrated on some erosional land surfaces associated with coal measures in the South Island. The main occurrences are at Mt Somers in Canterbury and at Charleston in Westland. There are other deposits in East Otago and Southland.

At Mt Somers, resources are estimated at 165,000 t of sand, containing more than 99% SiO_2, and other deposits are present in the same area. The several million tonnes of sand at Charleston contain mica (10%) and feldspar (30%), which make it unsuitable for glassware, but it has been used in cement-making. Silica sand (glass grade) at Hyde has resources estimated at a minimum of 134,000 t. The resources of mica-rich sands at Fairfield (Dunedin), in the Ida valley are probably large.

4.23.2.3 Quartzite Formed by Metamorphism of Quartz Sandstones of Paleozoic Age

Quartzites containing 90–93.7% SiO_2 occur in eastern Northland, formed by metamorphism of quartz sandstones within greywacke sequences. Deposits associated with schist at Aorere have a resource of about 1 Mt of quartzite (97–97.6% SiO_2) of ferrosilicon quality (Riley 1972). At Reefton, there is a maximum of 600,000 t of poor-quality quartzite associated with shist and containing 85–96% SiO_2 (Young 1964; Williams 1974).

4.23.2.4 Quartz Gravel Associated with Coal Measures

Quartz gravels in Southland (Part 1, Figure 9.1) are widespread and have potential for use in the production of ferrosilicon or silicon metal (Williams 1974; Strong et al. 2016). Preliminary tests conducted on the raw silica from Pebbly Hills by a ferrosilicon producer have indicated the suitability of this material for that purpose. The availability of abundant low ash coal and hydro-electricity are other factors favourable to a ferrosilicon industry in Southland. Material from Pebbly Hills is presently being investigated by Silicon Metal Industries (NZ) Ltd as a raw material for silicon metal production. Similar deposits occur elsewhere in Otago and northern Southland.

The quartz gravels around Pebbly Hills-Mabel Bush are inferred to contain more than 350 Mt, averaging 98% SiO_2 (MacFarlan and Barry 1991). Elsewhere the quantities are smaller – Waimumu (170+ Mt of 97.9% SiO_2), near Dunedin (5+ Mt), Central Otago (70 Mt of 97.7% SiO_2) and North Otago (small, 97.4% SiO_2).

4.23.2.5 Amorphous Silica and Chalcedonic Quartz Deposited in Hot Springs and Epithermal Quartz Veins

Amorphous silica is deposited by hot springs as silica sinter and by hydrothermal alteration of nearby rocks, mostly rhyolitic, in volcanically active areas. In the Taupō Volcanic Zone, acid sulfate alteration in the near-surface parts of active geothermal systems has resulted in the conversion of all minerals, except primary quartz, to an assemblage of amorphous silica + cristobolite ± native sulfur, alunite, cinnabar and barite (Roberts 1997). The end result is a low-density, white, porous rock composed primarily of amorphous silica and residual quartz phenocrysts. Three amorphous silica deposits have been explored recently, Tikitere and Taheke, near Rotorua, and Lake Rotokawa, near Taupō (Part 1, Figure 9.1). The Tikitere amorphous silica operation is owned by Microsilica New Zealand, a subsidiary of Golden Bay Cement. The plant currently produces about 3000 tpa of silica from two pits – a high grade and a low grade (Inside Resources). The material is processed to make products for a pozzolanic cement additive to produce high-quality, strong and durable concrete, sprayed tunnel linings, mortars and grouts.

The resource at Taheke is of the order of several million tonnes, and investigations in the 1990s outlined a resource of 4.5 Mt at Lake Rotokawa near Taupō (Roberts 1997).

Recent annual production statistics for silica are withheld. Last reported production statistics were:

- **Amorphous silica:** Last reported in 2016 at 29,531 t.
- **Silica sand:** Last reported in 2019 at 34,320 t (113,231 t in 2010).

Geo40 is currently extracting small quantities of amorphous silica from geothermal fluids at the Ohaaki geothermal field.

Key References: Williams (1974); Thompson (1989); MacFarlan and Barry (1991); Thompson et al. (1995); Roberts (1997); (Strong et al. 2016).

4.24 Sulfur (S)

4.24.1 International Description

International data for sulfur are listed in Table 4.19.

Table 4.19 Element properties, major minerals, world production, reserves and resources and major uses of sulfur.

Sulfur (S)		
International	**Ore Minerals:** Native sulfur (S) and sulfide minerals such as pyrite (FeS_2)	
	World mine production in 2023 (USGS 2024)	82 Mt
	Major world producers (% of total 2023 world production) (USGS 2024)	China (23%), the USA (10%), Saudi Arabia (10%), Russia (9%), United Arab Emirates (7%), Canada (6%), Kazakhstan (5%), India (4%), Japan (4%)
	World reserves (USGS 2024)	N/A
	World resources (USGS 2024)	Large (many billion tonnes)
	Uses: Worldwide, more than 80% is used for making sulfuric acid, mostly as a precursor to other chemicals and applications. Sulfur is used as a fertiliser, in car batteries, oil refining, water processing, mineral extraction, fungicides and pesticides, pharmaceuticals, rubber vulcanisation, bleaching paper and gunpowder.	

4.24.2 New Zealand Occurrences of Sulfur

Sulfur occurs mainly as native sulfur in volcanic areas and as the sulfide mineral pyrite (FeS_2). Native sulfur is associated with present-day and fossil geothermal areas in Northland at Ngawha and in the Bay of Plenty and Rotorua–Taupō areas, mainly on Whakaari / White Island, at Tikitere and Okere Springs near Rotorua, and at Lake Rotokawa near Taupō (Table 4.20). On Whakaari / White Island, sulfur is being deposited around active fumaroles and with gypsum in lake beds within the active crater.

Lake Rotokawa, 12 km northeast of Taupō, offers the best potential for sulfur mining, although the location of this resource within an active geothermal system poses some mining problems. Two types of deposits are present – lacustrine sulfur present within a buried lake-bed and surface mineralisation where crystalline sulfur impregnates a brecciated pumice horizon (Sinclair 1989). In the lacustrine type, the sulfur occurs in a colloidal state disseminated throughout the lake mud. The mineralisation is buried some 25–75 m below the present land surface and extends under Lake Rotokawa.

Pyrite is present in many types of metallic mineral deposits but only two have been investigated as a potential source of sulfur in New Zealand – one in the Kauaeranga Valley near Thames and the other at Copperstain Creek near Takaka. In the Kauaeranga Valley, high concentrations of pyrite are associated with hydrothermally altered andesitic lava and breccia and silty sediments of Miocene age. At Copperstain Creek, pyrite is present in a skarn deposit adjacent to an Early Cretaceous age granite that has intruded marble and biotite schist.

Table 4.20 Sulfur occurrences. Minerals: cp = chalcopyrite; py = pyrite.

Occurrence	**MM** [1]	**GERM** [2]	**Production (t)**	**Deposit Form**	**Minerals Major (Minor)**	**Host Rocks**	**Genesis**
Whakaari / White Island	I85	W14/e1	10,000 S	Stratiform beds and vent encrustations	Sulfur, gypsum	Andesite and lake beds	Fumarolic sublimation
Whale Island	I86	W15/e101	-	Encrustations in vents	Sulfur	Sinter and andesite	Fumarolic sublimation
Taheke	I87	U15/e104	2147 S	Encrustations in sinter	Sulfur	Sinter and ignimbrite	Fumarolic sublimation
Te Tarata	I88	U15/e106	5000 S	Massive encrustations	Sulfur	Pumice	Fumarolic sublimation
Postmaster Bath	I89	-	4800 S	Surface encrustations	Sulfur	Lake sediments	Fumarolic sublimation
Rotokawa	I95	U17/e104	16,141 S	Stratiform and encrustations	Sulfur, py, metastibnite	Lacustrine silt, pumiceous tuff	Hydrothermal – hot spring
Ahuahu Creek, Kaitake Range	I96	P19/e28	-	Chalcedonic quartz-pyrite veins	py, sulfur, cp, barite	Andesite, silicified tuff	Hydrothermal – hot spring

[1] MM = Metallogenic map code (Brathwaite and Pirajno 1993).

[2] GERM = Geological Resource Map code.

Sulfur is used to make sulfuric acid for the manufacture of superphosphate fertiliser. Sulfur has been mined mainly from Whakaari / White Island, Tikitere, Lake Rotorua and Lake Rotokawa, predominantly for use in making superphosphate fertilisers. There is currently no mining of sulfur in New Zealand.

At Lake Rotokawa, drilling has outlined a resource of 57 Mt of lake sediments containing an estimated 4.9 Mt of elemental sulfur (MacFarlan and Barry 1991). Although the overall grade for the lacustrine mineralisation is estimated at 10% sulfur, there are several layers within the bed where it is concentrated to 60–80% sulfur. The surface deposits are much smaller, with resources of approximately 100,000 t of pumice breccia containing between 10% and 15% sulfur (10,000–15,000 t of sulfur). These surface deposits were intermittently mined up to 1991 but are now considered too small for further commercial development.

Pyrite sulfur in the Kauaeranga Valley contains about 15–20 Mt of mineralised rock, averaging 7–8% sulfur (Kear 1957). Drilling at Copperstain Creek found resources of 10.5 Mt of 7.5% sulfur, with associated copper and molybdenum (Williams 1974). It is highly unlikely that pyrite would be mined for producing sulfur.

Key References: Williams (1974); MacFarlan and Barry (1991); Thompson et al. (1995).

4.25 Talc-Magnesite

See Magnesium (Section 3.11).

4.26 Wollastonite ($CaSiO_3$)

4.26.1 International Description

International data for Wollastonite are listed in Table 4.21.

Table 4.21 World production, reserves and resources and major uses of wollastonite.

Wollastonite ($CaSiO_3$)		
International	**World mine production in 2023 (USGS 2024)**	1.1 Mt
	Major world producers (% of total 2023 world production) (USGS 2024)	China (82%), India (9%), Mexico (7%), Canada
	World reserves (USGS 2024)	More than 100 Mt
	World resources (USGS 2024)	New Zealand. Large resources have been identified in China, Finland, India, Mexico and the USA.
	Uses: Wollastonite is widely used as a flux in the casting of steel and in the production of paints and coatings. In paints, wollastonite provides reinforcement, hardening and low oil absorption, as well as other benefits. In textured coatings, such as stucco, wollastonite provides crack resistance, reinforcement and high brightness. It is also used in the manufacture of adhesives, joint compounds, refractories and rubber.	

4.26.2 New Zealand Occurrences of Wollastonite

In the Holyoake Valley, west of Motueka, a reef-like body containing over 70% wollastonite occurs where the contact between Paleozoic age marble and schist has been partly intruded by the Cretaceous Separation Point batholith. About 500 t of wollastonite were produced in the 1960s and used in the manufacture of ceramics. Non-JORC compliant resources are 17,000 t proven and about 36,000 t indicated (Brathwaite et al. 1976).

Key References: Williams (1974); (Brathwaite et al. 1976); MacFarlan and Barry (1991).

4.27 Zeolite

4.27.1 International Description

International data for zeolite are listed in Table 4.22.

Table 4.22 Major minerals, world production, reserves and resources and major uses of zeolite.

Zeolite (Natural) $[(Ca,K,Na)_2Al_2Si_2O_8\ nH_2O]$		
International	**Major Minerals:** Analcime, chabazite, clinoptillite, mordenite, natrolite, heulandite, phillipsite and stillbite	
	World mine production in 2023 (USGS 2024)	1.1 Mt
	Major world producers (% of total 2023 world production) (USGS 2024)	Slovakia (20%), China (18%), South Korea (12%), New Zealand (9%), Indonesia (9%), USA (8%), Cuba (7%), Turkey (6%), Russia (3%), Hungary (3%)
	World reserves (USGS 2024)	N/A (although two companies in the USA reported combined reserves of 80 Mt in 2022)
	World resources (USGS 2024)	N/A
	Uses: Used as catalysts and sorbents, as molecular sieves, in ion-exchange beds and in water purification and softening (e.g. the world's largest use is in laundry detergents as a water softener to remove Ca^{2+} and Mg^{2+} ions). Other uses are in building materials as an additive in asphalt and a pozzolan in Portland cement, as pet litter and in agriculture as a soil treatment.	

4.27.2 New Zealand Occurrences of Zeolites

Zeolites are typically formed by low-temperature hydrothermal (<200°C) alteration and metamorphism in tuffs and volcanic sandstones, as well as volcanic-rich lake and deep-sea sediments. The main occurrences (Figure 4.13) are in:

1. Weakly metamorphosed marine tuffs and tuffaceous sandstones of Triassic age in Southland.
2. Marine tuffs of Miocene age in Northland and Auckland.
3. Hydrothermally altered tuffs and lake sediments of Quaternary age in the Taupō Volcanic Zone.

The Taupō Volcanic Zone hosts a number of zeolite deposits formed by hydrothermal alteration of suitable precursors such as vitric tuffs (Roberts 1997; Brathwaite 2003; Brathwaite et al. 2006; Brathwaite and Rae 2021). A large occurrence is at Ohakuri, where glass within the Ohakuri ignimbrite and younger pyroclastics has been hydrothermally altered to the zeolites mordenite and clinoptilolite, as well as smectite and opal.

The only deposits worked commercially were discovered in 1992 at Ngakuru, 20 km south of Rotorua. Pacific Blue Minerals mines zeolite from three deposits in the area and a further five large deposits have been identified. At Ngakuru, hydrothermally altered tuffaceous lacustrine sediments are exposed intermittently along several faults within a 6 x 3 km area and have a thickness in excess of 40 m. The alteration has produced a zeolite + smectite + cristobolite + amorphous silica assemblage, locally containing between 25 and 90% zeolites, mainly clinoptilolite and mordenite. When compared with zeolite deposits mined in other parts of the world, those from Ngakuru are young in geological terms (250,000 years) and have exceptional properties of adsorption. Current uses of zeolite are: (1) as adsorbents for soaking up oil/ chemical spills, as cat and animal litters and as a stockfeed additive; (2) as water softening, waste and potable water treatment, sports turf and potting mix amendment; and (3) as odour adsorbents and cosmetic additives. Blue Pacific Minerals has produced a modified zeolite (Aqual-P) that is has been used at Lake Okaro near Rotorua to absorb phosphate and nitrogen nutrients and control the growth of algal blooms that affect aquatic life.

Recent annual production statistics are withheld, with the last reported in 2011 at 3523 t (21,750 t in 2009), all from Ngakuru.

Other occurrences of zeolite in New Zealand are known from Southland (Coombs et al. 1959), and in Northland and Auckland (Sameshima 1978), but all are small.

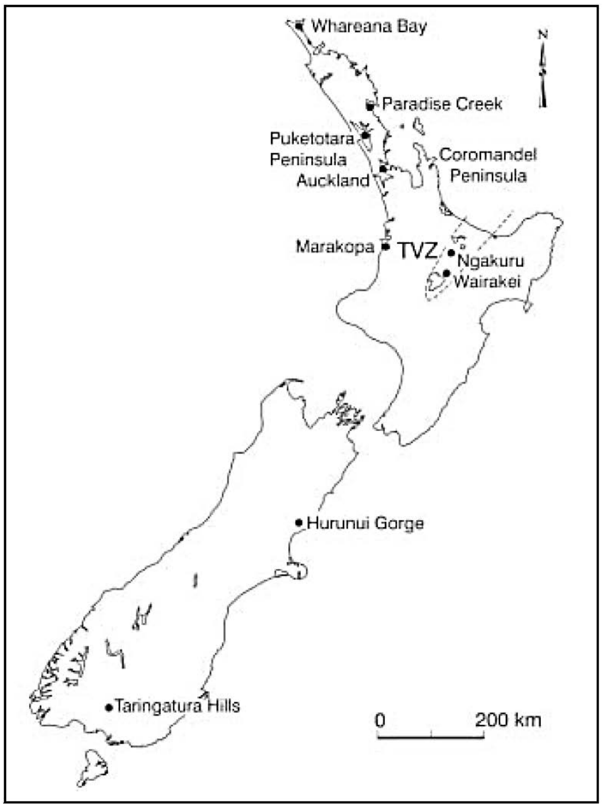

Figure 4.13 Location of zeolite deposits in New Zealand (after Christie et al. [2002]).

Key References: Christie et al. (2002); Brathwaite (2003, 2017); Brathwaite and Henderson (2016); Brathwaite and Rae (2021).

5.0 COAL

5.1 Coal Introduction

This section briefly reviews coal in New Zealand in terms of its occurrence, history, production, challenges and opportunities. For additional information and more detail, the reader is referred to descriptions by Barry et al. (1994), Edbrooke (1999) and Sherwood (2019).

5.2 Coal Occurrence

The economically significant coals were formed between 30 and 70 Ma in the Late Cretaceous, Eocene–Oligocene and Miocene as part of Cretaceous–Cenozoic sedimentary sequences. Their age contrasts with most of the world's coals, which were typically formed between 300 to 350 Ma. Also, many of New Zealand's coalfields are geologically and structurally complex.

In all, there are over 50 separate coalfields (Figure 5.1; Part 1, Figure 10.1). Bituminous coal is found almost entirely in Westland, sub-bituminous coal is found mainly in Waikato and lignite is located mainly in Southland and Central Otago.

5.2.1 North Island Coal

North Island coalfields are in Northland, Waikato and northern Taranaki (Figure 5.1a). Most known areas of sub-bituminous coal in Northland have been worked out, and the last mine closed in 1955.

Thirteen coalfields, extending from Drury (30 km south of Auckland) to Mangapehi (20 km south of Te Kūiti), are geologically grouped as Waikato coalfields. Much of their coal resources are in seams that are too deep to mine. In 2022, opencast mines at Maramarua and Rotowaro were the only Waikato mines still working.

Waikato coals are all sub-bituminous, deposited in the Eocene and Oligocene periods. Seams in the north of the region generally have low to medium ash and low sulfur contents, while seams in the south have medium to high ash and sulfur contents. The main seam is typically 3–10 m thick but reaches 20 m or more in parts of the Huntly and Waikare coalfields.

5.2.2 West Coast

The South Island's West Coast region (Figure 5.1b) contains New Zealand's only bituminous coals. Some have unusual properties that are in demand in international coal markets. There are 13 coalfields of various sizes between Greymouth and Seddonville (40 km north of Westport). The Buller, Greymouth, Inangahua and Reefton coalfields are the most economically important.

There are large quantities of in-ground coal remaining in the region, but most of the easily won coal has been mined. Over three-quarters of resources are in the Greymouth coalfield (mostly underground) and Buller coalfield (mostly opencast), but how much is mineable depends on coal prices, land access and a resumption of underground mining. After an explosion at the Pike River mine in 2010 that killed 29 men, the government decided that there would be no further mining in the area, which has been added to the Paparoa National Park.

There are two main types of coal measures on the West Coast: late Cretaceous to earliest Tertiary Paparoa coal measures and Eocene Brunner coal measures. Both Paparoa and Brunner coalfields contain seams up to 20 m thick. Paparoa coals are characterised by low ash and sulfur contents. Brunner coals have similar properties but with varying sulfur contents.

West Coast coals are almost all bituminous, with some exceptions, such as sub-bituminous Brunner (Echo, New Creek) and Rotokohu Coal Measures (Giles Creek) and a small deposit of anthracite at Fox River. Their properties see them valued as blending coals on world markets.

5.2.3 Otago and Southland

The bulk of New Zealand's coal resources are lignite (brown coal) in the south of the South Island. Over 7 Bt of mineable lignite resources have been proven in Otago and Southland, enough to provide a significant proportion of New Zealand's energy needs for a long period if needed.

Otago coalfields include very large lignite deposits in Central Otago, the Kaitangata coalfield south of Dunedin and several smaller coalfields (Figure 5.1b). Central Otago lignites are in seams up to 90 m thick and typically have 40–50% in-ground moisture and low to medium ash and low sulfur contents.

The eastern Southland lignite fields are comparable to other large brown coal deposits in the world and are, by far, New Zealand's largest known fossil fuel energy resource. These form extensive multiple seams up to 18 m thick and typically have 40–65% in-ground moisture and low to medium ash and low sulfur contents.

The Ōhai coalfield in central Southland has seams up to 23 m thick containing sub-bituminous and bituminous coals, generally with low ash and sulfur contents.

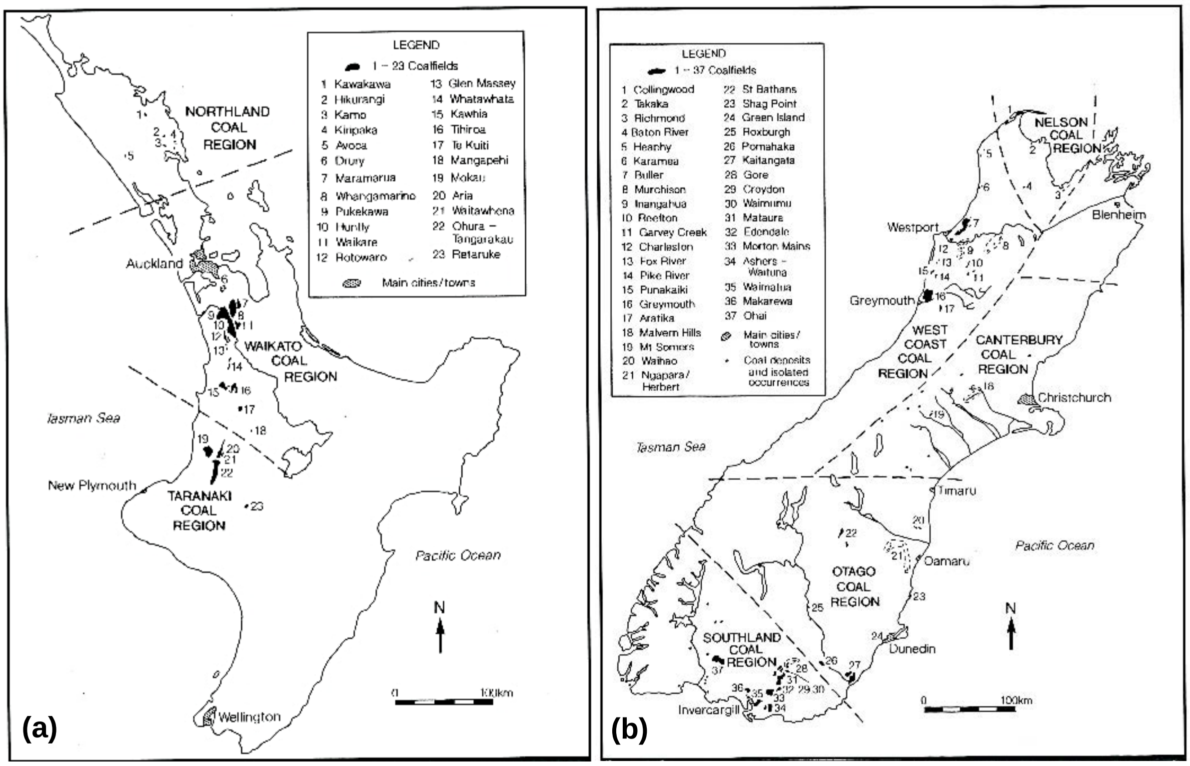

Figure 5.1 Coal regions and coalfields of the (a) North Island and (b) South Island, including small coal deposits for the latter (after Barry et al. [1994]).

5.3 History

Coal was discovered first in the South Island in the 1840s, and the first small coal mine was opened at Saddle Hill near Dunedin in 1849. North Island coal was not found until the 1860s.

The gold rushes of the 1860s resulted in rapid population booms that created much of the demand for coal, especially in Otago and the West Coast. For many years, coal was the main source of energy, but production fell from the 1960s once coal was no longer used by the railways and shipping, and most electricity was produced from hydro, natural gas and geothermal power stations. By the 1970s, most coal was extracted from opencast mines, being used for the Glenbrook steel mill, for Huntly power station and for dairy factories; high-quality coking coal from the West Coast was, and continues to be, exported.

About 1400 coal mines have operated in New Zealand, but most have been small in scale and run by private cooperatives. Sherwood (2019) noted that the key changes over the last 150 years of coal mining have been a steady reduction in the number of mines, increased mechanisation, the progressive displacement of underground mining by open-casting after World War II and the adoption of completely different standards of environmental management in modern mines.

The Government became a major coal miner following the establishment of State Coal Mines in 1901, and, by 1950, it was the largest producer of coal – at its operational peak in 1952, it operated 28 underground and 13 opencast mines. State Coal Mines was absorbed into the Mines Department in 1952 and in 1987 made into a state-owned enterprise, Coal Corporation of New Zealand or Coalcorp, which was rebranded as Solid Energy in 1996. Solid Energy got into financial trouble in the early to mid-2010s and its assets were closed or sold off to private companies in 2017, mostly to Bathurst Resources, which is now the major coal producer in New Zealand.

5.4 Production

New Zealand’s coal production can be divided into three areas:

1. In the North Island, coal production is centred in the Waikato region where large coalfields like Maramarua and Rotowaro produce sub-bituminous coal.
2. Coal extracted on the West Coast of the South Island is mostly bituminous coal, along with some sub-bituminous. The bituminous coal is mostly exported for steelmaking.
3. Otago and Southland production is sub-bituminous coal and also lower-energy lignite in Southland.

Fourteen mines were operating in New Zealand at the end of 2022 compared to 18 at the end of 2020 (Table 5.1). Production for 2023 is listed in Table 5.2 below; production trends between 1992 and 2023 are shown in Part 1 (Figure 4.4).

Table 5.1 Operating coal mines at the end of 2022 (Source: MBIE). B – Bituminous; SB – Sub-bituminous; L – Lignite.

Coalfield	Mine	Operator	Rank	Production 2022 (tonnes)
Waikato				
Maramarua	Kopuku	BT Mining	SB	204,790
Rotowaro	Awaroa	BT Mining	SB	406,848
West Coast				
Buller	Stockton	BT Mining	B	938,821
Buller	Escarpment [1]	Buller Coal	B	-
Reefton	Reefton Operations	Moore Mining	SB	56,210
Reefton	Boatmans [2]	Boatmans Coal	SB	-
Garvey Creek	Echo	Francis Mining	B	105,095
Inangahua	Giles Creek	Birchfield Coal	SB	202,219
Inangahua	Berlins Creek	Heaphy Mining	SB	-
Inangahua	New Creek	New Creek Mining	SB	0
Greymouth	Strongman	Birchfield Coal	B	54,810
Greymouth	Rajah	Roa Mining	B	129,866
Charleston	Charleston	Charleston Coal	SB	105
Otago				
Kaitangata	Castle Hill [2]	Kai Point Coal	SB	-
Southland				
Ohai	Takitimu [3]	Bathurst Coal	SB	221,982
Waimumu	New Vale [2]	New Vale and Ohai Coal	L	-
Ashers	Waituna [2]	Sinclair Contracting	L	-

[1] Production obtained from stockpiles or from former stockpiles as part of rehabilitation.

[2] Private coal operation.

[3] Mixture of Crown-owned and private coal. Only Crown-owned coal production is presented.

Table 5.2 Coal production by rank and region for 2023 (tonnes) (Source: MBIE).

	Rank			Total
	Bituminous (tonnes)	Sub-Bituminous (tonnes)	Lignite (tonnes)	
Waikato	-	535,079	-	535,079
NORTH ISLAND	**-**	**535,079**	**-**	**535,079**
West Coast	1,306,699	224,041	-	1,530,740
Canterbury	-	-	-	-
Otago	-	25,036	-	25,036
Southland	-	233,796	275,433	509,229
SOUTH ISLAND	**1,306,699**	**482,873**	**275,433**	**2,065,005**
NEW ZEALAND	**1,306,699**	**1,017,952**	**275,433**	**2,600,084**

5.5 Usage and Consumption

Most of New Zealand's premium bituminous coal is exported. It is valued internationally for its:

- Low ash, sulfur and phosphorous contents.
- Characteristics such as high swelling, fluidity and reactivity, which allow blending with other coals for use in the steel industry.

New Zealand domestic use of coal includes (Figures 5.2 and 5.3):

- Electricity generation at the Huntly Power Station as a back-up to renewable sources.
- Steel making at New Zealand Steel's Glenbrook Steel Mill.
- Cement and lime manufacture.
- Food processing – including milk powder and other dairy products; meat, vegetable canning, salt, gelatine and dried herbs.
- Heating commercial horticultural hothouses during cooler months.
- Other industrial process, including processing of timber, wool and leather.
- Heating commercial and public facilities, including schools, universities and hospitals.

Substitution of other energy sources have reduced the use of coal. Currently, renewables substitute for most coal-fired base load at Huntly, but the plant is still important as a back-up to renewable energy generation from hydroelectric, wind and solar sources, with coal playing a vital role in providing energy security in dry years and/or in periods of reduced wind and sunshine, and additionally in times of gas outages. Electricity generated from coal fell to 2.9% of total generation in 2022, a decrease from 7% of total electricity generation in 2021 (Figure 5.4).

New Zealand Steel is currently investigating a transition away from burning coal as part of its production processes with assistance from government funding. It is estimated that, if this transition is possible, it will reduce New Zealand's total greenhouse gas emissions by 1%. Similarly, the Golden Bay cement plant is investigating reducing its coal consumption. The diary industry and other food processors are major coal users, especially in the South Island, because gas is not reticulated there and other heating alternatives are more expensive.

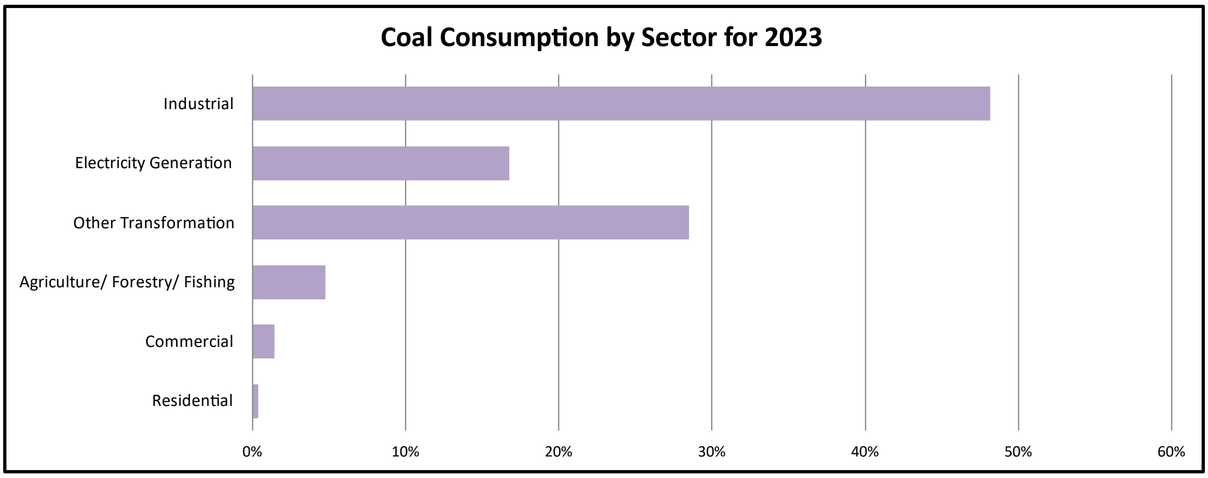

Figure 5.2 Coal consumption by sector for 2023 (percentage of total) (Source: MBIE).

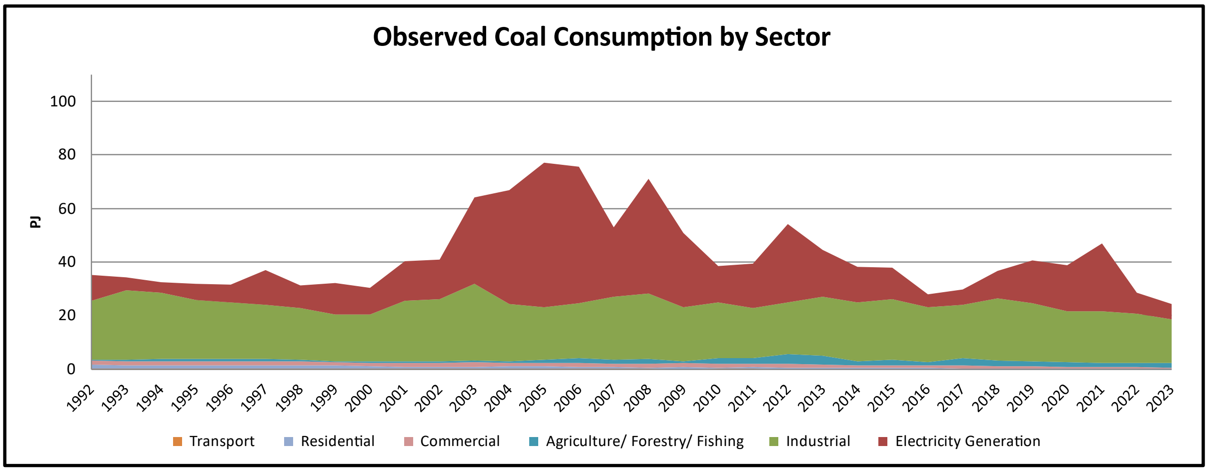

Figure 5.3 Coal consumption (PJ) by sector for 1992–2023 (tonnes) (Source: MBIE).

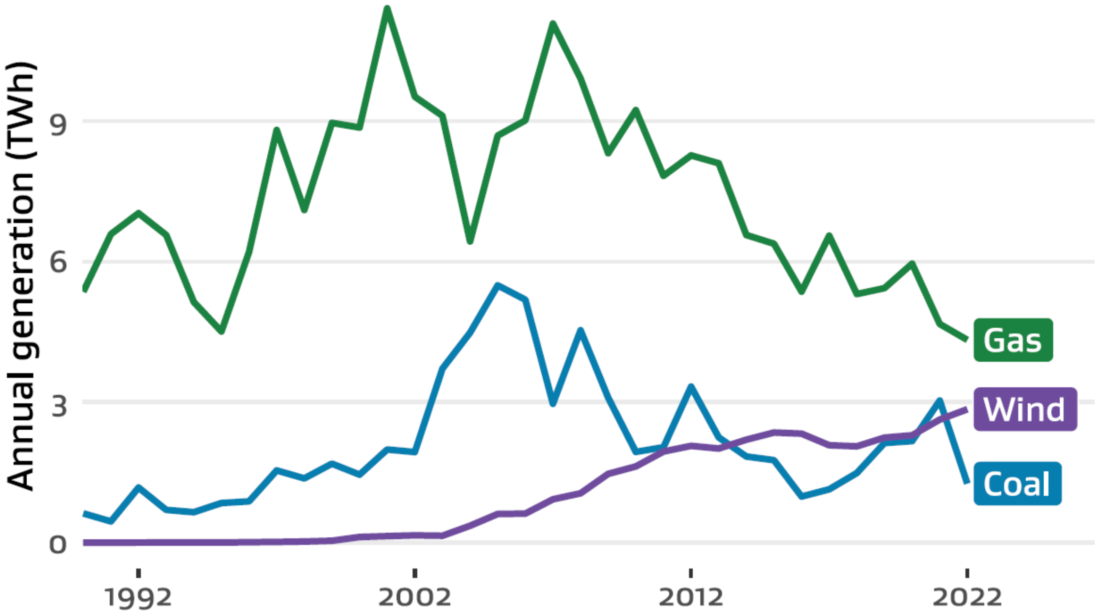

Figure 5.4 Share of total electricity generation by source, from 1990 to 2022 (Source: MBIE).

5.6 Resources

New Zealand's estimated in-ground coal resources are more than 15 Bt, being about 12 Bt of lignite and nearly 4 Bt of sub-bituminous and bituminous coal. However, most of these resources are classified as inventory coal and are largely non-recoverable (Sherwood 2019). Using a JORC-style classification scheme (Part 1, Table 7.1), Sherwood (2019) estimated that Coal Reserves were 38.5 Mt for bituminous coal and 9.0 Mt for sub-bituminous coal; and that Coal Resources were 230 Mt for bituminous coal and 66 Mt for sub-bituminous coal (Part 1, Table 7.3). Equivalent estimates for lignite resource are unavailable for these categories. Nevertheless, Southland's lignite resources are New Zealand's largest conventional energy resource. Coal Reserves and Resources reported to MBIE to the end of 2023 are listed in Part 1 (Table 7.4). Privately owned coal is not included because there is no requirement for reporting privately owned coal resource and reserve data.

5.7 Opportunities

Investigations have looked at developing the Southland lignite resources with a variety of projects, including the production of liquid fuels and fertiliser and as a petrochemical feedstock.

5.8 Challenges

- Because of the need to reduce emissions by substitution of renewable energy for coal, the market for coal is generally declining.
- The viability of coal exports from the West Coast are primarily dependent on global coking coal prices, as well as access to resources and controlling costs in production and transport to markets.

6.0 OFFSHORE METALLIC MINERALS

6.1 Offshore Placer Gold

In the South Island, gold-bearing sediments in beach deposits have been worked along the West Coast and south coast on a small scale. West Coast offshore deposits were investigated in some detail in the 1980s, along with areas off the south coast of the South Island and offshore from the Clutha River in Otago using geophysical surveys and dredge sampling.

Youngson and Stevenson (2016) noted that onshore gold production from the Westland placers has nearly all been recovered from downstream (west) of a succession of Pleistocene glacial moraines north of Ross (Figure 6.1). These moraines effectively form a ‘gold line’ that is oblique to the present coastline and crosses it in the vicinity of the Waitaha River just south of Ross. North/south of Waitaha River, most of the terminal moraines and any associated gold-bearing fluvial outwash systems are presently submerged on the inner continental shelf, where they are now overlain by a variable thickness of post-glacial marine sand, silt and mud. The now offshore terminal moraine deposits have been re-worked and upgraded by subsequent cycles of sea-level transgression and transgressive shoreface erosion, as well as by northward-directed storm and tidal currents.

6.1.1 Exploration

Four successive companies or groups have explored the West Coast offshore placer potential (Youngson 2006; Stevenson 2008):

1. In 1967, Alpine Geophysical Associates Inc (AGA 1968), under contract to Marine Mining Corporation, carried out extensive seismic (Sparker) surveys and some sampling.
2. In the early 1970s, Carpentaria Exploration Co Pty Ltd (Painter 1973) explored two near-shore areas of South Westland, largely to assess potential offshore extensions to heavy-mineral sands identified onshore.
3. In the 1980s, CRA Exploration Ltd (Price 1983a, 1983b; Price 1985, Price and Coles 1985; Wotherspoon 1986; Corner 1989) used the AGA seismic surveys as a basis for extensive grab-sampling of surface sediments and carried out vibro-coring programmes in an area offshore from the Arahura River (‘Harvester Project’). It defined a c. 400,000 oz resource within this area but considered the grade too low and abandoned the area.
4. From 2004, Seafield Resources, in a joint venture with DeBeers, carried out target development (Youngson 2006); offshore chirp sub-bottom profiling (Stevenson 2006); onshore ground magnetic surveys of beaches (Kirkpatrick 2006); offshore aeromagnetic surveys (Kirkpatrick 2007); seismic surveys (Hargrave 2006); and echo sounding, swath bathymetry and marine magnetic surveys (Sedyn and Esterhuizen 2007). These surveys defined two target areas referred to as the Northern target area and Southern target area, which were tested during 2010 by a coring programme using a Sonic Vibro-Coring (SVC) tool that could core to a maximum depth of 10 m but was restricted to operations in water depths greater that 20 m. A total of 55 cores were recovered from the two target areas, mostly in the CRA Harvester Project area. The seismic data provided information on the thicknesses, geometries, extents, inferred probable facies types and depositional environments of the different seismic stratigraphic units (Stevenson 2008). Using this data, the extension of some geological features on the present-day coastal plain were mapped into the offshore environment. The exploration programme was abandoned in mid-2011.

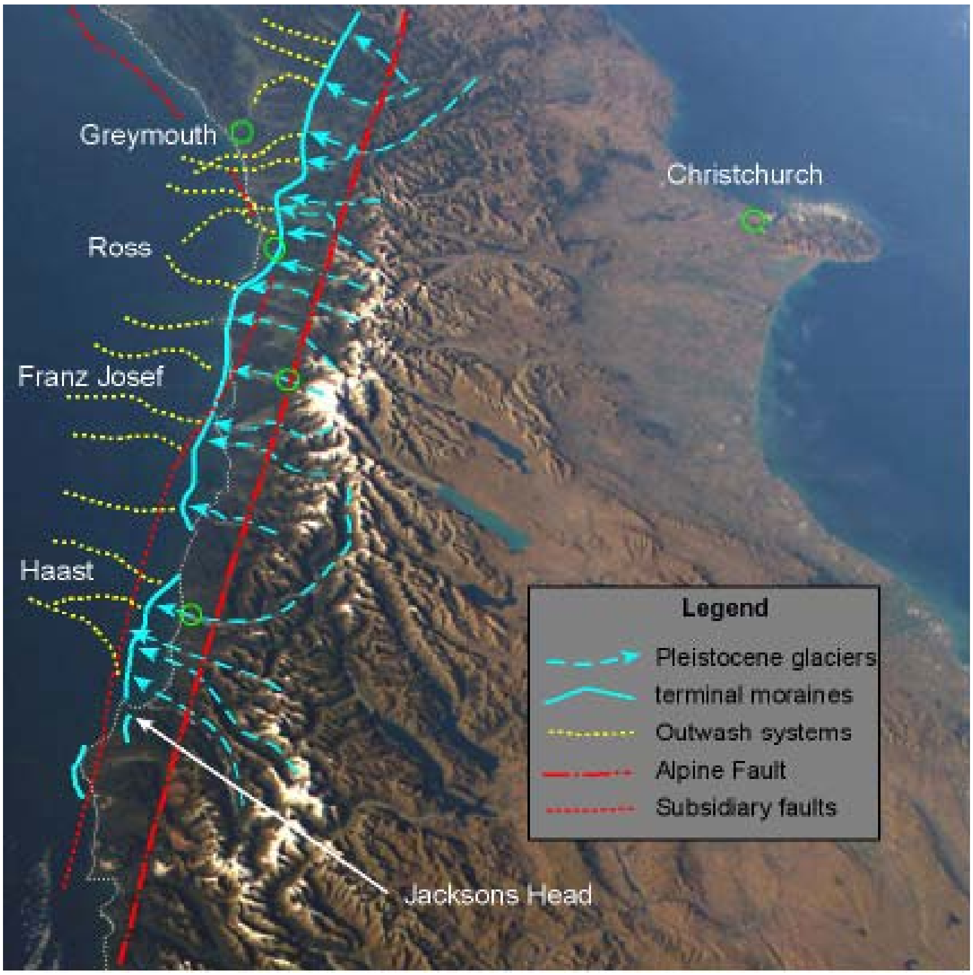

Figure 6.1 Schematic depiction of West Coast Late Pleistocene glaciers, terminal moraines and outwash systems, after Youngson (2006). Note that the terminal moraines south of Ross lie mainly offshore.

Resource estimates: A low-grade resource of about 400,000 oz of gold was defined by CRA in the West Coast offshore area.

Key References: Corner (1989); Youngson and Stevenson (2016).

6.2 Offshore Placer Titanomagnetite Ironsand

The Quaternary age titanomagnetite ironsand deposits found onshore along the western coast of the North Island have equivalent deposits offshore (Figure 3.21; Part 1, Figure 8.6). These are mostly interpreted as former beach, coastal dune and river deposits formed at times of lower sea level (Figure 6.2) and partly redistributed by the marine transgression and subsequent tidal currents and storm-wave action.

Figure 6.2 Past New Zealand sea levels. At the peak of the last glaciation about 20,000 years ago, temperatures were about 5°C below the current mean. Ocean water was locked up in massive ice sheets, so sea levels were 120–130 m lower than they are today. This extended the land area of New Zealand and the North and South Islands were joined. By 12,000 years ago, Cook Strait was flooded and the temperature had warmed sufficiently, so sea level was only about 70 m below present levels (after Mullan et al. [2006]).

Carter (1980) described cores taken from the seabed of the west coast continental shelf, penetrating as deep as 3 m, as exhibiting a transgressive sequence of shell-bearing sand with prominent gravely sand and sandy gravel horizons, overlain by fine to very fine terrigenous sand, locally capped by post-transgression mud. In most cores, the quantity of ironsand is highest in the shell-bearing layers, probably representing the highest-energy environments that redistributed the ironsand during the transgression.

In addition, the presence of ironsand below the depth of the piston cores was known from petroleum well samples and in samples from a drill hole for the Kupe well-head (P Vermeulen 2008, pers. comm.; Hartshorn and Selliani 2009).

6.2.1 Exploration

Concentrations of ironsand on the sea bottom were identified off the west coast of the North Island following sampling of offshore sediments during the 1960s to 1970s by the New Zealand Oceanographic Institute (now the National Institute of Water & Atmospheric Research [NIWA]) (Carter 1980). Sampling penetrated the seabed to a maximum depth of c. 3 m. Highest concentrations were identified in five areas: Manukau to the Waikato River mouth (Maukau),

c. 25 km offshore of Awakino, Mokau to Tongaporutu (Mokau), west of New Plymouth and west of Pātea (Figure 3.21; Part 1, Figure 8.6). From 2005, several companies followed up this work with offshore exploration, beginning with Iron Ore New Zealand (IONZ) and followed by Rio Tinto Mining and Exploration Limited (Rio Tinto), initially in joint venture with IONZ, Trans-Tasman Resources Ltd (TTR), Ironsands Offshore Mining Ltd and FMG Pacific (Fortescue Metals Group) (Figure 6.3). The larger exploration programmes undertook aeromagnetic surveys to identify target areas for bottom sampling and drilling. Aeromagnetic data exhibit positive magnetic anomalies interpreted to represent concentrations of ironsands in paleo-shorelines and paleo-river channels formed when sea level was lower than at present (Figure 6.2). Some may also represent lag deposits of ironsand left following winnowing by the marine transgression and more recent wave action during storms.

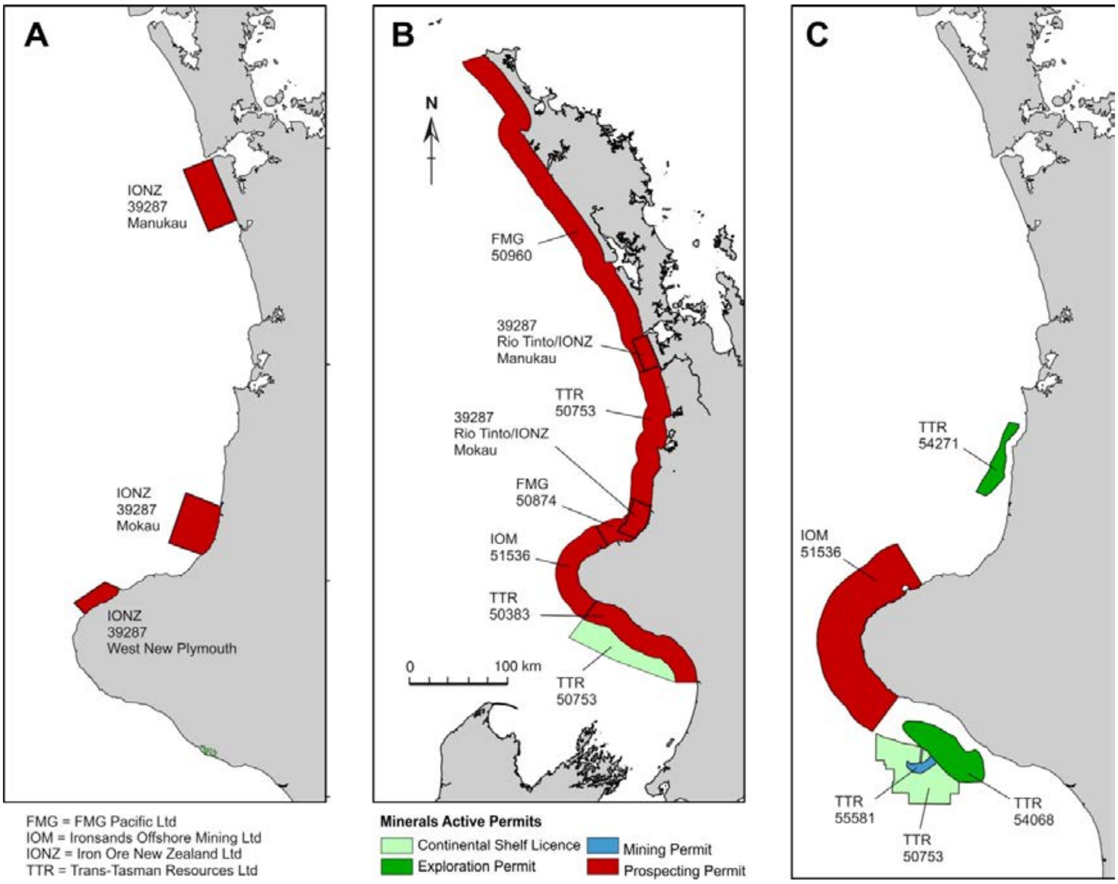

Figure 6.3 Mineral permits for offshore ironsand exploration in (a) 2005, (b) 2009 (c) and August 2016. Note that map B is at a smaller scale than maps A and C (after Christie [2016b]).

Marine geophysical surveys, such as shallow seismic profiling (e.g. boomer), and side-scan sonar and depth sounder surveys have also been used primarily to characterise the seafloor topography, sediment type and shallow stratigraphy. Some of the magnetic data was modelled in 3D to develop resource models for ironsand concentrations (modelled as TiFe) to depths up to 60 m below the seabed (e.g. Loftus 2010).

Sampling of the seafloor sands has included grab samples, core samples (to a maximum 5 m depth) collected using a vibracorer and reverse-circulation drilling using custom-developed equipment, the latter to attain deeper seafloor penetration than a vibracorer. For example, TTR developed two different submersible reverse-circulation drill rigs to obtain sediment samples; a versatile shallow system, fitted with drill strings of 5–11 m and a separate deep-drilling system with a depth penetration of up to 42 m and requiring a larger launching vessel. To 2014, more than 800 holes were drilled up to 11 m deep and an additional 17 deep holes up to 35 m deep.

6.2.2 Resources

TTR’s 2023 reported titanomagnetite JORC Resource of 3157 Mt of ironsand, producing a concentrate (56–57% Fe), includes 2073 Mt Indicated and 1083 Mt Inferred classification in deposits located offshore from Pātea in water depths of 20–50 m (Manuka Resources 2023).

6.2.3 Mining Proposal

A mining proposal was developed for excavation of up to 50 Mt (27 km^3) per year of seabed material containing ironsand. Processing on an offshore floating vessel would yield c. 10% iron ore for export, with the remaining material returned to the seabed. Mining permit MP55581 was granted to TTR in May 2014.

6.2.4 Challenges to Mining

The TTR seabed mining proposal has faced ongoing opposition from iwi, the fishing industry and environmental groups. Much of the opposition is focused on the potential environmental impact of the sediment plume generated by mining operations, particularly on the Pātea shoals, a shallow-water fishery nearer to the coast, and whether that could disrupt dolphins, whales and other marine mammals.

There is also opposition to any form of mining, as well as claims by iwi that the proposed mining harms the mauri of the South Taranaki Bight and also cuts across their rights and interests in their coastal waters and the fisheries within them.

6.2.5 Status

Following the granting of TTR’s mineral mining permit MMP55581, covering a JORC-reported vanadium-bearing titanomagnetite ironsand resource within the Exclusive Economic Zone (EEZ), outside the 12 nautical mile limit, a marine and discharge consent application to recover the resource was submitted by TTR to the Environmental Protection Agency (EPA) in August 2016, with consents granted in August 2017. These environmental consents to operate were then subject to court appeals and, following the Supreme Court’s judgment in 2021, returned to the EPA for reconsideration of the grants based on the Court’s rulings. In March 2024, TTR terminated the EPA’s reconsideration of the operating consents application but still retained MMP55581 within the EEZ and mineral exploration permit MEP54068, covering additional JORC-reported mineral resources inside the 12 nautical mile limit offshore of Pātea.

Key References: Carter (1980); Christie (2016c).

6.3 Offshore Placer Ilmenite

Ilmenite occurs offshore associated with placer gold deposits on the East Coast (see above, Section 6.1) and offshore in the Bay of Plenty (Figure 6.4). Little is known of the Bay of Plenty deposits; although several companies have proposed exploration, very little work has been carried out.

Figure 6.4 Area (brown) of Pacific Offshore Mining's prospecting permit 52474 to explore for ilmenite sands offshore of Waihi Beach in the Coromandel Peninsula (Source: NZP&M Minerals Permit Webmaps).

6.4 Offshore Volcanogenic Massive Sulfide Mineralisation

6.4.1 Introduction

The Kermadec arc, striking for 1200 km from Monowai volcano to the North Island of New Zealand, represents the southern portion of the contiguous ~2500 km Kermadec-Tonga arc (Part 1, Figure 11.1). The Kermadec arc is populated by 30 volcanic centres comprising single, large caldera or cone volcanoes or, less commonly, groups of relatively smaller cones. All of these volcanic centres lie to the west of the Kermadec Ridge in the southern and mid-parts of the arc – by up to 70 km in the case of Rumble II West – then merge with the Kermadec Ridge near the Kermadec Islands around 30°S. The volcanoes then diverge away (westward) from the Kermadec Ridge in the northern reaches of the arc (Part 1, Figure 11.1). Approximately 80% of these volcanoes are identified as hydrothermally active, and at least four of them have metal-rich fluids associated with the submarine volcanic activity, producing volcanogenic massive sulfide mineralisation (Figure 6.5). GNS Science (and, to a lesser extent, NIWA) and its international research partners have undertaken many research cruises to identify the volcanoes, their volcanic and hydrothermal activity and the presence of seafloor massive sulfide mineralisation.

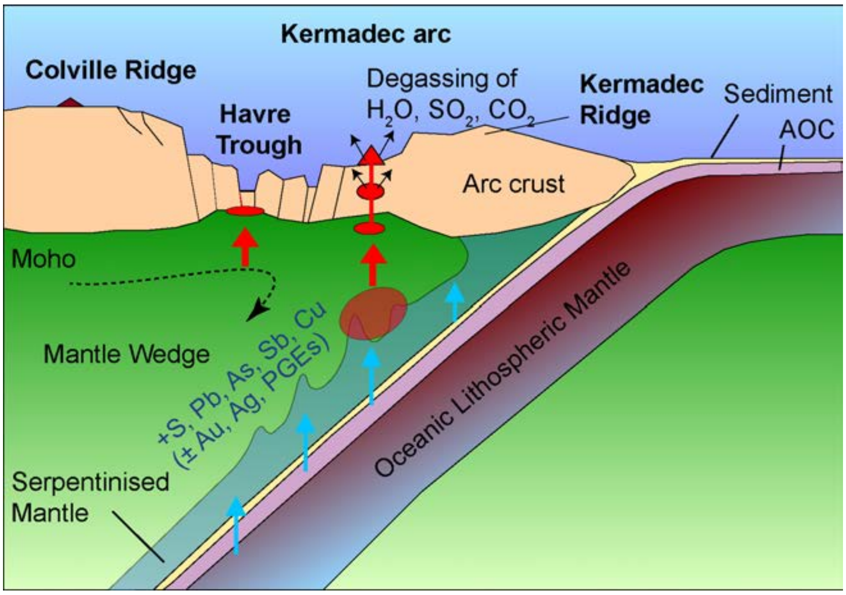

Figure 6.5 Schematic model of Kermadec arc petrogenesis (after Timm et al. [2016]).

6.4.2 Research Exploration

Since the serendipitous recovery of massive sulfide samples from Brothers and Rumble II West volcanoes in 1996 (Wright et al. 1998), subsequent research exploration initially focused on the discovery, spatial location and characterisation of seafloor hydrothermal systems of the Kermadec intraoceanic arc using hydrothermal plume surveys (Table 6.1). The plumes are used to vector in on the hydrothermal vent fields. The entire ~1300 km of the Kermadec arc that lies within New Zealand’s EEZ (Economic Exclusive Zone) has been surveyed for hydrothermal emissions, with about 80% of all the major submarine volcanoes being host to active vent fields (see Part 1, Figure 11.1). This makes the Kermadec arc the most hydrothermally active intraoceanic arc in the world (de Ronde et al. 2003a).

Additional cruises (see Table 6.1) have since re-visited several of the volcanoes as part of a time-series project to survey the hydrothermal plumes to model the chemical evolution of these seafloor systems. Considerably more samples of massive sulfide mineralisation have been recovered from Brothers volcano since 1996, using dredging, remotely operated vehicle (ROV) sampling and drilling (de Ronde et al. 2005, 2011, 2019).

Deployment of the manned submersibles *Shinkai 6500* in 2004 and *Pisces V* in 2005 meant that focused sampling of seafloor hydrothermal systems along the Kermadec arc was possible. Recovered chimney and other mineralised samples could then be placed in their proper geological and geochemical context, together with the analysis of vent fluids, with a view to further constructing a model for the formation of submarine arc-related massive sulfide deposits (e.g. de Ronde et al. 2011). In addition, the deployment at Brothers volcano in 2007 of the autonomous underwater vehicle (AUV) *ABE,* and later *Sentry* in 2011 and 2017, meant that high-resolution bathymetric maps (i.e. a resolution of ≤ 2 m compared to ~25 m using surface vessels) were obtained of the seafloor (Kusek 2007). Additional information obtained by an array of sensors that can be fitted to the vehicle (e.g. a magnetometer; and pH, Eh, light-scattering and temperature probes) enables precise location of the boundaries of the active and inactive hydrothermal fields, the location of the main active chimney clusters and the vertical extent of fluid up-flow zones within the volcanoes (Caratori Tontini et al. 2012; Caratori Tontini and de Ronde 2016). Deployment of the ROVs *Quest 4000* in 2016 and *Jason II* in 2018 meant that high-precision sampling continued at Brothers until it was drilled by the International Ocean Discovery Program (IODP) in 2018.

Massive sulfide mineralisation is known to occur at Brothers, Clark, Rumble II West and Hungaroa volcanoes (Part 1, Figures 11.1 and 11.2). At Brothers, numerous samples of what were either active chimneys or dead spires have been sampled from the main NW Caldera vent field, where at least 100 dead and active sulfide chimney spires occur, typically 2–3 m in height, with some reaching 6–7 m. More recently, chimneys up to 20 m tall have been sampled at the Upper Caldera site at Brothers (Figure 6.6). Ages of the NW Caldera chimneys fall into three groups: <4 years, 23 and 35 years old (at the time of sampling). Less common are massive sulfide crusts 2–3 m thick. Two main types of chimney predominate: Cu-rich (up to 28.5 14 wt.% Cu and including up to 91 ppm Au) and, more commonly, Zn-rich (up to 43.8 wt.% Zn; see Figure 6.6). Similarly, metal concentrations are relatively high for the limited number of samples recovered from Rumble II West (up to 9.8 wt. % Cu; 4.7 ppm Au; de Ronde et al. 2003b) and Clark volcanoes (5.8 ppm Au; de Ronde 2006).

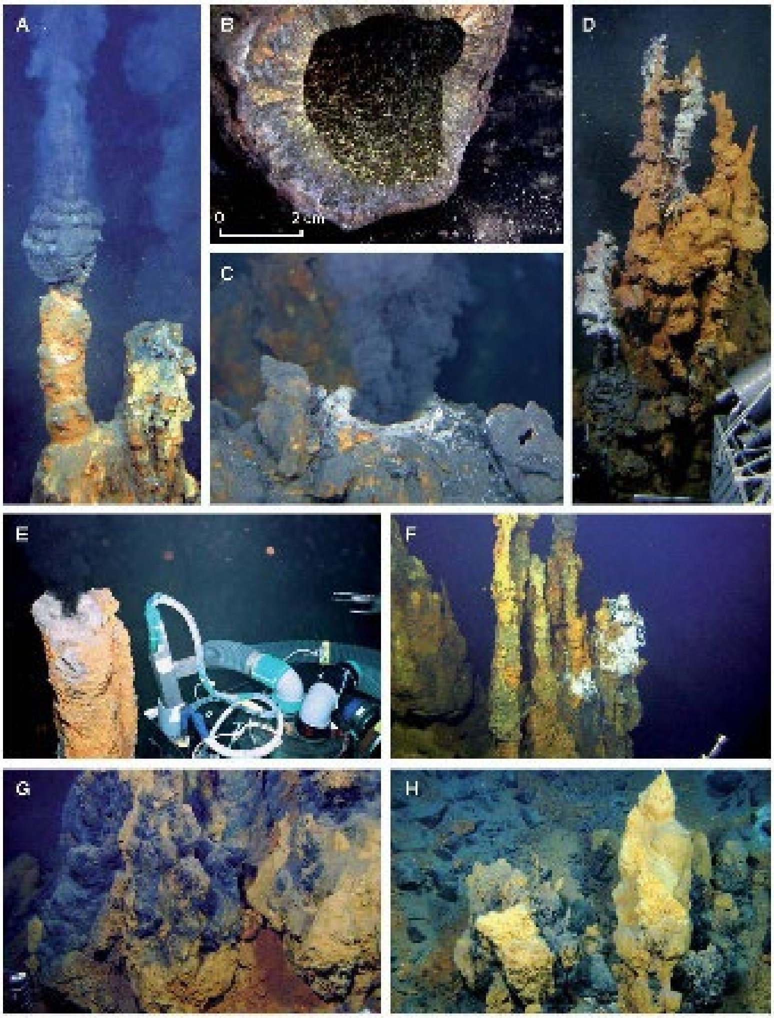

Figure 6.6 Brothers volcano chimneys *in situ*. (a) Classic beehive-type structure on the ~15-cm-tall, left-hand of the two smaller chimneys that sit atop this large ~4-m-high chimney complex. The maximum vent temperature within the NW Caldera field of 302°C was recorded at this chimney, at a depth of 1665 m. (b) Close-up of the left-hand chimney shown in (a) after being broken off by the submersible's robotic arm, showing predominantly Cu-rich mineralisation lining the orifice. (c) Vent orifice at what was the base of a small (~0.5 m tall) chimney sitting atop a 1–2-m-high sulfide mound with a vent temperature of 292°C (1627 m). Field of view is ~0.5 m. (d) Top of a ~4-m-tall, in-active chimney on the NW Caldera slopes. Depth is ~1610 m. (e) A ~2-m-tall chimney perched on a steep slope where other dead chimneys had fallen (1670 m). Vent fluid had a maximum temperature of 274°C. Field of view is ~1.5 m. (f) Cluster of dead chimney spires, all ~2 m high, seen ~25 m west of Marker #20 (1689 m). White material is bacterial mat. Chimney on left-hand side (partially obscured) is 5 m tall. (g) Base of cluster of Mn-coated, Fe-silica chimneys seen at a depth of ~1615 m. Field of view is ~2 m. (h) Another example of low temperature Fe-silica-rich chimneys seen here at a depth of ~1620 m. Field of view is ~3 m.

6.4.3 Mineral Exploration

Neptune Resources held prospecting permits over much of the Kermadec arc and part of the Colville Ridge and in 2008 applied for a mining permit over Brothers volcano. Its prospecting permits expired in 2010. The company conducted several surveys along both arcs that mapped the area with geophysical and multi-beam bathymetry data (e.g. Neptune Resources 2007; Downey and Perrin 2008; John 2011) and collected geological and biological seafloor and sediment samples (e.g. McConachy et al. 2005, 2006). Sampling was done with ROVs and seafloor drills that primarily targeted black-smoker chimney field and mineral-rich sediments to a maximum depth of 14.8 m below seafloor, for a total core recovery of 47.17 m from 107.3 m drilled. Neptune Resources also collected environmental data with oceanographic moorings.

Nautilus Resources Ltd applied for a prospecting permit along the back-arc region of the Kermadec arc but no work eventuated.

6.4.4 Prospectivity Categories

Datasets that are available for delineating the mineral prospectivity of offshore volcanoes include:

- Regional bathymetric mapping from surface vessels.
- Regional gravity.
- Regional magnetics.
- Hydrothermal plume mapping and water-column sampling over individual volcanoes.
- Dredge (rock and mineral) samples recovered using surface vessels.
- Vent fluid and chimney samples recovered using manned submersibles and ROVs.
- High-resolution seafloor mapping using AUVs.
- Precise location of vent field boundaries using AUVs.
- High-resolution magnetics using AUVs.
- Drilling (Brothers) using IODP.

Based on the information available, de Ronde et al. (2010) assigned the volcanoes of the Kermadec arc to four levels, or categories, of VMS mineral prospectivity: Category A being the highest and Category D the lowest level of prospectivity. Their assessments were confined to the volcanoes that make up the active arc front of the Kermadec arc. However, they also briefly referred to nearby regions, such as the Kermadec Ridge, the back-arc to the arc front (Havre Trough) and the Colville Ridge for their (sulfide) mineral potential. The following sections define each of these categories and outline the criteria used to delineate them, as well as update the prospectivity analyses with information available up to April 2024.

6.4.5 Category ‘A’ Volcanoes – High Prospectivity

Category ‘A’ volcanoes are those known to host VMS mineralisation. That is, samples of sulfide, typically collected using a manned submersible, ROV or dredge, have been recovered and/or sulfide chimneys have been observed. Mineralisation is of the massive sulfide type (i.e. rich in one or other of Cu, Zn or Pb, with accompanying Au making them more economically attractive), commonly mined from ancient, now land-based, deposits, and is the primary deposit type sought by mineral exploration companies in the offshore environment. Assignment of category ‘A’ to a volcano does not necessarily infer ‘economic’ concentrations, or grades of metal found in the mineralisation, nor the size of the resource (tonnage). However, limited information for both grade and tonnage is available (or can be inferred) for volcanoes presently assigned this category. Category 'A' volcanoes would be the most attractive to offshore mineral exploration companies, as they provide hard evidence for a possible ore deposit that could be exploited. Exploration companies could assess the viability of moving to more detailed sampling of the chimney fields, as well as geophysical surveys to delineate their boundaries (particularly depth), using ROVs or by seafloor drilling. Both are expensive operations. Thus, detailed information on the potential deposit site(s) would be advantageous and cost-effective prior to engaging these operations.

Four volcanoes have been given Category 'A' status: Brothers, Clark, Rumble II West and Hungaroa.

6.4.5.1 Brothers Volcano

Brothers volcano represents the most-studied arc volcano along the Kermadec arc (and likely the world), resulting in the availability of a considerable amount of data (see Table 6.1). This includes numerous plume, bathymetric, magnetic, gravity and towed-camera surveys, dredging, nine manned submersible dives, 14 ROV dives and a detailed AUV survey. It is the only volcano that has been drilled (e.g. seafloor drilling by Neptune Resources and IODP). One large site (main NW Caldera site) and another significant one (Upper Caldera site) are host to numerous chimneys and massive sulfide crusts. Approximately 25 sulfide chimneys have been sampled, dated and assayed from the NW Caldera site; fewer from the Upper Caldera site. Chimneys are typically 2–7 m tall, with 20-m-tall chimneys found at the recently discovered Upper Caldera site representing a large mass of sulfide. Two other sites (i.e. SE Caldera and W Caldera) have evidence for massive sulfides. However, except for one small sample recovered by dredging from the SE Caldera site, massive sulfides from the W Caldera and SE Caldera hydrothermal sites have effectively not been sampled.

6.4.5.2 Clark Volcano

Clark Volcano has had sulfide samples (and vent fluids) recovered by the submersible *Pisces V* during two dives in 2005. It has also been mapped by multi-beam for its bathymetry, by towed camera, and surveyed for hydrothermal plumes (several times). One main area and another, smaller, one have been identified as hosting active chimneys (up to 7 m tall) and what appear to be massive sulfide 'mounds', or probable remnants of older chimneys. These have been sampled, dated and assayed.

6.4.5.3 Rumble II West Volcano

Rumble II West has been surveyed with surface vessels for its bathymetry and hydrothermal plumes, the latter on several occasions. Rumble II West volcano is known to host at least one chimney field. Samples of massive sulfide have been recovered from this volcano during dredging operations in 1996 and 2011. In 2011, it was surveyed by the AUV *Sentry*, which revealed a more-detailed picture of hydrothermal activity and likely mineralisation that may extend over hundreds of metres.

6.4.5.4 Hungaroa Volcano

Hungaroa volcano was sampled in 2018 using the German research vessel *R/V Sonne* and three dives with the ROV *Quest 4000*. A number of sulfide samples were collected from massive sulfide mounds located in a hydrothermal vent field near the summit. The samples have been dated and assayed. They are dominated by sphalerite (Zn) and barite (Ba) and, to a lesser degree, chalcopyrite (Cu) mineralisation.

6.4.6 Category ‘B’ Volcanoes – Medium Prospectivity

Category ‘B’ volcanoes are those known to host active seafloor hydrothermal vents. That is, plume surveys conducted during the NZAPLUME series of cruises established that Category ‘B’ volcanoes were hydrothermally active. This category, as well as Category ‘A’ would be equivalent to the ‘brown fields’ category commonly referred to by on-land mineral exploration companies. The bathymetry of these volcanoes has also been mapped using various multi-beam systems. Recognition of hydrothermal activity does *not* automatically mean that there is associated VMS mineralisation, as not all vent fluids carry metals to the seafloor (e.g. de Ronde et al. 2001, 2003a, 2005, 2007, 2011). However, details of the plume chemistry can elucidate the composition of the fluid being expelled by the seafloor vents. This in turn can provide insight as to the likelihood of there being associated sulfide mineralisation.

Category ‘B’ volcanoes include (from south to north; see Part 1, Figure 11.1): Tangaroa, Rumble V, Rumble III, Healy, Kibblewhite, Sonne, Ngatoroirangi, Kuiwai, Hungaroa, Wright, Havre, Vulkanolog, Macauley cone, Macauley caldera, Giggenbach, Henetapeka, Putoto, Gamble, Rakahore, Hineputa and Monowai cone and caldera (volcanoes U and V shown in Figure 11.1 of Part 1 sit within Tonga’s territorial waters).

Pisces V submersible dives have been made on Monowai caldera (4), Macauley cone (2), Giggenbach (3), Wright (1), Healy (2), Rumble V (2) and Tangaroa (2). Massive sulfide mineralisation was not seen during any of these dives, although a later ROV dive on the Monowai site possibly identified mounds of sulfide on the seafloor. However, this has not been verified (i.e. by the recovery of any samples). All category ‘B’ volcanoes have been dredged to varying degrees, with mostly unmineralised rocks and, in some cases, samples of native sulfur having been recovered. Vent fluid samples were recovered during the *Pisces V* dives from all volcanoes mentioned above, with the exception of Wright volcano. ROV dives made by *Quest 4000* were conducted at Macauley cone (4), Hungaroa (3) and Rumble III (2), collecting vent fluids and select rock and/or mineralised samples.

6.4.7 Category ‘C’ Volcanoes – Low Prospectivity

Category ‘C’ volcanoes are those that have no evidence for hydrothermal activity from limited prospecting. That is, plume surveys conducted during the NZAPLUME series of cruises did not establish that the volcano was hydrothermally active. The volcanoes include (from south to north): Whakatane, Rumble IV, Lille, Rumble II East, Silent II, Cotton, Cole, Wright, Speight, Oliver and Q.

6.4.8 Category ‘D’ Volcanoes/Regions – Prospectivity Unknown

Category ‘D’ volcanoes/regions are those areas where we have little, or no, evidence to evaluate VMS prospectivity. That is, insufficient work has been done to determine the likelihood, or not, of a region being host to VMS mineralisation. This category would be similar to the ‘green fields’ category commonly referred to by on-land mineral exploration companies. This category includes the volcanoes Yokosuka, Rapuhia and Giljanes in the back-arc to the active arc front (not shown in Figure 11.1 of Part 1), as well as possible ancient volcanoes, or remnants thereof, on the Kermadec Ridge. This category also includes the immediate back-arc to the active arc front of the Kermadec arc (i.e. the Havre Trough), and the Colville Ridge (Part 1, Figure 11.1). The latter regions may be host to ancient equivalents of the active seafloor hydrothermal systems noted above. The southern parts of these areas to ~33°S have had regional bathymetry, gravity and magnetic surveys completed.

6.4.9 Research Required to Increase Prospectivity

The work required to elevate the prospectivity of hydrothermal systems in the four prospectivity categories described is illustrated in Figure 6.7.

Key References: Baker et al. (2003); Berkenbosch et al. (2012); Caratori Tontini et al. (2012); Caratori Tontini and de Ronde (2016); de Ronde et al. (2005, 2010, 2011, 2012).

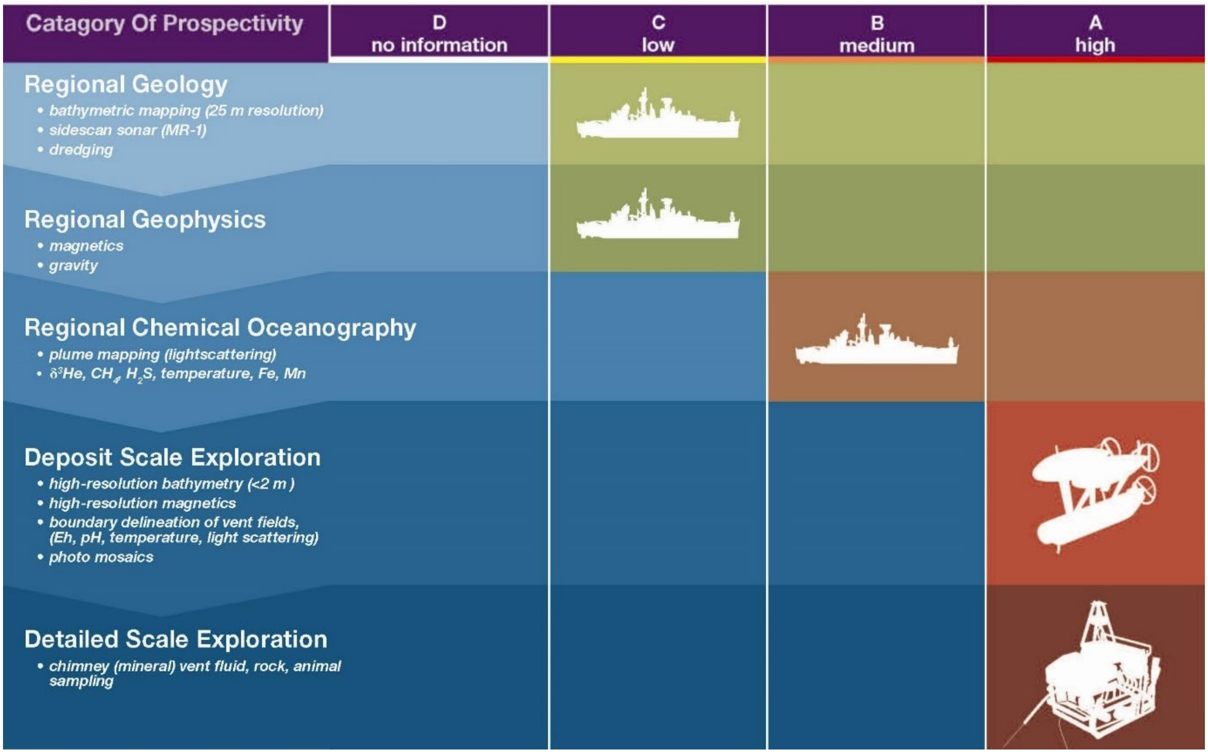

Figure 6.7 Recommended stages of exploration for seafloor massive sulfide deposits on the Kermadec Arc. Silhouettes are of preferred platforms (e.g. ships, AUVs, ROVs) (after de Ronde et al. [2010]).

This page left intentionally blank.

Table 6.1 Kermadec arc volcano inventory and prospectivity rank. * = Sub-aerial. Note: latitude and longitude are approximately the volcano centre. Cruise name: 1 = LAU HARVE 1997; 2 = SONNE 135 1998; 3 = NZAPLUME I 1999; 4 = NZAPLUME II 2002; 5 = NZAPLUME III 2004; 6 = SHINKAI 2004; 7a = PISCES leg I 2005; 7b = PISCES leg Iia 2005; 7c = PISCES leg Iib 2005; 8 = MANGO 192/2 2007; 9 = ROVARK 2007; 10 = UWASH 2009; 11 = *R/V Sonne* and *Quest 4000*; 12 = *R/V Thompson* and *Jason II*. Rank: A = massive sulfide recovered; B = Hydrothermally active; C = Inactive volcano/caldera; D = No data – including northern regions of Kermadec Ridge, Havre Trough and Colville Ridge. AUV = autonomous underwater vehicle.

Volcano		Latitude °S	Longitude °W	Cruise Name	Rank	Shipboard Bathymetry	AUV Bathymetry	Shipboard Gravity	Shipboard Magnetics	AUV Magnetics
Calypso Vent sites		37°41.7’	177°06’ E	2, 8	B	Y	N	N	N	N
Whakaari / White Island *		37°52’	177°58’	2, 3	B	N	N	N	N	N
Whakatane		36°49.545’	177°27.921’ E	3, 4	C	Y	N	N	N	N
Clark		36°27.653’	177°50.320’ E	2, 3, 4, 7b	A	Y	N	N	N	N
Tangaroa		36°19.750’	178°2.430’ E	3, 4	B	Y	N	N	N	N
Rumble IV		36°199’	178°079’	3	C	Y	N	N	N	N
Rumble V		36°8.390’	178°11.850’ E	3, 4, 6, 7a, 7c	B	Y	N	N	N	N
Lillie		35°51.217’	178°26.214’	3	C	Y	N	N	N	N
Rumble III		35°45.260’	178°30.00’ E	2, 3, 4, 10, 11	B	Y	N	N	N	N
Rumble II East		35°418’	178°585’	3, 6	C	Y	N	N	N	N
Rumble II West		35°21.270’	178°30.480’E	3, 4, 6, 10	A	Y	N	N	N	N
Thompson		35°17.100’	178°51.750’	3	D	Y	N	N	N	N
Silent II West		34°42.374’	178°34.269’	3, 4	D	Y	N	N	N	N
Silent II		35°172’	178°889’	3, 6	C	Y	N	N	N	N
Cotton		35°045’	178°973’	3	C	Y	N	N	N	N
Healy	Healy Cone (SW)	34°992’	178°994’	3, 4, 5, 6, 7c, 9	B	Y	N	N	N	N
	Healy Caldera	34°984’	178°999’	3, 4, 5, 6, 7c, 9	B	Y	N	N	N	N
Rapuhia		34°46.743’	178°30.322’	4	D	Y	N	N	N	N
Giljanes		34°46.570’	178°34.886’	4	D	Y	N	N	N	N
Yokosuka		34°42.544’	178°32.717’		D	Y	N	N	N	N
Brothers	Brothers Cone	34°53.01’	179°04.04’ E	2, 3, 4, 5, 6, 7c, 9, 10, 11, 12	A	Y	Y	N	Y	Y
	Brothers NW Caldera	34°52.29’	179°3.35’ E	2, 3, 4, 5, 6, 7c, 9, 10, 11, 12	B	Y	Y	N	Y	Y
	Brothers Lala (W)	34°53.78’	179°03.01’ E	2, 3, 4, 5, 9, 10	A	Y	Y	N	Y	Y
	Brothers SE Caldera	34°51.772’	179°05.894’ E	2, 3, 4, 5, 6, 9, 10	A	Y	Y	N	Y	Y
Kibblewhite		34°34.506’	179°15.300’	4, 6, 11	B	Y	N	N	N	N
Sonne		34°3.505’	179°35.336’	4	B	Y	N	N	N	N
Ngatoroirangi		33°43.850’	179°49.610’	4	B	Y	N	N	N	N
Cole		33°24.679’	179°52.337’	4	C	Y	N	N	N	N
Kuiwai		33°9.523’	179°57.475’	4	B	Y	N	N	N	N
Haungaroa	Haungaroa Vent one	32°36.38’	179°36.57’	4, 11	A	N	N	N	N	N
	Haungaroa Vent two	32°36.76’	179°36.42’	4	B	N	N	N	N	N
Wright		31°51.001’	179°11.258’	5, 7a	C	Y	N	N	N	N
Speight		32°23.289’	179°35.457’	4	C	N	N	N	N	N
Oliver		32°23.680’	179°40.150’	4	C	Y	N	N	N	N
Havre		31°20.710’	178°54.510’	4	B	Y	N	N	N	N
Vulkanolog		30°41.242’	178°27.188’	2, 4	B	Y	N	N	N	N
L’Esperence *		31°26’	178°54’	Curtis 2002	D	N	N	N	N	N
Curtis Island *		30°32.32’	178°26’	Curtis 2002	B	N	N	N	N	N
Macauley Island *		30°14’	178°26’	5	D	N	N	N	N	N
Macauley	Macauley Cone	30°12.789’	178°26.914’	4, 5, 7a, 11	B	Y	N	N	N	N
	Macauley Caldera	30°9.870’	178°27.730’	4, 5, 7a	B	Y	N	N	N	N
Giggenbach		30°2.780’	178°42.940’	4, 7a	B	Y	N	N	N	N
Raoul Island *		29°16.0’	177°55.10’	2, 5	B	N	N	N	N	N
Hinetapeka		28°33.813’	177°39.324’	5	B	Y	N	N	N	N
OP		27°42.546’	177°34.726’	5	D	N	N	N	N	N
Putoto		27°52.675’	177°36.004’	5	B	Y	N	N	N	N
Q		27°34.186’	177°35.289’	5	C	Y	N	N	N	N
Gamble		27°12.528’	177°25.999’	5	B	Y	N	N	N	N
Rakahore		26°51.771’	177°24.991’	5	B	Y	N	N	N	N
Hinepuia		26°05.305’	177°15.064’	5	B	Y	N	N	N	N
Monowai	Monowai Cone	25°53.509’	177°11.098’	5, 2, 8	B	Y	N	N	N	N
	Monowai Caldera	25°46.227’	177°10.207’	5, 2, 7a, 8	B	Y	N	N	N	N

Table 6.1 Continued.

Volcano		Plume								Vent T	Vent Fluids	Rock Samples	Massive Sulfides	Seafloor Photos	Seafloor Video
		L/S	pH	CH_4	δ^3He	Metals	Salinity	T	μ Biol						
Calypso Vent sites		N	N	N	N	N	N	N	N	N	Y	Y	N	Y	Y
Whakaari / White Island *		N	N	Y	N	N	N	Y	Y	Y	Y	Y	N	Y	Y
Whakatane		Y	Y	Y	Y	Y	Y	Y	N	N	N	N	N	N	N
Clark		Y	Y	Y	Y	Y	Y	Y	Y	Y	Y	Y	Y	Y	Y
Tangaroa		Y	Y	Y	Y	Y	Y	Y	Y	N	N	Y	Y	Y	N
Rumble IV		Y	Y	Y	Y	Y	Y	Y	N	N	N	N	N	N	N
Rumble V		Y	Y	Y	Y	Y	Y	Y	Y	Y	N	Y	N	Y	Y
Lillie		N	Y	Y	Y	Y	Y	Y	N	N	N	N	N	N	N
Rumble III		Y	Y	Y	Y	Y	Y	Y	Y	N	N	Y	N	Y	Y
Rumble II East		Y	Y	Y	Y	Y	Y	Y	N	N	N	N	N	N	N
Rumble II West		Y	Y	Y	Y	Y	Y	Y	Y	N	N	N	Y	N	N
Thompson		N	N	N	N	N	N	N	N	N	N	N	N	N	N
Silent II West		N	N	N	N	N	N	N	N	N	N	N	N	N	N
Silent II		Y	Y	Y	Y	Y	Y	Y	N	N	N	N	N	N	N
Cotton		Y	Y	Y	Y	Y	Y	Y	N	N	N	N	N	N	N
Healy	Healy Cone (SW)	Y	Y	Y	Y	Y	Y	Y	Y	Y	Y	Y	N	Y	Y
	Healy Caldera	Y	Y	Y	Y	Y	Y	Y	Y	Y	Y	Y	N	Y	Y
Rapuhia		Y	Y	Y	Y	Y	Y	Y	N	N	N	N	N	N	N
Giljanes		Y	Y	Y	Y	Y	Y	Y	N	N	N	N	N	N	N
Yokosuka		Y	Y	Y	Y	Y	Y	Y	N	N	N	Y	N	N	N
Brothers	Brothers Cone	Y	Y	Y	Y	Y	Y	Y	Y	Y	Y	Y	Y	Y	Y
	Brothers NW Caldera	Y	Y	Y	Y	Y	Y	Y	Y	Y	Y	Y	Y	Y	Y
	Brothers Lala (W)	Y	Y	Y	Y	Y	Y	Y	N	N	N	Y	Y	Y	Y
	Brothers SE Caldera	Y	Y	Y	Y	Y	Y	Y	N	N	N	Y	Y	Y	Y
Kibblewhite		Y	Y	Y	Y	Y	Y	Y	Y	N	N	N	N	N	N
Sonne		Y	Y	Y	Y	Y	Y	Y	N	N	N	Y	N	N	N
Ngatoroirangi		Y	Y	Y	Y	Y	Y	Y	Y	N	N	Y	N	N	N
Cole		Y	Y	Y	Y	Y	Y	Y	Y	N	N	N	N	N	N
Kuiwai		Y	Y	Y	Y	Y	Y	Y	Y	N	N	N	N	N	N
Haungaroa	Haungaroa Vent one	Y	Y	Y	Y	Y	Y	Y	N	N	N	Y	Y	Y	Y
	Haungaroa Vent two	Y	Y	Y	Y	Y	Y	Y	N	N	N	N	N	N	N
Wright		Y	Y	Y	Y	Y	Y	Y	Y	Y	N	Y	N	Y	Y
Speight		N	N	N	Y	N	N	N	N	N	N	N	N	N	N
Oliver		Y	Y	Y	Y	Y	Y	Y	Y	N	N	N	N	N	N
Havre		Y	Y	N	Y	Y	Y	Y	Y	N	N	N	N	N	N
Vulkanolog		Y	Y	Y	Y	Y	Y	Y	Y	N	N	Y	N	Y	Y
L'Esperence *		N	N	N	N	N	N	N	N	N	N	Y	N	Y	N
Curtis Island *		N	N	N	N	N	N	N	N	N	N	Y	N	Y	N
Macauley Island *		N	N	N	N	N	N	N	N	N	N	N	N	Y	N
Macauley	Macauley Cone	Y	Y	Y	Y	Y	Y	Y	Y	Y	N	Y	N	Y	Y
	Macauley Caldera	Y	Y	Y	Y	Y	Y	Y	Y	Y	N	Y	N	Y	Y
Giggenbach		Y	Y	Y	Y	Y	Y	Y	Y	Y	Y	Y	N	Y	Y
Raoul Island *		N	N	N	N	N	N	Y	N	N	Y	Y	N	Y	Y
Hinetapeka		Y	Y	Y	Y	Y	Y	Y	Y	N	N	Y	N	N	N
OP		N	N	N	N	N	N	N	N	N	N	N	N	N	N
Putoto		Y	Y	Y	Y	Y	Y	Y	Y	N	N	Y	N	N	N
Q		Y	Y	Y	Y	Y	Y	Y	N	N	N	N	N	N	N
Gamble		Y	Y	Y	Y	Y	Y	Y	Y	N	N	Y	N	N	N
Rakahore		Y	Y	Y	Y	Y	Y	Y	N	N	N	Y	N	N	N
Hinepuia		Y	Y	Y	Y	Y	Y	Y	Y	N	N	Y	N	N	N
Monowai	Monowai Cone	Y	Y	Y	Y	Y	Y	Y	Y	Y	Y	Y	N	Y	Y
	Monowai Caldera	Y	Y	Y	Y	Y	Y	Y	Y	Y	Y	Y	N	Y	Y

6.5 Offshore Ferromanganese Nodules

6.5.1 Introduction and Overview

Ferromanganese nodules (also known as polymetallic nodules) are accretions of manganese oxides and iron oxyhydroxides up to tens of centimetres in diameter, onto which metals such as cobalt (Co), nickel (Ni), copper (Cu), molybdenum (Mo), lithium (Li), titanium (Ti) and REE, as well as yttrium (REY) are scavenged. These form on or just below the sea floor on the abyssal plains of the deep ocean via precipitation from either ocean water or sediment pore water (e.g. Hein et al. 2020). Ferromanganese nodules cover vast areas of the global ocean floor, particularly in deep water (~3500–6500 m, below the carbonate compensation depth) where sedimentation is slow and bottom waters are well oxygenated.

Internally, ferromanganese nodules are concentrically layered and have numerous pores containing trapped silicate minerals and microfossils (Figure 6.8). Although relatively heavy and denser than sediment, they maintain their growth position on the seafloor for long periods of time via bottom currents winnowing away loose sediment that builds up around them as they rest on more-compacted sediment beneath.

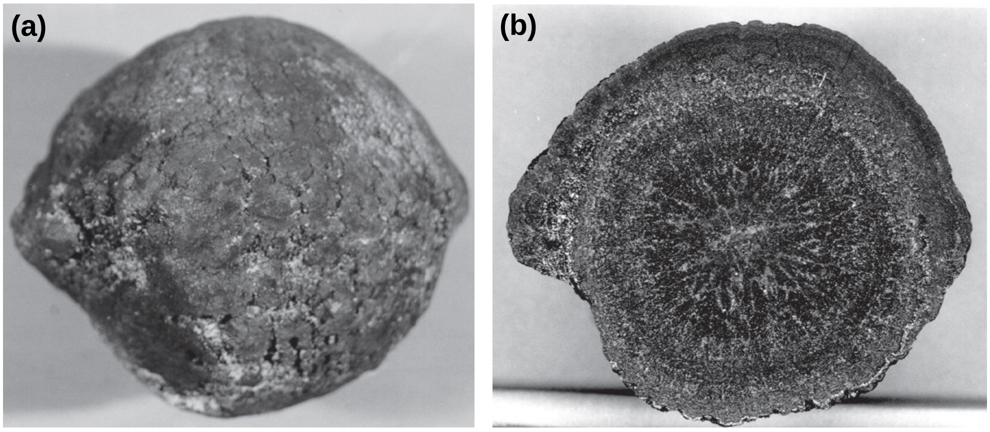

Figure 6.8 Discoidal shaped ferromanganese nodule from site U1413-1 (Latitude 49°30.0' S; Longitude 178°37.2' E; see Part 1, Figure 11.3): (a) Whole sample showing rough outer surface, with preferred growth along an equatorial plane. (b) Cross-section showing internal concentric layering with 'overgrowth' feature, possibly caused by over-crowding. Scale bars = 1 cm (after Graham and Wright [2006]).

There are two types of nodules, both of which require a nucleus (e.g. a rock, bone or tooth) around which metallic layers can precipitate (Figure 6.9). Hydrogenetic nodules form directly from oxygen-rich ocean waters via oxidation of dissolved Mn^{2+} and Fe^{2+}, which drives precipitation of Mn and Fe oxide colloids. These nodules form at very slow rates (a few millimetres per million years) and tend to contain roughly equal amounts of Fe and Mn (bulk Fe/Mn ~1) and very high concentrations of Co, Te, Ce and Pt. Diagenetic nodules form via precipitation from sediment-pore fluids just below the sea floor at faster rates of a few tens of millimetres per million years. These nodules are generally more Mn-rich (bulk Mn/Fe >10) and contain high levels of Ni, Cu and Li.

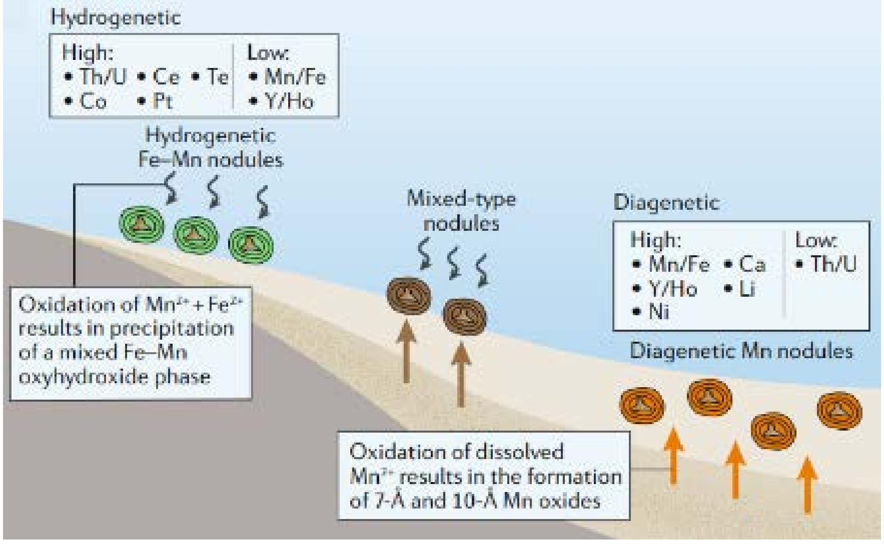

Figure 6.9 Schematic showing formation of hydrogenetic nodules via precipitation from seawater on the ocean floor, as well as diagenetic nodules via precipitation from pore fluids below the sediment-seawater interface. Mixed nodule types involve both precipitation mechanisms (after Hein et al. [2020]).

6.5.2 Distribution

Large nodule fields are common in the world's abyssal ocean, although most are in areas beyond national jurisdiction. Most well-studied fields are in the Pacific Ocean (e.g. Peru Basin and Penrhyn Basin-Cook Islands).

A large nodule field abuts the southeastern slope of the Campbell Plateau and extends into the Southwest Pacific Basin, beneath the Deep Western Boundary Current (DWBC) and Antarctic Circumpolar Current (ACC) (e.g. Carter 1989; Carter and McCave 1997). The field is inferred to be some 300–500 km wide in areas west of 174°E, between 59 and 48°S. Further east, it narrows to ~200 km at 55°S and 120 km at 49°S as the bottom currents are deflected eastward (Wright et al. 2005). Much of this field is within New Zealand's EEZ and/or Extended Continental Shelf.

The distribution of nodules within the northeastern sector of the Campbell field (the part closest to New Zealand) has been characterised in detail based on seafloor mapping (3.5 kHz profiling), photography and dredge sampling (Chang et al. 2003a, 2003b; Wright et al. 2005; Graham and Wright 2006). Here, abundant nodules form the substrate on undulating abyssal hills, locally eroded by scouring from the DWBC/ACC. The largest and oldest (~200 mm and 15 million years old [Graham et al. 2003]) nodules occur beneath the main flow axis of the DWBC-ACC. The seafloor density (i.e. areal coverage) of nodules in the southern part of this northeast sector increases eastward from <25% at the lower Campbell Slope to up to 84% on the Campbell skin drift. In the northern part of this sector, the highest densities (up to 90%) are on the lower Campbell Slope, decreasing to patchy coverage of 25–35% further east. No detailed studies of the distributions or compositions of nodules have been undertaken in other sectors of the field, adjacent to the southern or western Campbell Plateau. Estimates of seafloor densities vary here, from >75% (e.g. Glasby 1976) to patchier distributions of 25–75% (Carter and McCave 1997; Carter and Wilkin 1999).

6.5.3 Nodule Compositions and Economic Potential

The compositions of individual nodule layers and bulk samples from two dredge transects in the northeast sector of the Campbell field were studied by Chang et al. (2003b). Both were found to vary widely (e.g. Cu from 280 to 3100 ppm, Co from 320 to 4600 ppm [Table 6.2]), although most fall within the range typical of hydrogenetic growth (Mn/Fe <1). More recently, Davies (2018) analysed the outer-most rims (<1 mm) of nodules from these same transects and an additional site on the southwest corner of the Campbell Plateau. Her dataset includes a wider suite of elements and also highlights the dominance of hydrogenetic growth regimes, but it is of limited use for assessing bulk compositions and the overall resource.

Table 6.2 Mean concentrations of selected elements in nodules from the northeast part of the Campbell field (data from Chang et al. [2003b]) and four other fields in the Pacific and Indian Oceans (data compiled by Hein et al. [2020]). n.d. = Not determined.

	Northeast Campbell Field	Cook Island – Penrhyn Basin	Clarion-Clipperton Zone (Central-Eastern Pacific)	Central Indian Ocean Basin	Peru Basin
Fe/Mn	1.08	0.96	0.22	0.21	0.25
Mn (wt%)	15.17	16.9	28.4	24.4	34.2
Fe (wt%)	16.37	16.2	6.16	7.14	6.12
Ni (wt%)	0.27	0.377	1.3	1.1	1.3
Cu (wt%)	0.11	0.23	1.07	1.04	0.60
Ti (wt%)	0.90	1.28	0.32	0.42	0.16
Co (wt%)	0.15	0.375	0.21	0.111	0.048
Mo (ppm)	198	295	590	600	547
Total REE (ppm)	1535	1537	717	931	334
V (ppm)	298	504	445	497	431
Zr (ppm)	346	555	307	752	325
Tl (ppm)	n.d.	146	199	347	129
Li (ppm)	n.d.	51	131	110	311
Y (ppm)	101	141	96	108	69
As (ppm)	98	150	67	150	65
W (ppm)	n.d.	59	62	92	75

Based on an average nodule size of 3 cm, mass of 0.3 kg and seafloor density of 50%, Graham and Wright (2006) estimated a total mass of 2 x 10^9 kg for ferromanganese nodules within the 50,000 km^2 northeast part of the Campbell field. Taking average compositions from Chang et al. (2003b), these were equated to resources of 5 x 10^6 t of Ni, 2 x 10^6 t of Cu and 3 x 10^6 t of Co (of which 60–70% lies within New Zealand's EEZ). These resources were considered uneconomic at that time, given commodity prices and recovery costs. The average combined Ni + Cu + Co contents for the Campbell nodules are below the ~2–3 wt% cut-off that has more recently been considered to define 'resource-grade' nodules (e.g. Hein et al. 2020; Verlaan and Cronan 2022). However, the areal density of nodules and concentrations of other critical metals needs to be considered for a robust and up-to-date assessment of economic potential for the Campbell field. As for the Cook Islands–Penrhyn Basin nodules (Hein et al. 2015), relatively high Ti and REY contents of the Campbell nodules may make these a viable prospect despite their low Cu + Ni and modest Co contents (Table 6.2). The bulk abundances of a number of economically important metals (e.g. Li, Tl, W, Te, Pt) in the Campbell nodules are unknown and should be quantified as part of a more complete assessment of this resource.

Key References: Carter (1989); Carter and McCave (1997); Graham and Wright (2006).

7.0 OFFSHORE NON-METALLIC MINERALS

7.1 Chatham Rise Phosphorite

Deposits of phosphorite lie on the crest of the Chatham Rise at water depths of between 350 and 450 m (Cullen 1989) and were formed about 5 million years ago by phosphatisation of Miocene chalk (McArthur et al. 1990). The phosphorite occurs as irregularly shaped grains and nodules, ranging in size from 0.5 to 350 mm. The nodules lie on and within a thin layer of phosphorite-bearing glauconitic sand with an average thickness of 0.2 m but can reach thicknesses of more than 0.5 m in places. The sand layer consists of mainly silt and sand-sized sediments with the phosphorite nodules. The layers would have been originally stratified with phosphorite nodule layers, representing the periods of erosion and phosphatisation; however, later post-depositional modifications have resulted in these layers becoming disrupted. The underlying chalk layer occurs as a white ooze at the base on the sand. The upper 20–30 cm of this zone can be mixed due to bioturbation and include burrows filled with the overlying sand. The ooze also contains weathered chalk, an important constituent for phosphorite nodule formation. At depth, the ooze grades into an indurated chalk layer.

Phosphatisation is due to upwelling of nutrient-rich seawater. The flux of dead organic matter from high-productive waters to the seafloor supplies the phosphorus to the anoxic seabed. The decay of the organic matter and corresponding release of phosphorus from sulfate-reducing bacteria results in the precipitation of phosphorite (Wood et al. 2015; Wood and Falconer 2016). The Cenozoic-age chalk layers exposed on the central Chatham Rise provide the material for phosphorite nodules to form. The chalky seabed was intensively phosphatised, and biological activity produced the phosphoritic nodules as a lag deposit in the top sedimentary layer. When phosphatisation ceased, the phosphoritic nodules were coated with the mineral glauconite, protecting them from dissolution on the seabed.

Chemical analyses of the phosphorite nodules measured the abundance of major oxides and key environmental trace elements (Table 7.1). Analysis of trace elements in the phosphorite nodules showed that, compared to other phosphorite sources, cadmium levels are extremely low (Table 7.1) and that uranium abundance is somewhat elevated.

Table 7.1 Trace element abundances in Chatham Rise sediments, phosphorite nodules and glauconite-rich sands (after Wood and Falconer [2016]). Note: All units are mg/kg dry weight.

Parameter	**Phosphorite (Global)** [1]	**Coarse (>8 mm) Chatham Rise Phosphorites** [2]	**Fine (<8 mm) Chatham Rise Phosphorites** [3]
Arsenic	2–23	11 (5–39)	39 (5–79)
Barium	-	63 (0–300)	36 (4–140)
Cadmium	0.1–510	$<2^{-3}$	$<2^{-3}$
Chromium	1–160	0 (0–30)	9 (0–24)
Cobalt	0.37–385	14 (0–26)	15 (1–33)
Copper	5.5–130	10 (5–85)	7 (5–69)
Lead	50	7.0 (5.0–16)	15 (5–24)
Molybdenum	-	6.0 (3.0–17)	7.0 (3.0–10)
Nickel	2–120	15 (6–37)	30 (14–59)
Rubidium	-	16 (5–27)	52 (8–64)

Parameter	Phosphorite (Global) [1]	Coarse (>8 mm) Chatham Rise Phosphorites [2]	Fine (<8 mm) Chatham Rise Phosphorites [3]
Strontium	-	1600 (1400–1800)	1300 (1200–1700)
Thallium	-	12 (9–19)	11 (6–15)
Uranium	64–140	240 (20–480)	170 (120–310)
Vanadium	-	56 (0–140)	74 (61–91)
Yttrium	-	25 (19–54)	49 (23–91)
Zinc	6–520	11 (5–30)	22 (9–80)
Zirconium	-	5.0 (5.0–14)	12 (5–23)

[1] Aydin et al. (2010), except cadmium (Mar and Okazaki 2012), arsenic and uranium (Syers et al. 1986).

[2] Data from *R/V Sonne* survey, median data with range in parentheses.

[3] DD-4 median data with range in parentheses; n = 13.*n = 46, **n = 31.

7.1.1 Exploration

The Chatham Rise phosphorite deposits were discovered in 1952 when New Zealand Geological Survey geoscientists on board the *RRS Discovery II* dredged phosphorite from the seabed on the crest of the Chatham Rise. Between 1966 and 1981, several surveys and studies were undertaken for exploration by Global Marine Incorporated (1967–1968), JBL Exploration (NZ) New Zealand (1971) and Fletcher Challenge, as well as for research by the New Zealand Oceanographic Institute in collaboration with the German Geological Survey, resulting in research voyages by the *R/V Valdivia* (1978) and *R/V Sonne* (1981) and collection of more than 1100 seafloor samples (Table 7.2). In 2008, Chatham Rock Phosphate (CRP) was granted an exploration permit covering c. 3900 km^2 of the area identified as the most prospective by the earlier studies, and in 2011 it was granted a mining permit for the central 820 km^2 of the prospecting permit. Exploration by CRP included six cruises in the project area in 2011 and 2012, using the *M/V Tranquil Image* and *R/V Dorado* to validate the previous work and collect further geological, geotechnical, geophysical and environmental data. This work included collection of multi-beam bathymetry, side-scan sonar, magnetic data, additional seafloor samples for geological analysis and cone penetration test measurements of the physical properties of the sea floor. Seafloor traverses completed by the CRP surveys, and another by NIWA in 2013, used an ROV and deep-towed camera system to collect video and still images of the sea floor and samples of benthic fauna. Box cores were also collected along these traverses and analysed for infauna. In collaboration with its research partner, Royal Boskalis Westminster NV (‘Boskalis’), CRP proposed a mining system based on a conventional trailing suction hopper dredge, adapted for greater depth on the Chatham Rise. A mining permit was granted in December 2013 for a duration of 20 years but, in February 2015, New Zealand’s Environmental Protection Agency turned down CRP’s application for an environmental consent to begin mining. CRP is yet to re-apply.

Table 7.2 Exploration and sampling surveys of the Chatham Rise phosphorite.

Company or Vessel	Survey Dates	Seafloor Sampling Methods	Seafloor Sample Area	Sampling Depth
Global Marine Inc.	1967–1968	45-cm-diameter pipe dredge	-	-
R/V Tangaroa	1975–1978	No information	No information	No information
R/V Valdvia	1978	0.12 m^3 grab	45 x 45 cm to 66 x 66 cm	33 cm
R/V Sonne	1981	0.8 m^3 grab	1.06 x 1.90 m	38 cm
R/V Tranquil Image	2011	Van Veen grab sampler	0.25 m^2	-
R/V Dorado Discovery	2011–2012	Clamshell grab	2.03 x 1.42 m	-
		Box corer	20 x 30 cm to 50 x 50 cm	50 cm

7.1.2 Resources

Sterk (2014) reported a global JORC Inferred Mineral Resource totalling 80 Mm^3 at an average grade of 290 kg/m^3 and a cut-off grade of 100 kg/m^3 for a total contained 23.4 Mt of phosphorite (Table 7.3). The phosphorite is suggested to have an average grade of 18–19% P_2O_5 (of screened material). The average thickness of the resource is 0.20 m. The resource has an E–W extent of 60 km and N–S extent of 10–30 km. Additional exploration potential is in the order of 40 Mm^3, with 8–12 Mt of contained phosphorite at grades between 200 and 300 kg/m^3.

Table 7.3 Statement of Mineral Resources (phosphorite) for Mining Permit 55549, Chatham Rise (after Sterk [2014]). Estimates are rounded to reflect the level of confidence in these resources.

Classification	Volume (m^3)	Thickness (cm)	Ph kg/m^3	Contained Ph Mt
Inferred	80,000,000	20	290	23.4

Notes: The Mineral Resource is reported in accordance with the JORC Code, 2012 edition. The Mineral Resource is contained within MP 55549. All resources have been rounded to the nearest 0.1 Mt. Ph kg/m^3 is the weight of phosphorite per cubic metre. Contained Ph Mt is contained weight of phosphorite per million tonnes. Even though a representative average grade for the specification (phosphate grade) cannot be determined for the Mineral Resource, the tenor of the specification (in the order of 18–19% P_2O_5 of screened material) is suitable to allow classification into the Inferred Resource category. Mineral Resource is reported at 100 kg/m_3 cut-off grade.

Key References: Cullen (1989); Sterk (2014); Wood et al. (2015); Wood and Falconer (2016).

8.0 ACKNOWLEDGEMENTS

The manuscript was reviewed by Lyndon Murray, Tim Journeaux, Aidan Allan and Andy O'Loan of the Ministry of Business, Innovation & Employment (MBIE) and Phaedra Upton, Nyree Hill (Part 1) and Kevin Faure (Part 2) of GNS Science. Funding for the study was provided by MBIE. Coordination and general management of the project was provided by Kate Osborn, Business Development Manager – Environment and Climate, GNS Science. Kate Robb, Document Specialist Lead, GNS Science, checked and formatted the final version of the report.

9.0 REFERENCES

Adams CJ, Beck RJ, Campbell HJ. 2007. Characterisation and origin of New Zealand nephrite jade using its strontium isotopic signature. *Lithos*. 97(3):307–322. https://doi.org/10.1016/j.lithos.2007.01.001

[AGA] Alpine Geophysical Associates. 1968. Final report on the sparker survey of marine mining concession in New Zealand. Located at: Ministry of Business, Innovation & Employment, Wellington, NZ. 133 p. + enclosures. New Zealand Unpublished Mineral Report 2017.

Aldrich S. 2024. Technical report on the Reefton project, New Zealand. Dunedin (NZ): RSC Mining & Mineral Exploration. 172 p. Report. Prepared for Rua Gold; [accessed 2024 Jun]. https://ruagold.com/wp-content/uploads/2024/04/RUA-43-101-Technical-Report-UPDATED-April-18_-202443696308.1.docx.pdf

Allibone A, Jones P, Moore J, Craw D, MacKenzie DJ, Blakemore H. 2017. Kilometre-scale structural setting of ore shoots in the Frasers gold deposit, Macraes mine, New Zealand. *Ore Geology Reviews*. 89:1107–1121. https://doi.org/10.1016/j.oregeorev.2017.05.019

Allibone A, Blakemore, H, Gane J, MacKenzie D, Craw D. 2018a. Contrasting structural styles of orogenic gold deposits, Reefton Goldfield, New Zealand. *Economic Geology*. 113(7):1479–1497. https://doi.org/10.5382/econgeo.2018.4599

Allibone A, Jones P, Blakemore, H, Craw D, MacKenzie D, Moore J. 2018b. Structural setting of gold mineralisation within the Hyde-Macraes Shear Zone, southern New Zealand. *Economic Geology*. 113(2):347–375. https://doi.org/10.5382/econgeo.2018.4553

Angus P, Jongens R, Phillips M, McCulloch M, Nazimova Y, Ryan G. 2016. Exploration update (2011–2015) on the Sams Creek porphyry gold deposit, North-west Nelson. In: Christie AB, editor. *Mineral deposits of New Zealand: exploration and research*. Carlton (AU): Australian Institute of Mining and Metallurgy. p. 209–216. (Australasian Institute of Mining and Metallurgy monograph series; 31).

[AQA] Aggregate and Quarry Association. 2020. A briefing on the quarry sector and aggregate supply. Wellington (NZ): AQA; [accessed 2024 Jun]. https://www.aqa.org.nz/uploads/files/AQA%20Flyer_web%20file%20size%20small.pdf

[AQA] Aggregate and Quarry Association. 2024. New Zealand Quarry Database. Wellington (NZ): AQA.

Ashley P, Craw D, Mackenzie D, Rombouts M, Reay A. 2012. Mafic and ultramafic rocks, and platinum mineralisation potential, in the Longwood Range, Southland, New Zealand. *New Zealand Journal of Geology and Geophysics.* 55(1):3–19. https://doi.org/10.1080/00288306.2011.623302

Aydin I, Aydin F, Saydut A, Bakirdere EG, Hamamci C. 2010. Hazardous metal geochemistry of sedimentary phosphate rock used for fertilizer (Mazıdag, SE Anatolia, Turkey). *Microchemical Journal*. 96(2):247–251. https://doi.org/10.1016/j.microc.2010.03.006

Baker ET, Feely RA, de Ronde CEJ, Massoth GJ, Wright IC. 2003. Submarine hydrothermal venting on the southern Kermadec volcanic arc front (offshore New Zealand): location and extent of particle plume signatures. In: Larter RD, Leat PT, editors. *Intra-oceanic subduction systems: tectonic and magmatic processes*. London (GB): Geological Society of London. p. 141–161. (Geological Society special publication; 219). https://doi.org/10.1144/GSL.SP.2003.219.01.07

Baker T, Pollard PJ, Mustard R, Mark G, Graham JL. 2005. A comparison of granite-related tin, tungsten, and gold-bismuth deposits: implications for exploration. *SEG Newsletter*. 61:5–17. https://doi.org/10.5382/SEGnews.2005-61.fea

Barker RG, Christie AB. 2016a. Exploration for epithermal gold-silver deposits in the Hauraki Goldfield, North Island. In: Christie AB, editor. *Mineral deposits of New Zealand: exploration and research*. Carlton (AU): Australian Institute of Mining and Metallurgy. p. 225–236. (Australasian Institute of Mining and Metallurgy monograph series; 31).

Barker RG, Christie AB. 2016b. Exploration for epithermal gold-silver deposits in the Taupō Volcanic Zone, North Island, New Zealand. In: Christie AB, editor. *Mineral deposits of New Zealand: exploration and research*. Carlton (AU): Australian Institute of Mining and Metallurgy. p. 325–332. (Australasian Institute of Mining and Metallurgy monograph series; 31).

Barker RG, Christie AB. 2016c. Mineral exploration in the Northland Region. In: Christie AB, editor. *Mineral deposits of New Zealand: exploration and research*. Carlton (AU): Australian Institute of Mining and Metallurgy. p. 61–69. (Australasian Institute of Mining and Metallurgy monograph series; 31).

Barry JM. 1993. The history and mineral resources of the Reefton Goldfield. Wellington (NZ): Ministry of Commerce, Energy and Resources Division. 59 p. Report 15.

Barry JM. 1996. Mining history and geology of the Alpine Reef, Lyell Goldfield. In: *29th annual conference 1996: the changing face of West Coast mining*; 1996 Aug 20–23; Greymouth, New Zealand. Wellington (NZ): Australasian Institute of Mining and Metallurgy, New Zealand Branch. p. 3–46.

Barry JM, Duff SW, MacFarlan DAB. 1994. Coal resources of New Zealand. Wellington (NZ): Ministry of Commerce, Energy and Resources Division. 80 p. Report 16.

Bates TE. 1978. Final report on mineral exploration within prospecting licence 31253 Cascade Creek, Buller Gorge. Located at: Ministry of Business, Innovation & Employment, Wellington, NZ. 31 p. + 2 enclosures. New Zealand Unpublished Mineral Report 1337.

Bates TE. 1989a. Copper and nickel mineralisation in the Riwaka Complex, Northwest Nelson. In: Kear D, editor. *Mineral deposits of New Zealand*. Parkville (AU): Australasian Institute of Mining and Metallurgy. p. 119–123. (Australasian Institute of Mining and Metallurgy monograph series; 13).

Bates TE. 1989b. Te Aroha goldfield – Tui and Waiorongomai gold/silver/base metal prospects. In: Kear D, editor. *Mineral deposits of New Zealand*. Parkville (AU): Australasian Institute of Mining and Metallurgy. p. 79–81. (Australasian Institute of Mining and Metallurgy monograph series; 13).

Beach V, Hobbins JM. 2016. Puhipuhi – a high-level epithermal gold-silver prospect in Northland. In: Christie AB, editor. *Mineral deposits of New Zealand: exploration and research*. Carlton (AU): Australian Institute of Mining and Metallurgy. p. 219–224. (Australasian Institute of Mining and Metallurgy monograph series; 31).

Beck AC. 1965. Arahura River copper. *New Zealand Journal of Geology and Geophysics*. 8(6):1233–1238. https://doi.org/10.1080/00288306.1965.10428172

Beck RJ. 1984. New Zealand jade. Wellington (NZ): Reed. 173 p.

Beck RJ, Mason M. 2002. Mana pounamu: New Zealand jade. Auckland (NZ): Reed. 180 p.

Becker WN, Batt WD 2016. Waikaia placer gold mine, Southland. In: Christie AB, editor. *Mineral deposits of New Zealand: exploration and research*. Carlton (AU): Australian Institute of Mining and Metallurgy. p. 387–394. (Australasian Institute of Mining and Metallurgy monograph series; 31).

Bell JM, de C Clarke E. 1909. The geology of the Whangaroa subdivision, Hokianga division. Wellington (NZ): Department of Mines, New Zealand Geological Survey. 115 p. (New Zealand Geological Survey bulletin; 8).

Bell JM, de Courcy Clarke E, Marshall P. 1911. The geology of the Dun Mountain subdivision, Nelson. Wellington (NZ): Department of Mines, New Zealand Geological Survey. 71 p. (New Zealand Geological Survey bulletin; 12).

Bennett MC. 1976. The ultramafic-mafic complex at North Cape, northernmost New Zealand. *Geological Magazine.* 113:61–76.

Berkenbosch HA, de Ronde CEJ, Gemmell JB, McNeill AW, Goemann K. 2012. Mineralogy and formation of black smoker chimneys from Brothers submarine volcano, Kermadec Arc. *Economic Geology*. 107(8):1613–1633. https://doi.org/10.2113/econgeo.107.8.1613

Bishop DG, Braithwaite JC. 1969. Dolomite at Mt Burnett, Northwest Nelson. In: *The AusIMM proceedings 1969.* [Carlton (AU)]: Australasian Institute of Mining and Metallurgy. https://www.ausimm.com/publications/conference-proceedings/the-ausimm-proceedings-1969/dolomite-at-mount-burnett-north-west-nelson-new-zealand/

Black PM. 2009. Geologic inventory of North Island aggregate resources: influences on engineering materials properties [draft]. [Wellington] (NZ): Aggregate & Quarry Association (AQA); [accessed 2024 Jun]. www.aqa.org.nz/uploads/files/North%20Island%20Geological%20Inventory%202009.pdf

Black PM. 2014. South Island aggregate inventory: geological influences on materials properties [draft]. [Wellington] (NZ): Aggregate & Quarry Association (AQA); [accessed 2024 Jun]. www.aqa.org.nz/uploads/files/South%20Island%20Geological%20Inventory%202014.pdf

Bradley DC, McCauley AD, Stillings LM. 2017. Mineral-deposit model for lithium-cesium-tantalum pegmatites. Reston (VA): U.S. Geological Survey. 48 p. Scientific Investigations Report 2010–5070–O. https://doi.org/10.3133/sir20105070O

Braithwaite JC, Buckenham MH, Watters WA. 1976. Holyoake Valley wollastonite. *Industrial Minerals and Rocks*. 7:9–19.

Brathwaite RL. 1990. Ironsand resources of the west coast, North Island. Lower Hutt (NZ): Department of Scientific and Industrial Research, Geology and Geophysics. Contract Report 1990/5. Prepared for Electricorp Marketing, Hamilton.

Brathwaite RL. 2003. Geological and mineralogical characterization of zeolites in lacustrine tuffs, Ngakuru, Taupō Volcanic Zone, New Zealand. *Clays and Clay Minerals.* 51(6):589–598. https://doi.org/10.1346/CCMN.2003.0510601

Brathwaite RL. 2017. Zeolites in New Zealand and their use as environmental minerals. Lower Hutt (NZ): GNS Science. 27 p. (GNS Science report; 2017/27). https://doi.rg/10.21420/G2KP89

Brathwaite RL, Christie AB. 2006. Review of shoreline placer ilmenite deposits in New Zealand. In: Christie AB, Brathwaite RL, editors. *Geology and exploration of New Zealand mineral deposits*. Parkville (AU): Australasian Institute of Mining and Metallurgy. p. 43–48. (Australasian Institute of Mining and Metallurgy monograph series; 25).

Brathwaite RL, Christie AB. 2014. Titanomagnetite provenance in ironsands on the west coast of the North Island of New Zealand. In: Rendell C, editor. *47th New Zealand Branch annual conference on exploration, mining and New Zealand's mineral resources: conference proceedings;* 2014 Aug 24–27; Hamilton, New Zealand. [Place unknown] (NZ): Australasian Institute of Mining and Metallurgy, New Zealand Branch. p. 87–94.

Brathwaite RL, Christie AB. 2015. The contribution of titanomagnetite from the Taupō Volcanic Zone to ironsands on the west coast of the North Island of New Zealand. In: Sterk R, editor. *48th New Zealand Branch annual conference on exploration, mining and New Zealand's mineral resources: conference proceedings;* 2015 Aug 30 – Sep 2; Dunedin, New Zealand. [Place unknown] (NZ): Australasian Institute of Mining and Metallurgy, New Zealand Branch. p. 53–65.

Brathwaite RL, Christie AB. 2016. The rhyolite-hosted Matauri Bay and Maungaparerua halloysite clay deposits, Northland. In: Christie AB, editor. *Mineral deposits of New Zealand: exploration and research*. Carlton (AU): Australasian Institute of Mining and Metallurgy. p. 495–501. (Australasian Institute of Mining and Metallurgy monograph series; 31).

Brathwaite RL, Faure K. 2002. The Waihi gold-silver-base metal sulphide-quartz vein system, New Zealand: temperature and salinity controls on electrum and sulphide deposition. *Economic Geology*. 97:269–290. https://doi.org/10.2113/gsecongeo.97.2.269

Brathwaite RL, Henderson SM. 2016. Epithermal zeolite and gold-silver mineralisation in the Ngakuru Area, Taupō Volcanic Zone. In: Christie AB, editor. *Mineral deposits of New Zealand: exploration and research*. Carlton (AU): Australasian Institute of Mining and Metallurgy. p. 503–509. (Australasian Institute of Mining and Metallurgy monograph series; 31).

Brathwaite RL, Pirajno F. 1993. Metallogenic map of New Zealand. Lower Hutt (NZ): Institute of Geological and Nuclear Sciences. 215 p. (Institute of Geological & Nuclear Sciences monograph; 3).

Brathwaite RL, Rae AJ. 2021. Epithermal zeolite alteration associated with siliceous sinters, hydrothermal eruption breccias, and gold-silver mineralization, central Taupo Volcanic Zone, New Zealand. *Economic Geology.* 116(5):1093–1114. https://doi.org/10.5382/econgeo.4820

Brathwaite RL, Christie AB, Skinner DNB. 1989. The Hauraki goldfield – regional setting, mineralisation and recent exploration. In: Kear D, editor. *Mineral deposits of New Zealand*. Parkville (AU): Australasian Institute of Mining and Metallurgy. p. 45–56. (Australasian Institute of Mining and Metallurgy monograph series; 13).

Brathwaite RL, Isaac MJ, Challis GA, Brook FJ. 1990. Tertiary limestone and Zn-Pb mineralised skarn at Motukokako, Cape Brett, northern New Zealand. *Journal of the Royal Society of New Zealand.* 20(4):427–438.

Brathwaite RL, Simpson MP, Faure K, Skinner DNB. 2001. Telescoped porphyry Cu-Mo-Au, advanced argillic alteration and polymetallic quartz-sulfide-gold-anhydrite veins in the Thames District, New Zealand. *Mineralium Deposita*. 36(7):623–640. https://doi.org/10.1007/s001260100182

Brathwaite RL, Kamo SL, Faure K. 2004. U-Pb geochronology and geochemistry of molybdenum-bearing granodiorite porphyry at Copperstain Creek, west Nelson, New Zealand. *New Zealand Journal of Geology & Geophysics*. 47(2):219–225. https://doi.org/10.1080/00288306.2004.9515049

Brathwaite RL, Reynolds LJ, Faure K. 2006. Geology and exploration of the Sams Creek gold deposit, Northwest Nelson. In: Christie AB, Brathwaite RL, editors. *Geology and exploration of New Zealand mineral deposits*. Parkville (AU): Australasian Institute of Mining and Metallurgy. p. 247–252. (Australasian Institute of Mining and Metallurgy monograph series; 25).

Brathwaite RL, Sewell RJ, Christie AB. 2008. Nature and tectonic setting of massive sulfide mineralisation and associated sediments and volcanics in the Matakaoa Volcanics, Raukumara Peninsula, New Zealand. *New Zealand Journal of Geology and Geophysics*. 51(4):349–366. https://doi.org/10.1080/00288300809509870

Brathwaite RL, Christie AB, Faure K, Townsend MG, Terlesk S. 2012a. Origin of the Matauri Bay halloysite deposit, Northland, New Zealand. *Mineralium Deposita*. 47(8):897–910. https://doi.org/10.1007/s00126-012-0404-9

Brathwaite RL, Christie AB, Lukovic B. 2012b. Desktop study documenting the occurrence and geological characteristics of known VMS deposits associated with Northland's Tangihua Complex. Lower Hutt (NZ): Institute of Geological and Nuclear Sciences. 43 p. (GNS Science report; 2012/08).

Brathwaite RL, Jongens RJ, Christie AB, Lukovic B. 2012c. Dun Mountain Ophiolite Belt, East Nelson: desktop study and geochemical survey for chromite ± PGE deposits and Cu-rich VMS deposits. Lower Hutt (NZ): GNS Science. 43 p. + appendices. (GNS Science report; 2012/10).

Brathwaite RL, Christie AB, Faure K, Townsend MG, Terlesk S. 2014. Geology, mineralogy and geochemistry of the rhyolite-hosted Maungaparerua clay deposit, Northland. *New Zealand Journal of Geology and Geophysics.* 57(4):357–368. https://doi.org/10.1080/00288306.2014.920889

Brathwaite RL Christie AB, Jongens R. 2016. Exploration for chromite, platinum group element and nickel mineralisation in the Dun Mountain Ophiolite Belt, East Nelson. In: Christie AB, editor. *Mineral deposits of New Zealand: exploration and research*. Carlton (AU): Australasian Institute of Mining and Metallurgy. p. 463–470. (Australasian Institute of Mining and Metallurgy monograph series; 31).

Brathwaite RL, Christie AB, Gazley MF. 2021. Stratigraphy, provenance and localisation of the titanomagnetite placer at Waikato North Head, South Auckland, New Zealand. *Mineralium Deposita.* 56:343–362. https://doi.org/10.1007/s00126-020-00968-8

Bridson J. 2014. PP53798 – Otaka glauconite technical report – 2014. Located at: Ministry of Business, Innovation & Employment, Wellington, NZ. 18 p. + 1 enclosure. New Zealand Unpublished Mineral Report 5109.

Bridson J. 2015a. Annual progress report on PP 53798 to May 2015. Located at: Ministry of Business, Innovation & Employment, Wellington, NZ. 13 p. New Zealand Unpublished Mineral Report 5220.

Bridson J. 2015b. Surrender report on MPP 53798 – July 2015. Located at: Ministry of Business, Innovation & Employment, Wellington, NZ. 19 p. New Zealand Unpublished Mineral Report 5227.

Bridson J. 2015c. Surrender report for PP 55454, Nelson 2015. Located at: Ministry of Business, Innovation & Employment, Wellington, NZ. 7 p. New Zealand Unpublished Mineral Report 5221.

Briggs RM, Laurent JC, Hume TM, Swales A. 2009. Provenance of black sands on the west coast, North Island, New Zealand. In: *Proceedings of the 42nd New Zealand Branch annual conference: the NZ minerals industry – meeting the challenge*; 2009 Aug 25–28; Queenstown, New Zealand. [Place unknown] (NZ): Australasian Institute of Mining and Metallurgy, New Zealand Branch. p. 41–50.

Britten R. 2017. Regional metallogeny and genesis of a new deposit type – disseminated awaruite (Ni_3Fe) mineralisation hosted in the Cache Creek terrane. *Economic Geology*. 112(3):517–550. https://doi.org/10.2113/econgeo.112.3.517

Campbell HJ, Adams CJ, Beck RJ. 2008. Characterisation of New Zealand nephrite jade (pounamu) using strontium isotopes. *Archaeology in New Zealand*. 51(3):154.

Canyon Resources Pty Ltd. 1984. Progress report Aorere prospect, Northwest Nelson, New Zealand (PL 31723). Located at: Ministry of Business, Innovation & Employment, Wellington, NZ. 13 p. + 4 enclosures. New Zealand Unpublished Mineral Report 983.

Caratori Tontini F, de Ronde CEJ. 2016. Structural control on the development of submarine volcano hydrothermal systems in the Kermadec arc: near-sea floor magnetic mapping by Autonomous Underwater Vehicles. In: Christie AB, editor. *Mineral deposits of New Zealand: exploration and research*. Carlton (AU): Australasian Institute of Mining and Metallurgy. p. 403–412. (Australasian Institute of Mining and Metallurgy monograph series; 31).

Caratori Tontini F, Davy B, De Ronde CEJ, Embley RW, Leybourne M, Tivey MA. 2012. Crustal magnetization of Brothers Volcano, New Zealand, measured by autonomous underwater vehicles: geophysical expression of a submarine hydrothermal system. *Economic Geology*. 107(8):1571–1581. https://doi.org/10.2113/econgeo.107.8.1571

Carr RG, Rodgers KA, Black PM. 1980. The chemical and mineralogical changes accompanying the laterization of basalt at Kerikeri, North Auckland. *Journal of the Royal Society of New Zealand.* 10(3):247–258. https://doi.org/10.1080/03036758.1980.10415331

Carter L. 1980. Ironsand in continental shelf sediments off western New Zealand: a synopsis. *New Zealand Journal of Geology and Geophysics*. 23(4):455–468. https://doi.org/10.1080/00288306.1980.10424116

Carter L. 1989. New occurrences of manganese nodules in the Southwest Pacific Basin east of New Zealand. *New Zealand Journal of Marine and Freshwater Research.* 23(2):247–253. https://doi.org/10.1080/00288330.1989.9516361

Carter L, McCave IN. 1997. The sedimentary regime beneath the Deep Western Boundary Current inflow to the Southwest Pacific Ocean. *Journal of Sedimentary Research*. 67(6):1005–1017. https://doi.org/10.1306/D42686B2-2B26-11D7-8648000102C1865D

Carter L, Wilkin J. 1999. Abyssal circulation around New Zealand: a comparison between observations and a global circulation model. *Marine Geology.* 159:221–239. https://doi.org/10.1016/S0025-3227(98)00205-9

Carver R. 2009. Appendix 2 – Notes on the west Nelson geochemical data: stream sediment statistics and contours. In: Christie AB, Rattenbury MS, Brathwaite RL, Mortimer N, Tulloch AJ. *Mineral resource assessment of Kahurangi National Park, West Nelson*. Lower Hutt (NZ): GNS Science. Consultancy Report 2009/317. Prepared for Crown Minerals.

Challis GA. 1989. Platinum group metals in New Zealand. In: Kear D, editor. *Mineral deposits of New Zealand*. Parkville (AU): Australasian Institute of Mining and Metallurgy. p. 67–72. (Australasian Institute of Mining and Metallurgy monograph series; 13).

Challis GA, Lauder WR. 1977. Pre-Tertiary geology of the Longwood Range: parts NZMS 1 sheets S167, S168, S175 and S176. Wellington (NZ): Department of Scientific and Industrial Research. 1 map + 1 booklet, scale 1:50 000. (New Zealand Geological Survey miscellaneous series map; 11).

Challis GA, Long JVP. 1964. Wairauite: a new cobalt-iron mineral. *Mineralogical Magazine.* 33(266):942–948.

Chang SW, Choi H, Lee SR, Graham IJ, Wright IC. 2003a. Ferromanganese nodules in the vicinity of Bollons Seamount SE of the Campbell Plateau, SW Pacific Ocean. Part 1: Distribution and external morphology. Lower Hutt (NZ): Institute of Geological and Nuclear Sciences. 41 p. (Institute of Geological & Nuclear Sciences science report; 2003/13).

Chang SW, Choi H, Lee SR, Graham IJ, Wright IC. 2003b. Ferromanganese nodules in the vicinity of Bollons Seamount SE of the Campbell Plateau, SW Pacific Ocean. Part 2: Petrography and chemistry. Lower Hutt (NZ): Institute of Geological and Nuclear Sciences. 70 p. (Institute of Geological & Nuclear Sciences science report; 2003/14).

Christie AB. 1995. Mineral commodity report 7 – manganese. *New Zealand Mining.* 17:18–25.

Christie AB. 2002. Mesothermal gold deposits in New Zealand: mineral deposit model. Lower Hutt (NZ): Institute of Geological and Nuclear Sciences. 51 p. Client Report 2002/25. Prepared for Crown Minerals, Ministry of Economic Development.

Christie AB 2016a. Exploration of orogenic gold deposits in the Lyell goldfield, West Coast region. In: Christie AB, editor. *Mineral deposits of New Zealand: exploration and research*. Carlton (AU): Australasian Institute of Mining and Metallurgy. p. 109–117. (Australasian Institute of Mining and Metallurgy monograph series; 31).

Christie AB. 2016b. Exploration of placer titanomagnetite ironsand deposits offshore from the West Coast of the North Island. In: Christie AB, editor. *Mineral deposits of New Zealand: exploration and research*. Carlton (AU): Australasian Institute of Mining and Metallurgy. p. 443–450. (Australasian Institute of Mining and Metallurgy monograph series; 31).

Christie AB. 2016c. Introduction to epithermal gold-silver deposits in New Zealand. In: Christie AB, editor. *Mineral deposits of New Zealand: exploration and research*. Carlton (AU): Australasian Institute of Mining and Metallurgy. p. 218. (Australasian Institute of Mining and Metallurgy monograph series; 31).

Christie AB. 2019. Introduction to New Zealand hard rock gold deposits and their exploration models. *New Zealand Journal of Geology and Geophysics*. 62(4):394–413. https://doi.org/10.1080/00288306.2019.1653328

Christie AB, Barker RG. 2007. Mineral resource assessment of the Northland Region, New Zealand. Lower Hutt (NZ): Institute of Geological and Nuclear Sciences. 169 p. + 1 CD. (GNS Science report; 2007/06).

Christie AB, Barker RG. 2013. Mineral, coal and petroleum resources: production, exploration and potential. In: Dymond JR, editor. *Ecosystem services in New Zealand: conditions and trends*. Lincoln (NZ): Manaaki Whenua Press. p. 300–329.

Christie AB, Barker RG. 2016. Regional mineral resource assessments to promote recognition of mineral resource potential. In: Christie AB, editor. *Mineral deposits of New Zealand: exploration and research*. Carlton (AU): Australasian Institute of Mining and Metallurgy. p. 45–52. (Australasian Institute of Mining and Metallurgy monograph series; 31).

Christie AB, Brathwaite RL. 1993. Mineral commodity report 2: antimony. *New Zealand Mining.* 12:31–35.

Christie AB, Brathwaite RL. 1994. Mineral commodity report 4: copper. *New Zealand Mining.* 14:32–42.

Christie AB, Brathwaite RL. 1995a. Mineral commodity report 6: lead and zinc. *New Zealand Mining.* 16:22–30.

Christie AB, Brathwaite RL. 1995b. Mineral commodity report 10: nickel. *New Zealand Mining.* 18:39–45.

Christie AB, Brathwaite RL. 1996a. Mineral commodity report 11: tin. *New Zealand Mining.* 19:9–15.

Christie AB, Brathwaite RL. 1996b. Mineral commodity report 12: tungsten. *New Zealand Mining.* 19:19–27.

Christie AB, Brathwaite RL. 1996c. Mineral commodity report 13: silver. *New Zealand Mining.* 20:16–23.

Christie AB, Brathwaite RL. 1997a. Mineral commodity report 14: gold. *New Zealand Mining.* 21:21–40.

Christie AB, Brathwaite RL. 1997b. Mineral commodity report 15: iron. *New Zealand Mining.* 22:22–37.

Christie AB, Brathwaite RL. 1998. Mineral commodity report 16: titanium. *New Zealand Mining.* 23:15–25.

Christie AB, Brathwaite RL. 1999a. Mineral commodity report 19: beryllium, gallium, lithium, magnesium, uranium and zirconium. *New Zealand Mining*. 26:27–42.

Christie AB, Brathwaite RL. 1999b. Lower Hutt (NZ): Institute of Geological and Nuclear Sciences. 84 p. (Institute of Geological & Nuclear Sciences science report; 99/04).

Christie AB, Brathwaite RL. 2003. Hydrothermal alteration in metasedimentary rock-hosted orogenic gold deposits, Reefton goldfield, South Island, New Zealand. *Mineralium Deposita*. 38(1):87–107. https://doi.org/10.1007/s00126-002-0280-9

Christie AB, Brathwaite RL. 2006. Volcanogenic massive sulfide deposits in New Zealand: an overview. In: Christie AB, Brathwaite RL, editors. *Geology and exploration of New Zealand mineral deposits*. Parkville (AU): Australasian Institute of Mining and Metallurgy. p. 29–35. (Australasian Institute of Mining and Metallurgy monograph series; 25).

Christie AB, Challis GAC. 1995. Mineral commodity report 5: platinum group elements. *New Zealand Mining.* 15:31–37.

Christie AB, Herridge S. 2016. Alluvial gold mining at Earnscleugh, Alexandra, Otago. In: Christie AB, editor. *Mineral deposits of New Zealand: exploration and research*. Carlton (AU): Australasian Institute of Mining and Metallurgy. p. 353–357. (Australasian Institute of Mining and Metallurgy monograph series; 31).

Christie AB, Stewart TJ. 2016. Regional exploration geochemistry database of geochemical data compiled from open-file mineral reports. In: Christie AB, editor. *Mineral deposits of New Zealand: exploration and research*. Carlton (AU): Australasian Institute of Mining and Metallurgy. p. 543–548. (Australasian Institute of Mining and Metallurgy monograph series; 31).

Christie AB, Turnbull RE. 2016. Exploration of nickel-copper mineralisation in mafic and ultramafic rocks of the Riwaka Complex, West Nelson, South Island. In: Christie AB, editor. *Mineral deposits of New Zealand: exploration and research*. Carlton (AU): Australasian Institute of Mining and Metallurgy. p. 453–462. (Australasian Institute of Mining and Metallurgy monograph series; 31).

Christie AB, Brathwaite RL, Thompson BN. 1993. Mineral commodity report 1: aluminium. *New Zealand Mining.* 12:20–23.

Christie AB, Brathwaite RL, Johnston MR. 1994. Mineral commodity report 3: chromium. *New Zealand Mining.* 13:24–28.

Christie AB, Brathwaite RL, Tulloch AJ. 1998. Mineral commodity report 17: rare earth and related elements. *New Zealand Mining.* 24:7–19.

Christie AB, Thompson BN, Brathwaite RL. 2000. Mineral commodity report 20 – clays. *New Zealand Mining.* 27:26–43.

Christie AB, Thompson BN, Brathwaite RL. 2001a. Mineral commodity report 21: limestone, marble and dolomite. *New Zealand Mining.* 29:6–25.

Christie AB, Thompson BN, Brathwaite RL. 2001b. Mineral commodity report 22: aggregate. *New Zealand Mining.* 30:6–26.

Christie AB, Brathwaite RL, Thompson BN. 2002. Mineral commodity report 23: zeolites. *New Zealand Mining* 31:16–24.

Christie AB, Brathwaite RL, Mauk JL, Simpson MP. 2006a. Hauraki Goldfield: regional exploration databases and prospectivity studies. In: Christie AB, Brathwaite RL, editors. *Geology and exploration of New Zealand mineral deposits*. Parkville (AU): Australasian Institute of Mining and Metallurgy. p. 73–84. (Australasian Institute of Mining and Metallurgy monograph series; 25).

Christie AB, Cox SC, Rattenbury MS, Brathwaite RL, Whetter N. 2006b. Orogenic (mesothermal) gold deposits of the Reefton Goldfield, West Coast: review of exploration and geology. In: Christie AB, Brathwaite RL, editors. *Geology and exploration of New Zealand mineral deposits*. Parkville (AU): Australasian Institute of Mining and Metallurgy. p. 255–262. (Australasian Institute of Mining and Metallurgy monograph series; 25).

Christie AB, Mortimer N, Waterman P, Barker RG. 2006c. New Zealand platinum prospects in arc-type layered igneous complexes. In: Christie AB, Brathwaite RL, editors. *Geology and exploration of New Zealand mineral deposits*. Parkville (AU): Australasian Institute of Mining and Metallurgy. p. 37–42. (Australasian Institute of Mining and Metallurgy monograph series; 25).

Christie AB, Simpson MP, Brathwaite RL, Mauk JL, Simmons SF. 2007. Epithermal Au-Ag and related deposits of the Hauraki Goldfield, Coromandel Volcanic Zone, New Zealand. *Economic Geology*. 102(5):785–816. https://doi.org/10.2113/gsecongeo.102.5.785

Christie AB, Heron DW, Graham IJ, Davy BW. 2009. Genetic model for exploration of offshore West Coast ironsands, North Island, New Zealand. In: Williams PJ, editor. *Proceedings of the 10th Biennial SGA Meeting of the Society for Geology Applied to Mineral Deposits: smart science for exploration and mining*; 2009 Aug 17–20; Townsville, Australia. Townsville (AU): James Cook University. p. 979–981.

Christie AB, Barker RG, Brathwaite RL. 2010. Mineral resource assessment of the West Coast Region, New Zealand. *GNS Science report 2010/61.*

Christie AB, Barker RG, Brathwaite RL. 2010. Mineral resource assessment of the West Coast region, New Zealand. Lower Hutt (NZ): GNS Science. 238 p. + 1 CD. (GNS Science report; 2010/61).

Christie AB, Simpson MP, Barker RG, Brathwaite RL. 2019. Exploration for epithermal Au–Ag deposits in New Zealand: history and strategy. *New Zealand Journal of Geology and Geophysics*. 62(4):414–441. https://doi.org/10.1080/00288306.2019.1677251

Christie AB, Barker RG, Brathwaite RL, Rooyakkers SM, de Ronde CEJ. 2024. The mineral potential of New Zealand – Part 1: overview of New Zealand's mineral deposits and their resources. Lower Hutt (NZ): GNS Science. 83 p. Consultancy Report 2024/62A. Prepared for the Ministry of Business, Innovation & Employment.

Clark RJ, Norton AM. 1990. Report covering prospecting work carried out on PL 31-1862, Waipapa Beach. Located at: Ministry of Business, Innovation & Employment, Wellington, NZ. 20 p. New Zealand Unpublished Mineral Report 2710.

Coleman AC. 1980. Final report on the Wilberg area (PL 31527) Westland, New Zealand. Located at: Ministry of Business, Innovation & Employment, Wellington, NZ. 16 p. + 3 enclosures. New Zealand Unpublished Mineral Report 1664.

Coleman RG. 1966. New Zealand serpentinites and associated metasomatic rocks. Wellington (NZ): New Zealand Geological Survey. 101 p. (New Zealand Geological Survey bulletin; 76).

Coombs DS, Ellis AJ, Fyfe WS, Taylor AM. 1959. The zeolite facies, with comments on the interpretation of hydrothermal syntheses. *Geochimica et Cosmochimica Acta.* 17(1):53–107. https://doi.org/10.1016/0016-7037(59)90079-1

Cooper AF. 1971. Carbonatites and fenitization associated with a lamprophyric dike-swarm intrusive into schists of the New Zealand geosyncline. *Geological Society of America Bulletin.* 82:1327–1339.

Cooper AF. 1986. A carbonatitic lamprophyre dike swarm from the Southern Alps, Otago and Westland. In: Smith IEM. editor, Late Cenozoic volcanism in New Zealand. In: Smith IEM, editor. *Late Cenozoic volcanism in New Zealand*. Wellington (NZ): Royal Society of New Zealand. p. 313–336. (Royal Society of New Zealand bulletin; 23).

Cooper AF. 1996. Nb-rich biotite in carbonatites and fenites at Haast River, New Zealand. *Mineralogical Magazine.* 60:473–482.

Cooper AF, Paterson LA. 2008. Carbonatites from a lamprophyric dyke-swarm, South Westland, New Zealand. *Canadian Mineralogist*. 46(4):753–777. https://doi.org/10.3749/canmin.46.4.753

Cooper AF, Reay A. 1983. Lithology, field relationships, and structure of the Pounamu Ultramafics from the Whitcombe and Hokitika Rivers, Westland, New Zealand. *New Zealand Journal of Geology and Geophysics.* 26:359–379. https://doi.org/10.1080/00288306.1983.10422254

Cooper RA, Tulloch AJ. 1992. Early Paleozoic terranes in New Zealand and their relationship to the Lachlan Fold Belt. *Tectonophysics*. 214:129–144. https://doi.org/10.1016/0040-1951(92)90193-A

Corner NG. 1989. Final report on Harvester project 1989 Vibrocore drilling PLs 311326 to 311330, offshore Hokitika, Westland. Located at: Ministry of Business, Innovation & Employment, Wellington, NZ. 233 p. New Zealand Unpublished Mineral Report 2514.

Corner NG, Jennings WL. 1994. Mineral resources of the Northwest South Island National Park. Wellington (NZ): Ministry of Commerce, Energy and Resources Division. 104 p. Resource Information Report 19.

Cotton RJ, Birchfield A. 2006. The Grey River dredge, West Coast, South Island. In: Christie AB, Brathwaite RL, editors. *Geology and exploration of New Zealand mineral deposits*. Parkville (AU): Australasian Institute of Mining and Metallurgy. p. 275–278. (Australasian Institute of Mining and Metallurgy monograph series; 25).

Cotton RJ, Rose RV. 2006. The Ross alluvial goldfield, West Coast, South Island. In: Christie AB, Brathwaite RL, editors. *Geology and exploration of New Zealand mineral deposits*. Parkville (AU): Australasian Institute of Mining and Metallurgy. p. 279–284. (Australasian Institute of Mining and Metallurgy monograph series; 25).

Cotton RJ, Wood JW. 2016. Alluvial gold mining on the West Coast, South Island, 2005–2016. In: Christie AB, editor. *Mineral deposits of New Zealand: exploration and research*. Carlton (AU): Australasian Institute of Mining and Metallurgy. p. 335–340. (Australasian Institute of Mining and Metallurgy monograph series; 31).

Couper PG. 1981a. Progress report on the Scotia prospect, Waitekauri project, PL 31559, Coromandel Peninsula. Located at: Ministry of Business, Innovation & Employment; Wellington, NZ. 155 p. + 15 enclosures. New Zealand Unpublished Mineral Report 400.

Couper PG. 1981b. Progress report on the Maoriland prospect PL 31559, Waitekauri, Coromandel Peninsula. Located at: Ministry of Business, Innovation & Employment, Wellington, NZ. 98 p. + 6 enclosures. New Zealand Unpublished Mineral Report 425.

Couper PG. 1982. Progress report on the Scotia prospect PL 31559, Waitekauri, Coromandel Peninsula. Located at: Ministry of Business, Innovation & Employment, Wellington, NZ. 197 p. + 5 enclosures. New Zealand Unpublished Mineral Report 424.

Couper PG. 1983. Report on diamond drilling at Scotia prospect (PL 31-559) and Rahu prospect (PL 31-558), Coromandel Peninsula. Located at: Ministry of Business, Innovation & Employment, Wellington, NZ. 13 p. New Zealand Unpublished Mineral Report 439.

Cowden A, Ruddock R, Reay A, Nicolson P, Waterman P, Banks MJ. 1990. Platinum mineralisation potential of the Longwood Igneous Complex, New Zealand. *Mineralogy and Petrology.* 42:181–195. https://doi.org/10.1007/BF01162690

Cox DP. 1986. Descriptive model of W skarn deposit. In: Cox DP, Singer DA, editors. *Mineral deposit models*. Washington (DC): U.S. Government Printing Office. p. 55. (U.S. Geological Survey bulletin; 1693). https://pubs.usgs.gov/bul/b1693/

Cox DP, Singer DA, editors. 1986. Mineral deposit models. Washington (DC): U.S. Government Printing Office. 379 p. (US Geological Survey bulletin; 1693).

Cox SC, Nibourel L. 2015. Bedload composition, transport and modification in rivers of Westland, New Zealand, with implications for the distribution of alluvial pounamu (jade). *New Zealand Journal of Geology and Geophysics.* 58(2):154–175. https://doi.org/10.1080/00288306.2015.1025799

Cox SC, Adams CJ, Popham T, Goodall A, Campbell HJ. 2005. Pounamu resource assessment and characterisation. In: *2005 New Zealand Minerals Conference proceedings: realising New Zealand's mineral potential*; 2005 Nov 13–16; Auckland, New Zealand. Wellington (NZ): Crown Minerals. p. 365–366.

Craw D. 2006. Gold-bearing veins in the Southern Alps. In: Christie AB, Brathwaite RL, editors. *Geology and exploration of New Zealand mineral deposits*. Parkville (AU): Australasian Institute of Mining and Metallurgy. p. 285–288. (Australasian Institute of Mining and Metallurgy monograph series; 25).

Craw D, MacKenzie D. 2016. Macraes orogenic gold deposit (New Zealand): origin and development of a world class gold mine. Cham (CH): Springer. 127 p. (SpringerBriefs in World Mineral Deposits; 1).

Craw D, Norris RJ. 1991. Metamorphogenic Au-W veins and regional tectonics: mineralisation throughout uplift history of the Haast Schist, New Zealand. *New Zealand Journal of Geology and Geophysics.* 34(3):373–383. https://doi.org/10.1080/00288306.1991.9514476

Craw D, Rattenbury MS, Johnstone RD. 1987. Structural geology and vein mineralisation in the Callery River headwaters, Southern Alps, New Zealand. *New Zealand Journal of Geology and Geophysics*. 30(3):273–286. https://doi.org/10.1080/00288306.1987.10552622

Craw D, Begbie M, MacKenzie D. 2006. Structural controls on tertiary orogenic gold mineralisation during initiation of a mountain belt, New Zealand. *Mineralium Deposita*. 41(7):645–659. https://doi.org/10.1007/s00126-006-0088-0

Craw D, MacKenzie D, Ashley P. 2016. Longwood Range platinum, Southland. In: Christie AB, editor. *Mineral deposits of New Zealand: exploration and research*. Carlton (AU): Australasian Institute of Mining and Metallurgy. p. 481–486. (Australasian Institute of Mining and Metallurgy monograph series; 31).

Crump ME. 1994. A new source of gallium – geothermal muds. In: *Proceedings of the 28th annual conference*; 1994 Aug 17–19; Wairakei, New Zealand. [Place unknown] (NZ): Australasian Institute of Mining and Metallurgy, New Zealand Branch. p. 207–208.

Cullen DJ. 1989. The submarine phosphorite deposits of central Chatham Rise, east of New Zealand. In: Kear D, editor. *Mineral deposits of New Zealand*. Parkville (AU): Australasian Institute of Mining and Metallurgy. p. 201–206. (Australasian Institute of Mining and Metallurgy monograph series; 13).

Davies AML. 2018. Trace elements in New Zealand ferromanganese nodules: implications for deep sea environments [MSc thesis]. Wellington (NZ): Victoria University of Wellington. 231 p. https://doi.org/10.26686/wgtn.17131868

de Ronde CEJ. 2006. Mineralisation associated with submarine volcanoes of the southern Kermadec Arc, New Zealand. In: Christie AB, Brathwaite RL, editors. *Geology and exploration of New Zealand mineral deposits*. Parkville (AU): Australasian Institute of Mining and Metallurgy. p. 333–338. (Australasian Institute of Mining and Metallurgy monograph series; 25).

de Ronde CEJ, Baker ET, Massoth GJ, Lupton JE, Wright IC, Feely RA. Greene RG. 2001. Intra-oceanic subduction-related hydrothermal venting, Kermadec volcanic arc, New Zealand. *Earth and Planetary Science Letters.* 193(3):359–369. https://doi.org/10.1016/S0012-821X(01)00534-9

de Ronde CEJ, Faure K, Bray CJ, Chappell DA, Wright IC. 2003a. Hydrothermal fluids associated with seafloor mineralization at two southern Kermadec arc volcanoes, offshore New Zealand. *Mineralium Deposita.* 38(2):217–233. https://doi.org/10.1007/s00126-002-0305-4

de Ronde CEJ, Massoth,GJ, Baker ET, Lupton JE. 2003b. Submarine hydrothermal venting related to volcanic arcs. In: Simmons SF, Graham IJ, editors. *Volcanic, geothermal, and ore-forming fluids: rulers and witnesses of processes within the earth*. Littleton (CO): Society of Economic Geologists. p. 91–110. (Society of Economic Geologists special publication; 10).

de Ronde CEJ, Hannington MD, Stoffers P, Wright IC, Ditchburn RG, Reyes AG, Baker ET, Massoth GJ, Lupton JE, Walker SL, et al. 2005. Evolution of a submarine magmatic-hydrothermal system: Brothers volcano, southern Kermadec arc, New Zealand. *Economic Geology.* 100(6):1097–1133. https://doi.org/10.2113/gsecongeo.100.6.1097

de Ronde CEJ, Baker ET, Massoth GJ, Lupton JE, Wright IC, Sparks RJ, Bannister SC, Reyners ME, Walker SL, Greene RR, et al. 2007. Submarine hydrothermal activity along the mid-Kermadec Arc, New Zealand: large-scale effects on venting. *Geochemistry, Geophysics, Geosystems*. 8(7). https://doi.org/10.1029/2006GC001495

de Ronde CEJ, Leybourne MI, Berthelsen TJ. 2010. Prospectivity of Kermadec arc submarine volcanoes for massive sulfide mineralisation. Lower Hutt (NZ): GNS Science*.* 16 p. Consultancy Report 2010/119. Prepared for Crown Minerals, Ministry of Economic Development.

de Ronde CEJ, Massoth GJ, Butterfield DA, Christenson BW, Ishibashi J, Ditchburn RG, Hannington MD, Brathwaite RL, Lupton JE, Kamenetsky VS, et al. 2011. Submarine hydrothermal activity and gold-rich mineralization at Brothers Volcano, Kermadec Arc, New Zealand. *Mineralium Deposita.* 46(5):541–584. https://doi.org/10.1007/s00126-011-0345-8

de Ronde CEJ, Butterfield DA, Leybourne MI. 2012. Metallogenesis and mineralisation of intraoceanic arcs I: Kermadec Arc – introduction. *Economic Geology.* 107(8):1521–1525. https://doi.org/10.2113/econgeo.107.8.1521

de Ronde CEJ, Humphris SE, Höfig TW, Expedition 376 Scientists. 2019. Brothers Arc Flux: expedition 376 of the R/V JOIDES Resolution from and to Auckland, New Zealand. Sites U1527–U1531; 5 May–5 July 2018. College Station (TX): International Ocean Discovery Program. https://doi.org/10.14379/iodp.proc.376.2019

Dill HG. 2010. The ‘chessboard’ classification scheme of mineral deposits: mineralogy and geology from aluminum to zirconium. *Earth-Science Reviews*. 100(1):1–420. https://doi.org/10.1016/j.earscirev.2009.10.011

Douch C. 1988. Prospects for gold in New Zealand. In: *Gold mining 88: proceedings of the 2nd international conference on gold mining*; 1988 Nov 7–9; Vancouver, British Columbia, Canada. Littleton (CO): Society of Mining Engineers.

Douglas BJ. 1989. Phosphate resources within the area covered by EL 33493 Clarendon District, East Otago. Located at: Ministry of Business, Innovation & Employment, Wellington, NZ. 24 p. + 1 enclosure. New Zealand Unpublished Mineral Report 2638.

Downey JF. 1928. Quartz reefs of the West Coast mining district, New Zealand. Wellington (NZ): Government Printer. 144 p.

Downey JF. 1935. Gold mines of the Hauraki district, New Zealand. Wellington (NZ): Government Printer. 305 p.

Downey S, Perrin K. 2008. PL39-205 Colville partial surrender report for period ending 13 October 2008. Located at: Ministry of Business, Innovation & Employment, Wellington, NZ. 15 p. + 5 enclosures. New Zealand Unpublished Mineral Report 4447.

Doyle S, Christie AB, Martin AP. 2016. Mining and exploration at the Macraes orogenic gold deposit, East Otago. In: Christie AB, editor. *Mineral deposits of New Zealand: exploration and research*. Carlton, Vic.: Australasian Institute of Mining and Metallurgy. p. 183–189. (Australasian Institute of Mining and Metallurgy monograph series; 31).

Drew M. 2014. PP 54344 Wairarapa relinquishment report – 2014. Located at: Ministry of Business, Innovation & Employment, Wellington, NZ. New Zealand Unpublished Mineral Report 5114.

Durance PMJ, Polette D. 2016. A Review of the Kirwan Hill tungsten and gold prospect, West Coast. In: Christie AB, editor. *Mineral deposits of New Zealand: exploration and research*. Carlton (AU): Australasian Institute of Mining and Metallurgy. p. 471–479. (Australasian Institute of Mining and Metallurgy monograph series; 31).

Durance PMJ, Hill MP, Turnbull RE, Morgenstern R, Rattenbury MS. 2018. Nickel and cobalt mineral potential in New Zealand. Lower Hutt (NZ): GNS Science. 223 p. Consultancy Report 2018/64. Prepared for New Zealand Petroleum and Minerals.

Eckstrand OR, Sinclair, WD, Thorpe RI. 1995. Geology of Canadian mineral deposit types. Ottawa (ON): Geological Survey of Canada. (Geology of Canada; 8).

Edbrooke SW. 1999. Mineral commodity report 18: coal. *New Zealand Mining* 25:9–23.

Edwards AR. 1991. The Oamaru diatomite. Lower Hutt (NZ): DSIR Geology & Geophysics. 260 p. (New Zealand Geological Survey paleontological bulletin; 64).

Eggers AJ, Adams CJ. 1979. Potassium-argon ages of molybdenum mineralisation and associated granites of Bald Hill and correlation with other molybdenum occurrences in the South Island, New Zealand. *Economic Geology*. 74(3):628–637. https://doi.org/10.2113/gsecongeo.74.3.628

Emsbo P, Seal RR, Breit GN, Diehl SF, Shah AK. 2016. Sedimentary exhalative (sedex) zinc-lead-silver deposit model. Reston (VA): U.S. Geological Survey. 57 p. Scientific Investigations Report 2010-5070-N. https://doi.org/10.3133/sir20105070N

Evans HJ. 1963. Review of New Zealand bauxite. Located at: Ministry of Business, Innovation & Employment, Wellington, NZ. 6 p. + 1 enclosure. New Zealand Unpublished Mineral Report 15.

Faure K, Brathwaite RL. 2006. Mineralogical and stable isotope studies of gold-arsenic mineralisation in the Sams Creek peralkaline porphyritic granite, South Island, New Zealand. *Mineralium Deposita*. 40(8):802–827. https://doi.org/10.1007/s00126-005-0013-y

Ferrar HT. 1925. The geology of the Whangarei-Bay of Islands Subdivision, Kaipara Division. Wellington (NZ): Department of Mines, New Zealand Geological Survey. 134 p. (New Zealand Geological Survey bulletin; 27).

Fraser C. 1910. The geology of the Thames subdivision, Hauraki, Auckland. Wellington (NZ): Department of Mines, New Zealand Geological Survey. 136 p. (New Zealand Geological Survey bulletin; 10).

Fraser C, Adams JH. 1907. The geology of the Coromandel subdivision, Hauraki, Auckland. Wellington (NZ): Department of Mines, New Zealand Geological Survey. 154 p. (New Zealand Geological Survey bulletin; 4).

Fricker AG. 1970. Preliminary report on Russell antimony claim. Located at: Ministry of Business, Innovation & Employment, Wellington, NZ. New Zealand Unpublished Mineral Report 142.

Fulton GW. 2001. From paper to digital – the true value of historical mining information: Glenorchy scheelite project. In: *The Australasian Institute of Mining and Metallurgy: New Zealand Branch 34th Annual Conference*; 2001 Aug 29–31; Otago, New Zealand. [Place unknown] (NZ): Australasian Institute of Mining and Metallurgy, New Zealand Branch. p. 125–129.

Glasby GP. 1976. Surface densities of manganese nodules in the southern sector of the South Pacific. *New Zealand Journal of Geology and Geophysics.* 19(6):771–790. https://doi.org/10.1080/00288306.1976.10420739

Goldfarb RJ, Groves DI, Gardoll S. 2001. Orogenic gold and geologic time: a global synthesis. *Ore Geology Reviews*. 18(1):1–75. https://doi.org/10.1016/S0169-1368(01)00016-6

Goldfarb RJ, Baker T, Dubé B, Groves DI, Hart CJR, Gosselin P. 2005. Distribution, character, and genesis of gold deposits in metamorphic terran. In: Hedenquist JW, Thompson JFH, Goldfarb RJ, Richards JP, editors. *One Hundredth Anniversary Volume*. Littleton (CO): Society of Economic Geologists. p. 407–450. https://doi.org/10.5382/AV100.14

Gordon FR. 1959. The occurrence of diatomite near Middlemarch, Otago. In: *Proceedings of a mineral conference*; 1959 Sep 1–3; Dunedin, New Zealand. Dunedin (NZ): University of Otago. Paper 136.

Graham IJ, Wright IC. 2006. The Campbell ferromanganese nodule field in the southern part of New Zealand's Exclusive Economic Zone. In: Christie AB, Brathwaite RL, editors. *Geology and exploration of New Zealand mineral deposits*. Parkville (AU): Australasian Institute of Mining and Metallurgy. p. 339–347. (Australasian Institute of Mining and Metallurgy monograph series; 25).

Graham IJ, Ditchburn RG, Zondervan A, Chang SW, Choi H, Lee SR, Wright IC. 2003. Ferromanganese nodules in the vicinity of Bollons Seamount SE of the Campbell Plateau, SW Pacific Ocean. Part 3: beryllium isotope dating. Lower Hutt (NZ): Institute of Geological and Nuclear Sciences. 43 p. (Institute of Geological & Nuclear Sciences science report; 2003/15).

Grant M, Moore J, Madambi K, Leslie E, Carr D. 2024. NI 43-101 technical report: Macraes gold mine, Otago, New Zealand. Effective December 31, 2023. Otago (NZ): OceanaGold*.* 209 p.

Graves C. 1987. Six monthly report for the period 7 October 1986 to 7 March 1987 EL 33351, Takitimu Mountains area. Located at: Ministry of Business, Innovation & Employment, Wellington, NZ. New Zealand Unpublished Mineral Report 2069.

Green CJ, Lederer GW, Parks HL, Zientek ML. 2020. Grade and tonnage model for tungsten skarn deposits – 2020 update. Reston (VA): U.S. Geological Survey. 23 p. Scientific Investigations Report 2020–5085. https://doi.org/10.3133/sir20205085

Grieve PL. 2013. NI 43-101 technical report on resources at Muir's Project, Te Puke, Bay of Plenty, New Zealand. [Otago] (NZ): Glass Earth Gold Limited. 85 p.

Grieve PL, Corbett GJ, Leach TM. 2006. Conceptual models for gold exploration at Puhipuhi, Northland. In: Christie AB, Brathwaite RL, editors. *Geology and exploration of New Zealand mineral deposits*. Parkville (AU): Australasian Institute of Mining and Metallurgy. p. 65–70. (Australasian Institute of Mining and Metallurgy monograph series; 25).

Grindley GW, Watters WA. 1965. Geology. In: Ministry of Works, Town and Country Planning Branch, editor. *Nelson region*. Wellington (NZ): Government Printer. p. 17–37. (National resources survey; 4).

Grindley GW, Wodzicki A. 1960. Base metal and gold-silver mineralisation on the south-east side of the Aorere valley, north-west Nelson. *New Zealand Journal of Geology and Geophysics.* 3(4):585–592. https://doi.org/10.1080/00288306.1960.10420147

Groves DI, Goldfarb RJ, Gebre-Mariam M, Hagemann SG, Robert F. 1998. Orogenic gold deposits: a proposed classification in the context of their crustal distribution and relationship to other gold deposit types. *Ore Geology Reviews*. 13(1):7–27. https://doi.org/10.1016/S0169-1368(97)00012-7

Happy A. 1993. Aggregate production in New Zealand. *New Zealand Mining.* 9:29–34.

Happy AJ, Ashby JP. 1993. Production of aggregates in New Zealand – the trends. In: *The changing world of mining: proceedings of the 27th Annual Conference 1993*; 1993 Aug 24–27; Wellington, New Zealand. [Place unknown] (NZ): New Zealand Branch of the Australasian Institute of Mining and Metallurgy. p. 303–313.

Hargrave J. 2006. New Zealand South Island West Coast survey June 2006: operations report. Located at: Ministry of Business, Innovation & Employment, Wellington, NZ. 13 p. New Zealand Unpublished Mineral Report 4334.

Hart CJR. 2005. Classifying, distinguishing and exploring for intrusion-related gold systems. *The Gangue.* 87:1,4–9.

Hart CJR. 2007. Reduced intrusion-related gold systems. In: Goodfellow WD, editor. *Mineral deposits of Canada: a synthesis of major deposit types, district metallogeny, the evolution of geological provinces, and exploration methods*. St Johns (NL): Geological Association of Canada. p. 95–112. (Geological Association of Canada, Mineral Deposits Division special publication; 5).

Hartshorn G, Selliani S. 2009. Technical report on exploration activities within PP 39287 for the period 21 February 2007 to 20 February 2009. Located at: Ministry of Business, Innovation & Employment, Wellington, NZ. 38 p. + appendices. New Zealand Unpublished Mineral Report 4448.

Harvey CC, Townsend MG, Evans RB. 1990. The halloysite clays of Northland, New Zealand. In: *The Australasian Institute of Mining and Metallurgy 1990 Annual Conference: the mineral industry in New Zealand*; 1990 Mar 18–21; Rotorua, New Zealand. Parkville (AU): Australasian Institute of Mining and Metallurgy. p. 229–238.

Hawke AA, Price GD. 1983. Scheelite exploration in the Southern Alps. In: *Australasian Institute of Mining and Metallurgy, New Zealand Branch – annual conference: New Zealand energy and mineral resources;* 1983 Aug 17–19; Invercargill, New Zealand. [Place unknown] (NZ): Australasian Institute of Mining and Metallurgy, New Zealand Branch. p. 1–9.

Hawke AA, Price GD. 1989. Scheelite exploration in the Southern Alps. In: Kear D, editor. *Mineral deposits of New Zealand*. Parkville (AU): Australasian Institute of Mining and Metallurgy. p. 31–32. (Australasian Institute of Mining and Metallurgy monograph series; 13).

Hay KR. 1989. Precious metal exploration in the Longwood Range, Southland. In: Kear D, editor. *Mineral deposits of New Zealand*. Parkville (AU): Australasian Institute of Mining and Metallurgy. p. 197–199. (Australasian Institute of Mining and Metallurgy monograph series; 13).

Hayward BW. 1987. Granite and marble, a guide to building stones in New Zealand. Lower Hutt (NZ): Geological Society of New Zealand. 56 p. (Geological Society of New Zealand guidebook; 8).

Hein JR, Spinardi F, Okamoto N, Mizell K, Thorburn D, Tawake A. 2015. Critical metals in manganese nodules from the Cook Islands EEZ, abundances and distributions. *Ore Geology Reviews*. 68:97–116. https://doi.org/10.1016/j.oregeorev.2014.12.011

Hein JR, Koschinsky A, Kuhn T. 2020. Deep-ocean polymetallic nodules as a resource for critical materials. *Nature Reviews Earth & Environment*. 1(3):158–169. https://doi.org/10.1038/s43017-020-0027-0

Henderson J. 1917. The geology and mineral resources of the Reefton subdivision: Westport and north Westland divisions. Wellington (NZ): Department of Mines, New Zealand Geological Survey. 232 p. (New Zealand Geological Survey bulletin; 18).

Henderson SM, Fenton J, Bartle A, Hamilton A, Craw D. 2016. Manuherikia valley placer gold project, Central Otago. In: Christie AB, editor. *Mineral deposits of New Zealand: exploration and research*. Carlton (AU): Australasian Institute of Mining and Metallurgy. p. 367–372. (Australasian Institute of Mining and Metallurgy monograph series; 31).

Heron DW, custodian. 2024. Geological map of New Zealand. 4th ed. Lower Hutt (NZ): GNS Science. 1 USB, scale 1:250,000. (Institute of Geological & Nuclear Sciences 1:250,000 geological map; 1).

Hill MP. 2021. Aggregate opportunity modelling for New Zealand. Lower Hutt (NZ): GNS Science. 106 p. (GNS Science report; 2021/10). https://doi.org/10.21420/1RKC-QB05

Hill MP, Chilton MO. 2024a. Aggregate Opportunity Modelling for the Wellington Region of New Zealand. Lower Hutt (NZ): GNS Science. 20 p. (GNS Science report; 2024/09). https://doi.org/10.21420/JW09-RF66

Hill MP, Chilton MO. 2024b. Aggregate Opportunity Modelling for the Bay of Plenty area of New Zealand. Lower Hutt (NZ): GNS Science. 22 p. (GNS Science report; 2024/10). https://doi.org/10.21420/W34K-RR18

Hill MP, Chilton MO. 2024c. Aggregate Opportunity Modelling for the northern Auckland area of New Zealand. Lower Hutt (NZ): GNS Science. 23 p. (GNS Science report; 2024/11). https://doi.org/10.21420/DS28-ZG73

Hill MP, Chilton MO. 2024d. Aggregate Opportunity Modelling for the southern Auckland area of New Zealand. Lower Hutt (NZ): GNS Science. 22 p. (GNS Science report; 2024/12). https://doi.org/10.21420/J47S-NN09

Hill MP, Chilton MO. 2024e. Aggregate Opportunity Modelling for central and northwestern Otago area of New Zealand. Lower Hutt (NZ): GNS Science. 23 p. (GNS Science report; 2024/13). https://doi.org/10.21420/RFGE-SQ76

Höll R, Maucher A. 1976. The strata-bound ore deposits in the Eastern Alps. In: Wolf KH, editor. *Regional studies*. Amsterdam (NL): Elsevier Scientific Publishing Co. p. 1–36. (Handbook of strata-bound and stratiform ore deposits; 5).

Howard B. 1940. Rakiura: a history of Stewart Island, New Zealand. Wellington (NZ): A.H. & A.W. Reed. 415 p.

Hunter HW. 1977. Geology of the Cobb Intrusives, Takaka valley, north-west Nelson, New Zealand. *New Zealand Journal of Geology and Geophysics.* 20(3):469–501. https://doi.org/10.1080/00288306.1977.10427597

Hutton CO. 1950. Studies of heavy detrital minerals. *GSA Bulletin*. 61(7):635–710. https://doi.org/10.1130/0016-7606(1950)61[635:SOHDM]2.0.CO;2

Hutton CO, Seelye FT. 1945. Contributions to the mineralogy of New Zealand – part I. *Transactions of the Royal Society of New Zealand.* 75(2):160–168.

Ireland TR, Gibson GM. 1998. SHRIMP monazite and zircon geochronology of high-grade metamorphism in New Zealand. *Journal of Metamorphic Geology*. 16(2):149–167. https://doi.org/10.1111/j.1525-1314.1998.00112.x

John DA, Taylor RD. 2016. By-products of porphyry copper and molybdenum deposits. In: Verplanck PL, Hitzman MW, editors. *Rare earth and critical elements in ore deposits*. Littleton (CO): Society of Economic Geologists. p. 137–164. (Reviews in economic geology; 18). https://doi.org/10.5382/Rev.18.07

John DA, Ayuso RA, Barton MD, Blakely RJ, Bodnar RJ, Dilles JH, Gray F, Graybeal FT, Mars JC, McPhee DK, et al. 2010. Porphyry copper deposit model: chapter B of mineral deposit models for resource assessment. Reston (VA): U.S. Geological Survey. 169 p. Scientific Investigations Report 2010–5070–B.

John D, Vikre PG, du Bray EA, Blakely RJ, Fey DL, Rockwell BW, Mauk JL, Anderson ED, Graybeal F. 2018. Descriptive models for epithermal gold-silver deposits. Reston (VA): U.S. Geological Survey. 246 p. + 3 appendices. Scientific Investigations Report 2010-5070-Q. https://doi.org/10.3133/sir20105070Q

John F. 2011. PL39 195 (Kermadec 2011 – K11) Technical Report. Located at: Ministry of Business, Innovation & Employment, Wellington, NZ. 25 p. + 11 enclosures. New Zealand Unpublished Mineral Report 4732.

Johnston MR. 1987. High hopes: the history of the Nelson Mineral Belt and New Zealand's first railway. Nelson (NZ): Nikau Press. 152 p.

Johnston MR. 1993. The history of the eastern Marlborough goldfields: the Northbank, Mahakipawa and Queen Charlotte Sound. Nelson (NZ): Nikau Press. 456 p. (Gold in a tin dish; 2).

Jones GJ, Savory P. 1993. PP 39-003, Takaka area, NW Nelson, N.Z. report on prospecting activity January to March 1993. Located at: Ministry of Business, Innovation & Employment, Wellington, NZ. New Zealand Unpublished Mineral Report 3231.

Jongens R, Christie A, Leybourne M, Timm C, Smith-Lyttle G, Rattenbury M. 2012. Mineral potential of the Tapuaenuku and Blue Mountain Igneous Complexes, Kaikoura: desktop studies and geochemical survey. Located at: Ministry of Business, Innovation & Employment, Wellington, NZ. New Zealand Unpublished Mineral Report 5062.

Jury AP, Hancock PM. 1989. Alluvial gold deposits and mining opportunities on the West Coast, South Island, New Zealand. In: In: Kear D, editor. *Mineral deposits of New Zealand*. Parkville (AU): Australasian Institute of Mining and Metallurgy. p. 147–153. (Australasian Institute of Mining and Metallurgy monograph series; 13).

Kear D. 1957. Kauaeranga sulfide deposit, Thames, New Zealand. *New Zealand Journal of Science and Technology*. 38:483–495.

Kear D. 1979. Geology of ironsand resources of New Zealand. Wellington (NZ): Department of Scientific and Industrial Research. 154 p.

Kear D, Waterhouse BC, Swindale LD. 1961. Bauxite deposits in Northland. Wellington (NZ): Department of Scientific and Industrial Research. 58 p. (Department of Scientific and Industrial Research Information series; 32).

Kenex. 2011. New Zealand prospectivity study and exploration targeting review for orogenic Au mineralisation. Located at: Ministry of Business, Innovation & Employment, Wellington, NZ. New Zealand Unpublished Mineral Report 4842.

Kirkham RV, Sinclair WD, Thorpe RI, Duke JM, editors. 1993. Mineral deposit modelling. St Johns (NL): Geological Association of Canada. 770 p. (Geological Association of Canada special paper; 40).

Kirkpatrick L. 2006. Results of high resolution magnetic surveys, Westland, New Zealand. Located at: Ministry of Business, Innovation & Employment, Wellington, NZ. 19 p. New Zealand Unpublished Mineral Report 4336.

Kirkpatrick L. 2007. New Zealand airborne magnetic survey October 2006. Located at: Ministry of Business, Innovation & Employment, Wellington, NZ. 25 p. New Zealand Unpublished Mineral Report 4331.

Kusek KM. 2007. Robot paints stunning map of deep-sea volcano. *Oceanus*; [accessed 2024 Jul]. https://www.whoi.edu/oceanus/feature/robot-paints-stunning-map-of-deep-sea-volcano/

Kutsukake T. 1988. The Britannia granite pluton in the Karamea Batholith, South Island, New Zealand. *New Zealand Journal of Geology and Geophysics.* 31(3):275–286. https://doi.org/10.1080/00288306.1988.10417777

Landreth RF. 1946. Iron ore reserves of the Onekaka field, NW Nelson. Located at: Ministry of Business, Innovation & Employment, Wellington, NZ. 25 p. + 4 enclosures. New Zealand Unpublished Mineral Report 763.

Lang JR, Baker T. 2001. Intrusion-related gold systems: the present level of understanding. *Mineralium Deposita*. 36(6):477–489. https://doi.org/10.1007/s001260100184

Lang JR, Baker T, Hart CJR, Mortensen JK. 2000. An exploration model for intrusion-related gold systems. *SEG Discovery*. (40):1–15. https://doi.org/10.5382/SEGnews.2000-40.fea

Lay RE. 1976. Final report on the Otama area, Southland. Located at: Ministry of Business, Innovation & Employment, Wellington, NZ. 18 p. + enclosures. New Zealand Unpublished Mineral Report 2106.

Lefebure DV, Hart CJR. 2005. Plutonic-related Au quartz veins & veinlets. Victoria (BC): British Columbia Geological Survey. 8 p. (Mineral Deposit Profiles; L02).

Lefebure DV, Höy T, editors. 1996. Selected British Columbia mineral deposit profiles. Volume 2: metallic deposits. Victoria (BC): British Columbia Geological Survey. 172 p.

Lefebure DV, Ray GE, editors. 1995. Selected British Columbia mineral deposit profiles. Volume 1: metallics and coal. Victoria (BC): British Columbia Geological Survey. 136 p.

Lefond SJ. 1975. Industrial minerals and rocks: nonmetallics other than fuels. 4th ed. New York (NY): American Institute of Mining, Metallurgical, and Petroleum Engineers. 1360 p.

Loftus N. 2010. Chronological data review, airborne magnetic survey and 3D inversion report, Offshore Taranaki [PP51536]. Located at: Ministry of Business, Innovation & Employment, Wellington, NZ. New Zealand Unpublished Mineral Report 4667.

Long KR. 2004. Preliminary descriptive deposit model for detachment-fault-related mineralization. Reston (VA): U.S. Geological Survey; [accessed 2024 Jul]. http://pubs.usgs.gov/bul/b2004/html/bull2004detachmentfaultrelated_mineraliz.htm

Lowery JH. 1979. Mineragraphy and origin of copper-bearing sulphides at Waitahuna River, eastern Otago. *New Zealand Journal of Geology and Geophysics.* 22(1):29–40. https://doi.org/10.1080/00288306.1979.10422552

Luke KA. 1997. Geology and extraction of the Northland halloysite deposits. In: 1997 New Zealand Minerals & Mining conference proceedings; 1997 Nov 17–19; Auckland, New Zealand. Wellington (NZ): Publicity Unit, Crown Minerals, Ministry of Commerce. p. 193–198.

MacArthur NA. 1984. Final report on EL 33164 Charlton to Otama, Southland. Located at: Ministry of Business, Innovation & Employment, Wellington, NZ. 6 p. New Zealand Unpublished Mineral Report 2117.

MacDonell B. 1992. The Little Beach – Wallace Beach mineral sand deposit, Catlins area, New Zealand. In: R*ediscover Otago – new perspectives, new opportunities: proceedings of the 26th annual conference 1992, New Zealand Branch of the Australasian Institute of Mining and Metallurgy*; 1992 Aug 19–21; Dunedin, New Zealand. [Place unknown] (NZ): Australasian Institute of Mining and Metallurgy, New Zealand Branch.

MacFarlan DAB, Barry JM. 1991. Mineral resources of New Zealand. Wellington (NZ): Ministry of Commerce, Energy and Resources Division. 61 p. Resource information report 11.

MacKay DR. 1984. Report on scheelite exploration within Kakanui EL 33204, North Otago. Located at: Ministry of Business, Innovation & Employment, Wellington, NZ. New Zealand Unpublished Mineral Report 1957.

MacKenzie IF. 1984. Final report on exploration licence 33195, Whitcombe River, Westland, New Zealand. Located at: Ministry of Business, Innovation & Employment, Wellington, NZ. 99 p. + 5 enclosures. New Zealand Unpublished Mineral Report 1398.

MacPherson JM. 1970. Report on Longwoods Range, Southland Province, South Island. Located at: Ministry of Business, Innovation & Employment, Wellington, NZ. 8 p. + 3 enclosures. New Zealand Unpublished Mineral Report 2026.

Manhire DA, Loudon AG, Ryan MJ. 2006. L&M Mining Limited: large scale alluvial gold mining operations in Otago, Southland and Westland between 1987 and 2002. In: Christie AB, Brathwaite RL, editors. *Geology and exploration of New Zealand mineral deposits*. Parkville (AU): Australasian Institute of Mining and Metallurgy. p. 49–56. (Australasian Institute of Mining and Metallurgy monograph series; 25).

Manhire D, Ford S, Moriarty A, Manhire J. 2024. Final report: the viability, feasibility, and environmental effects from using New Zealand sourced phosphate. [Christchurch] (NZ): National Science Challenges, Our Land and Water; [accessed 2024 Jul]. https://ourlandandwater.nz/wp-content/uploads/2024/03/Final-Sustainable-Phosphate-Futures-report-1.pdf

Manuka Resources. 2023. Maiden vanadium resource at Taranaki VTM Iron Sand Project (New Zealand). Sydney (AU): Manuka Resources; [accessed 2024 Sep]. https://www.manukaresources.com.au/site/pdf/ba77d298-97c1-473d-b419-98b2ad54cda2/Maiden-Vanadium-Resource-at-Taranaki-VTM-Iron-Sand-Project.pdf

Mar SS, Okazaki M. 2012. Investigation of Cd contents in several phosphate rocks used for the production of fertilizer. *Microchemical Journal.* 104:17–21. https://doi.org/10.1016/j.microc.2012.03.020

Marsh E, Anderson E, Gray F. 2013. Nickel-cobalt laterites – a deposit model: chapter H of mineral deposit models for resource assessment. Reston (VA): U.S. Geological Survey. 38 p. Scientific Investigations Report 2010–5070–H.

Martin WRB, Long AM. 1960. Heavy mineral content and radioactivity counts of beach sands west of Oreti river mouth to Blue Cliffs, Southland, New Zealand. *New Zealand Journal of Geology and Geophysics*. 3(3):400–409. https://doi.org/10.1080/00288306.1960.10422085

Mason DO. 1973. Geology of the Parakao, Pakotai and Pupuke copper deposits, Northland [MSc thesis]. Auckland (NZ): University of Auckland. 175 p. + 3 fold. maps.

Mason DO, Kobe HW. 1989. Fe-Cu-(Zn) sulphide deposits associated with ophiolites in Northland: a summary. In: Spoerli B, Kear D, editors. *Geology of Northland: accretion, allochthons and arcs at the edge of the New Zealand micro-continent*. Wellington (NZ): Royal Society of New Zealand. p. 165–174. (Royal Society of New Zealand bulletin; 26).

Mathison I, Legge P, Crawford J. 1992. PP 39-003 – Takaka area, NW Nelson. Report on prospecting activity February to July 1992. Located at: Ministry of Business, Innovation & Employment, Wellington, NZ. New Zealand Unpublished Mineral Report 3178.

Maton T, Carr D, Church P. 2021. Waihi District – Martha underground feasibility study: NI 43-101 technical report. Effective date: 31st March 2021. Otago (NZ): *OceanaGold.* 330 p.

Mauk JL, Cocker HA, Rogers H, Ogiliev J, Padya AB. 2016. Process mineralogy of ironsands in the Waikato North Head deposit, Waikato Region, North Island. In: Christie AB, editor. *Mineral deposits of New Zealand: exploration and research*. Carlton (AU): Australasian Institute of Mining and Metallurgy. p. 435–442. (Australasian Institute of Mining and Metallurgy monograph series; 31).

Maxwell M. 1983. Drilling results PL 31338 Lake Stanley joint venture area. Located at: Ministry of Business, Innovation & Employment, Wellington, NZ. New Zealand Unpublished Mineral Report 976.

Maxwell MG. 1989. Greisen-related tin-tungsten mineralization at Doctor Hill, central Westland. In: Kear D, editor. *Mineral deposits of New Zealand*. Parkville (AU): Australasian Institute of Mining and Metallurgy. p. 143–146. (Australasian Institute of Mining and Metallurgy monograph series; 13).

McArthur JM, Sahami AR, Thirlwall M, Hamilton PJ, Osborn AO. 1990. Dating phosphogenesis with strontium isotopes. *Geochimica et Cosmochimica Acta.* 54(5):1343–1351. https://doi.org/10.1016/0016-7037(90)90159-I

McClelland DA. 1981a. NZ scheelite project: final report for EL 33145 Earnslaw, near Glenorchy. Located at: Ministry of Business, Innovation & Employment, Wellington, NZ. 13 p. + 1 enclosure. New Zealand Unpublished Mineral Report 1826.

McClelland DA. 1981b. NZ scheelite project: final report on EL 33161 and 33162, North and South Richardson Range. Located at: Ministry of Business, Innovation & Employment, Wellington, NZ. 10 p. + 6 enclosures. New Zealand Unpublished Mineral Report 1827.

McConachy TF, Yeats CJ, Binns RA, Quigley MA, Peet SC. 2005. Kermadec 05: preliminary report on coring program Brothers Seamount, PL39-195 New Zealand. Located at: Ministry of Business, Innovation & Employment, Wellington, NZ. 104 p. New Zealand Unpublished Mineral Report 4147.

McConachy TF, Yeats CJ, Quigley M. 2006. Completion Report Kermadec 05. Located at: Ministry of Business, Innovation & Employment, Wellington, NZ. 104 p. + appendices. New Zealand Unpublished Mineral Report 4191.

McConchie DM, Lewis DW. 1978. Authigenic, perigenic, and allogenic glauconites from the Castle Hill Basin, North Canterbury, New Zealand. *New Zealand Journal of Geology and Geophysics*. 21(2):199–214. https://doi.org/10.1080/00288306.1978.10424051

McConchie DM, Lewis DW. 1980. Varieties of glauconite in late Cretaceous and early Tertiary rocks of the South Island of New Zealand, and new proposals for classification. *New Zealand Journal of Geology and Geophysics*. 23(4):413–437. https://doi.org/10.1080/00288306.1980.10424113

McIlrath L, Harris T. 2024. Futureproofing access to aggregate: economic considerations. [Auckland] (NZ): Market Economics (M.E). Document Reference KAI 005.23.

McIntosh C, Cooksey R. 2016. The geology and mining of Globe-Progress orogenic gold deposit, Reefton Goldfield, from 2006 to 2015. In: Christie AB, editor. *Mineral deposits of New Zealand: exploration and research*. Carlton (AU): Australasian Institute of Mining and Metallurgy. p. 119–124. (Australasian Institute of Mining and Metallurgy monograph series; 31).

McKay A. 1883. On an antimony lode at Reefton, Inangahua County. *Reports of Geological Explorations.* 15:88–90.

McKay A. 1890. On the geology of Stewart Island and the tin-deposits of Port Pegasus district. *Reports of Geological Explorations.* 20:74–85.

McLaughlin RJW. 1973. Report on the ilmenite beach sands of the eastern Coromandel Peninsula. Located at: Ministry of Business, Innovation & Employment, Wellington, NZ. 35 p. New Zealand Unpublished Mineral Report 315.

McPherson RI. 1978. Geology of Quaternary ilmenite-bearing coastal deposits at Westport, South Island, New Zealand. Wellington (NZ): Department of Scientific and Industrial Research. 95 p. (New Zealand Geological Survey bulletin; 87).

Merchant RJ. 1978. Metallogenesis in the Thames-Tapu area Coromandel Peninsula, New Zealand [PhD thesis]. Auckland (NZ): University of Auckland.

Merchant RJ. 1986. Mineralization in the Thames district – Coromandel. In: Henley RW, Hedenquist JW, Roberts PJ, editors. *Guide to the active epithermal (geothermal) systems and precious metal deposits of New Zealand*. Berlin (DE): Gebrüder Borntraeger. p. 147–163. (Monograph series in mineral deposits; 26).

Merchant RJ. 2012. Glauconite – the future potash for fertilisers in New Zealand. *AusIMM Bulletin*. 1(6):78–81.

Merchant RJ. 2013. Glauconite resources at Otoka, East Cape: 12 month report on exploration activities. Located at: Ministry of Business, Innovation & Employment, Wellington, NZ. 62 p. New Zealand Unpublished Mineral Report 5015.

Middle Island. 2013. PP 54574 Castle Hill annual technical report – 2013. Located at: Ministry of Business, Innovation & Employment, Wellington, NZ. 24 p. + 2 enclosures. New Zealand Unpublished Mineral Report 5054.

Middle Island. 2015. PP 54610 Herbert Block North Otago partial surrender report 2015. Located at: Ministry of Business, Innovation & Employment, Wellington, NZ. 15 p. + 2 enclosures. New Zealand Unpublished Mineral Report 5215.

Middle Island. 2020. MEP60335 relinquishment report. Located at: Ministry of Business, Innovation & Employment, Wellington, NZ. 25 p. + 3 enclosures. New Zealand Unpublished Mineral Report 5693.

Minehan PJ. 1989. The occurrence and identification of economic detrital minerals associated with alluvial gold mining in New Zealand. In: Kear D, editor. *Mineral deposits of New Zealand*. Parkville (AU): Australasian Institute of Mining and Metallurgy. p. 159–167. (Australasian Institute of Mining and Metallurgy monograph series; 13).

Mineral Resources of New Zealand. 1998. Perth (AU): Louthean Publishing Pty Ltd.

Mitchell MJ. 1995. Alluvial platinum-group minerals from southern New Zealand. In: Mauk JL, St George JD, editors. *PACRIM Congress 1995: proceedings*; 1995 Nov 19–22; Auckland, New Zealand. Carlton (AU): Australasian Institute of Mining and Metallurgy. p. 377–382. (Australasian Institute of Mining and Metallurgy publication series; 95/9).

Morgan PG, Bartrum JA. 1915. Geology and mineral resources of the Buller-Mokihinui subdivision, Westport division. Wellington (NZ): Department of Mines, New Zealand Geological Survey. 210 p. (New Zealand Geological Survey bulletin; 17).

Morgenstern R. 2016. Hydrothermal alteration and rare earth element mineralisation in the French Creek Granite, Westland, New Zealand [MSc thesis]. Christchurch (NZ): University of Canterbury. https://doi.org/10.26021/7518

Morgenstern R, Turnbull RE, Hill MP, Durance PMJ, Rattenbury MS. 2018. Rare earth element mineral potential in New Zealand. Lower Hutt (NZ): GNS Science. 211 p. Consultancy Report 2018/23. Prepared for New Zealand Petroleum and Minerals.

Mortimer N, Strong DT. 2014. New Zealand limestone purity. *New Zealand Journal of Geology and Geophysics*. 57(2):209–218. https://doi.org/10.1080/00288306.2014.901230

Mortimer N, Tulloch AJ, Spark RN, Walker NW, Ladley E, Allibone AH, Kimbrough DL. 1999. Overview of the Median Batholith, New Zealand: a new interpretation of the geology of the Median Tectonic Zone and adjacent rocks. *Journal of African Earth Sciences*. 29(1):257–268. https://doi.org/10.1016/S0899-5362(99)00095-0

Morton J, editor. 2019. Lime use on New Zealand pastoral farms. Wellington (NZ): Fertiliser Association of New Zealand. 32 p.

Mosier DL, Singer DA, Bagby WC, Menzie WD. 1992. Grade and tonnage model of sediment-hosted Au. In: Bliss JD, editor. *Developments in mineral deposit modeling*. Washington (DC): U.S. Government Printing Office. (U.S. Geological Survey bulletin; 2004).

Mosier DL, Singer DA, Moring BC, Galloway JP. 2012. Podiform chromite deposits – database and grade and tonnage models. Reston (VA): U.S. Geological Survey. 45 p. Scientific Investigations Report 2012-5157.

Mullan B, Pearce P, Stuart S, Liley B, Mohan S. 2006. Climate change: New Zealand’s past land area. Wellington (NZ): Te Ara – the Encyclopedia of New Zealand; [updated 2020 Jul 20; accessed 2024 Jul]. https://teara.govt.nz/en/map/7543/new-zealands-past-land-area

Mustard R, Partington G. 2005. Granite gold mineral systems in New Zealand. In: *2005 New Zealand Minerals Conference proceedings: realising New Zealand's mineral potential*; 2005 Nov 13–16; Auckland, New Zealand. Wellington (NZ): Crown Minerals. p. 160–167.

Mutch AR, Baker LA. 1989. Recent exploration and evaluation of detrital gold in Otago and Southland. In: Kear D, editor. *Mineral deposits of New Zealand*. Parkville (AU): Australasian Institute of Mining and Metallurgy. p. 189–196. (Australasian Institute of Mining and Metallurgy monograph series; 13).

Nathan S. 1978. Sheets S31 and part S32 Buller-Lyell (1st ed), economic and engineering geology. Located at: Ministry of Business, Innovation & Employment, Wellington, NZ. New Zealand Unpublished Coal Report 742.

Nathan S, Rattenbury MS, Suggate RP, compilers. 2002. Geology of the Greymouth area [map]. Lower Hutt (NZ): Institute of Geological & Nuclear Sciences. 1 map + 1 book, scale 1:250,000. (Institute of Geological & Nuclear Sciences 1:250,000 geological map; 12).

Neptune Resources. 2007. Neptune CM07 GIS summary report. Located at: Ministry of Business, Innovation & Employment, Wellington, NZ. New Zealand Unpublished Mineral Report 4352.

[NERC] Natural Environment Research Council. 2011. Tungsten [commodity profile]. Nottingham (GB): British Geological Survey; [accessed 2024 Jun]. https://nora.nerc.ac.uk/id/eprint/17445/1/tungstenProfile%5B1%5D.pdf

New Talisman Gold Mines. 2022. Annual report 2022. Auckland (NZ): New Talisman Gold Mines. 35 p.

Nicholson DS. 1967. Distribution of economic minerals in South Island West Coast beach sands. *New Zealand Journal of Science.* 10:447–456.

Nicholson DS, Cornes JJS, Martin WRB. 1958. Ilmenite deposits in New Zealand. *New Zealand Journal of Geology and Geophysics.* 1(4):611–616. https://doi.org/10.1080/00288306.1958.10423169

Nicholson DS, Shannon WT, Marshall T. 1966. Separation of ilmenite, zircon and monazite from Westport beach sands. *New Zealand Journal of Science.* 9:586–598.

Nicholson KN, Black PM. 2004. Cretaceous to early Tertiary basaltic volcanism in the Far North of New Zealand: geochemical associations and their tectonic significance. *New Zealand Journal of Geology and Geophysics*. 47(3):437–446. https://doi.org/10.1080/00288306.2004.9515069

Nicolson P, Inger M, Cowden A. 1988. Geological and geochemical report Longwood Range project, Invercargill District (Final report EL 33-313; Progress report EL 33-423, PL 31-1573, and PL 31-1590). Located at: Ministry of Business, Innovation & Employment, Wellington, NZ. 400 p. + 35 enclosures. New Zealand Unpublished Mineral Report 2071.

[NZGS] New Zealand Geological Survey. 1970a. Minerals of New Zealand (Part A: metallics). 2nd ed. Lower Hutt (NZ): New Zealand Geological Survey. Report NZGS 38A.

[NZGS] New Zealand Geological Survey. 1970b. Minerals of New Zealand (Part B: non-metallics). 2nd ed. Lower Hutt (NZ): New Zealand Geological Survey. Report NZGS 38B.

[NZIC] New Zealand Infrastructure Commission Te Waihanga. 2021. Infrastructure resources study. Wellington (NZ): NZIC; [accessed 2024 Jul]. https://tewaihanga.govt.nz/our-work/research-insights/infrastructure-resources-study

OceanaGold. 2024 Feb 21. OceanaGold reports mineral reserves and resources for the year ended 2023 [news release]. Vancouver (BC): OceanaGold; [accessed 2024 Jun 24]. https://investors.oceanagold.com/2024-02-21-OceanaGold-Reports-Mineral-Reserves-and-Resources-for-the-Year-Ended-2023

Painter JAC. 1973. Progress report No 1 on MPW 8638 West Coast offshore No.1 (offshore Bruce Bay and Hunts Beach) – New Zealand. Located at: Ministry of Business, Innovation & Employment, Wellington, NZ. [7] p. + 1 enclosure. New Zealand Unpublished Mineral Report 1652.

Partington GA. 2009. Developing models using GIS to assess process an economic risk: examples from mineral exploration and wind energy development in New Zealand. In: *2nd Annual Geospatial Information Systems Summit*; 2009 Jun 22–23; Wellington, New Zealand. [Wellington (NZ)]: Kenex; [accessed 2024 Jul 4]. https://kenex.com.au/wp-content/uploads/2022/03/PartingtonWellingtonGIS2009.pdf

Pearson TR. 1973. Summary report bauxite prospect, Kerikeri area MPWs 451, 455, 479, and 480. Located at: Ministry of Business, Innovation & Employment, Wellington, NZ. 1 p. New Zealand Unpublished Mineral Report 81.

Phillips M. 2014. Geochemistry and timing, Sams Creek gold deposit, NW Nelson, New Zealand [MSc thesis]. Dunedin (NZ): University of Otago.

Phillips M. 2015. U-Pb dating of the Sams Creek dike: implications for genesis and exploration. In: Sterk R, editor. *48th New Zealand Branch annual conference on exploration, mining and New Zealand's mineral resources: conference proceedings*; 2015 Aug 30 – Sep 2; Dunedin, New Zealand. [Place unknown] (NZ): Australasian Institute of Mining and Metallurgy, New Zealand Branch. p. 351–364.

Phillips M, Angus P, MacKenzie D, Craw D. 2013. Geochemical variations in the Sams Creek gold prospect, NW Nelson, NZ. In: Taylor J, editor. *46th New Zealand Branch annual conference on exploration, mining and New Zealand's mineral resources: conference proceedings*; Nelson, New Zealand. Australasian Institute of Mining and Metallurgy, New Zealand Branch. p. 365–375.

Pirajno F. 1979. Geology, geochemistry, and mineralisation of the Endeavour Inlet antimony–gold prospect, Marlborough Sounds, New Zealand. *New Zealand Journal of Geology and Geophysics.* 22(2):227–237. https://doi.org/10.1080/00288306.1979.10424221

Pirajno F. 1982. Geology, geochemistry, mineralisation, and metal zoning of the McConnochie greisenised granite, Reefton district, Westland, New Zealand. *New Zealand Journal of Geology and Geophysics*. 25(4):405–425. https://doi.org/10.1080/00288306.1982.10421507

Pirajno F. 1985. Porphyry Mo and greisen W metallogeny related to the Karamea Batholith, South Island, New Zealand. *New Zealand Journal of Geology and Geophysics*. 28:187–191. https://doi.org/10.1080/00288306.1985.10422283

Pirajno F, Bentley PN. 1985. Greisen-related scheelite, gold and sulfide mineralisation at Kirwins Hill and Bateman Creek, Reefton district, Westland, New Zealand. *New Zealand Journal of Geology and Geophysics*. 28:97–109. https://doi.org/10.1080/00288306.1985.10422279

Pitcairn IK, Teagle DAH, Craw D, Olivo GR, Kerrich R, Brewer TS. 2006. Sources of metals and fluids in orogenic gold deposits: insights from the Otago and Alpine schists, New Zealand. *Economic Geology*. 101(8):1525–1546. https://doi.org/10.2113/gsecongeo.101.8.1525

Pitcairn IK, Craw D, Teagle DAH. 2014. The gold conveyor belt: large-scale gold mobility in an active orogen. *Ore Geology Reviews*. 62:129–142. https://doi.org/10.1016/j.oregeorev.2014.03.006

Price GD. 1983a. Final report on West Coast offshore project – northern exploration licences, New Zealand. Located at: Ministry of Business, Innovation & Employment, Wellington, NZ. 52 p. + 2 appendices + 7 enclosures. New Zealand Unpublished Mineral Report 977.

Price GD. 1983b. Final report on West Coast offshore project – central exploration licences, New Zealand, including Harvester prospect. Located at: Ministry of Business, Innovation & Employment, Wellington, NZ. 66 p. + 7 appendices + 10 enclosures. New Zealand Unpublished Mineral Report 1381.

Price GD. 1985. Harvester Project drilling report on 1984 vibrocoring programme: Offshore Hokitika. Located at: Ministry of Business, Innovation & Employment, Wellington, NZ. [14] p. + 4 appendices + 10 enclosures. New Zealand Unpublished Mineral Report 1428.

Price GD. 2013. PP52704 Hohonu project report for year 2 to 15 Dec 2012. Located at: Ministry of Business, Innovation & Employment, Wellington, NZ. 26 p. + 7 appendices + 2 enclosures. New Zealand Unpublished Mineral Report 4955.

Price GD. 2016. The Endeavour Inlet antimony mine, Marlborough. In: Christie AB, editor. *Mineral deposits of New Zealand: exploration and research*. Carlton (AU): Australasian Institute of Mining and Metallurgy. p. 99–107. (Australasian Institute of Mining and Metallurgy monograph series; 31).

Price GD, Coles G. 1985. Final report on West Coast offshore project – southern exploration licences, New Zealand, including Foulwind and Blaketown Els. Located at: Ministry of Business, Innovation & Employment, Wellington, NZ. 9 p. + 2 appendices + 4 enclosures. New Zealand Unpublished Mineral Report 998.

Price GD, Ryland CB. 2011. Annual report for PP 52704 – Hohonu project. Located at: Ministry of Business, Innovation & Employment, Wellington, NZ. 40 p. + 7 appendices + 2 enclosures. New Zealand Unpublished Mineral Report 4886.

Price GD, Aitchison JC, Wotherspoon BG. 1985. Final report on EL 33245 Mt Ward, Southern Alps, New Zealand. Located at: Ministry of Business, Innovation & Employment, Wellington, NZ. 23 p. + 2 enclosures. New Zealand Unpublished Mineral Report 1677.

Purvis G, Jamieson B, Hawke A, Foster J. 1982. Final report on exploration in the Southern Alps, Els 33079, Landsborough River, 33080 Huxley River, 33081 Wills River, 33150 Dobson River. Located at: Ministry of Business, Innovation & Employment, Wellington, NZ. 150 p. + 29 enclosures. New Zealand Unpublished Mineral Report 1667.

Rabone SDC. 1989a. Bismuth sulphosalts associated with molybdenite mineralisation in Northwest Nelson, New Zealand. In: Kear D, editor. *Mineral deposits of New Zealand*. Parkville (AU): Australasian Institute of Mining and Metallurgy. p. 139–142. (Australasian Institute of Mining and Metallurgy monograph series; 13).

Rabone SDC. 1989b. Molybdenum mineralisation at Taipo Spur, Karamea valley, Northwest Nelson, New Zealand. In: Kear D, editor. *Mineral deposits of New Zealand*. Parkville (AU): Australasian Institute of Mining and Metallurgy. p. 129–135. (Australasian Institute of Mining and Metallurgy monograph series; 13).

Railton GL, Watters WA. 1990. Minerals of New Zealand. Lower Hutt (NZ): New Zealand Geological Survey. 89 p. (New Zealand Geological Survey bulletin; 104).

Ramsay WHR, Kobe HW. 1974. Great Barrier Island silver-gold deposits, Hauraki province, New Zealand. *Mineralium Deposita.* 9(2):143–153.

Rattenbury MS, Partington GA. 2003. Prospectivity models and GIS data for the exploration of epithermal gold mineralisation in New Zealand. In: *Epithermal gold in New Zealand: GIS data package and prospectivity modelling*. Wellington (NZ): Ministry of Economic Development. 68 p.

Reed JJ. 1950. Spilites, serpentinites and associated rocks of the Mossburn district, Southland. *Transactions and Proceedings of the Royal Society of New Zealand.* 78:106–126.

Reed JJ. 1960. Manganese ore in New Zealand. *New Zealand Journal of Geology and Geophysics.* 3(3):344–354. https://doi.org/10.1080/00288306.1960.10422080

Richards RG. 1978. Utilisation of New Zealand dunites: an overview. Lower Hutt (NZ): Department of Scientific and Industrial Research, Industrial Processing Division. 22 p. Report IPD/IS 3.

Riley P. 1972. Quartzite investigations – Appos Flat, NW Nelson. Located at: Ministry of Business, Innovation & Employment, Wellington, NZ. 20 p. + 5 enclosures. New Zealand Unpublished Mineral Report 864.

Riley P, Ball JHT. 1971. Murray Creek antimony, Reefton. Located at: Ministry of Business, Innovation & Employment, Wellington, NZ. 11 p. + 5 enclosures. New Zealand Unpublished Mineral Report 1283.

Riley P, Ball JHT. 1972a. Auld's Creek antimony, Reefton. Located at: Ministry of Business, Innovation & Employment, Wellington, NZ. 8 p. + 1 appendix + 5 enclosures. New Zealand Unpublished Mineral Report 1294.

Riley P, Ball JHT. 1972b. Reefton antimony: Globe – Merrijigs prospect. Located at: Ministry of Business, Innovation & Employment, Wellington, NZ. 11 p. + 9 enclosures. New Zealand Unpublished Mineral Report 1295.

Riley P, Hume BJ. 1973. Wekakura fluorite prospect, NW Nelson. Located at: Ministry of Business, Innovation & Employment, Wellington, NZ. 3 p. + 4 enclosures. New Zealand Unpublished Mineral Report 887.

Ritchie JA. 1962. Diatomite deposits in New Zealand: a review. Wellington (NZ): Dominion Laboratory. Dominion Laboratory report 2054.

Ritchie TW. 2017. Placer garnet of the West Coast, New Zealand [MSc thesis]. Dunedin (NZ): University of Otago.

Ritchie TW, Scott JM. 2019. Placer garnet of the west coast of the South Island, New Zealand. In: *PACRIM 2019: mineral systems of the Pacific Rim conference proceedings*; 2019 Apr 3–5; Auckland, New Zealand. [Carlton (AU)]: Australasian Institute of Mining and Metallurgy.

Ritchie TW, Scott JM, Craw D. 2019. Garnet compositions track longshore migration of beach placers in western New Zealand. *Economic Geology*. 114(3):513–540. https://doi.org/10.5382/econgeo.4647

Roberts CJ. 1975. Progress report Haupiri property, Parapara River area, NW Nelson. Located at: Ministry of Business, Innovation & Employment, Wellington, NZ. [40] p. + 9 enclosures. New Zealand Unpublished Mineral Report 911.

Roberts PJ. 1989. Geology and mineralisation of the Monowai mine, Coromandel Peninsula. In: Kear D, editor. *Mineral deposits of New Zealand*. Parkville (AU): Australasian Institute of Mining and Metallurgy. p. 59–61. (Australasian Institute of Mining and Metallurgy monograph series; 13).

Roberts PJ. 1997. Zeolite and silica. In: *1997 New Zealand Minerals & Mining Conference: proceedings*; Auckland, NZ; 1997 Nov 17–19. Wellington (NZ): Crown Minerals, Ministry of Commerce. p. 199–203.

Robson RN. 1979. Geology of a mineralised porphyry system, Whangapoua, Coromandel Peninsula [MSc thesis]. Auckland (NZ): University of Auckland. 143 p.

Rogers MC. 1996. Grade-tonnage deposit models of selected Ontario mineral deposit types. Toronto (ON): Ontario Geological Survey. 105 p. Open File Report 5945.

Rogers MC, Thurston PC, Fyon JA, Kelly RI, Breaks FW. 1995. Descriptive mineral deposit models of metallic and industrial deposit types and related mineral potential assessment criteria. Toronto (ON): Ontario Geological Survey. 241 p. Open File Report 5916.

Roser BP. 1983. Comparative studies of copper and manganese mineralisation in the Torlesse, Waipapa and Haast Schist Terranes, New Zealand [PhD thesis]. Wellington (NZ): Victoria University of Wellington.

Rutherford PG, MacKay DR. 1984. Final report on Dansey Pass scheelite prospect, PL 31838, North Otago, New Zealand. Located at: Ministry of Business, Innovation & Employment, Wellington, NZ. 37 p. + 6 enclosures. New Zealand Unpublished Mineral Report 1958.

Sameshima T. 1978. Zeolites in tuff beds of the Miocene Waitemata Group, Auckland Province, New Zealand. In: Sand LB, Mumpton FA, editors. *Natural zeolites, occurrence, properties and uses*. New York (NY): Pergamon Press. p. 309–317.

Schulz KJ, Woodruff LG, Nicholson SW, Seal RR II, Piatak NM, Chandler VW, Mars JL. 2014. Occurrence model for magmatic sulfide-rich nickel-copper-(platinum-group element) deposits related to mafic and ultramafic dike-sill complexes. Reston (VA): U.S. Geological Survey. Scientific Investigations Report 2010–5070–I. https://doi.org/10.3133/sir20105070I

Sedyn PL, Esterhuizen G. 2007. Geophysical survey programme for 2007. Located at: Ministry of Business, Innovation & Employment, Wellington, NZ. 36 p. + 1 enclosure. New Zealand Unpublished Mineral Report 4335.

Sekula J. 1972. Manganese deposits and associated rocks of Northland, New Zealand [MSc thesis]. Auckland (NZ): University of Auckland.

Seward TM, Sheppard DS. 1986. Waimangu geothermal field. In: Henley RW, Hedenquist JW, Roberts PJ, editors. *Guide to the active epithermal (geothermal) systems and precious metal deposits of New Zealand*. Berlin (DE): Gebrüder Borntraeger. p. 81–91. (Monograph series on mineral deposits; 26).

Shanks III WCP, Koski RA, Mosier DL, Schulz KJ, Morgan LA, Slack JF, Ridley WI, Dusel-Bacon C, Seal Ii RR, Piatak NM. 2012. Volcanogenic massive sulfide occurrence model. Reston (VA): U.S. Geological Survey. Scientific Investigations Report 2010–5070–C. https://doi.org/10.3133/sir20105070C

Shannon WT, Kitt W, Marshall T. 1965. Separation of ilmenite and zircon from Waikato North head ironsands. *New Zealand Journal of Science.* 8:214–227.

Sherwood A. 2019. The geology and resources of New Zealand coalfields. Carlton (AU): Australasian Institute of Mining and Metallurgy. 364 p. (Australasian Institute of Mining and Metallurgy monograph series; 33).

Sillitoe RH. 1991. Intrusion-related gold deposits. In: Foster RP, editor. *Gold metallogeny and exploration*. Glasgow (GB): Blackie. p. 166–209.

Simandl GJ, Hora ZD, Lefebure DV, editors. 1999. Selected British Columbia mineral deposit profiles. Volume 3: industrial minerals and gemstones. Victoria (BC): British Columbia Ministry of Energy and Mines. 146 p.

Sinclair B. 1989. Lake Rotokaua sulphur deposits. In: Kear D, editor. *Mineral deposits of New Zealand*. Parkville (AU): Australasian Institute of Mining and Metallurgy. p. 89–91. (Australasian Institute of Mining and Metallurgy monograph series; 13).

Singer DA. 1998. Revised grade and tonnage model of carbonatite deposits. Reston (VA): U.S. Geological Survey. Open-file Report 98-235. https://doi.org/10.3133/ofr98235

Skinner DNB, Brathwaite RL. 1999. Mesozoic mesothermal quartz-gold-scheelite lodes, Wakamarina, Marlborough, New Zealand. *New Zealand Journal of Geology and Geophysics*. 42(3):335–348. https://doi.org/10.1080/00288306.1999.9514850

Smale D. 1970. Report on the examination of Copperstain Creek copper prospect, North-West Nelson. Located at: Ministry of Business, Innovation & Employment, Wellington, NZ. 12 p. + 2 appendices + 12 enclosures. New Zealand Unpublished Mineral Report 825.

Smale D. 1971. Report on examination of Nickel Prospect, Cobb-Takaka Area, North-West Nelson, New Zealand. Located at: Ministry of Business, Innovation & Employment, Wellington, NZ. 9 p. + 2 enclosures. New Zealand Unpublished Mineral Report 850.

Smith IEM, Chappell BW, Ward GK, Freeman RS. 1977. Peralkaline rhyolites associated with andesitic arcs of the southwest Pacific. *Earth and Planetary Science Letters*. 37(2):230–236. https://doi.org/10.1016/0012-821X(77)90167-4

Stanaway KJ. 1972. Manganese deposits and associated cherts and argillites of Auckland area [MSc thesis]. Auckland (NZ): University of Auckland.

Stanaway KJ, Kobe HW, Sekula J. 1978. Manganese deposits and the associated rocks of Northland and Auckland, New Zealand. New Zealand *Journal of Geology and Geophysics*. 21(1):21–32.

Stegman CL. 1987. Report on PL 311197 Asbestos Creek, Northwest Nelson, New Zealand to May 1987. CRA Exploration Pty. Located at: Ministry of Business, Innovation & Employment, Wellington, NZ. 299 p. + 29 enclosures. New Zealand Unpublished Mineral Report 1015.

Stegman CL. 1988a. Two drill-logs for PL 311197 Meter Creek, Asbestos Creek Project. Located at: Ministry of Business, Innovation & Employment, Wellington, NZ. 11 p. New Zealand Unpublished Mineral Report 2324.

Stegman CL. 1988b. Report on PL 311197 Asbestos Creek, including diamond drilling at the Meter Creek prospect, NW Nelson, New Zealand to March 1988. Located at: Ministry of Business, Innovation & Employment, Wellington, NZ. 101 p. + 10 enclosures. New Zealand Unpublished Mineral Report 1028.

Sterk R. 2014. Chatham Rise project: independent JORC (2012) technical report and mineral resource estimate on the Chatham Rise project in New Zealand. Wellington (NZ): RSC Consulting Ltd. 194 p. Prepared for Chatham Rock Phosphate Ltd.

Stevens MR. 1992. Final technical report on prospecting licence 31-1372, Wakapatu, Southland, New Zealand, for the period ended 19 November 1992. Located at: Ministry of Business, Innovation & Employment, Wellington, NZ. 20 p. + 1 enclosures. New Zealand Unpublished Mineral Report 3216.

Stevens MR, Phillip D. 1992. Waiau River, Southland New Zealand EL 33357 – final technical report for the period 11 April 1989 to 10 April 1991. Located at: Ministry of Business, Innovation & Employment, Wellington, NZ. 11 p. + 3 enclosures. New Zealand Unpublished Mineral Report 3109.

Stevenson I. 2006. Interpretation of data collected from the June 2006 evaluation geophysical survey. Located at: Ministry of Business, Innovation & Employment, Wellington, NZ. 28 p. New Zealand Unpublished Mineral Report 4333.

Stevenson I. 2008. Review of the offshore geophysical model for the Seafield Project Northern & Southern Target areas. Located at: Ministry of Business, Innovation & Employment, Wellington, NZ. 145 p. + 1 enclosure. New Zealand Unpublished Mineral Report 4332.

Stewart RT. 1906. Mining at Waikaia. In: Galvin P, editor. *The New Zealand mining handbook*. Wellington (NZ): Government Printer. p. 197–198.

Strategic Materials. 2013. EP 53058 Mandamus exploration report – 2013. Located at: Ministry of Business, Innovation & Employment, Wellington, NZ. 19 p. + 4 enclosures. New Zealand Unpublished Mineral Report 4986.

Strong DT, Turnbull IM, Glassey PJ. 2016. Silica deposits of Southland. In: Christie AB, editor. *Mineral deposits of New Zealand: exploration and research*. Carlton (AU): Australasian Institute of Mining and Metallurgy. p. 511–515. (Australasian Institute of Mining and Metallurgy monograph series; 31).

Suggate RP. 1957. The geology of the Reefton subdivision. Wellington (NZ): New Zealand Geological Survey. 146 p. + 10 folded maps. (New Zealand Geological Survey bulletin; 56).

Syers JK, Mackay AD, Brown MW, Currie LD. 1986. Chemical and physical characteristics of phosphate rock materials of varying reactivity. *Journal of the Science of Food and Agriculture.* 37(11):1057–1064. https://doi.org/10.1002/jsfa.2740371102

Tay SL, Scott JM, Palmer MC, Reid MR, Stirling CH. 2021. Occurrence, geochemistry and provenance of REE-bearing minerals in marine placers on the West Coast of the South Island, New Zealand. *New Zealand Journal of Geology and Geophysics*. 64(1):89–106. https://doi.org/10.1080/00288306.2020.1736585

Taylor RD, Hammarstrom JM, Piatak NM, Seal RR II. 2012. Arc-related porphyry molybdenum deposit model. Reston (VA): U.S. Geological Survey. Scientific Investigations Report 2010-5070-D. https://doi.org/10.3133/sir20105070D

Tennant WC, Sewell JR. 1967. A survey of the rare earth contents in stream sediments of the Paparoa Range, New Zealand. *New Zealand Journal of Science*. 10:721–735.

Thalhammer OAR, Stumpfl EF, Jahoda R. 1989. The Mitersill scheelite deposit, Austria. *Economic Geology*. 84(5):1153–1171. https://doi.org/10.2113/gsecongeo.84.5.1153

Thompson BN. 1989. Non-metallic minerals. In: Kear D, editor. *Mineral deposits of New Zealand*. Parkville (AU): Australasian Institute of Mining and Metallurgy. p. 15–23. (Australasian Institute of Mining and Metallurgy monograph series; 13).

Thompson BN, Reed JJ, Dunn LRL, Billinghurst WM. 1954. Perlite deposits in New Zealand. Part 1: geology. Part 2: evaluation. *New Zealand Journal of Science and Technology.* B36(3):208–226.

Thompson JFH, Newberry RJ. 2000. Gold deposits related to reduced granitic intrusions. In: Hagemann SG, Brown PE, editors. *Gold in 2000*. Littleton (CO): Society of Economic Geologists. p. 377–400. (Reviews in Economic Geology; 13). https://doi.org/10.5382/Rev.13.11

Thomson BC, Ward KR, Muir PD. 2021. Purity of agricultural lime and dolomite used in New Zealand. [Wellington] (NZ): Ministry for Primary Industries. 12 p. (MPI Technical Paper; 2022/04).

Timm C, Wysoczanski RJ, de Ronde CEJ. 2016. Potential sources of metals in Kermadec arc lavas. In: Christie AB, editor. *Mineral deposits of New Zealand: exploration and research*. Carlton (AU): Australasian Institute of Mining and Metallurgy. p. 397–402. (Australasian Institute of Mining and Metallurgy monograph series; 31).

Torckler, LK, Hobbins JM, Christie AB. 2016. Mining and exploration of the epithermal gold-silver deposits at Waihi, Hauraki Goldfield. In: Christie AB, editor. *Mineral deposits of New Zealand: exploration and research*. Carlton (AU): Australasian Institute of Mining and Metallurgy. p. 303–312. (Australasian Institute of Mining and Metallurgy monograph series; 31).

Townsend MG. 1989. Halloysite clay deposits in Northland. In: Kear D, editor. *Mineral deposits of New Zealand*. Parkville (AU): Australasian Institute of Mining and Metallurgy. p. 39–43. (Australasian Institute of Mining and Metallurgy monograph series; 13).

Tulloch AJ. 1988a. Batholiths, plutons, and suites: nomenclature for granitoid rocks of Westland – Nelson, New Zealand. *New Zealand Journal of Geology and Geophysics*. 31(4):505–509. https://doi.org/10.1080/00288306.1988.10422147

Tulloch AJ. 1988b. Metamorphic core complexes and detachment faults in Westland, New Zealand – implications for precious metal mineralisation. Lower Hutt (NZ): New Zealand Geological Survey. 44 p. Report M 172.

Tulloch AJ. 1992. Petrology of the Sams Creek peralkaline granite dyke, Takaka. *New Zealand Journal of Geology and Geophysics*. 35(2):193–200. https://doi.org/10.1080/00288306.1992.9514513

Tulloch AJ. 1995. Precious metal mineralisation associated with the Cretaceous Paparoa metamorphic core complex, New Zealand. In: Mauk JL, St George JD, editors. *PACRIM Congress 1995: proceedings*; 1995 Nov 19–22; Auckland, New Zealand. Carlton (AU): Australasian Institute of Mining and Metallurgy. p. 575–580. (Australasian Institute of Mining and Metallurgy publication series; 95/9).

Tulloch AJ, Brathwaite RL. 1986. C7: Granitoid rocks and associated mineralisation of Westland-west Nelson. In: Houghton BF, Weaver SD, editors. *International volcanological congress New Zealand, 1986: South Island igneous rocks – tour guides A3, C2 and C7*; Auckland, New Zealand. Lower Hutt (NZ): New Zealand Geological Survey. p. 65–92. (New Zealand Geological Survey record; 13).

Tulloch AJ, Christie AB. 2000. Reconnaissance rare earth element (REE) geochemistry of Ohika Detachment Fault (Buller) and Mandamus Intrusives (North Canterbury). Lower Hutt (NZ): Institute of Geological and Nuclear Sciences. 26 p. (Institute of Geological & Nuclear Sciences science report; 2000/10).

Tulloch AJ, Dunlap WJ. 2006. A Carboniferous ^{40}Ar/^{39}Ar amphibole emplacement age for the Au-bearing Sams Creek alkali–feldspar granite dike, west Nelson, New Zealand. *New Zealand Journal of Geology and Geophysics*. 49(2):233–240. https://doi.org/10.1080/00288306.2006.9515162

Tulloch AJ, Kimbrough DL. 1989. The Paparoa Metamorphic Core Complex, New Zealand: Cretaceous extension associated with fragmentation of the Pacific margin of Gondwana. *Tectonics.* 8(6):1217–1234. https://doi.org/10.1029/TC008i006p01217

Tulloch AJ, Mackenzie IF. 1986. Tin-tungsten granites in New Zealand. *Bureau of Mineral Resources, Geology and Geophysics record*. 86/10:75–76.

Tulloch AJ, Rabone SDC. 1993. Mo-bearing granodiorite porphyry plutons of the Early Cretaceous Separation Point Suite, west Nelson, New Zealand. *New Zealand Journal of Geology and Geophysics*. 36(4):401–408. https://doi.org/10.1080/00288306.1993.9514586

Turnbull IM, Smith Lyttle B. 1999. Annotated 1:1 million maps of limestone regions of New Zealand. Lower Hutt (NZ): Institute of Geological and Nuclear Sciences. 2 p. + maps. Client Report 1999/118. Prepared for Department of Conservation.

Turnbull IM, Allibone AH, Jongens R, compilers. 2010. Geology of the Fiordland area. Lower Hutt (NZ): GNS Science. 97 p. + 1 map, scale 1:250,000. (Institute of Geological & Nuclear Sciences 1:250,000 geological map; 17).

Turnbull RE, Size WB, Tulloch AJ, Christie AB. 2017. The ultramafic–intermediate Riwaka Complex, New Zealand: summary of the petrology, geochemistry and related Ni–Cu–PGE mineralisation. *New Zealand Journal of Geology and Geophysics*. 60(3):270–295. https://doi.org/10.1080/00288306.2017.1316747

Turnbull RE, Morgenstern R, Hill MP, Durance PMJ, Rattenbury MS. 2018. Lithium mineral potential in New Zealand. Lower Hutt (NZ): GNS Science. 210 p. Consultancy Report 2018/63. Prepared for New Zealand Petroleum & Minerals.

Turnbull RE, Hill MP, Morgenstern R, Rosenberg MD. 2019. Lithium mineral potential in the Taupō Volcanic Zone. Lower Hutt (NZ): GNS Science. 70 p. Consultancy Report 2019/61. Prepared for New Zealand Petroleum & Minerals.

Turnbull RE, Christie AB, Georgatou AA, de Ronde CEJ, Brathwaite RL, Chambefort I, Hill MP. 2023. Copper as a critical metal for New Zealand’s transition to a low-carbon economy. Lower Hutt (NZ): GNS Science. 88 p. (GNS Science report; 2022/43). https://doi.org/10.21420/NYEJ-XG27

Turner PD. 2015. Carbonatite veins in lamprophyre dykes, Mt Tapuaenuku, New Zealand [MSc thesis]. Christchurch (NZ): University of Canterbury. https://doi.org/10.26021/8606

[USGS] U.S. Geological Survey. 2024. Mineral commodity summaries 2024. Reston (VA): U.S. Geological Survey. https://doi.org/10.3133/mcs2024

van de Ven M, Gazley M, Sterk R, Aldrich S, Werner E. 2020. Exploration for Lithium-Caesium-Tantalum (LCT) pegmatites in New Zealand. In: *Mining's role in a prosperous low-emissions economy: New Zealand minerals forum 2020 in partnership with AusIMM conference proceedings*; 2020 Oct 13–14; Hamilton, New Zealand. [Place unknown] (NZ): New Zealand Minerals Forum. p 87–91.

Van Gosen BS, Fey DL, Shah AK, Verplanck PL, Hoefen TM. 2014. Deposit model for heavy-mineral sands in coastal environments. Reston (VA): U.S. Geological Survey. Scientific Investigations Report 2010-5070-L. https://doi.org/10.3133/sir20105070L

Verlaan PA, Cronan DS. 2022. Origin and variability of resource-grade marine ferromanganese nodules and crusts in the Pacific Ocean: a review of biogeochemical and physical controls. *Geochemistry*. 82(1):125741. https://doi.org/10.1016/j.chemer.2021.125741

Verplanck PL, Van Gosen BS, Seal RR, McCafferty AE. 2014. A deposit model for carbonatite and peralkaline intrusion-related rare earth element deposits. Reston (VA): U.S. Geological Survey. Scientific Investigations Report 2010-5070-J. https://doi.org/10.3133/sir20105070J

Viljoen RP. 1972. The geology and economic potential of antimony mineralization of the South Island of New Zealand with particular reference to the mineral holdings of Antimony Mines Ltd (Endeavour Inlet, Middlemarch and Reefton). Located at: Ministry of Business, Innovation & Employment, Wellington, NZ. 29 p. New Zealand Unpublished Mineral Report 877.

Waterhouse BC. 1967. Diatomite at Mercer. In: *Industrial Minerals and Rocks 1966.* Wellington (NZ): Department of Scientific and Industrial Research. p. 35–37. (DSIR information series; 63).

Wellman HW. 1942. Talc-magnesite and quartz-magnesite rock, Cobb – Takaka district. *New Zealand Journal of Science and Technology*. B24:103-127.

Wellman HW. 1943. Talc in North-West Nelson and North Westland. *New Zealand Journal of Science and Technology*. B24:227–235.

Whattam SA, Malpas JG, Ali JR, Smith IEM, Lo C-H. 2004. Origin of the Northland Ophiolite, northern New Zealand: discussion of new data and reassessment of the model. *New Zealand Journal of Geology and Geophysics.* 47(3):383–389. https://doi.org/10.1080/00288306.2004.9515064

Whattam SA, Malpas JG, Ali JR, Lo C-H, Smith IEM. 2005. Formation and emplacement of the Northland Ophiolite, northern New Zealand: SW Pacific tectonic implications. *Journal of the Geological Society*. 162(2):225–241. https://doi.org/10.1144/0016-764903-167

Williams GJ. 1934. The auriferous tin placers of Stewart Island, New Zealand. *New Zealand Journal of Science and Technology.* 15:344–357.

Williams GJ. 1974. Economic geology of New Zealand. Rev. ed. Victoria (AU): Australasian Institute of Mining and Metallurgy. 490 p. (Australasian Institute of Mining and Metallurgy monograph series; 4).

Williams GJ, Katz HR. 1974. Recent progress in the mineral industry. In: Williams GJ, editor. *Economic geology of New Zealand.* Rev. ed. Victoria (AU): Australasian Institute of Mining and Metallurgy. p. 371–382. (Australasian Institute of Mining and Metallurgy monograph series; 4).

Williams GJ, Mackie JB. 1959. Economic minerals in Stewart Island. In: *Proceedings of the fourth triennial mineral conference*; 1959 Sep 1–3; Dunedin, New Zealand. [Dunedin (NZ)]: University of Otago. Paper 125.

Williams GJ, et al. 1959. Economic minerals at Canaan, NW Nelson. Located at: Ministry of Business, Innovation & Employment, Wellington, NZ. 9 p. New Zealand Unpublished Mineral Report 774.

Wilson D, Sharp B, Sheng MS, Sreenivasan A, Kieu M, Ivory V. 2022. Aggregate supply and demand in New Zealand. Wellington (NZ): Waka Kotahi NZ Transport Agency. 89 p. (Waka Kotahi NZ Transport Agency research report; 693).

Wodzicki A. 1972. Mineralogy, geochemistry and origin of hydrothermal alteration and sulphide mineralization in the disseminated molybdenite and skarn-type copper sulphide deposit at Copperstain Creek, Takaka, New Zealand. *New Zealand Journal of Geology and Geophysics*. 15(4):599–631. https://doi.org/10.1080/00288306.1972.10423987

Wodzicki A, Thompson BN. 1970. The geology and mineralisation of Coppermine Island. *New Zealand Journal of Geology and Geophysics*. 13(3):631–646. https://doi.org/10.1080/00288306.1970.10431334

Wood BL. 1966. Geological map of New Zealand 1:250,000: sheet 24 Invercargill. Wellington (NZ): Department of Scientific and Industrial Research. 1 fold. map. (Geological map of New Zealand 1:250,000; 24).

Wood BL. 1983. Widespread scheelite in Mesozoic schists of South Island, New Zealand [abstract]. In: *Pacific Science Association 15th Congress: programme, abstracts and congress information*. Dunedin (NZ): Pacific Science Association. p. 258.

Wood J, Meyers J, Vidanovich P. 2016. Aotea ironsand deposit, Waikatro region, North Island. In: Christie AB, editor. *Mineral deposits of New Zealand: exploration and research*. Carlton (AU): Australasian Institute of Mining and Metallurgy. p. 427–433. (Australasian Institute of Mining and Metallurgy monograph series; 31).

Wood RA, Falconer R. 2016. Chatham phosphate: a strategic resource. In: Christie AB, editor. *Mineral deposits of New Zealand: exploration and research*. Carlton (AU): Australasian Institute of Mining and Metallurgy. p. 517–522. (Australasian Institute of Mining and Metallurgy monograph series; 31).

Wood RA, Falconer R, Kudrass H. 2015. Seabed fertiliser. In: Graham IJ, editor. *A continent on the move: New Zealand geoscience revealed*. 2nd ed. Wellington (NZ): Geoscience Society of New Zealand. p. 312–313. (Geoscience Society of New Zealand miscellaneous publication; 141).

Woodruff LG, Nicholson SW, Fey DL. 2013. A deposit model for magmatic iron-titanium-oxide deposits related to Proterozoic massif anorthosite plutonic suites. Reston (VA): U.S. Geological Survey. Scientific Investigations Report 2010–5070–K.

Wotherspoon BG. 1986. Harvester project: final report on EL 33254 Rimu and 33255 Gladstone. Located at: Ministry of Business, Innovation & Employment, Wellington, NZ. 8 p. + 1 enclosure. New Zealand Unpublished Mineral Report 1449.

Wright IC, de Ronde CEJ, Faure K, Gamble JA. 1998. Discovery of hydrothermal sulfide mineralization from southern Kermadec arc volcanoes (SW Pacific). *Earth and Planetary Science Letters.* 164(1):335–343. https://doi.org/10.1016/S0012-821X(98)00225-8

Wright IC, Graham IJ, Chang SW, Choi H, Lee SR. 2005. Occurrence and physical setting of ferromanganese nodules beneath the Deep Western Boundary Current, SW Pacific Ocean. *New Zealand Journal of Geology and Geophysics.* 48(1):27–41. https://doi.org/10.1080/00288306.2005.9515096

Yardley B. 2002. Mining assessment and prospecting potential of the Glenorchy gold-tungsten prospect. Located at: Ministry of Business, Innovation & Employment, Wellington, NZ. 61 p. New Zealand Unpublished Mineral Report 3972.

Young DJ. 1964. Ganister and silica sand deposits of the west coast, South Island. *New Zealand Journal of Geology and Geophysics*. 7(3):508–524. https://doi.org/10.1080/00288306.1964.10422098

Youngson JH. 2006. A gold placer genesis model for the Westland continental shelf, New Zealand: projection and first-order targeting: revision 1. Dunedin (NZ): Youngson Geoscience Consultants Ltd. 93 p. Unpublished confidential report.

Youngson JH, Stevenson I. 2016. An overview of offshore placer gold exploration: the Seafield project, Westland, 2006–2010. In: Christie AB, editor. *Mineral deposits of New Zealand: exploration and research*. Carlton (AU): Australasian Institute of Mining and Metallurgy. p. 345–352. (Australasian Institute of Mining and Metallurgy monograph series; 31).

Zientek ML. 2012. Magmatic ore deposits in layered intrusions – descriptive model for reef-type PGE and contact-type Cu-Ni-PGE deposits. Reston (VA): U.S. Geological Survey. Open-file report 2012–1010. 48 p.

Zuckerman MB. 1972a. Progress report no.1 Birchfield MPW 14591 and MPW applications 48/69, 115/70. Located at: Ministry of Business, Innovation & Employment, Wellington, NZ. 62 p. + 5 enclosures. New Zealand Unpublished Mineral Report 869.

Zuckerman MB. 1972b. Progress report – Takaka No. 3, Nelson. Located at: Ministry of Business, Innovation & Employment, Wellington, NZ. 13 p. + 2 enclosures. New Zealand Unpublished Mineral Report 874.

Zuckerman MB. 1972c. Progress report No.1 – Takaka areas, New Zealand. Located at: Ministry of Business, Innovation & Employment, Wellington, NZ. 29 p. + 6 enclosures. New Zealand Unpublished Mineral Report 873.

www.gns.cri.nz

Principal Location

1 Fairway Drive, Avalon
Lower Hutt 5010
PO Box 30368
Lower Hutt 5040
New Zealand
T +64-4-570 1444
F +64-4-570 4600

Other Locations

Dunedin Research Centre
764 Cumberland Street
Private Bag 1930
Dunedin 9054
New Zealand
T +64-3-477 4050
F +64-3-477 5232

Wairakei Research Centre
114 Karetoto Road
Private Bag 2000
Taupo 3352
New Zealand
T +64-7-374 8211
F +64-7-374 8199

National Isotope Centre
30 Gracefield Road
PO Box 30368
Lower Hutt 5040
New Zealand
T +64-4-570 1444
F +64-4-570 4657